Head to Head Tests of the Hydrodynamic Support for Saturn V

ER 14036

December 1965

Prepared by:

H. Bone

W. R. Case

F. T. Gordon

Approved by:

R. A. Hirsch

P. A. Milleson

E. J. Weber

FOREWORD

This report has been prepared by the Baltimore Division of the Martin Company, a division of the Martin Marietta Corporation, in partial fulfillment of the requirements of Contract NAS 8-11903, dated 15 February 1965.

ABSTRACT

This report covers the Head to Head tests done on the Saturn V Hydrodynamic Support at Martin-Baltimore during the period from 1 August to 6 October 1965. Included are descriptions of the specimens, procedures, and results of the tests conducted during this period.

CONTENTS

CONTENTS (continued)

LIST OF FIGURES

LIST OF FIGURES (continued)

LIST OF FIGURES (continued)

LIST OF FIGURES (continued)

LIST OF FIGURES (continued)

LIST OF FIGURES (continued)

LIST OF TABLES

SUMMARY

The purpose of the test program reported herein was twofold: First, to demonstrate compliance with certain performance requirements specified contractually, and second, to generate data for comparison with the mathematical model. The characteristics to be demonstrated, the specified values and the test results are summarized in tabular form below.

Characteristic	Specified Value	Test Result
Operating Range	Raise 3 in. Operate ±1 in. vertical ±4 in. lateral	Successfully demonstrated
Spring Rate	Bounce frequency 0.6 cps with heavy vehicle, 5 to 1 adjustment in spring rate	Minimum spring rate successfully demonstrated
Bearing Surface Misalignment	2 minute misalignment angle under maximum eccentric load	Test stand deflections obscured results
Moving Mass	Vertical Mass < 16,000 lb/support Effective Mass < 5,000 lb/support	Successfully demonstrated
Damping Constant	Lateral: 2.0 lb sec/in., light vehicle 3.2 lb sec/in., heavy vehicle	Successfully demonstrated within the limits of the test stand configuration
	Vertical: Can be made positive under all conditions 24 lb sec/in., 1 cps) heavy 40 lb sec/in., .5 cps) vehicle 15 lb sec/in., light vehicle	Total damping can be limited to the piston viscous damping which is 30 lb sec/in.
Local Resonances	None below 20 cps	Successfully demonstrated
Bearing Redundancy	Bearings to operate when 1/2 of the flow control valves are inoperable.	Successfully demonstrated

In summary, it can be stated that the hydrodynamic support performed in a predictable manner and in accordance with the analytical model. The only exceptions to the foregoing statement are that the flat bearing gaps under high load were less than predicted, and the piston viscous damping during vertical motion was higher than predicated. Various tests were performed in an attempt to isolate the source of these discrepancies but they were not found. It is believed, however, that the hydrodynamic support can be fully utilized to serve its intended purpose.

The details of the test program including the instrumentation utilized, the test procedures employed and the results obtained are reported herein. Also included herein are the details of any changes in components, design details or procedures which were required in order to successfully complete the program.

I. INTRODUCTION

The Hydrodynamic Support provides a six degree-of-freedom system for dynamic testing of the Saturn V. The system consists primarily of four pedestals and associated fluid and electrical supplies and controls.

The Saturn V in its heaviest configuration weighs about 7.2×10^6 lb or 1.8×10^6 lb per support. To prove the design of the supports for design assurance and compliance with design specifications before a vehicle was available, it was necessary to simulate the bearing loads associated with the various Saturn configurations. Since proving the design with a weight this large was not a realistic solution, another method of producing a large bearing load had to be found. The solution was to place two supports in a rigid framework and let them push against each other to produce the desired bearing load. The check of design assurance and design specifications on the Hydrodynamic Supports was accomplished in this Head-to-Head configuration.

The four piston-cylinders and associated hydraulic, pneumatic and electrical systems have been tested in the Head-to-Head Tests. The Head-to-Head Tests can be divided into six broad categories:

1. Design Assurance Tests
2. Vibration Surveys
3. Cylinder Supply Panel Tests
4. Static Piston Characteristics
5. Damping Tests
6. Miscellaneous Testing

The testing was conducted in two sets. The first set consisted of Units 1 and 2 and the second set consisted of Units 3 and 4. Units 1 and 3 were the upper assemblies.

Sixty-nine test conditions in all six categories were tested on Set #1 during the period of 8-1 through 9-2-65. Sixty-four test conditions in categories 1, 4, 5 and 6 were tested on Set #2 during the period 9-8 through 9-26. Also individual vertical and rotational damping tests were conducted on piston cylinder #5 on 10-6-65.

II. DESCRIPTION OF SPECIMENS

Two piston cylinder assemblies (Ref. 1) were installed in the Head-to-Head Test Stand (Ref. 2) utilizing the production hydraulic supply system, operating console, and a majority of the production components of this system (Refs. 3 through 8). Two overall views of the Head-to-Head installation are given in Fig. II-1 and Fig. II-2. The operating console is shown in Fig. II-3.

Figure II-4 shows a schematic of a hydraulic support unit providing six degrees of freedom. In the Head-to-Head testing the upper assembly spherical bearing was locked to the flat bearing thus preventing rotation. The stem connecting the upper and lower assemblies was guided by rollers in one translational direction and restrained by springs in the second horizontal translation direction (Fig. II-5).

The supply lines feeding the bearings and capillary seal were constructed to approximate the longest test site line runs on the bottom piston assembly (Unit 2 on Set #1 and Unit 4 on Set #2) and the shortest test site line runs on the upper piston assembly (Unit 1 on Set #1 and Unit 3 on Set #2).

III. TEST REQUIREMENTS

The Head-to-Head Test requirements are set forth in the Head-to-Head Test Specification (88A4100403) which is included as Appendix I. This specification covers the testing of both sets of piston and cylinders with the exception that the only requirement for testing on the second set was to demonstrate their functional operation.

IV. TEST DESCRIPTION SUMMARY

A. SUMMARY OF TESTS

To implement the test requirements a detailed test procedure was written (Ref. 9) to serve as a guide during the Head-to-Head testing. The first set was to be tested for all the requirements and the second set was just to be functionally checked. Because of problems along the way this plan had to be revised. Some additional tests were added to both sets and some of the tests planned for the first test were deferred until the second set. These problems will be discussed in detail under the Discussion and Results section of this report.

The tests can be broken into six main divisions and then subdivided. The tests conducted on both sets are listed below using this breakdown. Some tests were repeated, but these are not included in the following listing.

	No. of Tests Conducted Set #1	Set #2
a. Design Assurance		
(1) Piston Cylinder Gap and Bearing Gaps	10	9
(2) Bearing Redundancy and Separation	4	0

		No. of Tests Conducted Set #1	Set #2
a.	Design Assurance (Continued)		
	(3) Air Spring Loss	0	1
	(4) Floating Procedure	0	1
	(5) Operating Range	6	2
	(6) Sink Rate	2	2
	(7) Eccentric Loading	1	0
b.	Vibration Surveys		
	(1) Lateral	1	0
	(2) Vertical	1	0
c.	Cylinder Supply Panel		
	(1) K_Q Breadboard Tests	12 - done in Laboratory	
	(2) System K_Q Tests	9	0
	(3) System Component Tests	3	0
d.	Static Piston Characteristics	10	6
e.	Damping		
	(1) Head-to-Head		
	(a) Lateral	2	2
	(b) Vertical	15	36
	(2) Unit Tests		
	(a) Vertical and Rotational	5	7
f.	Miscellaneous Testing		
	(1) Ovality	0	1
	(2) Temperature Investigation	0	1

A summary of all tests conducted on Set #1 and Set #2 is given in Table IV-A-1. This table is divided into six main divisions like the listing above.

A summary list of the measurements taken for each type of test is given in Table IV-A-2. The general location of the instrumentation is also given on this table. Specific instrumentation locations will be discussed in the Instrumentation Section and Results Section .

B. INSTRUMENTATION

The measurements taken during the Head-to-Head tests included displacements, gaps, temperatures, flows, accelerations, forces, pressures, and phase. Instrumentation locations are given on Table IV-A-2. A block diagram of the overall system instrumentation is given on Fig. IV B-1 and a photograph of the recording equipment is given in Fig. IV-B-2.

Detail block diagrams of the conditioning equipment for displacement, gaps, and temperatures are given in Figs. IV-B-3, IV-B-4, and IV-B-5. Because of possible physical damage to the production displacement potentiometer, during some tests the potentiometer was secured to the vibration support stand with the stem riding on the lower piston top. This installation was used on nearly all the vertical damping tests and is shown on Fig. IV-B-6. This figure also shows some of the flat and spherical bearing gap measurement installations.

The inlet oil temperature to the capillary seal for both pistons and the return oil temperature were recorded during most of the tests. These temperature locations are shown schematically on Table IV-A-2 and

Figures IV-B-7 and IV-B-8 show the installation of T_1 (inlet to lower piston) and T_3 (return). Two flows were monitored during the testing. These flows were FL_1 (lower cylinder capillary flow) and FL_2 (upper cylinder capillary flow). Fig. IV-B-7 shows where FL_1 was installed. Notice in this Figure the proximity of the flow transducer and the temperature sensor.

Figure IV-B-9 shows the installation (on the lower flat and spherical bearing) of the vertical and lateral accelerometers used in the vertical and lateral vibration surveys. Similar installations were made on the lower piston and cylinder.

All the pressure transducer general locations are indicated on Table IV-A-2. Of particular interest are the pressures and differential pressures associated with the upper and lower cylinders (P_9, P_{10}, P_{9A}, P_{10A}, P_{9D}, P_{10D}, P_{9VEC}, P_{10VEC}). Pressures P_9 and P_{10} monitored the total lower and upper cylinder pressures respectively. In addition to the P_9 transducer a pressure gage(P_{9G}) was also installed to monitor the lower cylinder pressure (Fig. IV-B-7). P_{9A} and P_{10A} were the differential pressures obtained after nulling out the static values of P_9 and P_{10}. These differential pressures (P_{9A} and P_{10A}) were generally recorded during all the Static Piston Characteristic Tests and Vertical Damping Tests. Pressures P_{9D} and P_{10D} were the differential pressures from the Wianco Differential Transducers. These pressures (P_{9D} and P_{10D}) were used in the Static Piston Characteristic Tests on the second set of piston-cylinders and P_{9D} was used on the first set during Vertical Damping. The differential pressures P_{10VEC} and P_{9VEC} refer to the

pressures obtained with the Statham Differential Transducers. These differential pressures were used during the Vertical Damping Tests of the second set to obtain phase between the pressure and lower piston displacement. Some of the above pressure and differential pressure transducer locations are identified on Figs. IV-B-10 and IV-B-11.

The amount of damping in the system was determined, on the first set, by measuring the phase angle between the upper cylinder pressure (P_{10D}) and the lower piston displacement. The phase angle was very small and difficult to measure during the Vertical Damping Tests. The technique for measuring small phase angles was furnished by Marshall Space Flight Center (R-ASTR-F dated May 19, 1965). This technique was checked out and works extremely well under laboratory conditions. The application of this phase measurement technique in the Head-to-Head Tests was difficult. Noise in the system, for example, tended to mask the results. These problems are discussed in Section V of this report. The phase measurement instrumentation used on the first set is presented in block diagram on Fig. IV-B-12.

Several improvements in the phase measuring instrumentation were made prior to Vertical Damping Tests on the second set of piston-cylinders. The block diagram of the phase instrumentation used on the second set is given on Fig. IV-B-13 and a photograph of the conditioning equipment is given on Fig. IV-B-14. In these tests the Statham differential pressure transducers were used and the balance network used with these pressure transducers is given on Fig. IV-B-15.

tests is somewhat erratic, probably because the cylinder and piston temperatures had not fully stabilized. Data from the Static Piston Characteristics and Vertical Damping tests is more consistent, probably because the system was operated continuously for many hours during these tests, assuring temperature stabilization.

The capillary seal flow versus capillary seal length, at constant pressure, is shown in Figs. VA-5 and VA-6 for cylinders No. 2 and No. 4. This data is from static flow and piston characteristics tests at capillary seal lengths of 4, 6 and 8 in. The measured flow are compared to the theoretical flow versus seal length relationship around a 6 in. length. The high pressure curve is shown with and without correction for the theoretical gap deflection. On the low pressure curve the correction is negligible (cf. Ref (10). The effect of the theoretical gap deflection is very small and is less than the spread in the measured data. Generally, the measured data was in agreement with the flow versus length theory but was not sufficiently accurate to verify the deflection theory.

All flow data is adjusted to the equivalent flow at an average oil temperature of 105° F. This adjustment was made using the average of the measured inlet and outlet oil temperatures and finding the equivalent oil viscosity from a viscosity versus temperature curve (Fig. VA-7). The equivalent flow equals the measured flow multiplied by the oil viscosity at the average measured temperature, divided by the oil viscosity at 105° F.

The average oil temperatures measured during the tests were slightly higher than 105° F at the high bearing loads and slightly lower than

105°F at the low bearing loads. The temperature rise through the capillary was approximately 12° F at the high bearing loads.

2. Bearing Gap Test

The test objective was to verify proper hydrostatic bearing operation by measuring pressures and gaps in the flat, spherical and ring bearings. The bearing supply flow control valves were to be readjusted, if required.

The flat bearing pressures and gap versus load are shown in Fig. VA-8. The recess pressure was not measured, but it was accurately calculated from the load and the bearing geometry. The supply pressure which is the pressure between the outlet of the supply flow control valves and the inlet of the stabilizing orifices, should equal the recess pressure plus a constant pressure drop of 400 psi across the stabilizing orifices. The measured supply pressure, P_{11}, was in good agreement with the theoretical value.

The flat bearing gap was measured at two places, 90° apart, on the periphery of the bearing. The measured gap was in good agreement with the theoretical value at light loads, but at the higher loads the gap was less than expected. Subsequent tests indicated that the flat bearing gap at the 1.8×10^6 lb load was 0.002 to 0.003 in. rather than 0.004 in. Special test No. 109 was run to get additional data on the flat bearing pressures, flows and gap. This test confirmed the previous data. The pressures and flow were in good agreement with the design values, but the measured gap at the maximum load was down to approximately 0.002 in. The reason for this was not found. The lateral damping tests indicated satisfactory operation of the flat bearings, so the small measured gap was not considered a significant problem.

The spherical bearing pressure and gap versus load are shown in Fig. VA-9. The measured recess pressure was in excellent agreement with the theoretical value. The measured spherical bearing gap was in good agreement with the theoretical value at light loads, but at the higher loads the indicated gap was larger. The reason for this was not found. There were no problems with the spherical bearing in the Head to Head test.

The ring bearing recess pressures were measured and compared. The pressures were found to be in the range of 400 to 1200 psi, and within each bearing the pressures were balanced within 20% total variation. This is considered to be the acceptable operating range for recess pressures, and therefore, it was not necessary to readjust any of the supply flow control valves.

3. Bearing Redundancy and Separation Tests

The test objectives were to demonstrate bearing redundancy, which requires that the bearings operate without contact when the flow to any one flow control valve is shut off; and to demonstrate that the bearing surfaces can be separated after bearing contact.

The bearing pressures and gaps which were recorded during the redundancy and separation tests are summarized in Table VA-1, for the flat and spherical bearing tests, and in Table VA-2, for the ring bearing tests. The gap measurements are intended to show changes only and not the absolute values.

Test No. 14, Flat and Spherical Bearing Redundancy - The flat and spherical bearings were operated at a 1.8×10^6 lb bearing load. The flow to one of the two flow control valves feeding the flat bearing and to one of the two flow control valves feeding the spherical bearing was shut off. The flow to the auxiliary centering recesses in the spherical bearing was not changed.

The flat bearing gap was reduced by approximately 20%, and the flat bearing pressure, upstream of the stabilizing orifices, was reduced from approximately 2600 psi to 2400 psi. There was no evidence of bearing contact.

The spherical bearing gap was reduced by approximately 20%, and the spherical bearing pressure, in the main recess, was unchanged at approximately 2500 psi. There was no evidence of bearing contact.

The flow to the flat and spherical bearings was restored to normal and the gaps and pressures immediately returned to the values recorded prior to the flow shutoff.

Test No. 13, Flat and Spherical Bearing Separation - The flat and spherical bearings were operated at 1.8×10^6 bearing load. All flow to the flat and spherical bearings was shut off.

The flat bearing gap went to zero and the pressure upstream of the stabilizing orifices dropped to approximately 2100 psi.

The spherical bearing gap went to zero and the pressure in the main recess dropped to approximately 2400 psi.

The flow was rapidly restored to the flat and spherical bearings by opening the ball shutoff valves in the bearing supply lines. All bearing gaps and pressures immediately increased to the values recorded prior to the flow shutoff.

Test No. 15, Upper Ring Bearing Redundancy - The ring bearings were operated at a concentric load of 1.8×10^6 lb. The flow to one of the six recesses in the upper ring bearing was shut off.

The gap at the shutoff recess was reduced by approximately .003 in. and the pressure in the recesses were redistributed. There was no evidence of bearing contact.

The flow was restored to normal and the bearing gap and pressures returned to essentially the values recorded prior to the flow shutoff.

Test No. 16, Lower Ring Bearing Redundancy - The ring bearings were operated at a concentric load of 1.8×10^6 lb. The flow to one of the six recesses in the lower ring bearing was shut off.

The gap at the shutoff recess was reduced by approximately .002 in. and the pressures in the recesses were redistributed. There was no evidence of bearing contact

The flow was restored to normal, and the bearing gap and pressures returned to essentially the values recorded prior to the flow shutoff.

4. Air Spring Loss Test (Test No. 36)

The test objective was to measure the downward velocity of the piston when a simulated failure of the air spring supply has occurred and to verify that this rate did not exceed the design limit.

For this test the solenoid valve (SOV-1) which is normally used as the bailing purge valve was installed between the piston and the orifice fitting which is normally screwed directly into the piston. This arrangement closely simulated the failure condition in that the orifice discharged directly into the atmosphere. During the test a load of 1.8×10^6 lb was provided by maintaining constant pressure in the upper cylinder. The hose failure was simulated by opening the solenoid valve.

A piston velocity of .041 in/sec or 2.46 in./min was obtained (Fig. VA-10). This velocity is less than 1/10 the dynamic design load requirement and its low value is due to an error in sizing the orifice which is .080 in. in diameter. The orifice was not changed because its small size does not present an operational problem.

5. Float Refloating Test

The test objective was to demonstrate the procedure for raising and refloating a piston float after it had been sunk.

The float in cylinder No. 4 was successfully refloated, after several unsuccessful trails. The floating procedure was revised and retested several times until a workable procedure was developed.

The final refloating procedure was as follows. The lower piston was loaded so that it would not lift when the lower cylinder was pressurized up to 150 psi. In normal use, the piston will be held in the "Park" position by the test vehicle weight.

The jacking valve (ROV-1) was energized to start oil flow to the cylinder at a constant rate of approximately 6 gpm. The purge valve (ROV-6) was opened to vent gas, or oil, from the top of the piston.

When the oil level reached the bottom of the bailing tube, as indicated by the start of oil flow, the piston pressure was increased to approximately 60 psi by adding gas through pressurization valve (CV-5). The oil inflow was then adjusted by means of bleed valve (FCV-5), to maintain the piston pressure constant at approximately 100 psi. This procedure set up a constant oil flow through the piston, in under the float and out from above the float, which slowly lifted the float to the top of the piston.

When the float was raised, it contacted the bottom of the bailing tube stopping the outflow of oil. The inflow of oil was reversed by de-energizing the jacking valve, allowing the float to slowly drop and continue bailing. It was important in this operation that the piston pressure did not exceed 120 psi, otherwise the float would not release from the bailing tube.

When the oil level droppped below the bottom of the bailing tube, as indicated by the start of gas flow from the bailing hose, the jacking valve was re-energized to again raise the float. The bleed valve (FCV-5) was adjusted to increase the cylinder inflow by approximately 3 gpm in order to raise the float at approximately 1 in. per minute.

When the float again contacted the bailing tube, as indicated by stoppage of outflow, the jacking valve was immediately de-energized. It was important that the inflow be reversed immediately, otherwise oil would spill over the sides of the float and refill it.

The jacking valve was cycled to raise and lower the float for approximately 6 cycles until the quantity of oil expelled as the float dropped away from the bailing tube was near zero. Then, the purge valve was closed

and gas was added to the piston through the pressurization valve, CV-5, to drive the float down to its seat. This completed the floating procedure.

During the refloating tests, the float sunk indicating system was not operable and therefore was not used in the refloating procedure. In normal operation the float sunk indicating system will be used as a primary indicator in the refloating procedure. As the float is cycled up and down during the bailing operation, the system will be monitored to determine when the "SUNK" indication changes to "FLOAT." After this indication, the bailing will be continued for several more cycles, and then the float will be driven down to its seat to conclude the refloating procedure.

The cylinder sight glass and the float height indicator on the control panel were not used in the refloating procedure. It was found that the sight glass did not correctly indicate the piston oil level when the float was sunk. The indicated level was approximately 10 in. higher than the actual level. Because of this condition, and because of its slow response, the sight glass was not found to be useful in the refloating procedure.

A positive indication of the oil level was obtained by monitoring the flow from the bailing hose. This was monitored by a man at the cylinder and relayed to the operator at the control panel. An indication of the height of the oil level above the bottom of the bailing tube was obtained from the increase in piston pressure as the oil level increased and compressed the trapped gas volume. During the bailing

operation, the jacking valve was cycled to raise the oil level when it fell below the level of the bailing tube, and to lower the oil level when the float contacted the bailing tube, or when the piston pressure increased by 50 percent.

6. Operating Range Tests

The test objectives were to demonstrate the jacking of the piston from the park position to the 3 in. operating position at various bearing loads and spring rates, and to measure the times required.

The jacking and lowering operations at bearing loads of 0.1×10^6, 0.44 and 10^6, and 1.8×10^6 lb, and at minimum and maximum spring rates were demonstrated in the operating range tests (Nos. 64 through 69 for Set No. 1, and Nos. 28, 31 and 32 for Set No. 2), and also as a part of the setup for most of the other Head to Head tests.

The normal jacking operation takes place in two phases. First, the compression of the air spring from the piston precharge pressure to the operating pressure while the piston height is held constant in the park position. Second, the raising of the piston from the park position to the 3 in. operating height while the pressure is held constant at the operating pressure.

The flow input to the lower cylinder was set up so as to produce equilibrium at the 3 in. operating height. The test was started by energizing the jacking valve to start flow to the lower cylinder and no further adjustment was made to the lower cylinder controls. When the air spring had compressed to the operating pressure, the piston was allowed to rise at constant load. When a height of 2.8 in. was reached, the test was ended. The times required for the compression and jacking phases of the tests are shown below.

Operating Range Tests

Test No.	66	67	68	69	28	31
Load x 10^{-6} lb.	.44	.44	1.8	1.8	1.8	1.8
Spring rate	min	max	max	min	min	max
Times, minutes, compression	-	73	18	-	2.5	45
Jacking	20	37	10	10	10.3	-
Total	-	110	28	-	12.8	-

It was found that the times required for jacking at the low bearing loads and for air spring compression at the maximum spring rates were unreasonably long. A total time of 110 minutes was recorded for the 0.44 x 10^6 load at the maximum spring rate.

This shows that the jacking procedure based on not changing the cylinder supply flow or bleed flow controls during the jacking operation is unsatisfactory for all but the minimum spring rates and the higher loads.

Operation of the sight glass was monitored during the compression phase of test No. 31. As the air spring was compressed, the float height increased from 10 in. to 80 in. at an average rate of 1.55 in. per minute. The oil level in the sight glass lagged the float height by approximately 15 minutes to catch up after the float height stabilized.

7. Sink Rate Tests

The objective of the tests was to demonstrate that the pistons would lower from the 3 in. raised position to the park position in less than 1.5 min. (the period for which emergency flow is provided

to the bearings) at the maximum and minimum vehicle weight. When the pistons are lowered to the park position the oil in the cylinder is discharged through a flow control valve (FCV-9) set at 10 gpm. This assures an adequate sink rate for the light vehicle weights and the heavy vehicles come down slightly faster due to increased flow over the capillary seal.

During these tests the load was provided by pressurizing the upper cylinder. During some tests, particularly the low load test (Fig. V A-11), the pressure decreased slightly permitting the air spring to expand. The resulting float motion displaces oil which must be discharged at a constant rate through the flow control valve thus reducing the sink rate of the piston.

Test results (Figs. V A-11 and V A-12) on piston-cylinder No. 4 agree with the predicted sink rates when corrected for air spring expansion which occurred on the minimum weight condition and gave a lowering time of 60 seconds which is well below the allowable 1.5 minutes.

The test results (Figs. V A-15 through A-18) from piston-cylinder No. 2 when corrected for air spring expansion indicate that the controlled outflow of oil was 4 gpm rather than 10 gpm which gives lowering times of about 70 seconds for the maximum weight. This could have been caused by dirt in the flow control valve. On the low load ($.1 \times 10^6$ lb) tests No. 71 and 71A on piston-cylinder No. 2, the pressure fell below the desired value of 150 psi to less than 125 psi which is the lower limit of the pressure at which the flow control valve has satisfactory regulation (Figs. VA-13 and V A-14). The pressure regulation was corrected on later tests.

8. Eccentric Loading Test

The test objective was to measure the angle between the piston face and a horizontal reference under a 4-in. eccentric load of 1.8×10^6 lb.

The test was performed by displacing the stem assembly laterally relative to the piston centerline. Measurements were made relative to the two piston faces rather than relative to a true horizontal plane. It was found that test stand deflections caused the piston centerlines to tilt thus preventing meaningful measurement of the desired angle. The ring bearing recess pressures and gaps were recorded and the changes in these quantities, due to the eccentric load, were found to agree with predicted results.

9. Effective Moving Mass

It was intended to determine the vertical mass in the Head to Head configuration by measuring the pressure in the lower piston required to support the weight of both pistons, stems, and the four bearings. This method was not employed as the separate components were weighed during assembly.

It is required that the vertical mass not exceed 16,000 lb/support and that the effective moving mass of each support not exceed 5000 lb.

The vertical mass per support was determined by actual measurement to be as follows:

Piston assembly	12,400 lb.
Flat bearing assembly	590
Spherical bearing assembly	625

Stem assembly	570
Interface disc assembly (Not part of Head to Head)	829
	15,014 lb.

The effective moving mass was determined by the following equation:

Effective moving mass = horizontal mass + 1/10 vertical mass

This calculation is given below.

$$\text{Effective moving mass} = 590 + 625 + 570 + 829 + \frac{15,014}{10}$$

$$= 2614 + 1501$$

$$+ 4115 \text{ lb/support}$$

B. VIBRATION SURVEYS

The purpose of the vibration surveys were to ensure that the Hydrodynamic Supports and associated components have natural frequencies above 20 cps. In order to avoid exciting the system through the air spring resonance, and also due to the lower frequency limitation on the shaker, it was originally decided to perform the vibration surveys from 5 to 20 cps and to monitor the system accelerations and displacements at key locations on the pistons, cylinders and bearings. Measurement of system performance parameters, in terms of oil flow, oil temperature, nitrogen gas temperature and hydrostatic bearing gaps were included in the test specification (Appendix A) but were omitted when the tests were run since it was felt that they would not contribute any significant information. The vibration surveys, which were conducted in both the vertical and lateral directions at a bearing load of 1.8×10^6 lb are summarized below.

1. Vertical

The vertical vibration survey was conducted by attaching two C-5 electrodynamic shakers, each rated at 650 lb and with their output automatically controlled to be in phase, to the lower piston as shown on the schematic on Table IV A-2 (F_3 and F_4 on the side view of Head to Head test fixture). The output of accelerometers mounted on the upper and lower piston, cylinder and flat bearing and the lower cylinder spherical bearing were monitored continuously through the frequency range 5 to 20 cps and recorded at 0.5 cps increments. The seven accelerometer locations are indicated on the schematic on Table IV A-2 as A_1 through A_8. Figures V B-1 through V B-4 show the recorded peak to peak accelerations at the 7 locations. As indicated on the figures, the maximum accelerations measured were less than 0.01 g for the shaker input force of 1090-1190 lb and no resonances were found. Some of the recorded data points, particularly in the 5-10 cps range are not shown due to high noise levels at 180-240 cps. The acceleration levels in the 5-10 cps range are, however, less than in the 10-20 cps range where the same noise levels were present.

2. Lateral

The lateral vibration survey was conducted by attaching the C-5 shakers to the piston as shown on the front view of the Head to Head test fixture in Table IV A-2 (F_1 and F_2 inputs represent the two shakers). Accelerations were measured at 0.5 cps increments at 4 locations, indicated by A_1, A_2, A_3 and A_4 on Table IV A-2, with the system excited through the 5 to 20 cps range. Figures V B-5 and

V B-6 show the peak to peak accelerations recorded for the input force of 600-650 lb. As indicated on Fig. V B-5, no resonances were detected on either the piston or cylinder through the 5 to 20 cps frequency range. Figure V B-6 indicates an apparent 11 cps resonance on the flat bearing and a 16.5-17.0 cps resonance on both the flat bearing and spherical bearing. During the lateral vibration survey, the shakers were bolted to a separate structure alongside the Head to Head test fixture and this separate structure indicated an 11 cps resonance as shown on Fig. V B-7. Also, the stem connecting the upper and lower pistons in the Head to Head test stand had to be restrained from lateral motion at the 1.8×10^6 lb bearing load. This was due to the fact that the 1 cps lateral restraint springs used to center the stem could not overcome the lateral force produced by the pistons cocking relative to one another in the test stand at the high bearing load. In order to prevent the stem from moving off center, a wood block was inserted between the stem and the Head to Head test stand. This block was not rigidly attached to either the stem or test stand and therefore provided a rather sloppy connection. The A_4 accelerometer, attached to the spherical bearing, did not show the 11 cps buildup as did A_3 (Fig. V B-6) but did show a large 44 cps response (4 harmonic) at the 11 cps excitation frequency.

This nonlinearity and the 11 cps apparent resonance on the flat bearing (which could be rigid body rotation of the flat bearing) and also the 16.5-17.0 cps response on both bearings may or may not be legitimate resonances but the sloppy connection of the stem to the Head to Head test stand and the 11.0 cps shaker stand resonance make these apparent resonances suspect.

C. CYLINDER SUPPLY PANEL

1. Breadboard Tests

The hydraulic supply flow to the support cylinders is required to have a particular flow variation with cylinder pressure in order to overcome the low frequency instability problem with the capillary seal. The cylinder supply panel system is designed to produce decreasing supply flow rates with increasing cylinder pressures. The rate of change of supply flow with cylinder pressure is designated by the symbol K_Q. The flow gain, K_Q, is adjustable from zero to approximately .030 gpm per psi. The nominal cylinder supply flow is adjustable from zero to approximately 12 gpm.

The objectives of this test were to demonstrate that the cylinder supply system as designed would produce the required range of K_Q values, and to determine how the K_Q values varied with changes in

excitation frequency, excitation amplitude, pressure levels, and flow rates. The test parameters were selected to cover the full range of conditions possible in normal operation of the cylinder supply system.

The cylinder supply system is as shown in Fig. VC-1. An adjustable capillary valve (CV-1) produces the required flow variation (K_Q). A dome loaded pressure regulator (PRV-1) operates to maintain a constant oil pressure upstream of the capillary valve. A pressure compensated flow control valve (FCV-1), connected in parallel with the capillary valve, operates to provide additional supply flow at a constant flow rate.

A pressure compensated flow control valve (FCV-2), connected to the downstream side of the capillary valve, operates to provide a bleed flow at a constant flow rate.

In the test setup, the downstream side of the capillary valve was connected to a throttling valve which simulated the support cylinder pressure drop. A servo valve in parallel with the throttling valve, was driven to produce sine wave pressure oscillations of the simulated cylinder pressure. Hydraulic power was supplied by a portable hydraulic power cart having a capacity of approximately 35 gpm at 3000 psi. The hydraulic fluid was Humble Nuto 146 at a test system inlet temperature of approximately 95°F.

Test instrumentation was as shown in Fig. VC-1. Flow measurements were made by means of Rampo strain gage type dynamic flowmeters connected to a recording oscillograph. These flowmeters

were calibrated against a Buffalo positive displacement type flow-meter which in turn had been calibrated by a weight per time method using the Nuto 146 oil. Pressure measurements were by means of gages for static pressures and transducers for dynamic pressures. Temperature measurements were by means of thermocouples.

The supply system outlet flow (Q_3) and the supply system outlet pressure (P_3) were recorded simultaneously on the oscillograph while the servo valve was driven to produce sine wave variations in outlet pressure (P_3) at prescribed frequencies and amplitudes. The resulting flow gain, K_Q, was determined by dividing the peak to peak flow variation by the peak to peak pressure variation.

A series of 18 frequency response tests were run, each consisting of measuring the flow gain, K_Q, at ten frequencies in the range of 0 to 20 cps. The test conditions were selected to produce the maximum, midpoint, and minimum values of K_Q obtainable at various simulated loads, flows, and amplitudes. The various K_Q's were produced by passing 100%, 50% and 0% of the supply flow through the capillary valve (CV-1) and the balance through the supply flow control valve (FCV-1). The system outlet pressure was adjusted to simulate various loads. The supply flow was maintained constant at the level required by the maximum load, and the bleed flow (FCV-2) was increased to produce lower cylinder flows at lower simulated loads.

A series of 4 flow gain tests were run, each consisting of measuring the flow gain, K_Q, at approximately 7 settings of the

capillary valve and at three frequencies at each setting. The four tests simulate three different bearing loads.

Typical results of the frequency response tests are shown in Figs. VC-2, VC-3, and VC-4. The flow gain, K_Q, was reasonably constant with frequency from zero to one cycle per second which is the critical operating range. Above 1 cps, the high level K_Q's decreased with increasing frequency and the low level K_Q's increased with increasing frequency. These variations resulted from the decreasing ability of the pressure and flow regulating components to provide ideal regulation at increasing frequencies.

When the pressure regulator (PRV-1) permitted a variation in the pressure upstream of the capillary valve, the resulting flow gain, K_Q, was reduced as shown in tests 2C 5C and 6C. Another example of this is shown in Test No. 6B in which the pressure regulator failed to regulate properly and produced a dip in the K_Q curve. This failure was due to a damaged regulator which was later repaired.

When the supply flow control valve (FCV-1) permitted variations in the supply flow rate, the resulting flow gain, K_Q, was increased as shown in tests 2A, 5A and 6A. Also in these tests, in which all of the supply flow was through FCV-1, the phase angle between the cylinder flow, Q_3, and the cylinder pressure, P_3, shifted with frequency. In the frequency range of 0.1 to 2 cps, the flow was 60° to 120° out of phase with the pressure (flow loading). At higher frequencies the flow approached the normal in-phase relationship.

The out of phase condition makes the effective (in-phase component) K_Q approach zero, which is the desired value for this system setting. In the series "B" and "C" tests in which the capillary valve was set to produce a moderate to large K_Q, there was essentially no phase shift from the normal. The normal relationship is for the minimum flow to be in phase with the maximum pressure.

During the early breadboard tests, it was found that the supply flow control valve (FCV-1) had poor frequency response in the viscous oil. The valve was reworked by increasing the size of several damping orifices and increasing the spool clearance. This substantially improved the frequency response. Also during the tests, there were two failures of the pressure regulator (PRV-1). The regulators were reworked by adding holes in the valve body to make the pressure loading on the diaphragm symmetrical. After the rework, no further difficulty was experienced with the regulators. See Development Test Report ER 14037, Ref. (12) for details of the rework of the pressure regulator and flow control valve.

The results of the flow gain tests are shown in Figs. VC-5, VC-6, VC-7 and VC-8 which compare the dynamic K_Q values with the theoretical static value. The static value was determined by measuring the capillary valve flow versus setting at a constant pressure drop of 300 psi, and calculating the K_Q as the flow divided by the pressure drop. In the tests simulating the maximum vehicle weight (Figs. VC-5 and VC-6) and the medium vehicle weight (Fig. VC-7), the dynamic K_Q's were in reasonably

good agreement with the theoretical static valves within the significant K_Q range of 0 to .025 gpm per psi. In the test simulating the low vehicle weight (1.76×10^6 lb), (Fig. VC-8), the dynamic K_Q's were substantially higher than the static values. The reason for this was not apparent.

The data from all of the breadboard tests shows considerable scatter. This can be accounted for by the many inaccuracies inherent in the test setup and instrumentation. The oil temperature was not well controlled and stabilized, since this had to be done manually. Temperature variations affect the generated K_Q's by approximately 3% per ^{o}F. The sine waves produced by the servo valve were far from perfect. The system inlet pressure (P_1) did not stay constant at large flow variations. The flowmeter calibration was very sensitive to oil temperature. The quantities being measured were small changes in large values. These factors, plus the normal inaccuracies in the instrumentation, indicate that the test results may be up to 25% in error.

From the breadboard tests, it was concluded that the cylinder supply system was capable of generating the required range of flow gains, and that the system frequency response was reasonably flat in the critical operating range. It was also concluded that the generated K_Q's could be related to the static calibration of the capillary valve. It was decided that additional K_Q tests would be run during the Head to Head tests to get additional data using the production version of the cylinder supply panel and using the production hydraulic supply system.

2. Component Tests

The objective of test No. 100 was to determine the in-place static calibration of the capillary valve, CV-1, and the associated plumbing. The cylinder supply line was disconnected at the cylinder and was connected to a throttling valve and a positive displacement flowmeter. The supply and bleed flow control valves were set for zero flow. The pressure regulator and the throttling valve were set to produce a constant 300 psi pressure drop from the upstream side of the capillary valve to the downstream end of the cylinder supply line. At various settings of the capillary valve, the resultant flow was measured. The predicted flow gain, K_Q, for the combined capillary valve and cylinder supply line was calculated by dividing the measured flow by 300 psi. The results of this test are shown in Fig. VC-9.

The objective of test No. 101 was to measure the flow resistance of the cylinder supply line from the downstream side of the capillary valve to the cylinder connection. In the Head to Head test setup this line contained a dynamic flowmeter and various fittings which were expected to have a significance resistance.

The results of this test showed that the resistance of the cylinder supply line, downstream of the capillary valve, was 10 psi per gpm in the range of 0 to 10 gpm.

3. System K_Q Test

The objective of this test was to measure the flow gain, K_Q, generated by the production version of the cylinder supply panel and to relate the flow gain to the setting of the capillary valve.

For this test the outlet of the lower cylinder supply panel was disconnected from the cylinder inlet and was connected through a throttling valve to the return line. A servo valve was connected in parallel with the throttling valve and was driven to produce sine wave oscillations of the simulated cylinder pressure. This part of the setup was the same as for the breadboard tests (see Fig. VC-1). The simulated cylinder flow, FL_1, and simulated cylinder pressure, P_9, were recorded simultaneously on the oscillograph, and the K_Q value was calculated in the same manner as for the breadboard tests (see Para. V C-1).

The results of the first set of K_Q tests, Nos. 6 through 11, were not meaningful due to an error in the test operation. The K_Q tests were rerun as special test No. 102. In this test, the capillary valve was tested at eight different settings. At each setting the pressures and flows were set to simulate the 1.8×10^6 lb bearing load, and the cylinder pressure was oscillated at three frequencies, 0.05, 0.2 and 1.0 cps, and at three amplitudes at the high frequency. The hydraulic power unit was operated at the pressures and oil temperature associated with the 1.8×10^6 lb bearing load.

The results of test No. 102 are shown in Fig. VC-9 as a plot of the generated K_Q versus the capillary valve setting. Also plotted in this figure are the predicted K_Q's from the static in place calibration of the capillary valve, test No. 100. These results show that the generated K_Q's are in good agreement with the predicted K_Q's in the range of 0.003 to 0.025 gpm/psi. Values beyond this

range are not significant. The generated K_Q's were reasonably constant with frequency and amplitude variations.

4. Cylinder Supply Panel Test Summary

Figure VC-9 shows good agreement between K_Q determined by static in place calibration of the capillary panel and K_Q measured at various frequencies in test No. 102. In test No. 101 the resistance of the line between the capillary valve and the cylinder was measured making it possible to relate the bench calibration of the capillary valve to the in-place calibration. Figure VC-10 shows that the computed K_Q curve versus the laboratory calibration of the prototype capillary valve is in good agreement. The laboratory calibration of the prototype valve gives points that fall on a very smooth curve which tends to further substantiate the data. The production valves were made to the same drawing (88A4100483) as the prototype. The drawing tolerances are very small on critical dimensions so that the prototype calibration can be used for all valves.

D. STATIC PISTON CHARACTERISTICS TESTS

The purposes of the static piston characteristics tests were to determine the Hydrodynamic Support static stiffness by measuring the piston displacement-piston load relationship and also to determine the gas spring rate by measuring the float displacement-piston load relationship. This latter objective was not accomplished, however, due to operational difficulties with the float height indicator. A discussion of the problem is given in Ref. (12).

The Hydrodynamic Support static stiffness is important, in conjunction with the characteristics of the lateral restraint system to be employed in the Saturn V testing, in determining the static stability of the vehicle. As indicated by the theory (Ref. 10), the static stiffness of the support is uniquely determined by the bearing load, capillary seal length and input flow gain (K_Q), for a given piston-cylinder geometry and oil temperature. It was therefore decided that tests would be conducted to determine the static stiffness of two of the supports under various conditions of the three parameters-bearing load, seal length and K_Q at the design operating temperature of 95° F at the pump inlet.

Briefly, the procedure for performing these tests was to establish a bearing load at a given capillary seal length, temperature and input flow gain (capillary restrictor valve setting CV-1), for the lower piston-cylinder in the Head to Head setup and then to vary the lower piston displacement using the upper piston as an actuator. The displacements were varied in increments up to ± 1 in. about the original capillary seal length (positive direction is up) and held at each increment for a sufficient time to allow the pressure and displacements to come to equilibrium, at which time the data were recorded. Repeat tests were necessary in some cases due to too much scatter in the data, probably caused as a result of taking the data too fast, that is, not simulating static conditions. Since the static and dynamic spring rates can be widely different depending upon the input flow gain, care had to be taken in performing the static piston characteristic tests to ensure that the data would be representative of static conditions.

Of particular interest from the tests performed, are the cylinder inlet oil flow rate variations with cylinder pressure and the cylinder pressure variations with piston displacement. From the first, the actual input flow gain (K_Q) that was attained during the test can be determined and compared with the expected value based on the relationship between the capillary restrictor vavle (CV-1) setting and the input flow gain established during the cylinder supply panel calibrations (tests Nos. 100 and 102). From the cylinder pressure variations with piston displacement the static stiffness can be determined and compared with the theory at the input flow gain attained during the test. Excluding repeats, there were 10 tests performed on piston-cylinder No. 2, and 6 tests performed on piston-cylinder No. 4. A summary of the static stiffnesses and input flow gains determined from the data of the original test or of at least one repeat test is shown below.

Summary of Static Piston Characteristic Tests

Test Number	Test Conditions: Piston-Cylinder Tested	Bearing Load (10^6 lb)	Capillary Seal Length (inch)	CV-1 Setting (turns open)	Results: K_Q Input Flow gain (gpm/psi)	K Static Stiffness (lb/in.)
41.5	2	1.8	6	0	-.00055	480,000
39-B	2	1.8	6	2.95	.0094	120,400
40-A	2	1.8	6	3.75	.0155	73,140
41	2	1.8	6	4.65	.0204	56,620
41-A	2	1.8	6	4.65	.0219	55,680
57A	2	1.8	4	2.50	.0061	385,800
53	2	1.8	4	5.40	.0294	91,960
56-A	2	1.8	8	3.65	.0167	46,240
45	2	0.44	6	4.66	.0215	12,840
46	2	0.44	6	2.95	.0157	20,100
47	2	0.44	6	3.75	.0163	16,550
18-A	4	1.8	6	3.20	.0152	62,890
19	4	1.8	6	4.00	.0120	51,750
24	4	1.8	4	4.50	.0155	85,630
27	4	1.8	8	3.60	.0148	42,710
20	4	0.44	6	3.20	.0166	11,020
21	4	0.44	6	4.00	.0205	8,890

As indicated in the summary above, test results are presented for two of the piston-cylinders for variations in the three parameters: bearing load, capillary seal length, and input flow gain (indicated by the CV-1 setting). The static stiffnesses shown are seen to decrease with increasing input flow gain for the first four tests which are at a constant bearing load and seal length. This relationship, which is substantiated by the theory, is evident for all sets of tests in which the only parameter varied was input flow gain.

The curves of input oil flow rate versus cylinder pressure and cylinder pressure versus piston displacement from which the above results were obtained, are shown on Figs. VD-1 through VD-34. From these curves the static stiffness is obtained as the slope of the pressure-displacement curve times the cylinder internal cross-sectional area (755 $in.^2$) and the input flow gain is obtained as the slope of the flow rate-pressure curve. In all cases, these slopes were obtained from a least squares linear fit to the data.

As indicated on Figs. VD-1 through VD-34, the data generally appears to follow this linear fit. The oil temperature variation during each test are indicated on the figures and can explain some of the scatter in the data. Figures VD-11 and VD-28 show the results of a test in which wide variations in temperature occurred. On the pressure-displacement curve (Fig. VD-28) the data indicates an apparent zero stiffness for the first three data points. However, Fig. VD-11 shows that this is due to the flow decreasing at constant pressure due to the large decreases in temperature. That is, as the

oil temperature is decreased, the flow rate required to maintain constant pressure decreases. For capillary flow, the capillary seal length is inversely proportional to the product of the flow rate and the viscosity at constant pressure and capillary gap; that is,

$$\ell = \frac{c}{Q\mu}$$

From VD-11, the flow rate changes from 2.6 gpm at 110°F to 1.6 gpm at 100° F while the pressure remains constant. One would therefore expect that a change in seal length of:

$$\Delta \ell = \ell_o \left(\frac{Q\mu}{Q\mu_o} - 1 \right) \qquad = -.87 \text{ in.}$$

would occur, where the subscript "o" refers to the initial conditions ℓ_o = 6", Q_o = 2.6 gpm, T_o = 110° F and the subscript "f" refers to the condition of Q_f = 1.6 gpm, T_f = 100° F. As seen from Fig. VD-28, the piston did, in fact, displace -.95 in. at constant pressure. Therefore, the first two data points, over which the temperature changed from 110° to 100° F, should not be used and only the last four data points, over which the temperature remained constant, should be used in the data interpretation.

In order to substantiate the theory regarding the independence of the static stiffness on the gas spring rate, several of the static piston characteristic tests were performed with a minimum gas spring rate and then repeated with the float locked on the seat in the piston. In the latter configuration, the gas is isolated and cannot contribute to the piston deflection. The comparison of test No. 41, which was done with a minimum gas spring rate, and test No. 41-A, which was

with the float locked, indicates that the gas spring rate does not affect the static stiffness.

From the input flow gains obtained from the test data (Figs. VD-1 through 17) and the capillary restrictor valve settings for each of the Static Piston Characteristic tests, a curve can be drawn of input flow gain versus capillary valve settings similar to the static calibration of the cylinder supply panel (test No. 100). Figure VD-35 shows such a curve, where the dotted line is drawn through the data obtained from the Static Piston Characteristic tests and the solid line was obtained from a separate static calibration of the cylinder supply panel (test No. 100). The dotted line fits all but 5 of the data points within 10%, but is higher than the data from test No. 100. Differences in temperature from test to test as well as temperature variations during the Static Piston Characterisc tests may account for the scatter in the data as well as the difference between the two curves shown.

E. DAMPING

1. Head to Head

a. Lateral

The purpose of the lateral damping test was to determine the magnitude of the lateral dashpot constant under bearing loads of 0.44×10^6 lb and 1.8×10^6 lb.

The combined stem, spherical bearing, and flat bearing can normally be moved freely on top of the piston surface. Because of this negligible horizontal spring rate, it was necessary for the Head to

Head tests that the stem be put between two springs to provide an oscillating system from which the viscous damping could be measured. The damping due to the viscous shear of the oil between the flat bearing and the piston top was expected to be very small. The extraneous effects due to springs, roller bearings, and other contributors was expected to add an unknown amount of damping, possibly of the same order of magnitude as that being investigated.

Because of the unknown amount of damping in the springs, it was decided to use two different sets of springs in the testing. After excitation, the springs provided a decaying free oscillation from which the logarithmic decrement was determined and hence the damping coefficient.

The system was excited by displacing the centering block in the lateral direction by hand excitation when the soft (1 cps) springs were installed and by a loading jack when the hard (5 cps) springs were installed. It was intended to do both bearing loads with both sets of springs, however, it was impossible to obtain high bearing load lateral damping with the soft springs installed. The reason for this was that the free oscillation frequencies decreased with increasing bearing load up to some critical load beyond which the stem became statically unstable. The critical bearing load for this condition was about 1×10^6 lb and the instability was caused by test stand deflection inducing a force on the stem that the soft springs could not overcome. The stiff springs did not allow this instability. In addition to the North-South spring restraint the stem was restrained

from moving in the East-West direction by channels attached to the test stand. Rollers between the stem and the channel permitted the stem to move with spring compression but prevented the stem from moving normal to the centerline of the two springs.

Four lateral damping tests were conducted on the first set of piston-cylinders and two on the second set. Generally three trials were made at each test condition. The 1 cps springs were used on the first set of piston-cylinders and the 5 cps springs on the second set. A summary of the six tests is given below.

Summary of Lateral Damping Tests

Test Condition				Results	
Test No.	Piston Cylinders Tested	Bearing Load (10^6 lb)	Centering Spring Frequency	C for Both Pistons lb sec/in	C per Support lb sec/in.
108	1	None	1 cps	3.0	1.5
108	1	0.1	1 cps	3.3	1.65
108	1	0.44	1 cps	5.2	2.6
108A	1	0.75	1 cps	5.3	2.65
38	2	0.44	5 cps	6.2 and 6.07	3.1 and 3.03
39	2	1.8	5 cps	7.15	3.57

Figures V E-1 through V E-4 give the results for tests on the first set. Figures V E-5 and -6 give the results of damping on the second set. These curves show the viscous damping to be independent of amplitude.

Figure V E-7 gives a plot of the damping coefficient per piston versus bearing load in relation to the maximum allowable specification

levels. Both damping coefficients measured at the 0.44×10^6 and 1.8×10^6 lb bearing loads are slightly over the maximum specification levels. For the tests done with the 1 cps spring a cable was attached to the stem from about a 40 ft distance with about 100 lb to relieve the stem roller bearing load on the channels that restrict movement from the centerline of the springs. This was not done for the tests with the 5 cps springs installed. The only comparison between the damping with the different springs is shown at the 0.44×10^6 bearing load. The 0.5 lb sec/in. difference between the damping coefficients measured with the two springs could be due to:

(1) Differences in damping contributed by the springs;

(2) Differences in oil temperature between the two tests;

(3) Variations between the two piston-cylinders in flow control valves and orifices feeding oil to the flat bearing thereby causing different gaps between the piston and flat bearing.

If the differences are due to the damping contributed by the springs, then the damping at the 1.8×10^6 bearing load would be within specification if it could have been done with the 1 cps springs.

b. Vertical

The purpose of the vertical damping tests was to measure the total vertical damping of the Hydrodynamic Support to ensure that the support damping would be less than the maximum positive values specified between 0.5 and 1.0 cps and above 1.0 cps and also to ensure that it would be non-negative at all frequencies.

As indicated by the theory (Ref.(10)), the total support damping can be considered to be the sum of a viscous damping and a flow damping. The viscous damping, which is due to the laminar shear forces on the piston in the capillary seal and ring bearing areas, is a function of the capillary seal length and bearing load for a given piston-cylinder and oil temperature. The bearing load affects the capillary seal gap and ring bearing gap while the oil temperature controls the viscosity of the oil. The flow damping, which is due to the cylinder input and capillary seal oil flows, is primarily a function of the bearing load, capillary seal length, gas volume, excitation frequency and input flow gain and can be either positive or negative. The total support damping can therefore be either positive or negative depending upon the relative magnitudes of the viscous and flow damping. For a given configuration, that is, a particular piston-cylinder, bearing load, capillary seal length, gas spring rate and oil temperature, the total support damping is adjustable at all frequencies within varying limits by changing the input flow gain. Equation V E(1) below gives the total damping (from Ref. (10)) as a function of the dynamic stiffness, K_p (which is a function of bearing load and gas volume) and of frequency:

$$\bar{C} = \frac{K_p\left(\frac{1}{\tau_2} - \frac{1}{\tau_1}\right)}{\omega^2 + \frac{1}{\tau_2^2}} + C_p \qquad \text{VE-(1)}$$

where τ_1 and τ_2 are time constants and C_p is the viscous damping.

Since the total vertical damping is dependent on so many parameters, it was decided that testing would be limited to determining the vertical damping under various conditions of bearing load, frequency and input flow gain while maintaining a capillary seal length of 6 in., a minimum gas spring rate and the operating oil temperature. It was originally anticipated that a gas spring could be obtained in the inverted piston in the Head to Head configuration thus providing a mass (the two pistons) between two springs (the upper and lower piston gas springs) that could be excited with a shaker both on and off resonance. At resonance the total damping would be primarily the viscous damping of both piston-cylinders since the flow damping, which is inversely proportional to the square of the frequency, would be essentially nonexistent. Therefore, the total damping could have been determined by cutting the shaker off and measuring the free oscillation decay rate. Below resonance the total damping was to be determined by measuring the phase angle between the shaker force and the piston displacement. However, it was found that a gas spring could not be obtained in the upper piston thereby eliminating this method of determining the total vertical damping.

The method of determining the total damping that was then decided upon was to fill the inverted piston-cylinder with oil, attach a servo valve to its inlet oil line and to oscillate the input oil flow, thereby using the upper piston as a means of excitation. The flow damping of the lower cylinder plus the viscous damping of both piston-cylinders could then be obtained at any frequency by measuring

the phase between the excitation (the upper piston pressure) and the displacement. This procedure was used to determine the damping for the first set of piston-cylinders installed in the Head to Head configuration. For the first set, which had piston-cylinder #1 in the upper (inverted) position and #2 in the lower position, 15 damping tests were conducted. Of these, 8 were done at the 1.8×10^6 lb bearing load, 4 at the 0.44×10^6 lb bearing load and 3 at the 0.10×10^6 lb bearing load. From the measured phase angles the lower cylinder flow damping (C_{f_2}) plus the upper and lower cylinder viscous damping (C_{V_1} and C_{V_2}) was determined from:

$$\tan\phi_1 = \frac{(C_{f_2} + C_{V_1} + C_{V_2})}{K_2 - m\omega^2}$$

where K_2 is the stiffness of the lower system.

The results of the tests on the first set of piston-cylinders at the 1.8×10^6 lb bearing load, 0.5 cps are shown on Fig. V E-8 as a function of the input flow gain. The phase angles were measured using the technique shown on Fig. IV B-12 and the total damping was calculated from these phase angles using the above equation. The average dynamic stiffness from the four tests, which is needed to calculate the damping from the phase angle, is indicated on the figure and was determined from the lower cylinder pressure and displacement oscillations. Also shown on Fig. V E-8 is the theoretical damping curve for comparison with those determined from the measured phase angles. As indicated by the comparison, the test results are

significantly higher than the theoretical values in most instances. There are several reasons, some of which were not really evaluated until after the 15 tests, that tend to make the test results suspect. These are listed below:

(1) Insufficient electronic filtering of the signals in the phase measurement. The filtering used, which is shown on Fig. IV B-12, was an SKL filter on the pressure signal. In order to avoid low frequency phase shifting of the pressure signal, the filter cutoff frequency had to be set high and consequently did not sufficiently filter the 60 cycle noise that was present. Also, the SKL filter used was found to have some internal noise that affected the measurements.

(2) Carrier amplifier noise. Since Wianco pressure transducers were used in the first 15 damping tests, carrier amplifiers were needed. The carrier frequency proved to be a source of interference in making the phase measurements.

(3) Non-sinusoidal excitation. The servo valve which was used to oscillate the flow in the upper piston to provide excitation for the lower piston generally produced a non-sinusoidal wave form (in some cases practically a triangular waveform). Since the flow damping is frequency dependent, the resulting phase measurement from the non-sinusoidal excitation represented some weighted average of the damping values at each frequency component of the excitation. The

servo valve produced this non-sinusoidal wave form due to clogging of the servo valve filter and also due to poor location of the servo valve and its pressure regulator relative to the upper cylinder inlet.

Due to the inconsistency of the test data with the theory it was obvious that the above problems would have to be corrected in order to obtain meaningful data. It was therefore decided that while better instrumentation was being installed for the phase measurement, a change-over to piston-cylinders Nos. 3 and 4 would be made in the Head to Head test stand and that a comprehensive set of vertical damping tests would then be performed on this set. Figure IV B-13 shows a schematic of the phase measuring circuit that was finally decided upon, which includes: better filtering, better filter location (filtering after the two signals are added) and strain gage pressure instruments which do not need the previously used carrier amplifier system. During the change-over to piston-cylinders Nos. 3 and 4, the servo valve and pressure regulator were moved closer to the upper cylinder inlet in order to provide a better flow oscillation wave form.

With the above changes in the phase measuring system and excitation, testing was begun on piston-cylinders Nos. 3 and 4 to determine the total vertical damping (lower cylinder flow damping plus upper and lower cylinder viscous damping). As was done on the first set of piston-cylinders, the total damping was to be determined from the phase angle between the upper cylinder pressure and the piston displacement. When these damping tests were begun it was discovered

that the upper cylinder pressure exhibited a waveform similar to the displacement but with a square wave superimposed. Figure V E-9 shows the upper cylinder pressure and piston displacement time histories from a typical test during which this phenomena was present. Since the phase measuring technique used in these tests is only applicable to signals that have identical waveforms, it is obvious that the "clipping" on the upper cylinder pressure would make the phase measurements difficult to interpret. The clipping on the pressure signal was believed to be due to some physical interference within the lower piston-cylinder (No. 4)--a possibility that was also discovered in some separate tests of this piston-cylinder prior to its installation in the Head to Head test fixture. The results of the vertical damping tests performed with this clipping present again proved to be higher than the theory, but in view of the apparent interference problem, this is not surprising.

Since it was felt that the interference problem was peculiar to piston-cylinder No. 4 and not the others, and in order to avoid immediate removal of the Nos. 3 and 4 setsfrom the test fixture to fix the problem, testing was continued in order to obtain data on at least the flow damping. By measuring the phase angle between the lower cylinder pressure and piston displacement the viscous damping of the two piston-cylinders plus the extraneous damping due to the apparent interference problem would be avoided and only the lower cylinder flow damping would be obtained. Separate tests on the individual piston-cylinders could be performed after removal from the Head to Head test stand to determine the viscous damping. The total damping (assuming a fix on

the apparent interference problem could be made) would then be the sum of the flow damping obtained during tests in the Head to Head configuration plus the viscous damping from the side tests. Using this approach, 30 tests were conducted to determine the flow damping under various conditions of bearing load, frequency and input flow gain. At the 1.8×10^6 lb and 0.44×10^6 lb bearing loads, the flow damping was determined for several input flow gains at each of 4 frequencies. For the 0.10×10^6 lb bearing load, the damping was determined for one input flow gain at each of 4 frequencies.

Of the 30 tests performed, the results of 13 are shown on Figs. V E-10 through V E-15 as flow damping (obtained from the measured phase angles between the lower cylinder pressure and the piston displacement) versus input flow gain. On these figures are also shown the theoretical flow damping curves obtained from Ref. (10), which is the same as equation V E-(1) and assumes adiabatic behavior of the nitrogen gas, and the theoretical flow damping including the nitrogen gas dynamics, which is a modification of Ref. (10) using the analysis of Ref. (11). At each bearing load, the theoretical curves were evaluated for the conditions of: 6 in. capillary seal length, .007 in. capillary gap, and the average dynamic stiffness from the tests at each frequency. As indicated by the curves, the flow damping calculated from the measured phase angles follows the theoretical curves. Deviations between the data points and the theoretical curves shown could be due to the fact that the capillary gap is less than the .007 in. used for the theoretical curves.

Figures V E-13, E-14 and E-15, which are the only cases shown where the nitrogen gas dynamics appreciably modify the original theory of Ref. (10), indicates that the modified theory may be slightly conservative.

The remainder of the 30 flow damping tests on piston-cylinder No. 4 were done at the high bearing load, high frequency (1.8×10^6 lb, 1.0 cps) and the lighter bearing loads (0.44×10^6 and 0.10×10^6 lb) above 0.1 cps. These tests, which were all done using a 10 psi Statham pressure transducer for the pressure signal in the phase measurement, all gave damping values that were lower than expected. In fact, the phase angles measured appeared to be lower than the theory in an increasing manner with frequency indicating that the pressure transducer and/or the hydraulic lines used to connect it to the cylinder were introducing a phase lag and therefore giving indicated flow damping values that were too low. Figure V E-16 shows the layout of the hydraulic lines, accumulator and pressure transducer setup which was connected to the piston-cylinder in the Head to Head damping tests. In order to determine whether any phase lag was being introduced by the pressure transducer and/or the hydraulic lines, this whole assembly was removed from the Head to Head setup and separate tests were performed on it. These tests consisted of measuring pressure signals with two transducers (side by side) installed in the hydraulic lines as during the Head to Head tests, and the phase between them recorded at several frequencies. One of the transducers was then moved to a location near the excitation (which was provided by a mechanical piston oscillating the flow in the

lines) and the test was repeated. The difference between the phase lags from the two tests is the true phase lag between the excitation (which is simulating the cylinder pressure in the Head to Head tests) and the pressure transducer. The results of the tests indicated the following:

(1) The pressure transducer and/or the associated hydraulic lines used to connect the transducer to the piston-cylinder in the Head to Head test did introduce a phase lag.

(2) The phase lag increases with frequency.

(3) The magnitude of the phase lag measured depended upon how well the hydraulic lines, accumulators, etc. were tied down (vibrations of the lines affected the phase lag).

(4) The magnitude of the measured phase lag at 1.0 cps was on the order of 0.7 to 2.0 degrees (high enough to explain the difference between the measured and theoretical damping in the Head to Head tests).

Based on the above, it is concluded that the only good data from the 60 tests performed on piston-cylinders Nos. 2 and 4 are the 13 previously mentioned tests on Cylinder No. 4 (Figs. V E-10 through V E-15) and that these data generally agree well with the theory. In the cases where the theory predicts an appreciable influence due to the nitrogen gas dynamics, the agreement is not as good as those cases where the theoretical effect is small. Since this test data agrees well with theoretical flow damping versus K_Q curves shown on Figs. V E-10-E-15, then it is also inversely proportional to frequency

as indicated by equation V E-(1). At higher frequencies (above 1.0 cps) the total damping will therefore be primarily due to the viscous damping as indicated in Ref. (10).

Having substantiated the theory regarding the flow damping, the total system damping can be considered to be the sum of the flow damping and the viscous damping which, as previously mentioned, can be evaluated from separate tests on the piston-cylinders.

2. Unit Tests - Vertical and Rotational

The separate tests that were conducted on the piston-cylinders to determine the viscous damping consisted of two types: vertical oscillation of the piston in the cylinder, and rotation of the piston in the cylinder. In both cases, the particular piston-cylinder being tested was removed from the Head to Head test fixture as shown in Fig. V E-17. A gas spring rate was established at a gas pressure and input oil flow rate sufficient to support the weight of the piston in the cylinder. (This operation is identical to that used in the Head to Head tests except that now the bearing load is merely the piston weight.) For the vertical oscillation tests, the piston was oscillated in the cylinder at the resonance of the piston mass on the gas spring (approximately 0.8 cps), and the damping was determined from the free oscillation decay rate of the piston. For the rotational tests, the piston was rotated in the cylinder (no vertical motion) and the damping was determined from the exponential decay rate following release of the piston. In both types of test the damping should be due to the viscous shear of the oil flow in the capillary seal and ring bearing

areas and, disregarding secondary effects, should be identical. Figure V E-18 shows the results of the vertical oscillation and rotational tests performed on piston-cylinder No. 4, the one which exhibited the apparent interference problem in the Head to Head damping tests. For this particular piston-cylinder the separate vertical and rotational tests were done prior to installation in the Head to Head test fixture. As indicated on Fig. V E-18, the damping obtained from the vertical oscillation tests is approximately 50% higher than that obtained from the rotational tests. It was noted during these tests that the accelerometer signal which was recorded and used to determine the damping exhibited the same "clipped" waveform as was noted on the upper cylinder pressure signal during the Head to Head damping tests. After completion of the vertical and rotational damping tests and the Head to Head damping tests on this piston-cylinder, the piston and float were removed from the cylinder and inspected. Figure V E-19, which is a photograph of the float from piston No. 4, shows that the float was rubbing on the piston, as evidenced by the scratch marks. Measurements made of the float diameter indicated that it was out of tolerance by .022 in, enough to interfere with the piston. This float was subsequently remachined to be within the specified dimensions, and piston-cylinder No. 5 was substituted for No. 4 for the Saturn V support. Cylinder No. 4 is presently planned to be used as a spare.

Figure V E-20 shows the vertical and rotational damping obtained from separate tests on piston-cylinder No. 2. These results also show

that the damping determined from the vertical tests is significantly higher than that obtained from the rotational tests. For this piston-cylinder, vertical and rotational tests were done with and without the float in the piston. As indicated, the damping curves shown with and without the float are slightly different but the difference between them is within the scatter of the data. The float for piston No. 2 was inspected and no indication of float-piston interference was found. It was therefore concluded that, since the results with and without the float were essentially the same, the float was not responsible for the difference between the damping obtained from the vertical and rotational tests.

Figures V E-21 and 22 show the results of the separate damping tests on piston-cylinders Nos. 3 and 5, and again it is evident that the damping obtained from the vertical tests is higher than that from the rotational tests. For piston-cylinder No. 3 several tests were done in an effort to determine the effect of temperature and piston pressure on the damping. According to the theory the viscous damping should be proportional to the oil viscosity, whose temperature dependence is shown on Fig. V A-7. For the vertical damping curves of Fig. V E-21 at 124°F and 110°F the average ratio of the damping values is 0.75. From Fig. V A-7, the viscosity ratio at 124°F and 110°F is 0.65 indicating that the vertical damping does not decrease as much as the viscosity ratio would indicate. Similarly, for the rotational damping on piston-cylinder No. 3 the average damping ratio at 123°F and 110°F is 0.83 while the viscosity ratio indicates that it should be 0.68. To determine the effect of piston pressure on the vertical and rotational damping, tests were done with two piston pressures. In the

first case, the nitrogen gas pressure was 17 psig, just enough to support the weight of the piston and provide 0.8 cps gas spring at the maximum gas volume. In the second case the piston was pressurized to 2400 psig above the float with low volume, 17 psig gas spring below the float. The 2400 psig piston pressure and 17 psig cylinder pressure should have made the capillary seal gap smaller than in the tests where the piston and cylinder pressures were 17 psig. With a smaller capillary gap the damping would have been higher, however, inspection of Fig. V E-21 shows that for the vertical tests the damping decreased approximately 12 lb-sec/in. between the 17 psig piston pressure test and the 2400 psig piston pressure test while for the rotational damping tests the damping remained the same for both piston pressures. Since pure rotation of the piston in the cylinder does not involve gas volume oscillations, the rotational damping tests are essentially independent of the gas and would therefore not be expected to differ between the tests run with the gas above and below the float. In the vertical oscillation tests the gas dynamics can contribute to the damping as indicated in Ref. (11) depending primarily upon the gas pressure, frequency and the coefficient of the heat transferred from the gas. Although estimates of the effect using the analysis of Ref. (11) amount to only 2.0 lb-sec/in. for the vertical oscillation tests with the gas above the float, this estimate is proportional to an experimental heat transfer coefficient obtained from Ref. (11). Figure V E-23 summarizes some of the test results shown on Figs. V E-18, 20, 21 and 22, and compares the test results with the theoretical viscous damping. As indicated, the results from the rotational damping tests are in good agreement with the theory. The vertical damping results are, as previously mentioned, significantly higher than expected.

F. MISCELLANEOUS TESTING

1. Ovality Check

During the vertical damping tests on the second set of piston-cylinders there was intermittent indication of some physical interference within one of the two piston-cylinder combinations. It was decided to check for physical interference by performing an ovality test of piston-cylinder No. 3 (as a separate unit) and to disassemble No. 4 for inspection.

The No. 3 piston-cylinder was set out on the floor after the Head to Head tests and a six-inch capillary seal length established with a 17 psi air spring in the piston. Four dial gages were attached to the top of the cylinder at 90° to each other such that the dial plunger rested against the side of the piston. The two gap sensors (G_1 and G_2) used in the Head to Head test were also installed again at the top right and bottom left of the cylinder. The cylinder was marked off in 30° increments, then the piston was rotated relative to the cylinder and stopped at every 30° mark and data recorded from all sensing devices. The piston was concentric within the drawing tolerance (.002 TIR).

2. Temperature Time Histories

The gaps between the piston and cylinder are influenced by the relative piston and cylinder temperatures which in turn are a function of the ambient air temperatures. If the cylinder heaters are left off and the ambient temperature is less than the normal operating oil temperature of about 110°F then the cylinder does not expand as much as the piston, thus decreasing the gap between the piston and cylinder.

Most of the Head to Head tests were conducted with the cylinder heaters on, thus the cylinder and piston could be kept near the same temperature.

The temperature difference between the piston and cylinder and also the elapsed time for temperature stabilization was checked with the cylinder heaters turned off. This check was made on the morning of 9-23-65 when the ambient temperature was about 75°.

One temperature sensor was placed on the piston side near the top and the other was placed on the outside of the cylinder near the upper ring bearing. After completing a Static Piston Characteristic Test the cylinder heaters were turned off and about 3 hours lapsed before the temperature test was run. The two temperatures were monitored every 5 minutes for 3-1/2 hours. Both piston and cylinder started out at 92°F. At the end of the 3-1/2 hours the piston was at 113° and the cylinder was at 106°. The piston-cylinder temperatures stabilized at about 113° (piston) and 107° (cylinder). The temperatures read at 5 minute intervals are given on Table V F-1.

VI. CONCLUSIONS

Based on the tests performed on the Hydrodynamic Support in the Head to Head configuration it is concluded that, in general, the system and components function as designed and that the measured performance parameters are in good agreement with the theory (where comparisons are made) with few exceptions.

From the Design Assurance Tests several conclusions were drawn. Some of these are listed below:

(1) The capillary seal gaps are slightly smaller than anticipated.

(2) The flat and spherical bearing gaps are in good agreement with the theory at the light bearing loads. At the high bearing loads the flat bearing gap is 0.001 to 0.002 in. less than anticipated while the spherical bearing gap is higher than the theoretical value.

(3) The flat and spherical bearings operate without contact when flow to one of the bearing flow control valves is shut off. The bearing gaps and pressures return immediately to their normal values when the flow is resumed.

(4) There was no evidence of piston-cylinder contact when flow to one of the ring bearing recesses was shut off. The gaps and pressures reutrn to essentially the normal values when flow was resumed.

(5) The piston sink rate due to an air spring pressure loss was considerably less than the maximum permitted descent rate due to an error in sizing the gas discharge orifice.

(6) The jacking procedure based on not change the cylinder supply flow or bleed flow controls during the operation is unsatisfactory for all but the minimum spring rates and the higher loads.

(7) The float can be refloated without disassembly of the piston and cylinder but the sight glass was of no use in the refloating procedure.

(8) The time for the piston to go from 3 in. above the park position to the park position was about 50 seconds which is within the desired time of 90 seconds and well below the rate for allowable impact loads.

(9) The ring bearing gaps change approximately 0.001 inches when the flat and spherical bearing assembly is displaced 4 inches off center.

Data from the vibration surveys conducted in both the lateral and vertical directions at the 1.8×10^6 lb bearing load indicate that there are no resonances in the vertical direction in the frequency range 5-20 cps. In the lateral direction no resonances were detected on either the piston or cylinder but two apparent resonant peaks were found on the flat bearing and one on the spherical bearing. These apparent resonances which were found at 11 and 17 cps, may be attributed to the stem centering block and/or the shaker support stand.

Tests conducted on the cylinder supply panel to determine the flow variation with cylinder pressure through the flow control valves, capillary restrictor valve and hydraulic lines indicate that the supply panel can produce the range of K_Q's theoretically required for the vehicle-suspension system stability. Results of the tests also indicate that the system K_Q is flat within .002 to .005 gpm/psi with frequency variations but is not the same for all cylinder supply pressures.

Results of the Static Piston Characteristics tests which were performed to determine the static stiffness of the Hydrodynamic Support, indicate that the stiffness is linear with piston deflection, at least up to the ±1.0 in. deflections tested and that the static stiffness is independent of the gas spring rate. Due to temperature variations during the tests and also due to mean temperature differences among the tests, no comparisons were made of the static stiffness determined with theoretical values. However, the static stiffness was shown to decrease with increasing K_Q with values that indicate good agreement with the theory can be made if the data is normalized to a uniform temperature.

Damping tests, made to determine the lateral damping due to the viscous forces between the flat bearing and piston surface indicate that the lateral damping is slightly higher than the maximum specified values. Differences between the measured values and the maximum specified values are attributed to the springs used to center the stem in the Head to Head tests.

In the vertical damping tests conducted in the Head to Head configuration many problems were encountered that prevented the tests from being conducted as originally anticipated. The method of determining the total vertical damping that was finally decided upon was to measure the low frequency flow damping by measuring the phase angle between the lower cylinder pressure and the piston displacement and to measure the higher frequency viscous damping in separate tests on the piston-cylinders out of the Head to Head configuration. The total damping would then be the sum of the flow damping and the viscous damping.

Results of the flow damping test indicate excellent agreement with the theory for the low frequency, high bearing load tests. At the lighter bearing loads and higher frequencies the flow damping, and consequently the phase angle representing it, theoretically became small. The small phase angle measured under these conditions did not agree well with the theory but the difference was attributed to a phase lag introduced by the phase measuring instrumentation. Separate tests on the phase measuring circuit showed that the lag introduced was sufficient to account for the difference between the theoretical flow damping and the measured values at the light bearing loads and higher frequencies. It was therefore concluded that the actual flow damping of the Hydrodynamic Support agrees with the theory and is therefore linear with K_Q and decreases quadratically with increasing frequency and can be adjusted with K_Q to give positive or negative flow damping.

The piston-cylinder viscous damping; which, together with the flow damping determine the total support damping, was determined from separate tests on the supports. Results of these tests indicate that the high frequency damping (where the flow damping is negligible) is significantly higher than the theoretical damping and is, in fact, higher than the maximum specified values. Measured values of the viscous damping determined from the free oscillation decay rate of the piston in the cylinder were on the order of 30 lb-sec/in. in comparison to to 15 lb-sec/in. theoretical. No explanation for this was found and, in fact, several tests conducted to determine the relationship between the measured damping and piston pressure and also oil temperature either yielded results contradictory to expectations or did not change the damping as much as anticipated.

Following the separate damping tests, checks were made on the ovality of the piston relative to the cylinder to determine if there could be either interference between the piston and cylinder at the low piston pressure used in the damping tests. Results of the ovality tests indicated that the piston and cylinder were concentric within tolerance.

VII. REFERENCES

1. Martin Dwg. 88A4100410 - Piston and Cylinder Assembly - Saturn V Hydrodynamic Support

2. Martin Dwg. 88A4100402 - Head to Head Test Stand - Saturn V Hydrodynamic Support

3. Martin Dwg. 88A4100486 - Equipment and Piping Installation - Saturn V Hydrodynamic Support

4. Martin Dwg. 88A4100488 - Tubing Installation - Saturn V Hydrodynamic Support

5. Martin Dwg. 88A4100486 - Equipment and Piping Installation- Saturn V Hydrodynamic Support

6. Martin Tool Dwg. 8831-2631 - Hydraulic Pressure Piping - Upper and Lower Cylinders and Sub Panels - Saturn V Hydrodynamic Support

7. Martin Tool Dwg. 8831-2628 - Hydraulic Return System - Saturn V Hydrodynamic Support

8. Martin Dwg. 88A4100903 - Wiring Schematic, Control Panel, Head to Head Test - Saturn V Hydrodynamic Support

9. Head to Head Test Procedure - Martin ER 14035, July 1965.

10. Prause, R. H., "Dynamic Response of the Hydrodynamic Support for Saturn V," Martin ER 13915, June 1965.

11. von Pragenau, G. L., "Approximation of Free Flight for Ground Vibration Tests on Saturn V Space Vehicle Implemented by Hydraulic Support - Specifications, Analysis, Stabilization and Results," (unpublished).

12. Frost, R., "Development Test Report," Martin ER 14307, Nov. 1965.

VIII. TABLES

SUMMARY OF HEAD TO

TABLE IV A

Test No.	Set No.	1965 Test Date	Description	Bearing Load x 10^6	Lower Piston Spring Rate	Force
			A) DESIGN ASSURANCE			
			1 & 2 Gaps			
2	1	8-4	Piston cylinder gap test (3.1) * Adjust flow control valves (3.2)	0.1	Min	
3	1	8-4	↓	0.44	Min	
4	1	8-5	↓	1.0	Min	
5	1	8-7	↓	1.8	Min	
51	1	8-15	Static flow characteristics (5.2.1)	0.1	None	Forced disp by
52	1	8-14	↓	0.44	↓	↓
53	1	8-12	Static flow & piston characteristics	1.8	↓	↓
54	1	8-15	Static flow characteristics	0.1	↓	↓
55	1	8-14	↓	0.44	↓	↓
56	1	8-12	Static flow & piston characteristics	1.8	↓	↓
1	2	9-8	Piston cylinder gap test (3.1) Adjust flow control valves (3.2)	0.1	Min	
2	2	9-8	↓	0.44	Min	
4	2	9-8	↓	1.8	Min	
22	2	9-25	Static flow characteristics (5.2.1)	0.1	Min	Forced disp. b
23	2	9-25	↓	0.44	Min	↓
24	2	9-24	Static flow & piston charac.	1.8	↓	↓
25	2	9-25	Static flow characteristics	0.1	Min	↓
26	2	9-25	Static flow characteristics	0.44	Min	↓
27	2	9-25	Static flow & piston characteristics	1.8	↓	↓
			3. BEARING REDUNDANCY & SEPARATION			
13	1	8-8	Bearing Separation (3.4)	1.8	Min	
14	1	8-8	Bearing Redundancy (3.3)	1.8	Min	
15	1	8-9	Bearing Redundancy (3.3)	1.8	Min	
16	1	8-9	Bearing Redundancy (3.3)	1.8	Min	
			4. AIR SPRING LOSS			
36	2	9-25	Air spring loss (3.5)	1.8	Min	Simulated weig
			5. FLOATING PROCEDURE			
37	2	9-14	Floating procedure (3.5.2)	0		Simulated weig
			6. OPERATING RANGE TEST			
64	1	8-27	Operating range test (3.6)	0.1	Min	Simulated weig
65	1	8-27	↓	0.1	Max	Simulated weig
66	1	8-10	↓	0.44	Min	Simulated weig
67	1	8-14	↓	0.44	Max	Simulated weig
68	1	8-11	↓	1.8	Max	Simulated weig
69	1	8-10	↓	1.8	Min	Simulated weig
28	2	9-17	Operating range test (3.6)	1.8	Min	Simulated weig
32	2	9-23	Operating range test	0.1	Min	Simulated weig

* Numbers in parentheses indicate paragraph in Head to Head Test Specification, Appen

) HEAD TEST

-1

Input	Capillary Seal Length Upper	Capillary Seal Length Lower	K_o Set In	General Information
	6	6	N.A.	
	6	6	N.A.	
	6	6	N.A.	
	6	6	N.A.	Stem went hard over and applied eccentric load
upper piston	8	4	N.A.	
	8	4	N.A.	
	8	4	.046(Max)	
	4	8	N.A.	
	4	8	N.A.	
	4	8	.015	Repeat is 56A (8-13)
	6	6		
	6	6		
	6	6		
upper piston	8	4		
	8	4		
	8	4	.025	
	4	8		
	4	8		
	4	8	.015	
	6	6	N.A.	Flow cut to lower flat & spherical bearing.
	6	6	N.A.	One flat and spherical flow valve closed.
	6	6	N.A.	One upper ring flow control valve closed.
	6	6	N.A.	One lower ring flow control valve closed.
t	6	6		Bleed N_2 from lower piston
t				
t	6	6	N.A.	From park to operate position
t	↓	↓		
t				
t				
t				
t				
t	6	6		
t	6	6		

lix A.

67-2

68-1

SUMMARY OF HEAD

TABLE IV

Test No.	Set No.	1965 Test Date	Description	Bearing Load x 10^6	Lower Piston Spring Rate	Force
			7. SINK RATE TEST			
70	1	8-10	Sink rate test (3.7)	1.8	Min	Simulated Weigh
71	1	8-27		0.1	Min	Simulated weigh
29	2	9-17	Sink rate test (3.7)	1.8	Min	Simulated weigh
33	2	9-23	Sink rate test	0.1	Min	Simulated weigh
			8. ECCENTRIC LOADING TEST			
5	1	8-7	Adjust flow control valves (3.2)	1.8	Min	
			9. EFFECTIVE MOVING MASS			
1	1	8-1	Determine moving mass (8.9)			
			B. VIBRATION SURVEYS 1. LATERAL			
63	1	8-30	Lateral resonance survey (4.0)	1.8	Min	C-5 constant fo 5 to 20 cps
			2. VERTICAL			
62	1	8-31	Vertical resonance survey (4.0)	1.8	Min	C-5 Constant fo 5 to 20 cps
			C. CYLINDER SUPPLY PANEL 1. BREADBOARD TESTS			
12						
			2. SYSTEM K_Q TEST			
6	1	8-9	Determine K_Q values	1.8	N.A.	Piston disconne oil supply and loads simulated pressure
7	1	8-9		1.8	N.A.	
8	1	8-9		0.44	N.A.	
9	1	8-9		0.44	N.A.	
9.5.1	1	8-10		0.9	N.A.	
9.5.2	1	8-9		0.9	N.A.	
10	1	8-9		0.1	N.A	
11	1	8-9		0.1	N.A.	
102	1	8-19	Additional K_Q tests	1.8 Simulated		Piston disconne
			3. SYSTEM COMPONENT TESTS			
100	1	8-18	Calibration of CV-1 in system	1.8 Simulated		Piston disconne
101	1	8-18	Calibration of FCV-1 in system	1.8 Simulated		Piston disconne
104	1	8-21	Check on calibration of CV-2	1.8	Min	
			D. STATIC PISTON CHARACTERISTICS			
39	1	8-12	Static piston characteristics (5.2.1)	1.8	Min	Forced disp. by
40	1	8-12		1.8	Min	
41	1	8-12		1.8	Min	
41.5	1	8-17	Static piston characteristics	1.8	None	Forced disp. by
45	1	8-14		0.44	None	
46	1	8-14		0.44	None	
47	1	8-14		0.44	None	

Input	Capillary Seal Length Upper	Lower	K_Q Set In	General Information
t	6	6	N.A.	From operate to park position
t	6	6	N.A.	From operate to park position
t	6	6		From operate to park
t	6	6		From operate to park
	6	6	N.A.	Stem went hard over & applied eccentric load.
				Components were subsequently weighed.
rce	6	6	N.A.	
rce	6	6	N.A.	
				Done in laboratory
cted from bearing by line	N.A.	N.A.	CV-1=350	Checked at 0.5 & 1.0 cps; 6A is repeat test
	N.A.	N.A.	440	Checked at 0.5 & 1.0 cps; 7A is repeat test (8-14)
	N.A.	N.A.	350	Checked at 0.5 & 1.0 cps; 8A is repeat test (8-15
	N.A.	N.A.	440	Checked at 0.5 & 1.0 cps; 9A is repeat test (8-15
	N.A.	N.A.	440	Checked at 0.5 & 1.0 cps;
	N.A.	N.A.	350	
	N.A.	N.A.	350	
	N.A.	N.A.	440	
cted				0,1,2,3,4,5,6, & 7 CV-1 settings at 0.05, 0.2, & 1.0 cps
cted				Measure flow with variations of CV-1 settings @ 2400 psi
cted				Measure flow and line pressure drop for FCV-1 settings @ 2400 psi
				CV-2 settings of 3.5 and 5.5
upper piston	6	6	.008	Repeat 39A (8-15) & 39B (8-20) W/O Airspring
	6	6	.016	Repeat 40A (8-13) & 40B (8-19) W/O Airspring
	6	6	.032	Repeat 41A (8-16) W/O airspring
upper piston	6	6	0	
	6	6	.008	Repeat is 45A (8-20)
	6	6	.016	Repeat is 46A (8-20)
	6	6	.032	

SUMMARY OF HEAD TO
TABLE IV A

Test No.	Set No.	1965 Test Date	Description	Bearing Load x 10^6	Lower Piston Spring Rate	Force I
			D. STATIC PISTON CHARACTERISTICS			
53	1	8-12	Static flow & piston characteristics	1.8		
56	1	8-12	Static flow & piston charac.	1.8		
57A	1	8-13	Static piston characteristics	1.8	None	Forced disp. b
18	2	9-23	Static piston characteristics	1.8	Min	Forced disp. b
19	2	9-24	Static piston charac. (5.2.1)	1.8	Min	Forced disp. b
20	2	9-25	Static piston charac. (5.2.1)	0.44	Min	Forced disp. b
21	2	9-25	Static piston charac. (5.2.1)	0.44	Min	Forced disp. b
24	2	9-24	Static flow & piston charac.	1.8	↓	Forced disp. b
27	2	9-25	Static flow & piston charac.	1.8	↓	Forced disp. b
			E. DAMPING			
			1. HEAD TO HEAD			
			a. LATERAL			
60	1	8-10	Lateral Damping (5.1)	0.44	Min	Stem excited m
108	1	8-27	Lateral damping			Stem excited m
38	2	9-26	Lateral damping (5.1)	0.44	Min	Stem excited b
39	2	9-26	Lateral damping (5.1)	1.8	Min	Stem excited b
			b. VERTICAL			
22	1	8-25	Vertical damping (5.2.2)	1.8	Min	Servo-valve us upper piston a
24	1	8-25	↓	1.8	Min	0.5 cps
25	1	8-25		1.8	Min	0.5 cps
26	1	8-25		1.8	Min	1.5 cps
27	1	8-24		1.8	Min	0.05 cps
28	1	8-24		1.8	Min	0.1 cps
30	1	8-24		1.8	Min	0.2 cps
31	1	8-24		1.8	Min	0.5 cps
32	1	8-23		0.44	Min	0.05 cps
33	1	8-23		0.44	Min	0.1 cps
34	1	8-24		0.44	Min	0.5 cps
35	1	8-24		0.44	Min	0.8 cps
36	1	8-26		0.1	Min	0.05 cps
37	1	8-26		0.1	Min	0.1 cps
38	1	8-26	↓	0.1	Min	0.5 cps
6.0	2	9-19	Vertical damping (5.2.2)	1.8	Min	0.05 cps
6.1	2	9-19	↓	1.8	Min	0.1
6.2	2	9-19		1.8	Min	0.2
6.3	2	9-20		1.8	Min	1.0
7.0	2	9-20		1.8	Min	1.0
7.1	2	9-1C		1.8	Min	0.2
7.2	2	9-17		1.8	Min	0.1
7.3	2	9-19		1.8	Min	0.05
8.0	2	9-20		1.8	Min	0.05
8.1	2	9-20		1.8	Min	0.1
8.2	2	9-20		1.8	Min	0.2
8.3	2	9-21		1.8	Min	1.0
9.0	2	9-21		1.8	Min	1.0
9.1	2	9-20		1.8	Min	0.2
9.2	2	9-20		1.8	Min	0.1
9.3	2	9-20	↓	1.8	Min	0.05

69-1

put	Capillary Seal Length Upper	Lower	K_0 Set In	General Information
	8	4	.046(Max)	
	4	8	.015	Repeat is 56A (8-13)
upper piston	8	4	.005	First test was called 57A
upper piston	6	6	.010	18A (9-25)
upper piston	6	6	.020	
upper piston	6	6	.010	
upper piston	6	6	.020	
upper piston	8	4	.025	
upper piston	4	8	.015	
nually	6	6	N.A.	One cps lateral springs installed.
nually (1 cps)			N.A.	Varying bearing loads (zero to 1.0×10^6)
quick release	6	6		5 cps lateral springs installed.
quick release	6	6		
d to oscillate 0.5 cps	6	6	All flow thru FCV	Phase between lower cylinder displacement and upper cylinder pressure (ϕ_1)
	6	6	.008	
	6	6	.016	
	6	6	.025	
	6	6	.025	
	6	6	.025	
	6	6	.025	
	6	6	.025	
	6	6	.018	
	6	6	.018	
	6	6	.018	
	6	6	.018	
	6	6	.018	
	6	6	.018	
	6	6	.018	
	6	6	.030	Measured ϕ_2 — Phase between upper cylinder pressure and lower piston displacement is ϕ_1
	6	6	.030	ϕ_1&ϕ_2
	6	6	.030	ϕ_2 — Phase between lower cylinder pressure and lower piston displacement is ϕ_2
	6	6	.030	ϕ_2
	6	6	0	ϕ_2
	6	6	0	ϕ_1& ϕ_2(9-20)
	6	6	0	ϕ_1& ϕ_2(9-20)
	6	6	0	ϕ_1
	6	6	.020	ϕ_2
	6	6	.020	ϕ_2
	6	6	.020	ϕ_2
	6	6	.020	ϕ_2
	6	6	.005	ϕ_2
	6	6	.005	ϕ_2
	6	6	.005	ϕ_2
	6	6	.005	ϕ_2

SUMMARY OF HEAD TO

TABLE IV A-

Test No.	Set No.	1965 Test Date	Description	Bearing Load x 10^6	Lower Piston Spring Rate	Forc
10.0	2	9-22	Vertical damping (5.2.2)	0.44	Min	Servo 0.05
10.1	2	9-21		0.44	Min	0.2
10.2	2	9-16		0.44	Min	0.5
10.3	2	9-21		0.44	Min	1.0
11.0	2	9-16		0.44	Min	1.0
11.1	2	9-16		0.44	Min	0.5
11.2	2	9-16		0.44	Min	0.2
11.3	2	9-15		0.44	Min	0.05
12.0	2	9-22		0.44	Min	0.05
12.1	2	9-21		0.44	Min	0.2
12.2	2	9-22		0.44	Min	0.5
12.3	2	9-22		0.44	Min	1.0
13.0	2	9-22		0.44	Min	1.0
13.1	2	9-22		0.44	Min	0.5
13.2	2	9-22		0.44	Min	0.2
13.3	2	9-22		0.44	Min	0.05
14	2	9-23		0.1	Min	0.05
15	2	9-23		0.1	Min	0.1
16	2	9-23		0.1	Min	0.5
17	2	9-23		0.1	Min	1.0
			2. UNIT TESTS a. VERTICAL AND ROTATIONAL			
105	1	8-22	Vertical damping		39 psi	Foot dampin
106	1	8-24	Vertical damping	0.44	Min	Servo at 0.
107	1	8-26	Vertical damping	0.1	Min	0.
	1	9-2	Vertical damping Unit No. 2		17 psi	Bounce by h
	1	9-2	Rotational damping Unit No. 2		17 psi	Rotated by
	2	8-27	Vert. & Rotational Damping Unit #4		17 psi	Hand excita
	2	10-1	Vert. & Rotational Damping Unit #3			Vert. quick rotation by
	2	10-1	Vert. & Rotational Damping Unit #3			
	2	9-30	Vert. & Rotational Damping Unit #3		17 psi	Hand excita
	2	10-1	Vert. & Rotational Damping Unit #3		17 psi	
	2	10-6	Vert. & Rotational Damping Unit #5		17 psi	
	2	10-6	Rotational Damping Unit #5			
			F. MISCELLANEOUS TESTING			
103	1	8-19	Check of P_{9A} & P_{10A} for consistency	1.8	Min	Displaced b
109	1	8-28	Flat bearing investigation			
	2	10-1	Ovality check on Unit #3			
	2	9-23	Press. check in cavity between upper and lower ring bearings	1.8	Min	
	2	9-23	Temp. time histories on piston and cylinder.	1.8	Min	

HEAD TEST

Input	Capillary Seal Length Upper	Capillary Seal Length Lower	K_Q Set In	Measured	General Information
cps	6	6	.030	ϕ_2	Phase between upper cylinder pressure & lower piston displacement is ϕ_1
	6	6	.030	ϕ_2	
	6	6	.030	ϕ_1	Phase between lower cylinder pressure & lower piston displacement is ϕ_2
	6	6	.030	ϕ_2	
	6	6	0	ϕ_1	
	6	6	0	ϕ_1	
	6	6	0	ϕ_1	
	6	6	0	ϕ_1	
	6	6	.020	ϕ_2	
	6	6	.020	ϕ_2	
	6	6	.020	ϕ_2	
	6	6	.020	ϕ_2	
	6	6	.005	ϕ_2	
	6	6	.005	ϕ_2	
	6	6	.005	ϕ_2	
	6	6	.005	ϕ_2	
	6	6	.030	ϕ_2	
	6	6	.030	ϕ_2	
	6	6	.030	ϕ_2	
	6	6	.030	ϕ_2	
g					Head to head tests with no upper piston pressure
5 cps			0		Same as test 34 except all flow thru FCV-1
5 cps			.025		Same as test 38 except K_Q suddenly increased
and excitation					(Side tests on Unit #2 with & without float at 4,5,6,7,8 inch capillary seal lengths)
hand					
tion					At 4,5,6,7, & 8 inch capillary seal lengths.
release hand					At 2,4 & 6 in seal lengths; high temp;2400 psi locked up inside piston;17 psi pressure below piston.
					Vert. at 2,4 & 6; rotational at 4,5,6 & 8 inch seal lengths; 2400 psi piston pressure; 17 psi below piston.
tion					At 4,5,6 & 8 inch capillary seal lengths.
					High temp. at 4, 6 & 8 inch seal lengths.
					At 4, 6 & 8 inch seal lengths.
					At 4, 6 & 8 inch seal lengths; 2400 psi piston pressure.
y upper piston	6	6			Measure gaps & pressures with various loads.

SUMMARY OF ALL MEASUREMENTS AND INS

TABLE IV A-2

INST NO.	LOCATION	DESIGN ASSURANCE TESTS					
		PISTON-CYL GAP	BEARING GAP	BEARING REDUNDANCY & SEPARATION	AIR SPRING LOSS	OPERATING RANGE	SINK RATE
P_1	L. ASSY., L. R. BEARING, L. FRONT		X	X		X	
P_2	L. ASSY., L. R. BEARING, R. SIDE		X	X		X	
P_3	L. ASSY., L. R. BEARING, L. REAR		X	X		X	
P_4	L. ASSY., U. R. BEARING, R. FRONT		X	X		X	
P_5	L. ASSY., U. R. BEARING, R. REAR		X	X		X	
P_6	L. ASSY., U. R. BEARING, L. SIDE		X	X		X	
P_7	U. ASSY., U. R. BEARING, R. SIDE		X	X		X	
P_8	U. ASSY., U. R. BEARING, L. REAR		X	X		X	
P_9	L. ASSY., FRONT CYLINDER	X	X	X	X	X	X
P_{9A}	L. ASSY., FRONT CYLINDER	X					
P_{9D}	L. ASSY., FRONT CYLINDER						
P_{9G}	L. ASSY., REAR CYLINDER	X					
P_{10}	U. ASSY., FRONT CYLINDER	X	X	X	X	X	X
P_{10A}	U. ASSY., FRONT CYLINDER	X					
P_{10D}	U. ASSY., FRONT CYLINDER						
P_{11}	L. ASSY., FLAT BEARING, R. REAR	X	X	X		X	
P_{12}	L. ASSY., SPH. BEARING, R. SIDE	X	X	X		X	
P_{13G}	U. ASSY., U. R. BEARING, L. FRONT		X	X			
P_{14G}	U. ASSY., L. R. BEARING, R. FRONT		X	X			

ECCENTRIC LOADING	VIBRATION SURVEYS		CYLINDER SUPPLY PANEL	STATIC PISTON CHART		DAMPING			
						HEAD TO HEAD			UNIT
							VERT		
	LATERAL	VERTICAL	KQ	SET 1	SET 2	LAT	SET 1	SET 2	VERT-ROTAT
X								X	
X								X	
X								X	
X								X	
X								X	
X								X	
X								X	
X								X	
X	X	X	X	X	X	X	X	X	X
				X	X		X		X
					X			X	
				X	X			X	
X	X	X		X	X	X	X	X	
				X	X		X		
					X		X	X	
X				X	X	X		X	
X				X	X	X		X	
X								X	
X								X	

71-2

SUMMARY OF ALL MEASUREMENTS AN

TABLE

INST NO.	LOCATION	DESIGN ASSURANCE TESTS				
		PISTON-CYL GAP	BEARING GAP	BEARING REDUNDANCY & SEPARATION	AIR SPRING LOSS	OPERATING RANGE
P_{15G}	U. ASSY., L. R. BEARING, R. REAR		X	X		
P_{16G}	U. ASSY., L. R. BEARING, L. SIDE		X	X		
P_{17G}	L. ASSY., FLATBEARING, R. FRONT		X	X		
FL_1	L. ASSY., SUPPLY FLOW, REAR	X	X	X	X	X
FL_{1D}	L. ASSY., SUPPLY FLOW					
FL_2	U. ASSY., SUPPLY FLOW, REAR	X	X	X	X	X
P_{10} VEC	PHASE MEASUREMENT					
P_9 VEC	PHASE MEASUREMENT					
D_1 VEC	PHASE MEASUREMENT					
V_{MIN}	PHASE MEASUREMENT					
ϕ	CALCULATED (PHASE ANGLE)					
δ	LOG DECREMENT					
D_1	L. ASSY. VERTICAL	X	X	X	X	X
D_2	LATERAL	X	X	X		
T_1	L. ASSY. SUPPLY	X	X	X	X	X
T_2	U. ASSY., SUPPLY	X	X	X	X	X
T_3	RETURN	X	X	X	X	X
T_4	L. ASSY. NITROGEN	X	X	X	X	X
G_1	L. ASSY., L. R. BEARING, L. SIDE		X	X		X
G_2	L. ASSY., U. R. BEARING, R. SIDE		X	X		X

D INSTRUMENTATION LOCATIONS

V A-2

SINK RATE	ECCENTRIC LOADING	VIBRATION SURVEYS		CYLINDER SUPPLY PANEL	STATIC PISTON CHART		DAMPING			UNIT
							HEAD TO HEAD			
		LATERAL	VERTICAL	KQ	SET 1	SET 2	LAT	VERT SET 1	VERT SET 2	VERT-ROTAT
	X								X	
	X								X	
	X								X	
X	X	X	X	X	X	X	X	X	X	X
				X				X	X	X
	X	X	X		X	X				
									X	
									X	
									X	
									X	
								X	X	
									X	
X	X	X	X		X	X		X	X	X
	X				X	X	X			
X	X	X	X	X	X	X	X	X	X	X
X	X	X	X		X	X	X	X	X	X
X	X	X	X	X	X	X	X	X	X	X
X	X	X	X		X	X	X	X	X	X
	X								X	
	X								X	

72-2

SUMMARY OF ALL MEASUREMENTS AI

TABLE I

INST NO.	LOCATION	DESIGN ASSURANCE TESTS				
		PISTON-CYL GAP	BEARING GAP	BEARING REDUNDANCY & SEPARATION	AIR SPRING LOSS	OPERATING RANGE
G_3	L. ASSY., FLAT BEARING, FRONT		X	X		X
G_4	L. ASSY., FLAT BEARING, L. SIDE		X	X		X
G_5	L. ASSY., SPH. BEARING, R. SIDE		X	X	X	
G_6	L. ASSY., SPH. BEARING, REAR		X	X		X
FO_1	L. ASSY., L. SIDE					
FO_2	L. ASSY., R. SIDE					
FO_3	L. ASSY., FRONT					
FO_4	L. ASSY., REAR					
A_{1V}	L. ASSY., CYLINDER					
A_{1L}	L. ASSY., CYLINDER					
A_{2V}	L. ASSY., PISTON					
A_{2L}	L. ASSY., PISTON					
A_{3V}	L. ASSY., FLAT BEARING					
A_{3L}	L. ASSY., FLAT BEARING					
A_{9V}	L. ASSY., SPH. BEARING					
A_{4L}	L. ASSY., SPH. BEARING					
A_{6V}	U. ASSY., FLAT BEARING					
A_{7V}	U. ASSY., PISTON					
A_{8V}	U. ASSY., CYLINDER					

ID INSTRUMENTATION LOCATIONS

/ A-2

SINK RATE	ECCENTRIC LOADING	VIBRATION SURVEYS		CYLINDER SUPPLY PANEL	STATIC PISTON CHART		DAMPING			UNIT
							HEAD TO HEAD			
		LATERAL	VERTICAL	NQ	SET 1	SET 2	LAT	VERT SET 1	VERT SET 2	VERT-ROTAT
X	X	X					X		X	
X	X	X					X		X	
X							X		X	
	X						X		X	
		X								
		X								
			X							
			X							
			X							
		X								
			X							X
		X								
			X							
		X								
			X							
		X								
			X							
			X							
			X							

73-2

SUMMARY OF ALL MEASUR

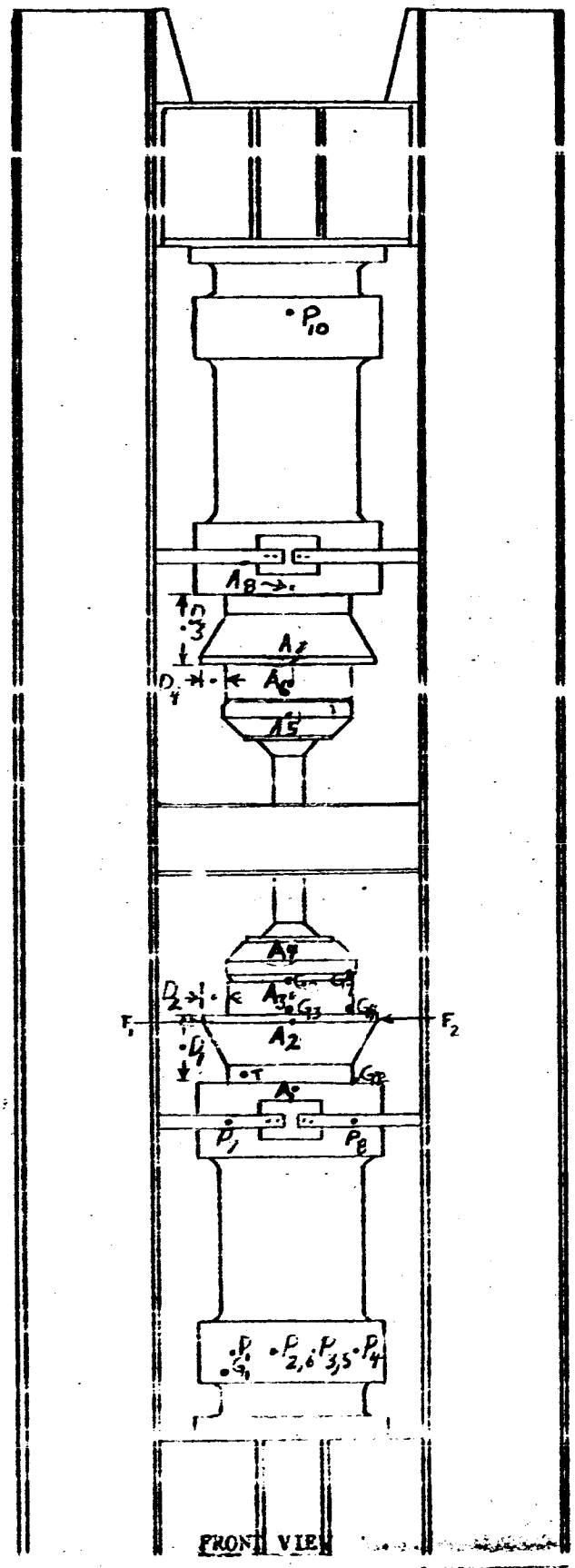

FRONT VIEW

ABBREVIATIONS:

P	-	Pressure transducer
FL	-	Flow meter
T	-	Thermocouple (temperature)
G	-	Gap (distance detector)
D	-	Displacement
FO	-	Force
	-	Damping (log decrement)
	-	Damping (phase angle)
AV	-	Accelerometer - vertical
AL	-	Accelerometer - lateral

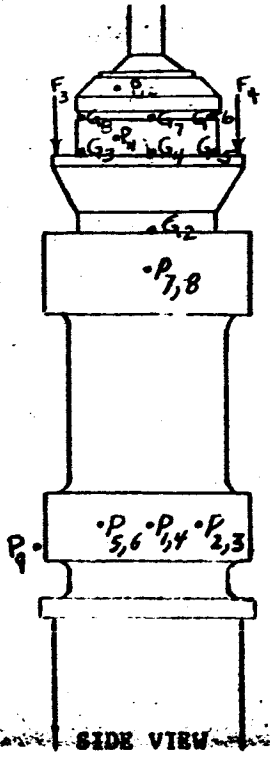

SIDE VIEW

74-1

TABLE IV A-2

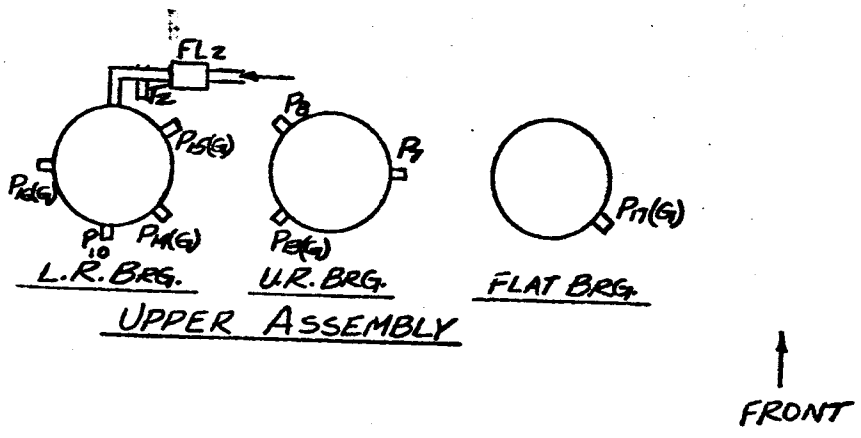
FL2
T2
P8
P9(G)
P7
P6(G)
P10
P11(G)
P12(G)
L.R. BRG.
U.R. BRG.
FLAT BRG.
UPPER ASSEMBLY
FRONT

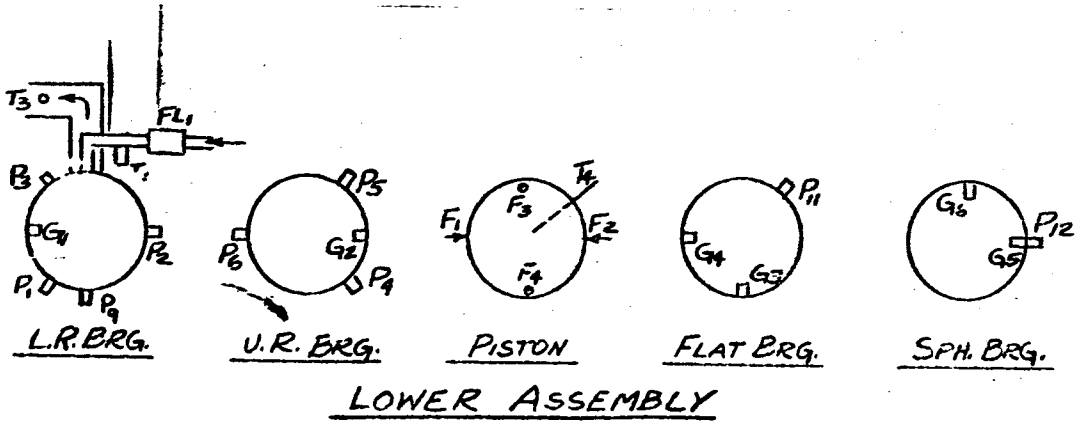
T3
FL1
T1
P3
G1
P2
P1
P5
P6
G2
P4
T4
F1
F3
F2
F4
P11
G4
G3
G6
P12
G5
L.R.BRG.
U.R. BRG.
PISTON
FLAT BRG.
SPH. BRG.
LOWER ASSEMBLY

TABLE IIA-1
FLAT & SPHERICAL BEARING SEPARATION

TEST NO.			14 BEFORE	14 DURING	14 AFTER	13 DURING	13 AFTER		15 AFTER	16 AFTER		14 Δ	13 Δ		AVG @
FLOW			FULL	1/2	FULL	0	FULL		FULL	FULL					FULL
CYL	P_9		2390	2370	2370	2390	2410		2360	2380		-12	8		2382
FLAT	P_{11}		2575	2400	2630	2090	2665		2580	2615		-215	-523		2613
SPH.	P_{12}		2510	2480	2490	2410	2520		2505	2505		-26	-96		2506
GAP	G_3		.0020	.0020	.0023	0	.0023		.0016	.0017		-.0002	-.0022		.0022
(FLAT)	G_4		.0010	.0006	.0012	0	.0013		.0024	.0025		-.0006	-.0012		.0012
GAP	G_5		.0063	.0041	.0070	.0016	.0068		.0052	.0067		-.0026	-.0051		.0067
(SPH)	G_6		.0091	.0088	.0089	.0037	.0089		.0090	.0096		-.0002	-.0053		.0090
	$P_{11}-P_9$		185	30	250	-300	255		220	235					229
	$P_{12}-P_9$		120	110	120	20	110		145	125					124

ENG. REP. NO.

PAGE 75

060501

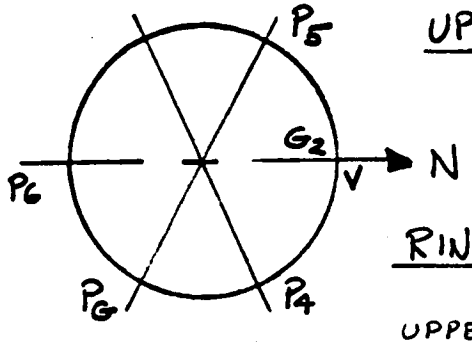

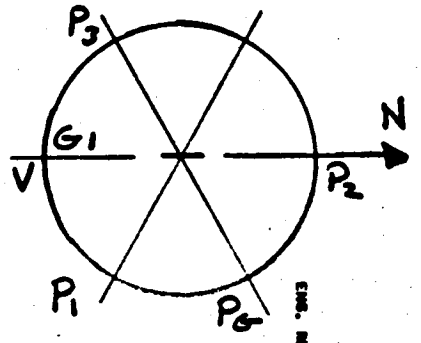

TABLE V A-2

RING BEARING REDUNDANCY, LOWER ASS'Y

			UPPER					LOWER						
TEST NO.			15 BEFORE	15 DURING	15 AFTER	15 Δ		16 BEFORE	16 DURING	16 AFTER	16 Δ			
FLOW	*		NORM	OFF	NORM			NORM	OFF	NORM				
CYL	P9		2360	2360	2360	0		2350	2350	2380	-15			
LOWER RING	P1		1215	1205	1200	-3		1200	1215	1209	11			
	P2		1270	1250	1240	-5		1209	1050	1213	-161			
	P3		1185	1168	1168	8		1180	1196	1188	12			
	P6		1100	1090	1090	-5		1035	885	1045	-155			
UPPER RING	P4		1170	1180	1154	18		1190	1170	1170	-10			
	P5		1050	1070	1048	21		1078	1065	1072	-10			
	P6		1105	920	1075	-170		1105	1100	1100	-2			
	P6		990	780	960	-195		990	990	990	0			
GAP.L	G1		.0102	.0103	.0105	0		.0099	.0079	.0097	-.0019			
GAP.U	G2		.0049	.0013	.0044	-.0033		.0045	.0047	.0044	.0003			

060501 * RECESS IN LINE WITH GAP MEASURING DEVICE.

TABLE V F-1

Time Histories of #4 Cylinder and Piston Temperatures During Test 18

TABLE V F-1

Real Time	t (Min.)	Cylinder Temperature	Piston Temperature
0105	0	92.1	92.7
0120	0	92.2	92.2
0133	Main Pumps on Hyd. Press. - 1000 psi	92.0	91.6
0143	10	91.4	91.8
0148	15	91.4	92.8
0155	22	92.2	93.7
0200	27	92.1	94.9
0205	32	92.4	94.1
0210	37	92.7	94.7
0215	42	92.8	96.8
0220	47	93.1	96.8
0225	52	94.1	97.1
0230	57	93.8	97.9
0235	62	94.0	99.1
0240	67	93.8	99.4
0245	72	94.9	101.8
	Hyd. Press.-3000 psi		
0250	77	95.6	103.1
0255	82	97.0	104.2
0300	87	97.1	105.4
0305	92	98.8	106.2
0310	97	98.8	107.2
0320	107	99.7	108.1
0330	117	101.6	109.9
0340	127	102.9	110.1
0355	142	103.8	111.8
0410	157	104.9	112.8
0425	172	105.2	112.7
0440	187	105.8	113.1
0500	247	106.4	113.3

IX. FIGURES

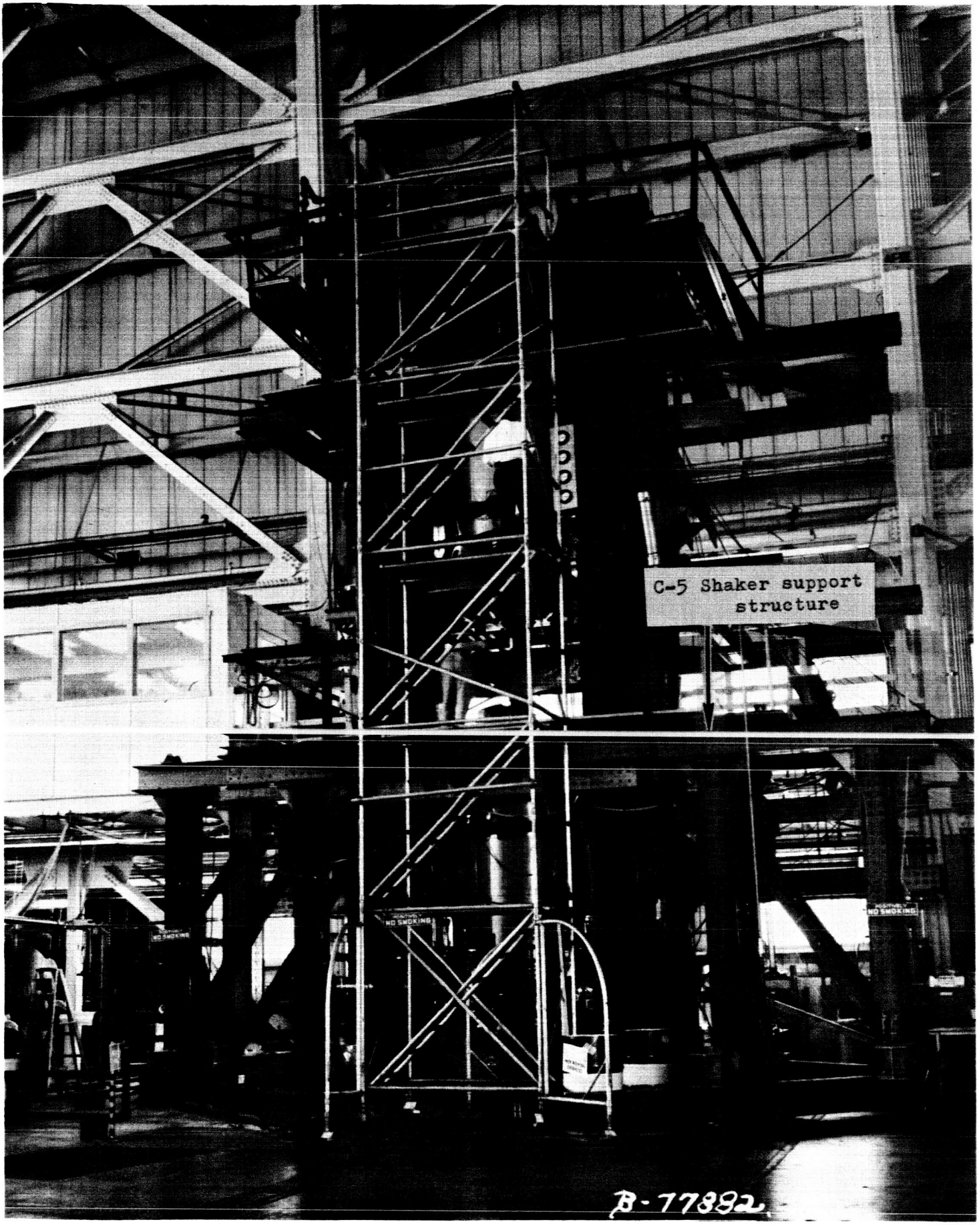

HEAD TO HEAD TEST - OVERALL FRONT VIEW
FIGURE II-1

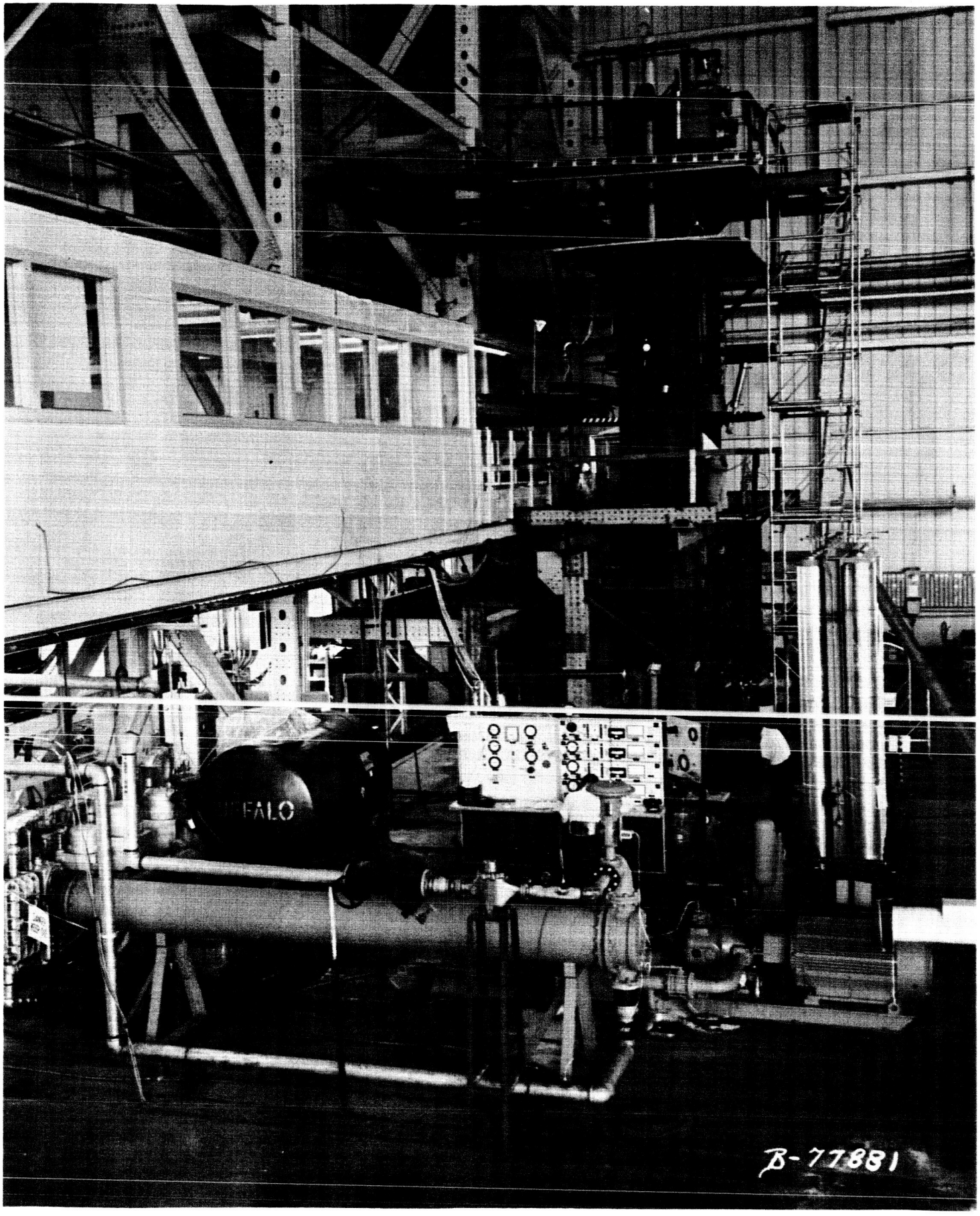

HEAD TO HEAD TEST - OVERALL SIDE VIEW
FIGURE II-2

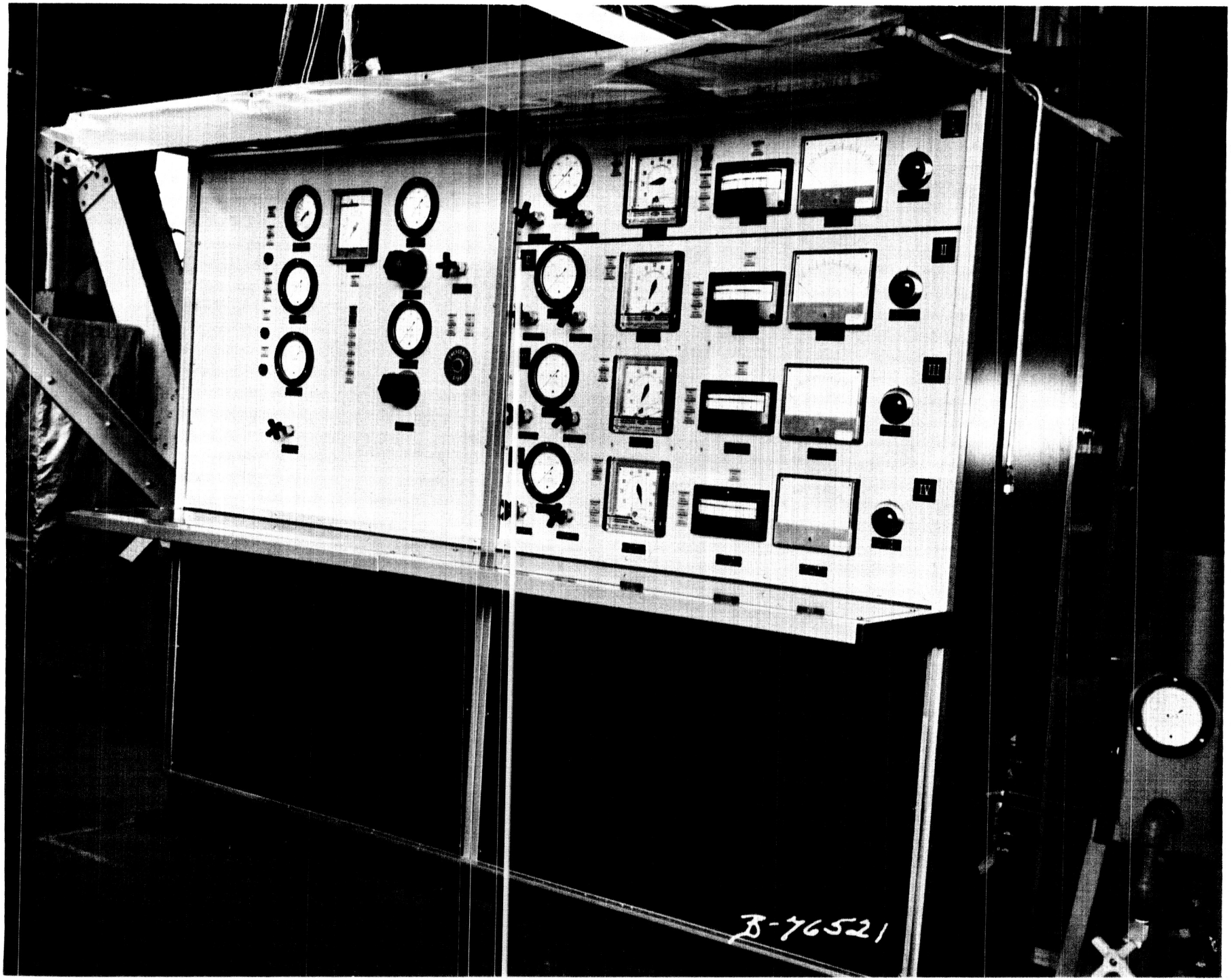

OPERATING CONSOLE
FIGURE II-3

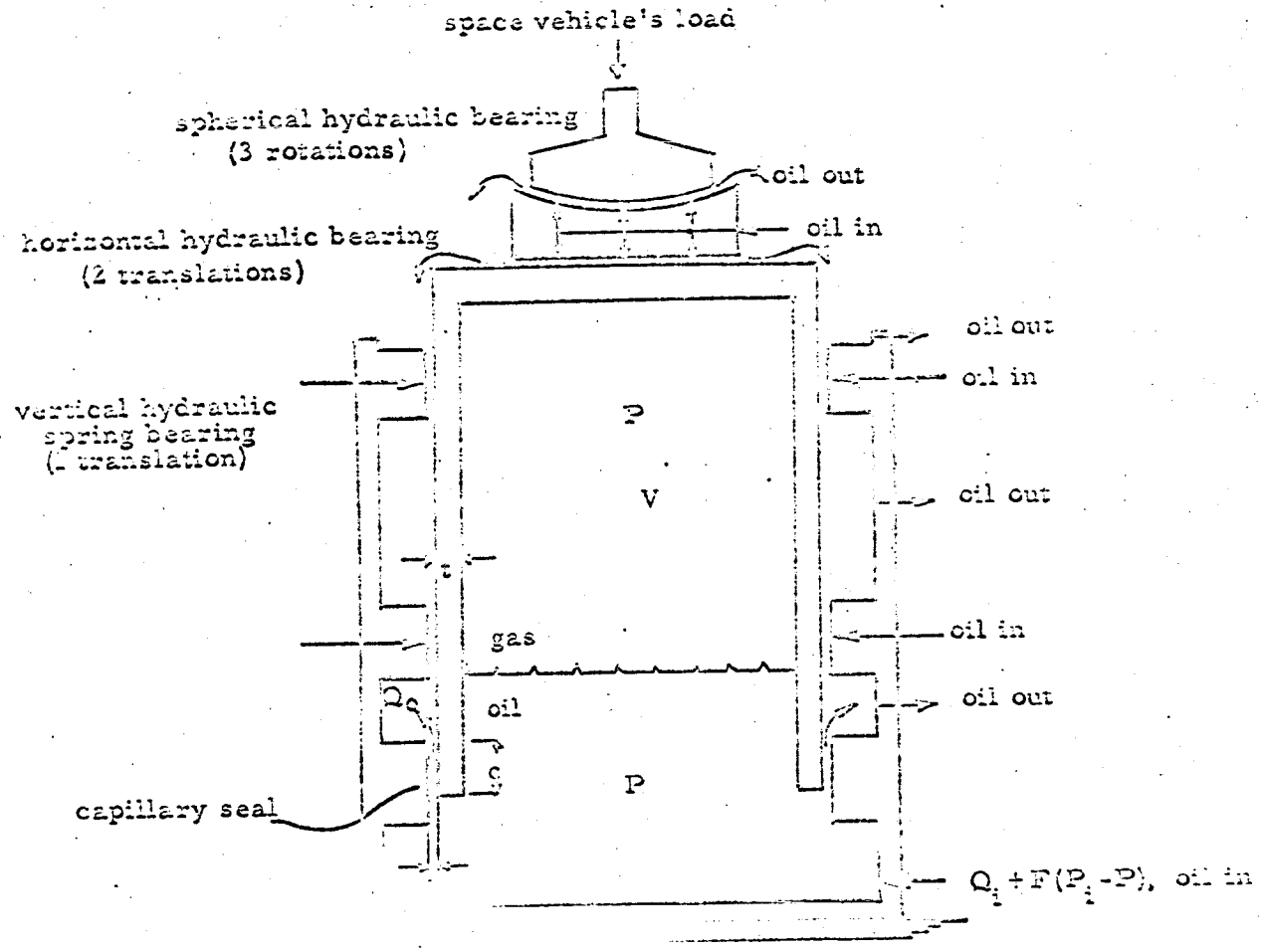

Figure II-4 - Schematic of hydraulic support unit providing six degrees of freedom

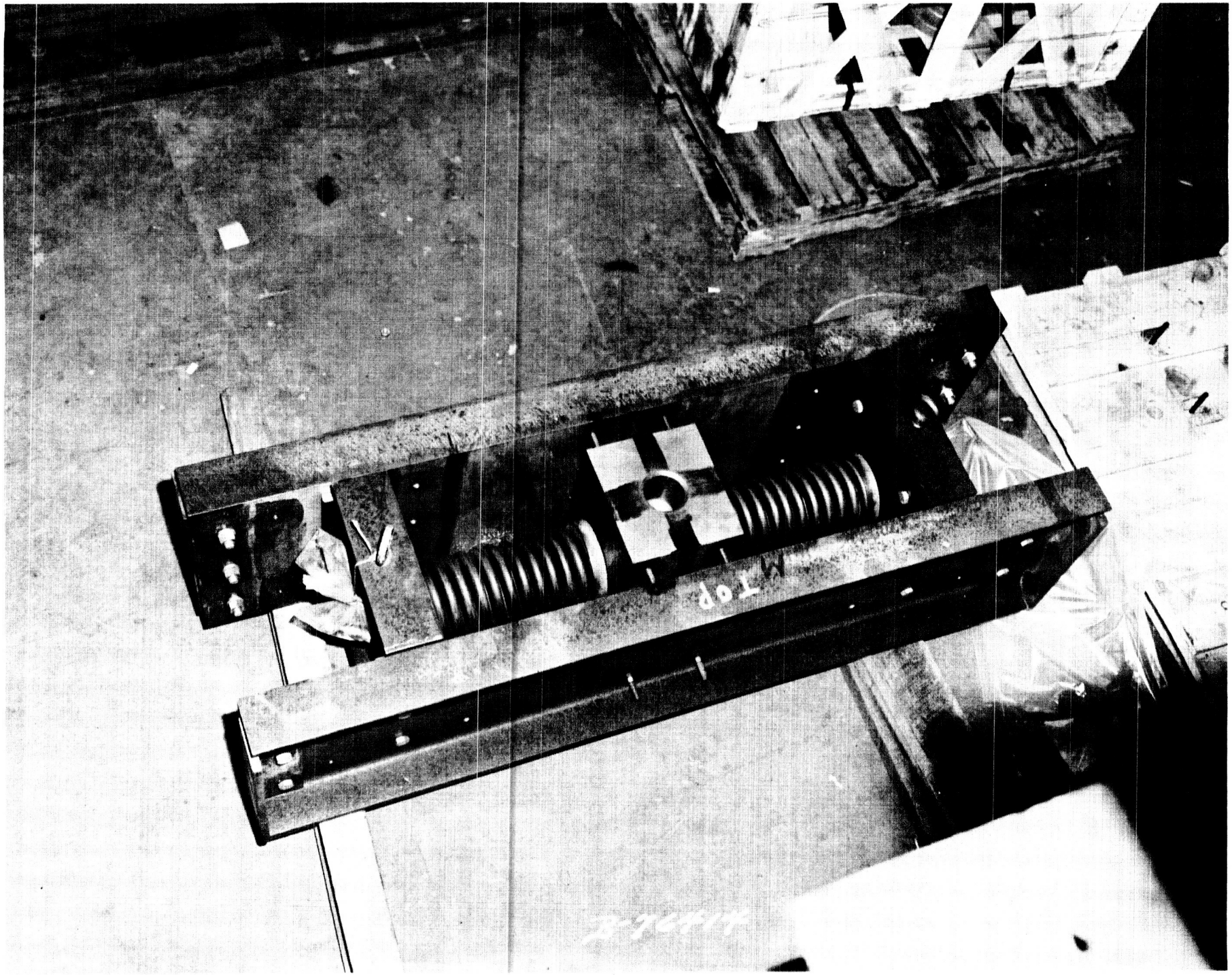

STEM CENTERING CONFIGURATION
FIGURE II-5

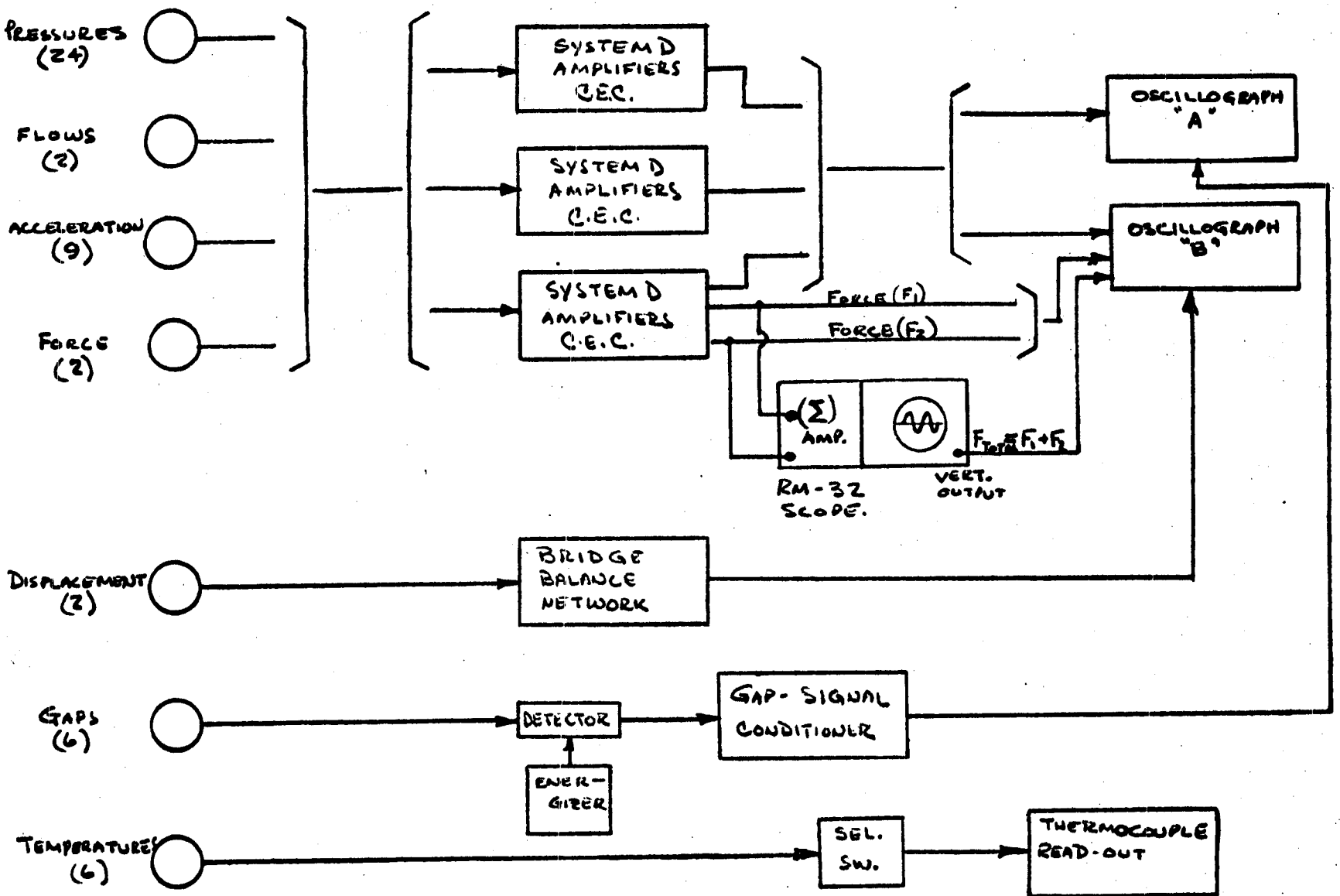

FIGURE IV B-1

BLOCK DIAGRAM OF OVERALL SYSTEM INSTRUMENTATION

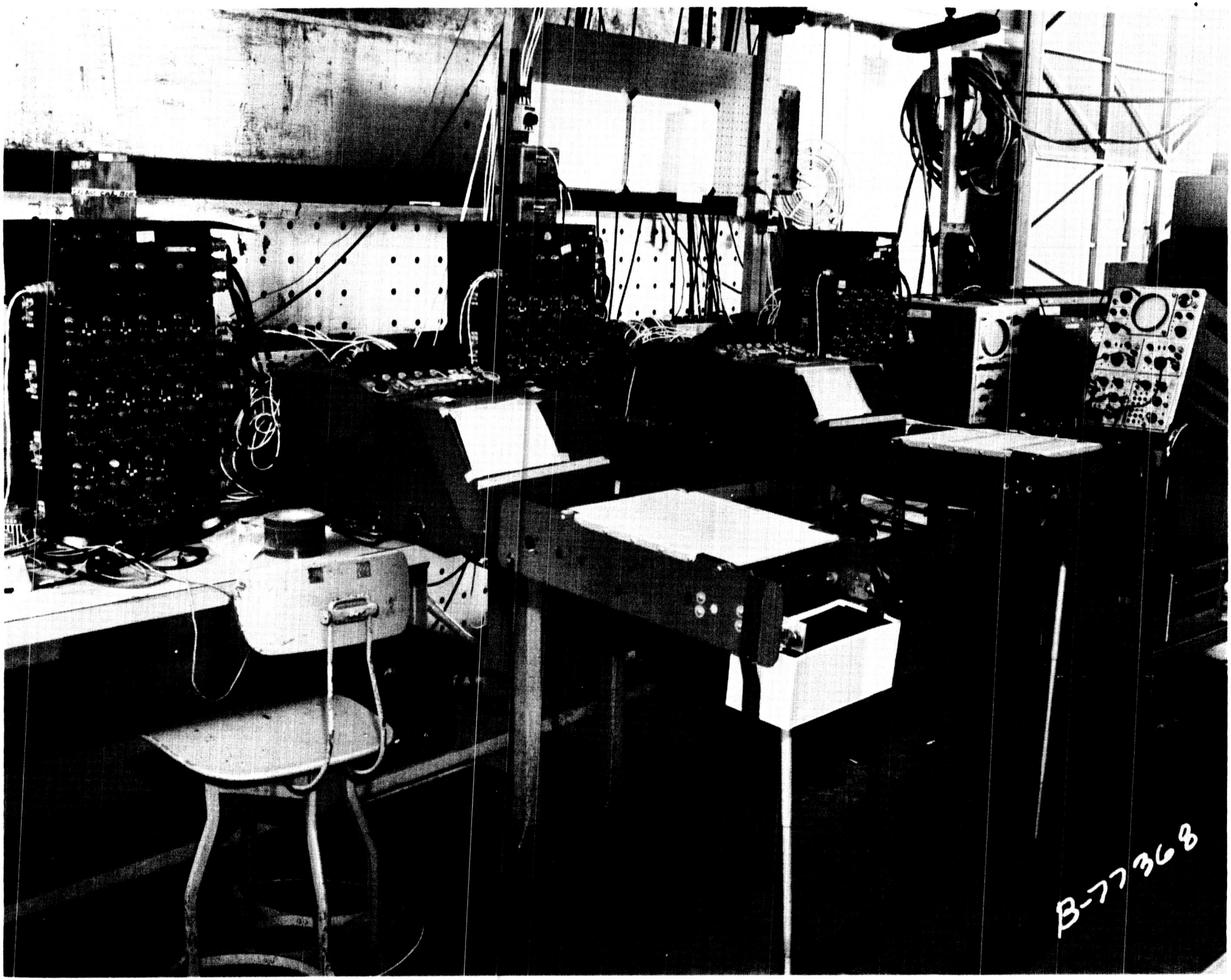

RECORDING EQUIPMENT
FIGURE IV B-2

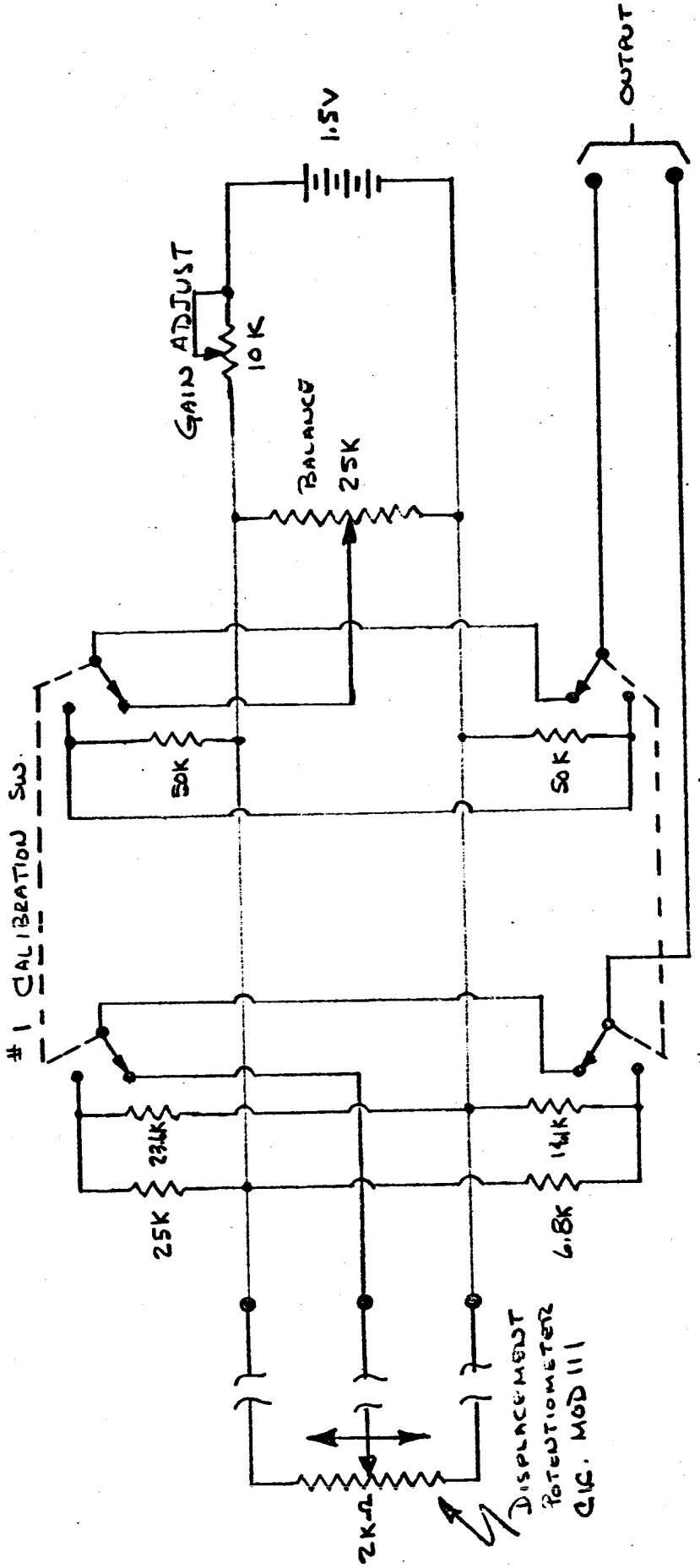

FIGURE IV B-3

BLOCK DIAGRAM FOR DISPLACEMENT MEASUREMENT

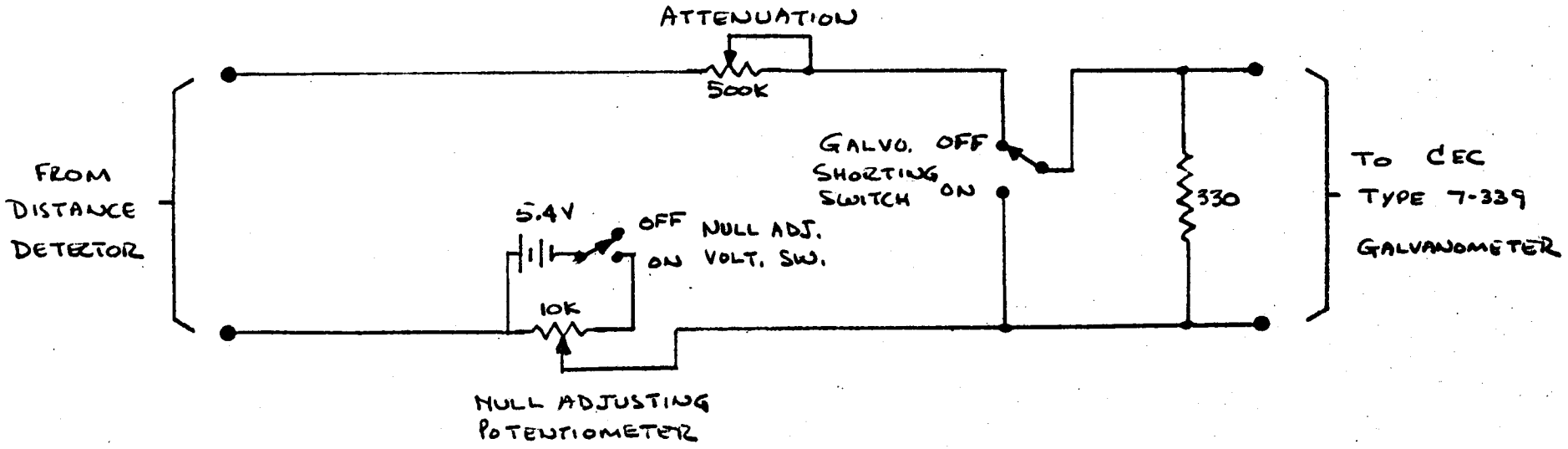

FIGURE IV B-4

BLOCK DIAGRAM FOR GAP
MEASUREMENT

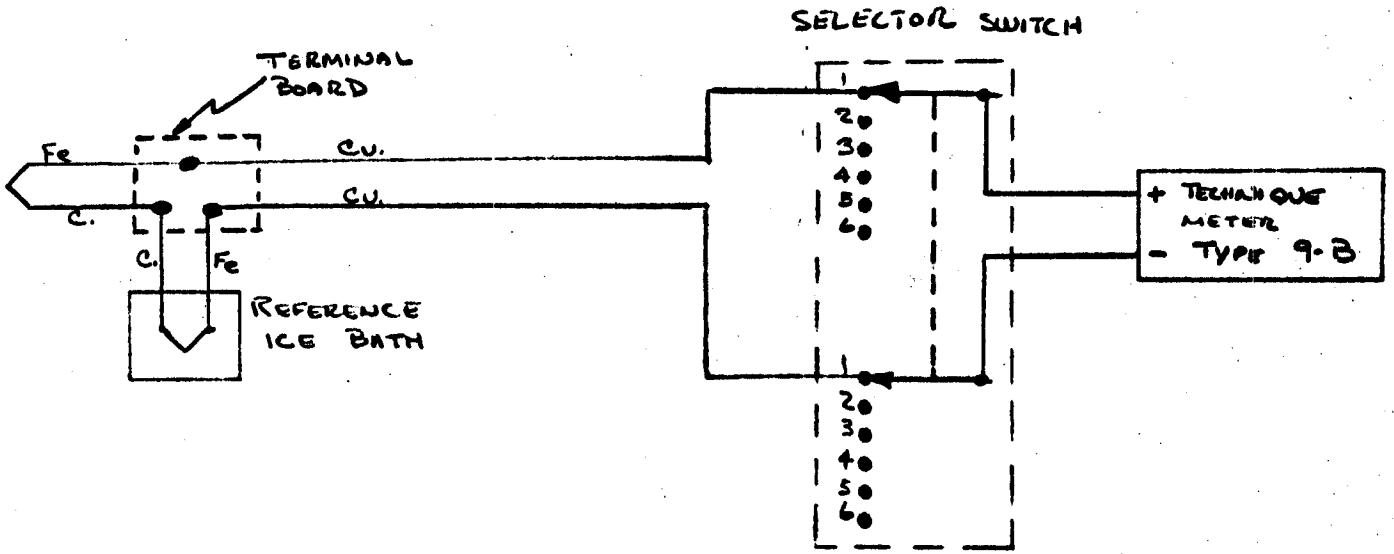

THERMOCOUPLE TYPE J IRON-CONSTANTAN

FIGURE IV B-5

BLOCK DIAGRAM FOR TEMPERATURE MEASUREMENT

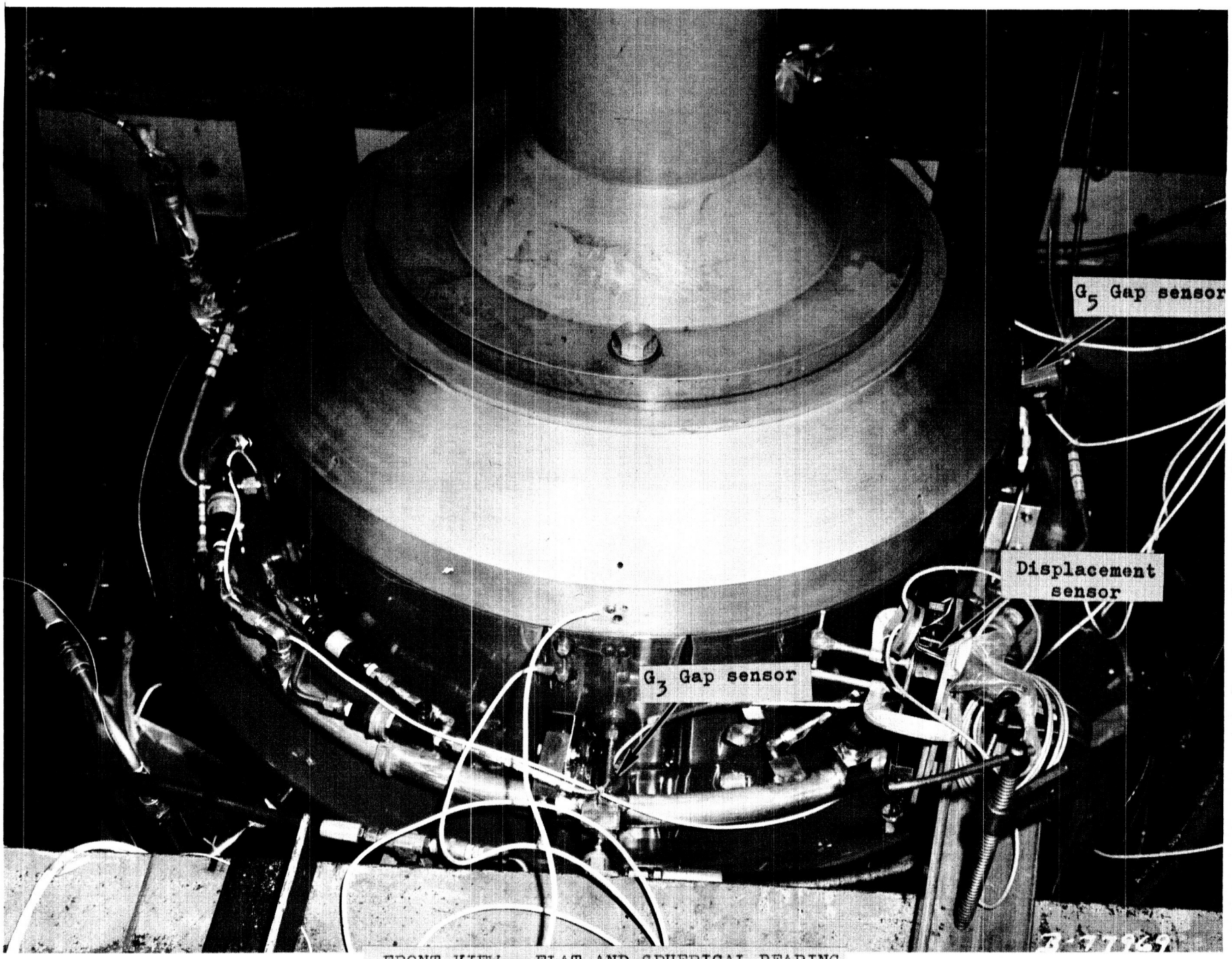

FRONT VIEW - FLAT AND SPHERICAL BEARING
LOWER ASSEMBLY
FIGURE IV B-6

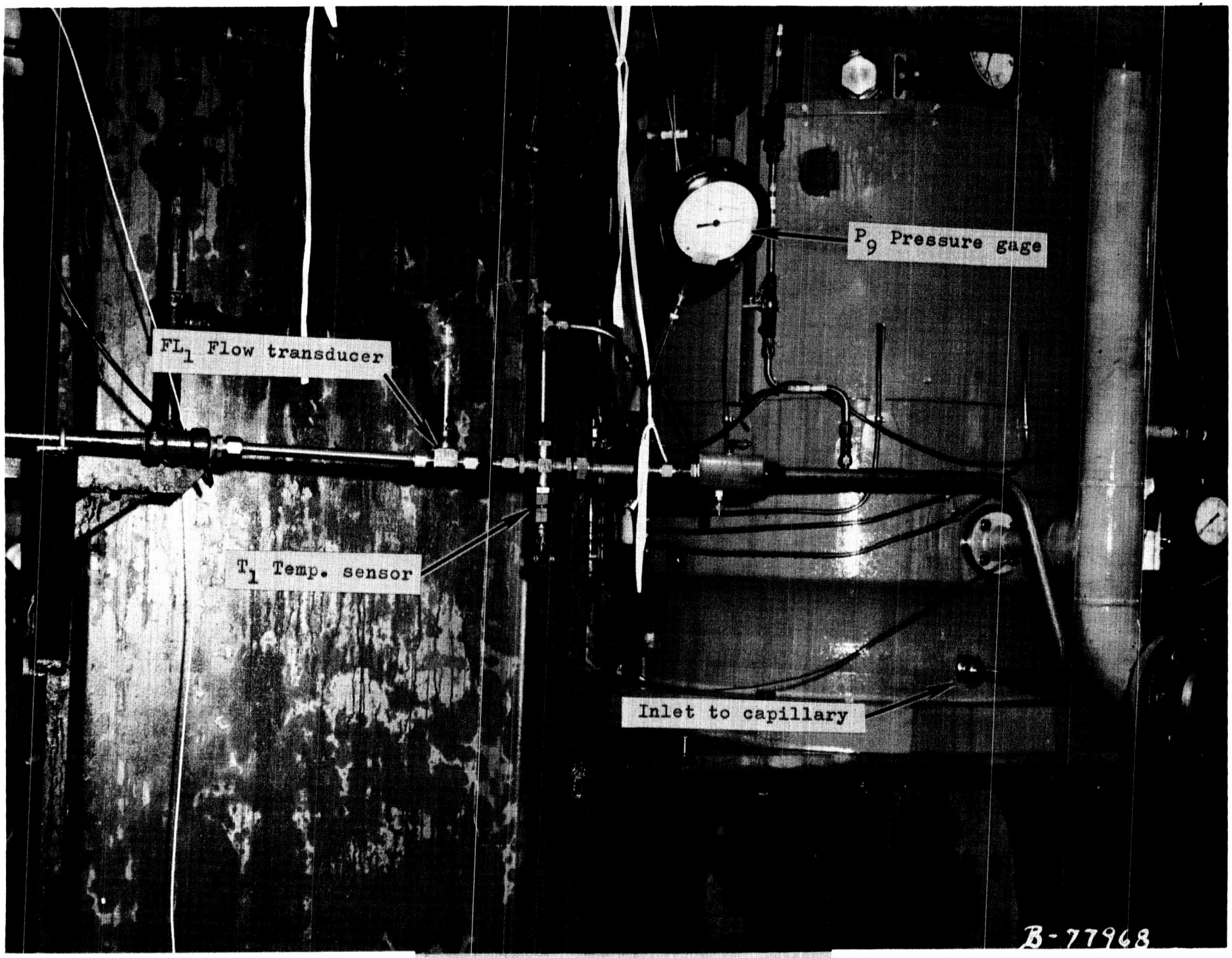

REAR VIEW OF LOWER PISTON ASSEMBLY
FIGURE IV B-7

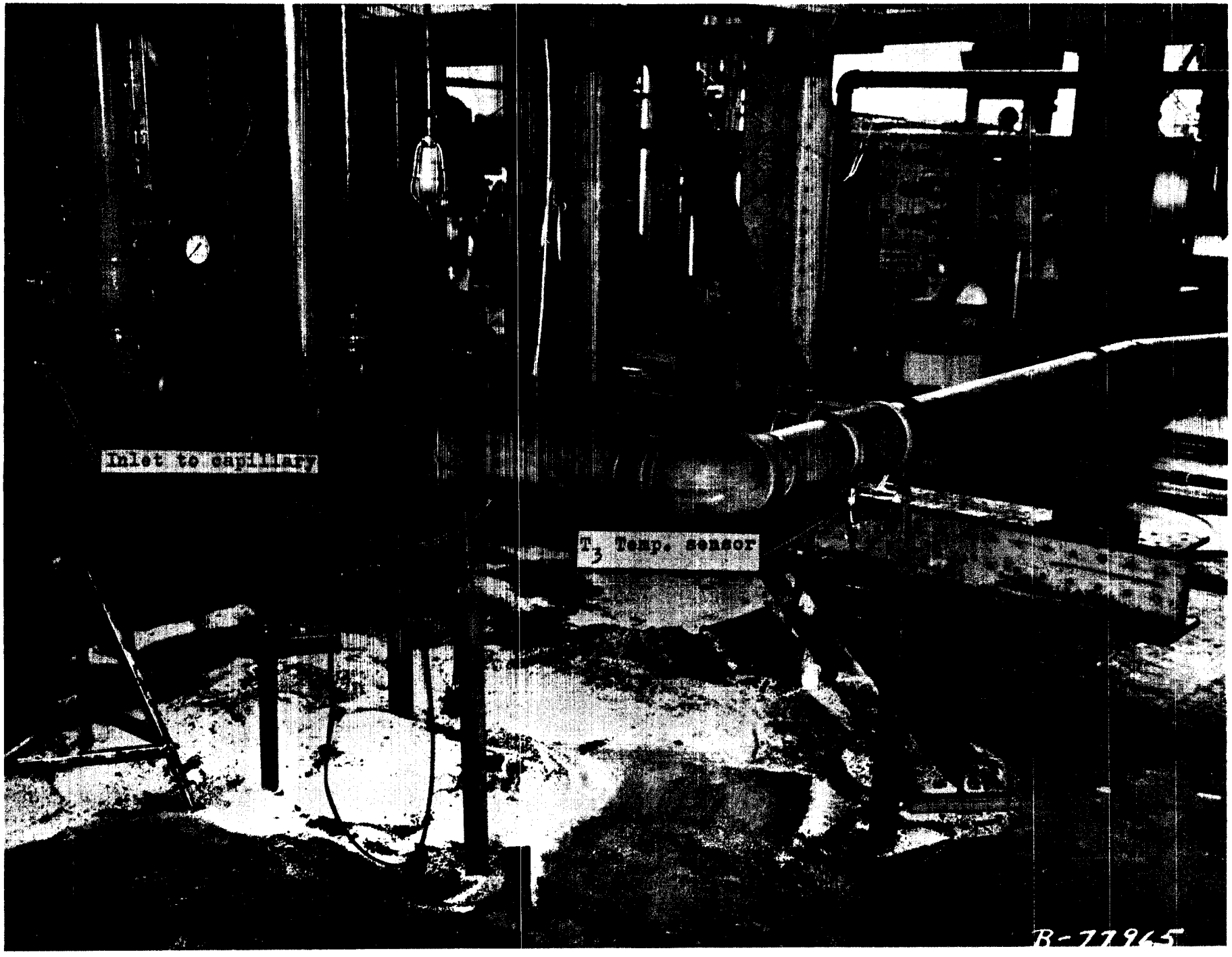

RETURN LINE FROM LOWER ASSEMBLY
FIGURE IV B-8

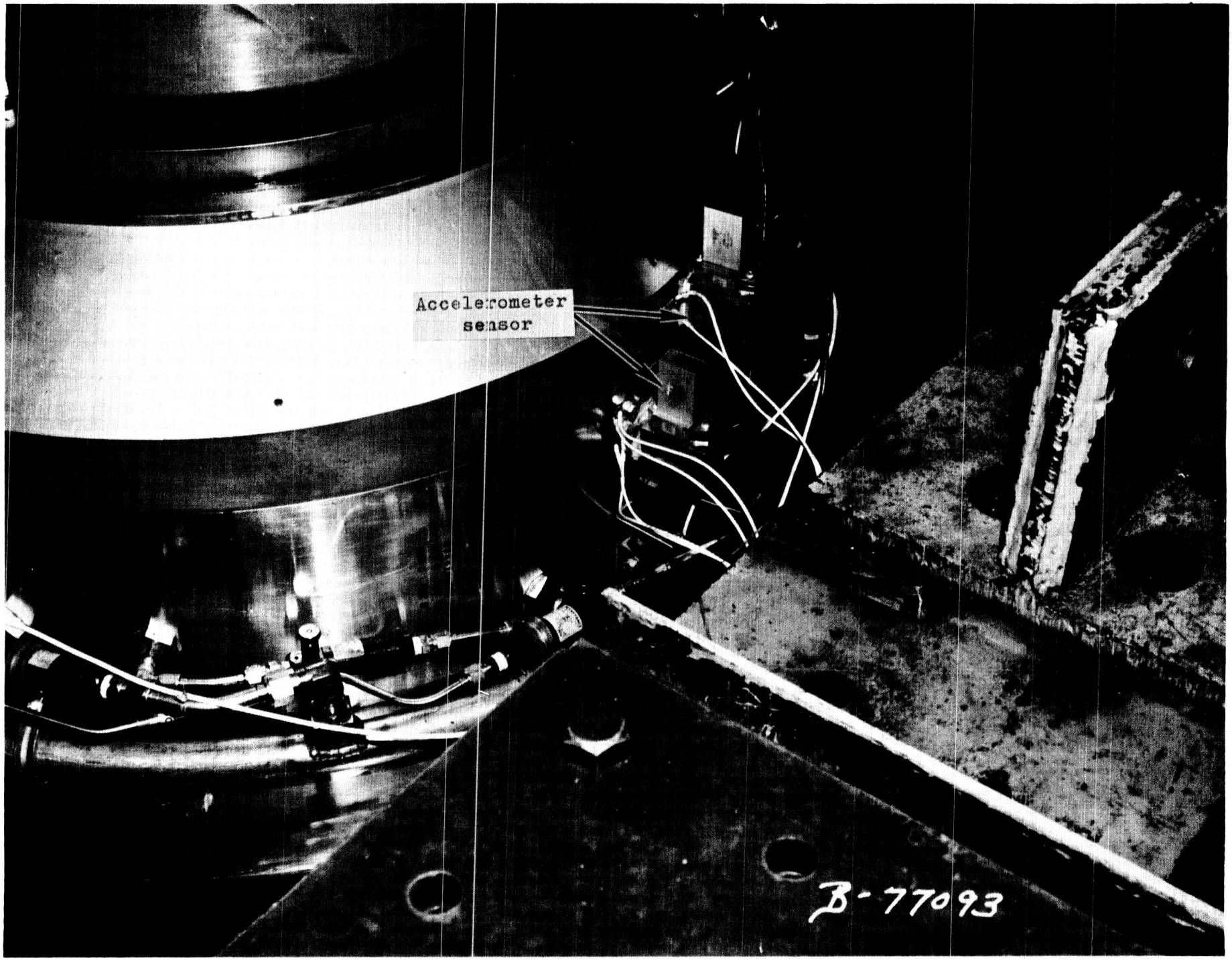

FLAT AND SPHERICAL BEARING - LOWER ASSEMBLY
FIGURE IV B-9

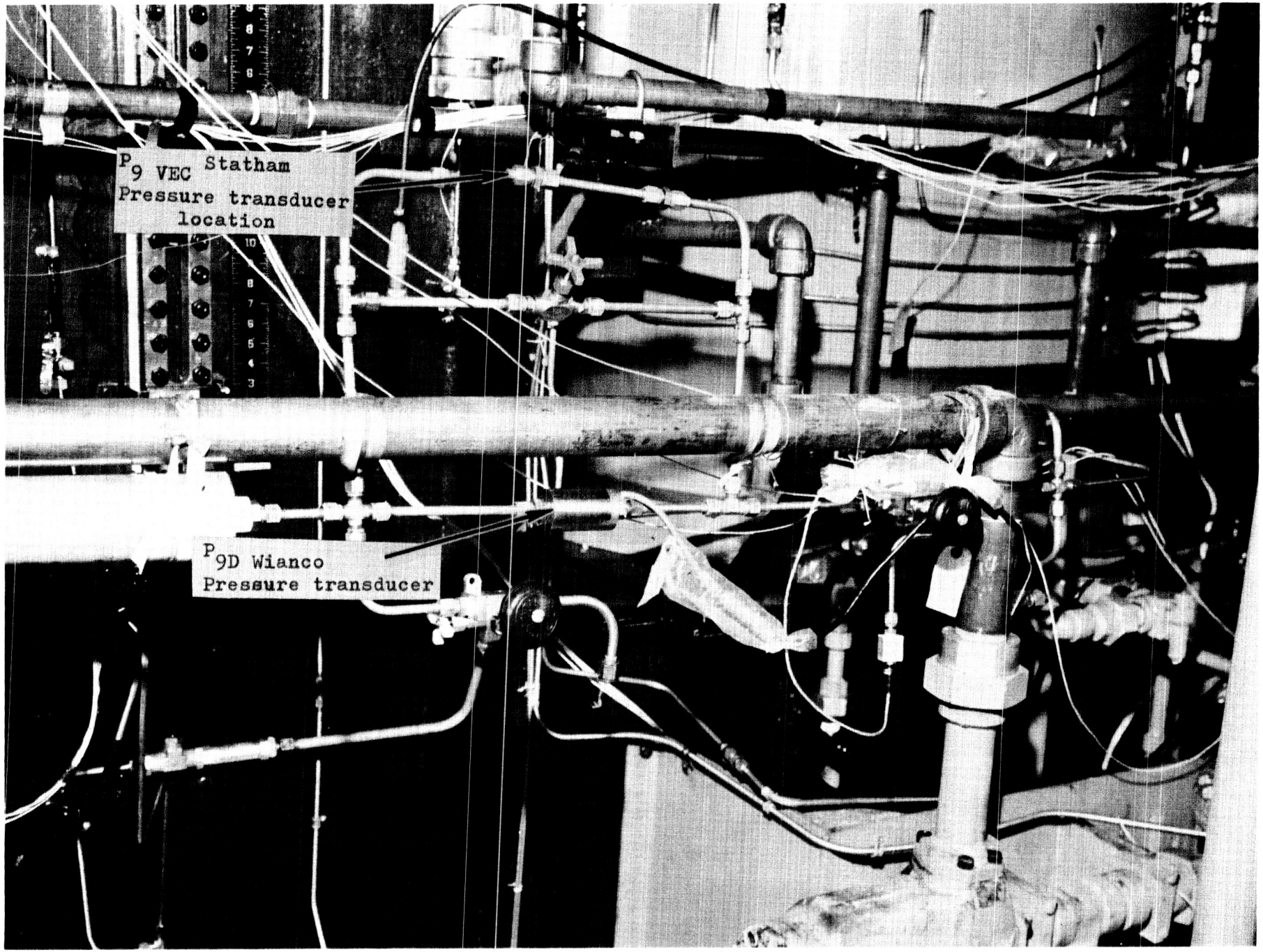

BOTTOM FRONT OF LOWER ASSEMBLY
FIGURE IV B-10

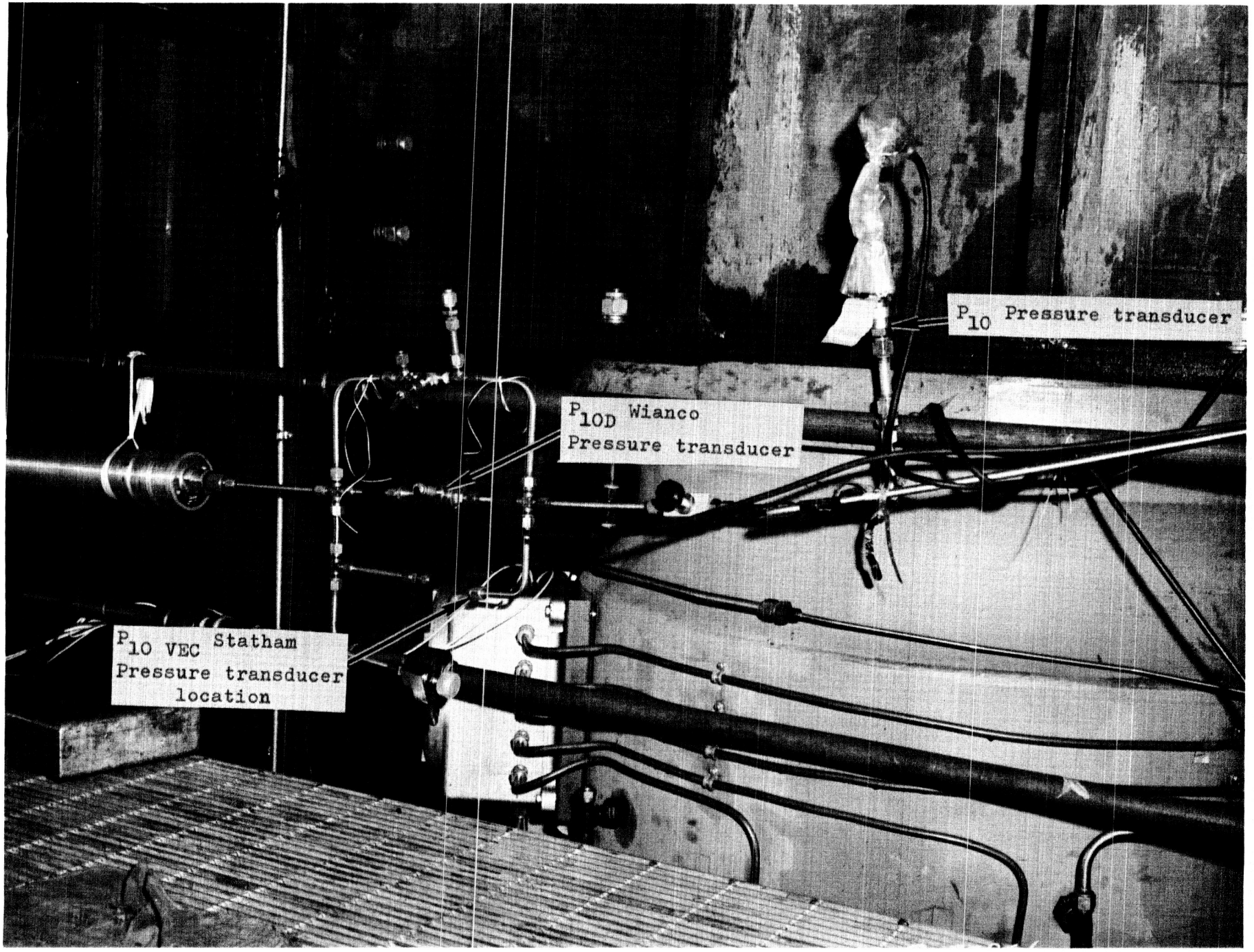

FRONT OF UPPER ASSEMBLY
FIGURE IV B-11

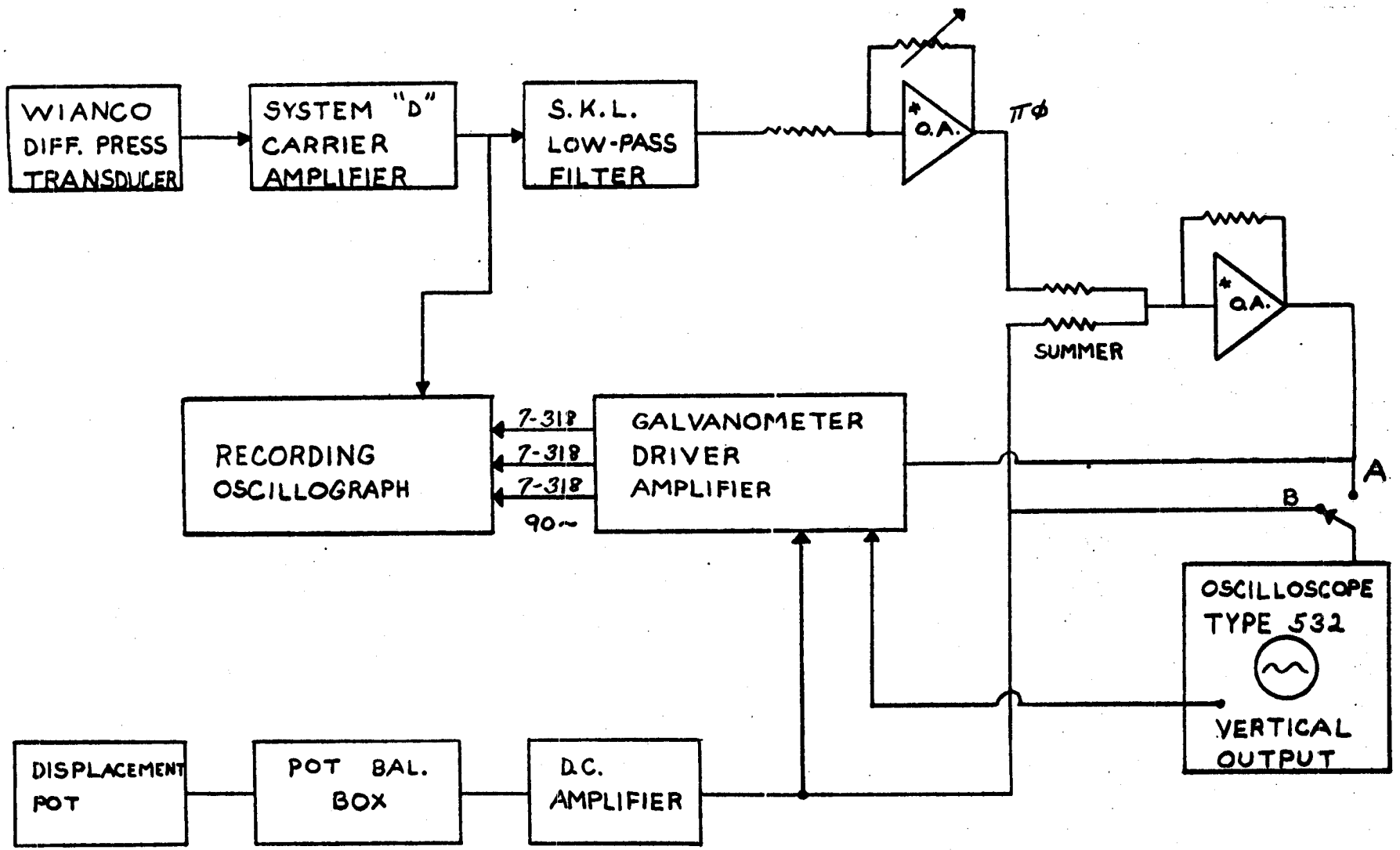

(NULL) $\frac{A}{B} \times 57.3 =$ DEGREES
(DISP.)

* USED IN TYPE 555 OSCILLOSCOPE
(OPERATIONAL AMPLIFIERS)

FIGURE IV B-12

BLOCK DIAGRAM FOR PHASE ANGLE MEASUREMENT
(FIRST SET)

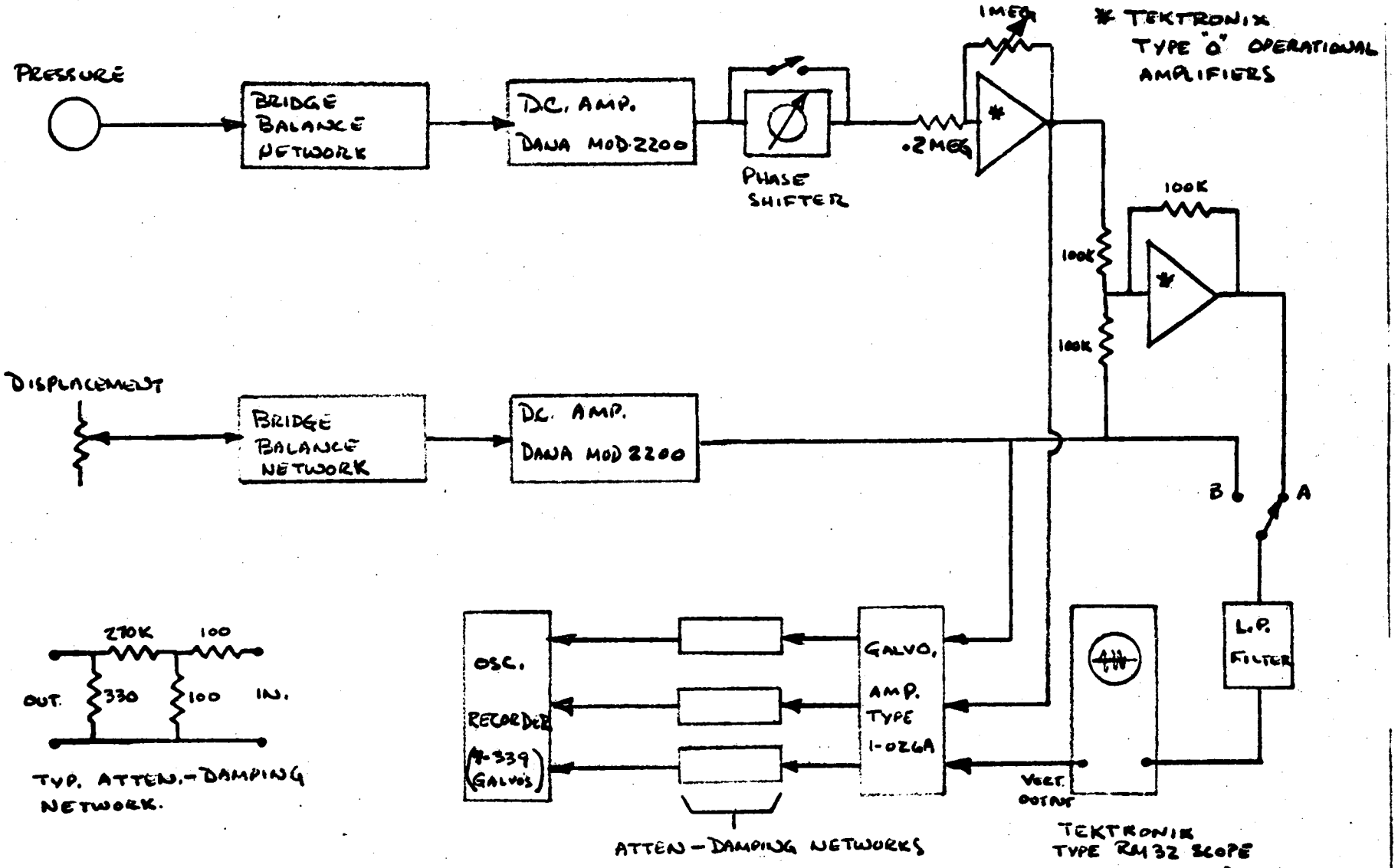

FIGURE IV B-13

BLOCK DIAGRAM FOR PHASE ANGLE MEASUREMENT

(SECOND SET)

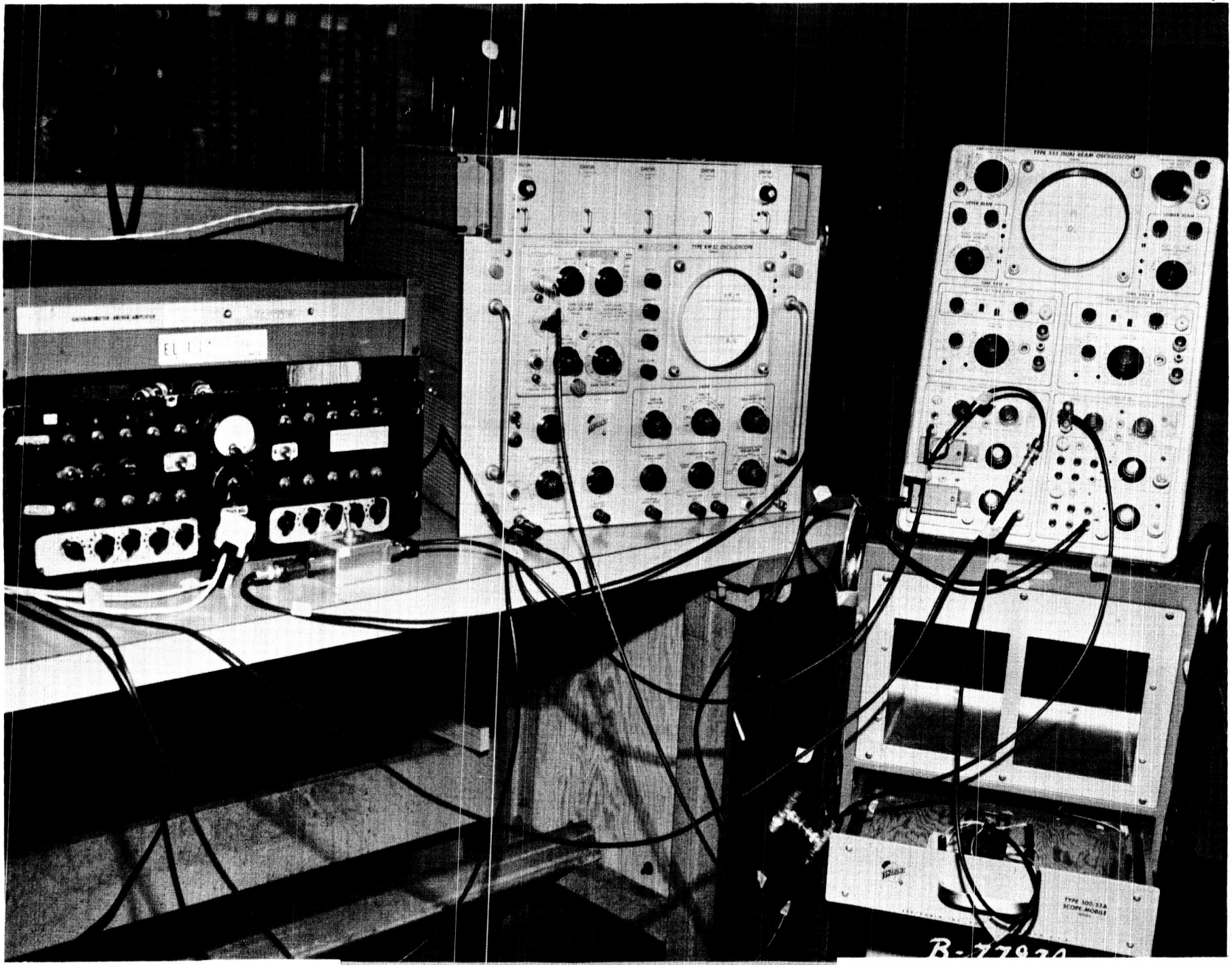

PHASE CONDITIONING EQUIPMENT - SECOND SET
FIGURE IV B-14

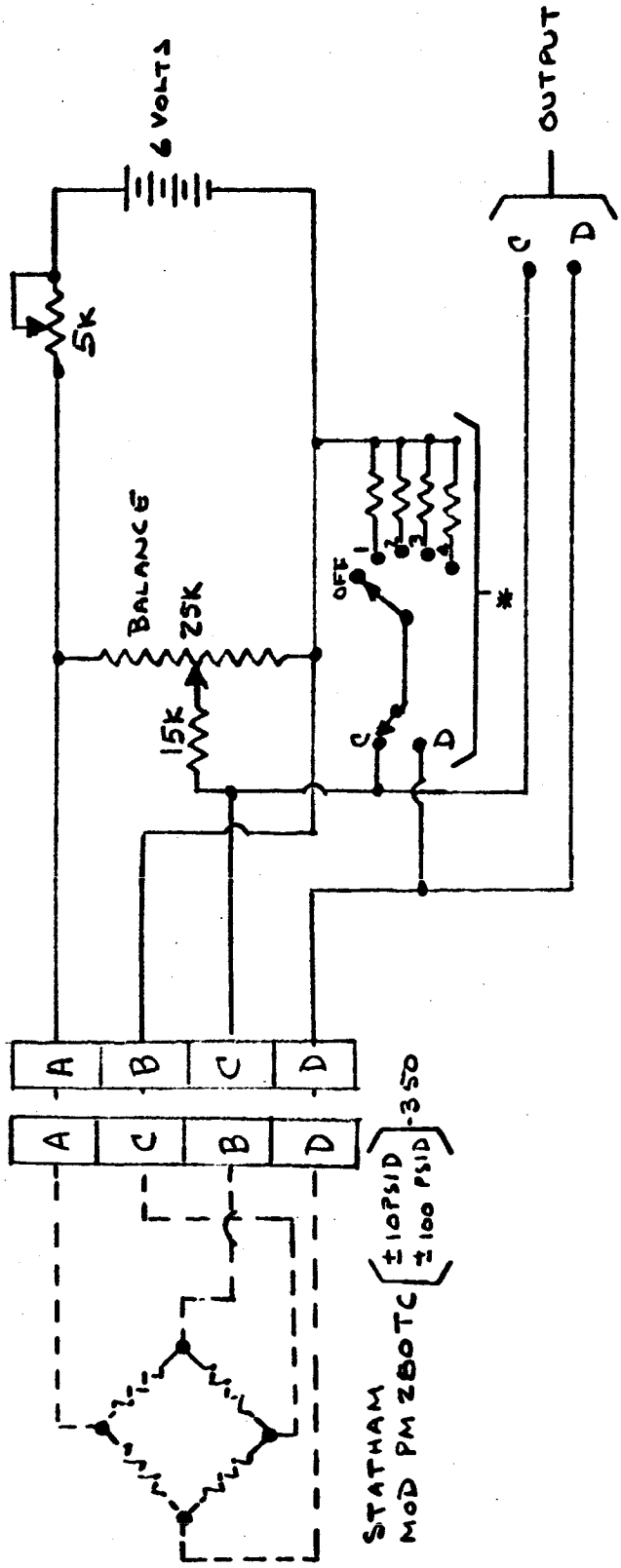

* CALIBRATION CIRCUIT
1) 560K, 2) 220K, 3) 104.5K, 4) 51K

FIGURE IV B-15

PRESSURE BRIDGE BALANCE NETWORK FOR PHASE MEASUREMENT

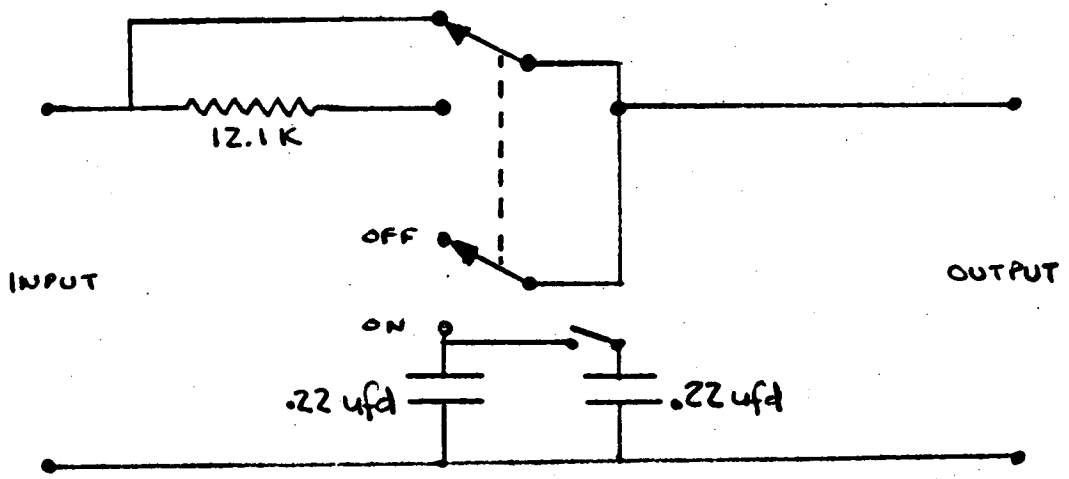

FIGURE IV B-16

PHASE SHIFTER (LAG) CIRCUIT

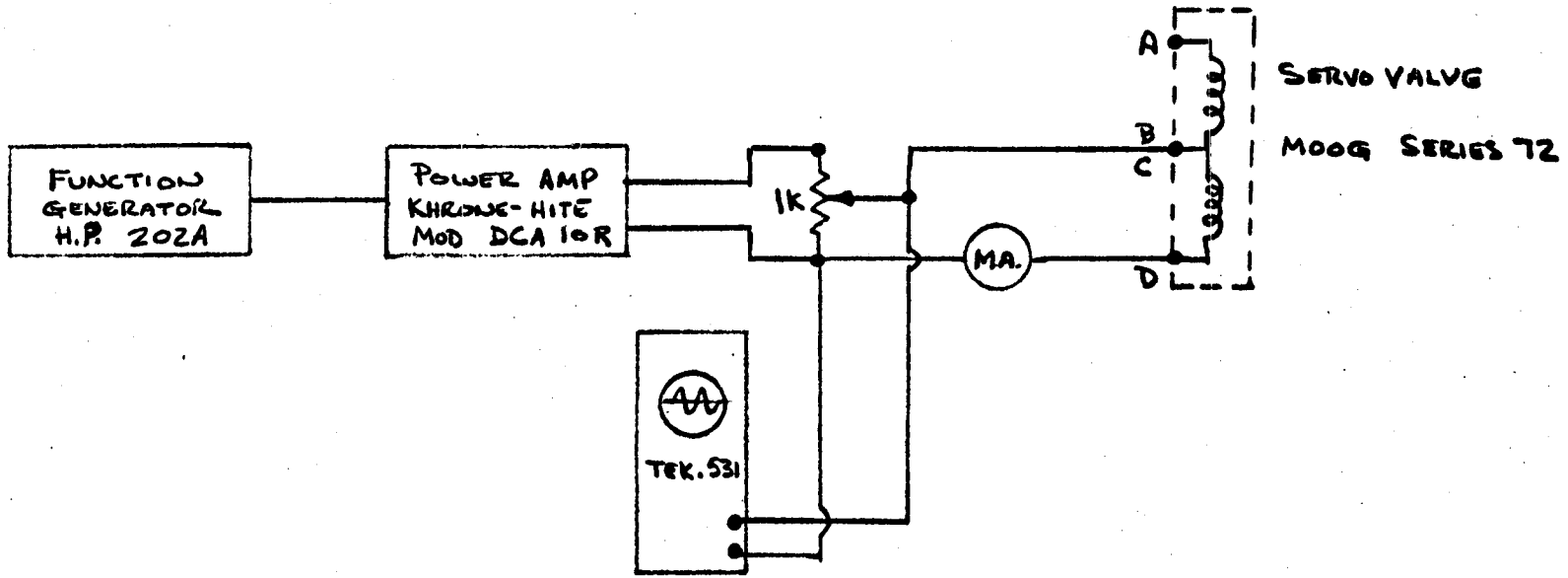

FIGURE IV B-17

BLOCK DIAGRAM OF HYDRAULIC EXCITATION SYSTEM

FIGURE V A-1
CAPILLARY FLOW VS PRESSURE
CYLINDER SER. NO. 1

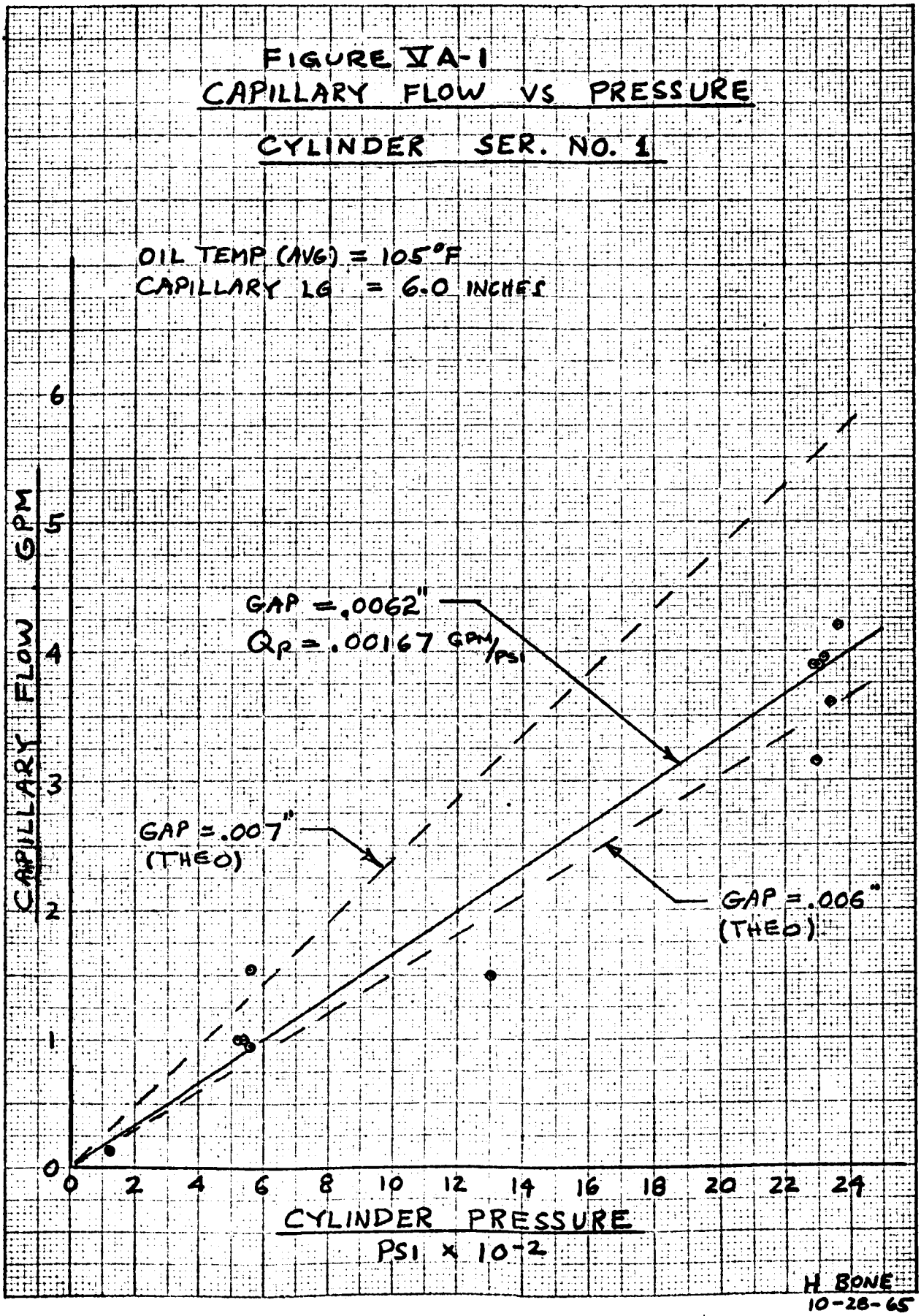

FIGURE V A-2

CAPILLARY FLOW VS PRESSURE

CYLINDER SER. NO. 2

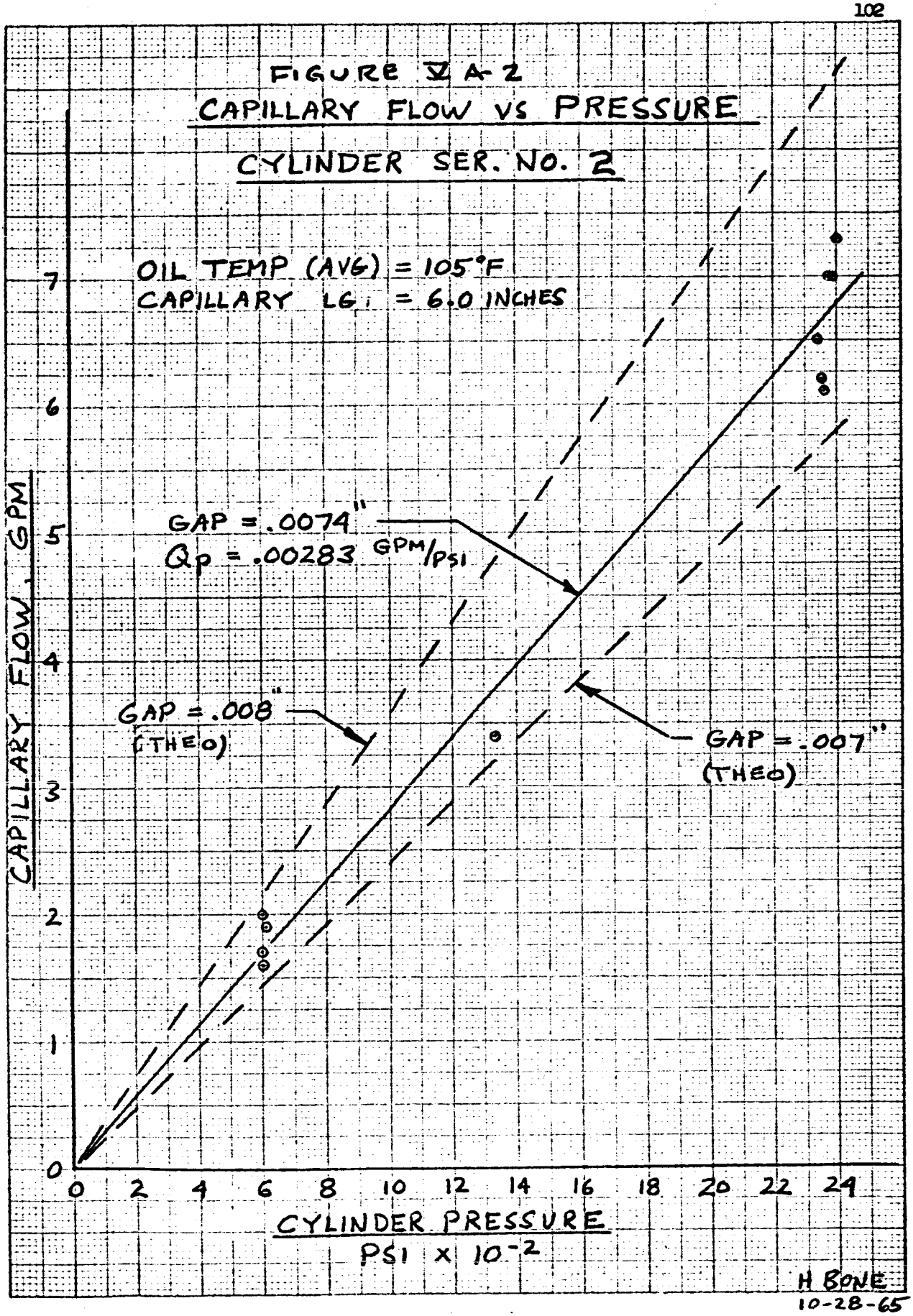

H BONE
10-28-65

FIGURE V A-3

CAPILLARY FLOW VS PRESSURE

CYLINDER SER. NO. 3

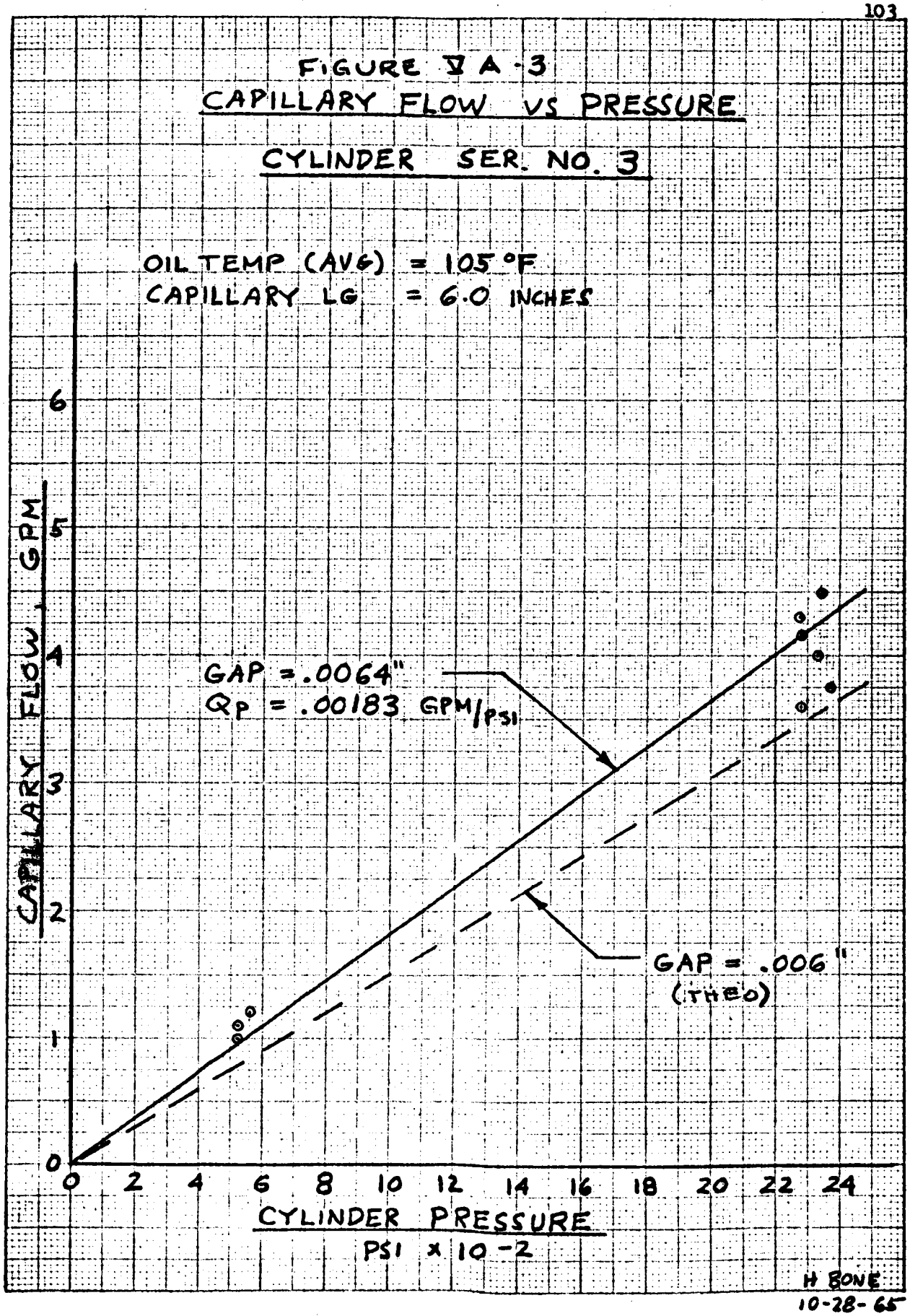

H BONE
10-28-65

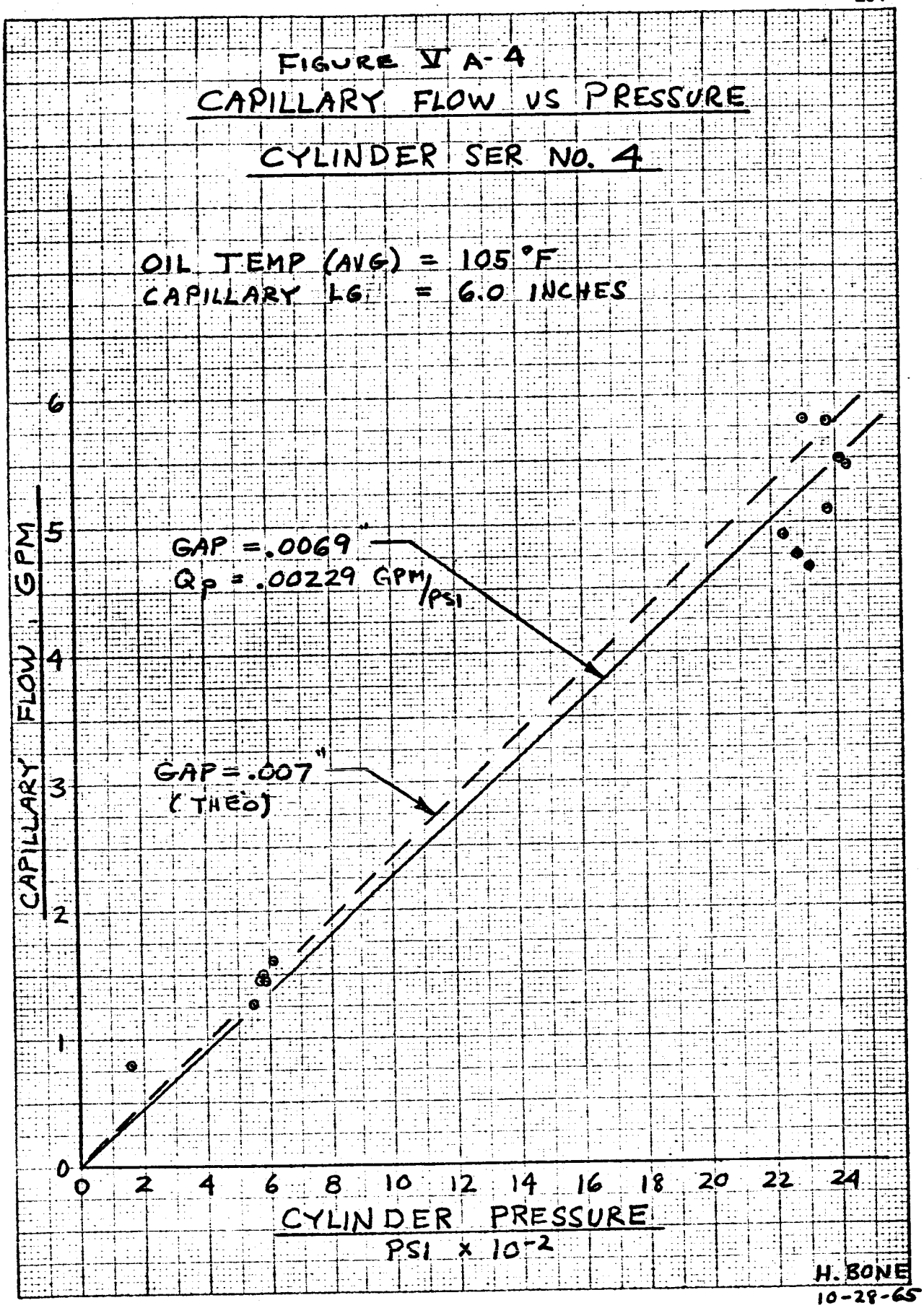
FIGURE V A-4
CAPILLARY FLOW VS PRESSURE
CYLINDER SER NO. 4
OIL TEMP (AVG) = 105 °F
CAPILLARY LG = 6.0 INCHES
GAP = .0069"
Qp = .00229 GPM/PSI
GAP = .007"
(THEO)
CAPILLARY FLOW, GPM
0
1
2
3
4
5
6
0 2 4 6 8 10 12 14 16 18 20 22 24
CYLINDER PRESSURE
PSI x 10-2
H. BONE
10-28-65

FIGURE IV A-5
CAPILLARY FLOW VS LENGTH
CYLINDER SER NO 2.

OIL TEMP (AVG) = 105°F

——— FLOW WITH NO GAP DEFLECTION

– – – FLOW CORRECTED FOR THEO. GAP DEFLECTION

⊙— TEST DATA (NUMBERS INDICATE TEST NO.)

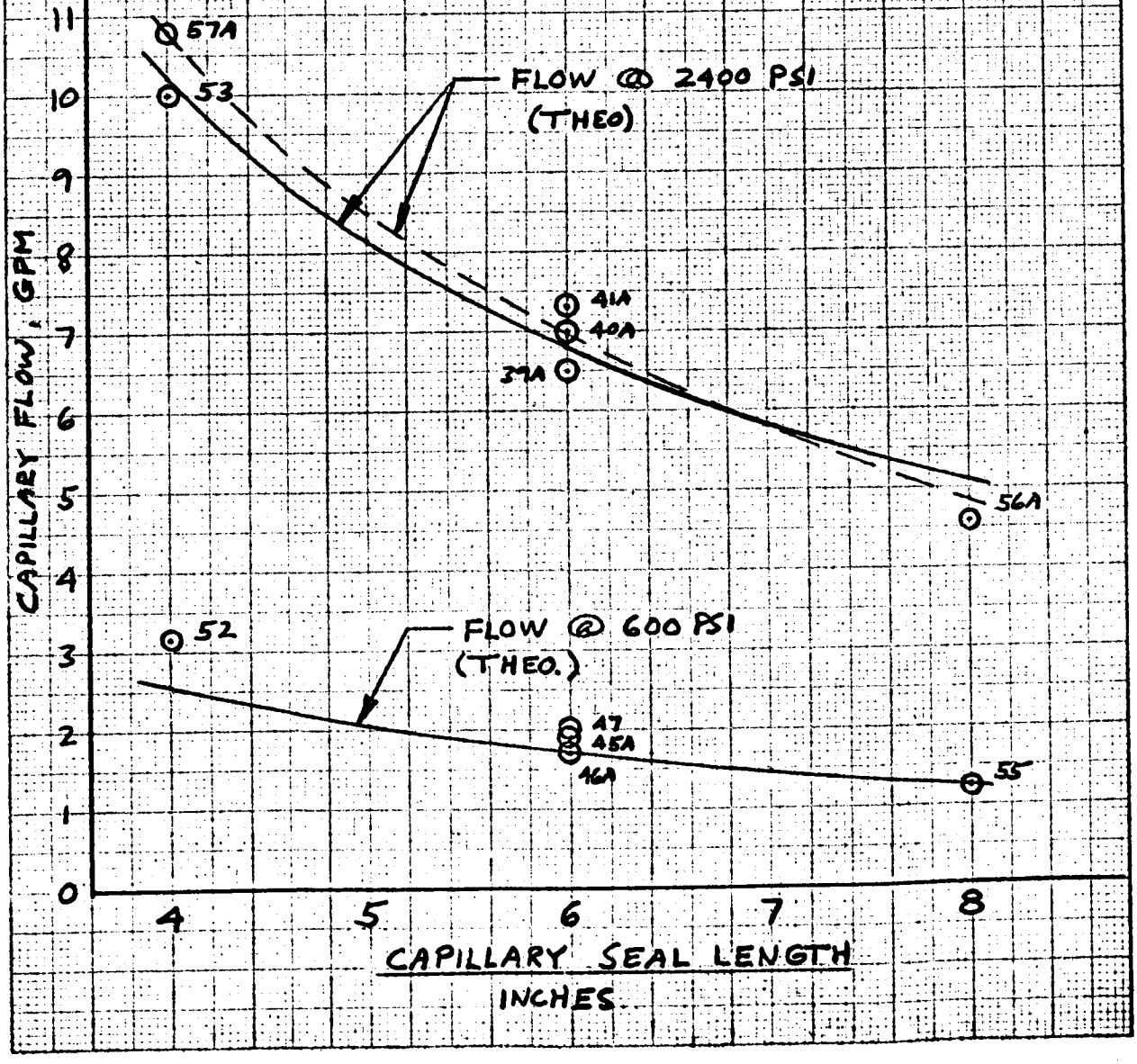

FIGURE V A-6
CAPILLARY FLOW vs LENGTH
CYLINDER SER NO. 4

OIL TEMP (AVG) = 105°F

——— FLOW WITH NO GAP DEFLECTION

- - - - FLOW CORRECTED FOR THEO. GAP DEFLECTION

⊙ — TEST DATA (NUMBERS REFER TO TEST NO.)

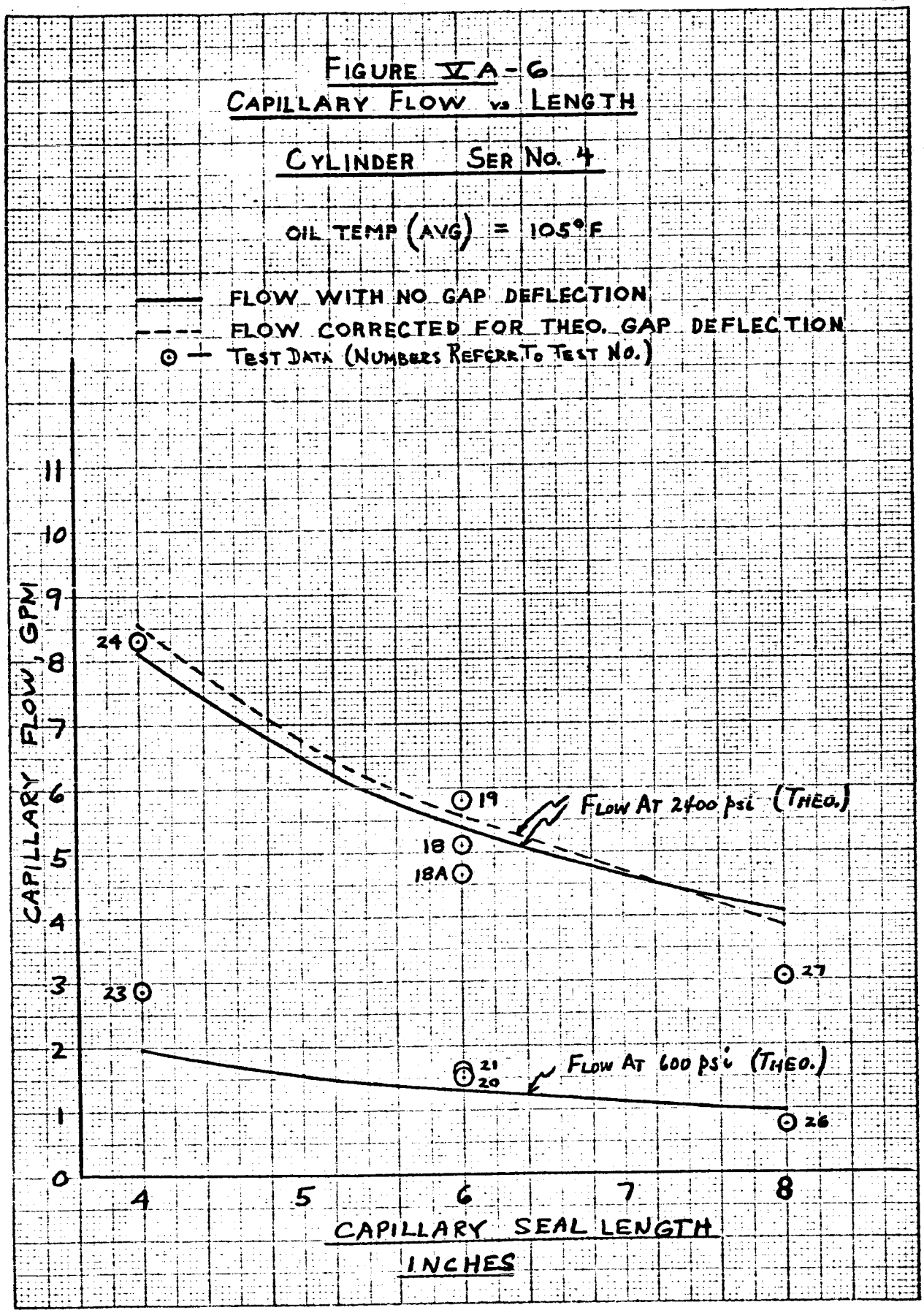

FIGURE V A-7

HUMBLE NUTO 146 OIL VISCOSITY VS. TEMPERATURE

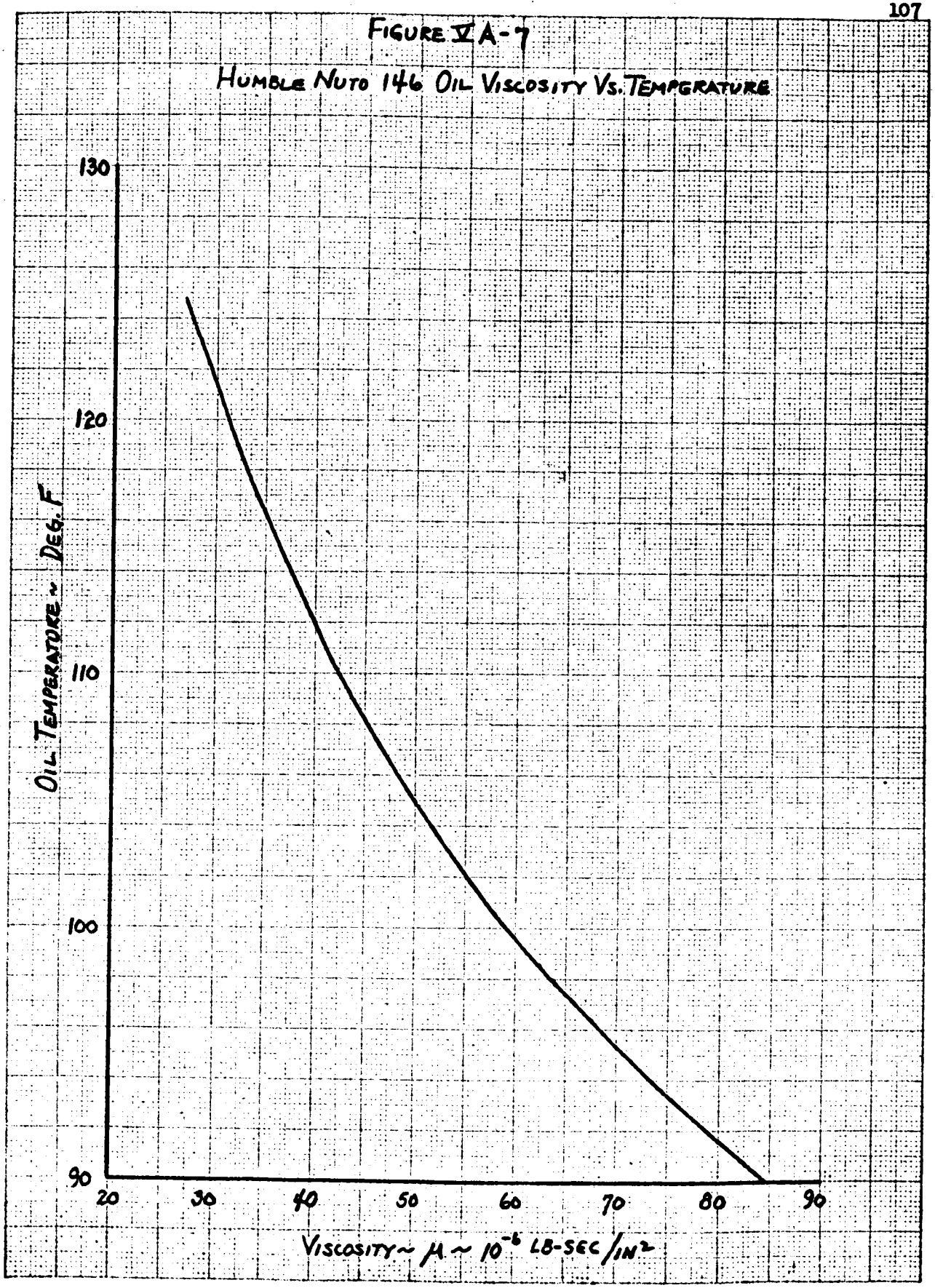

FIGURE V A-8
FLAT BEARING
PRESSURE AND GAP VS LOAD
CYL. NO. 2, TEST NOS. 2, 3, 4, 4A, 5 & 5A

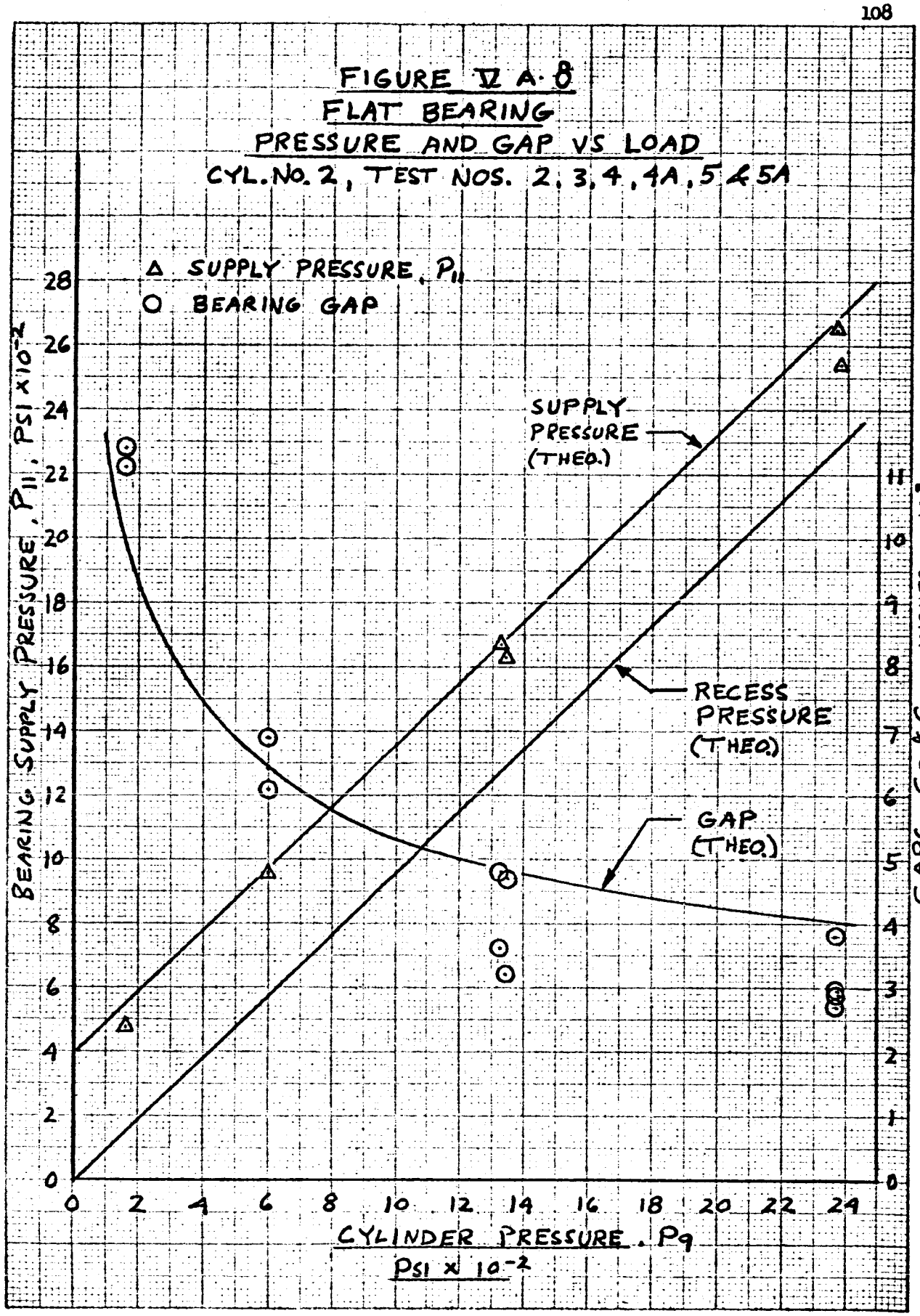

FIGURE VA-9
SPHERICAL BEARING
PRESSURE AND GAP VS LOAD
CYL. NO. 2, TEST NOS. 2, 3, 4, 4A, 5, & 5A

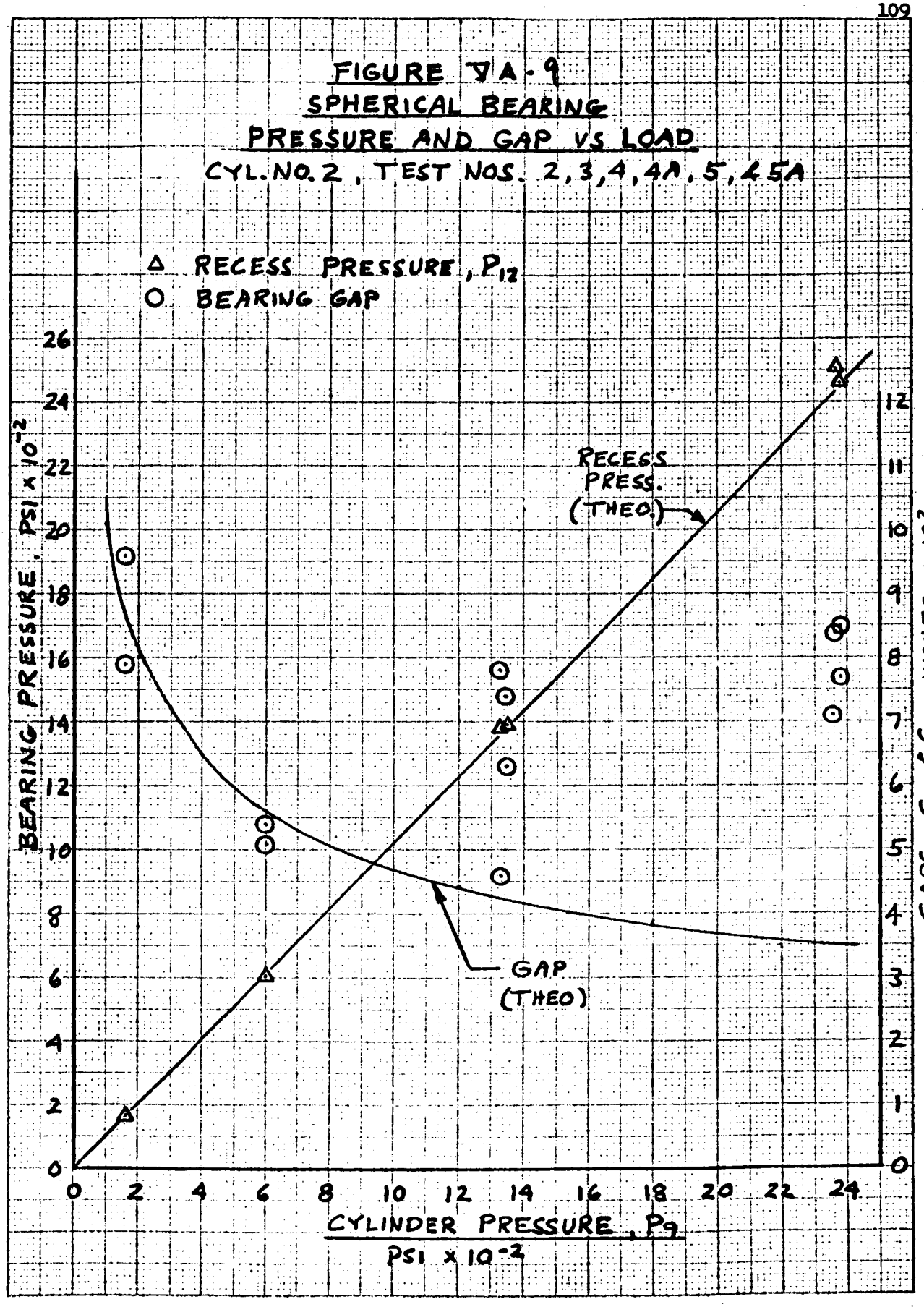

FIGURE IV A-10

TEST NO. 36

AIR SPRING PRESSURE LOSS

(PISTON-CYL. NO. 4, 1.8 × 10⁶ LB BEARING LOAD, 6" CAPILLARY SEAL)

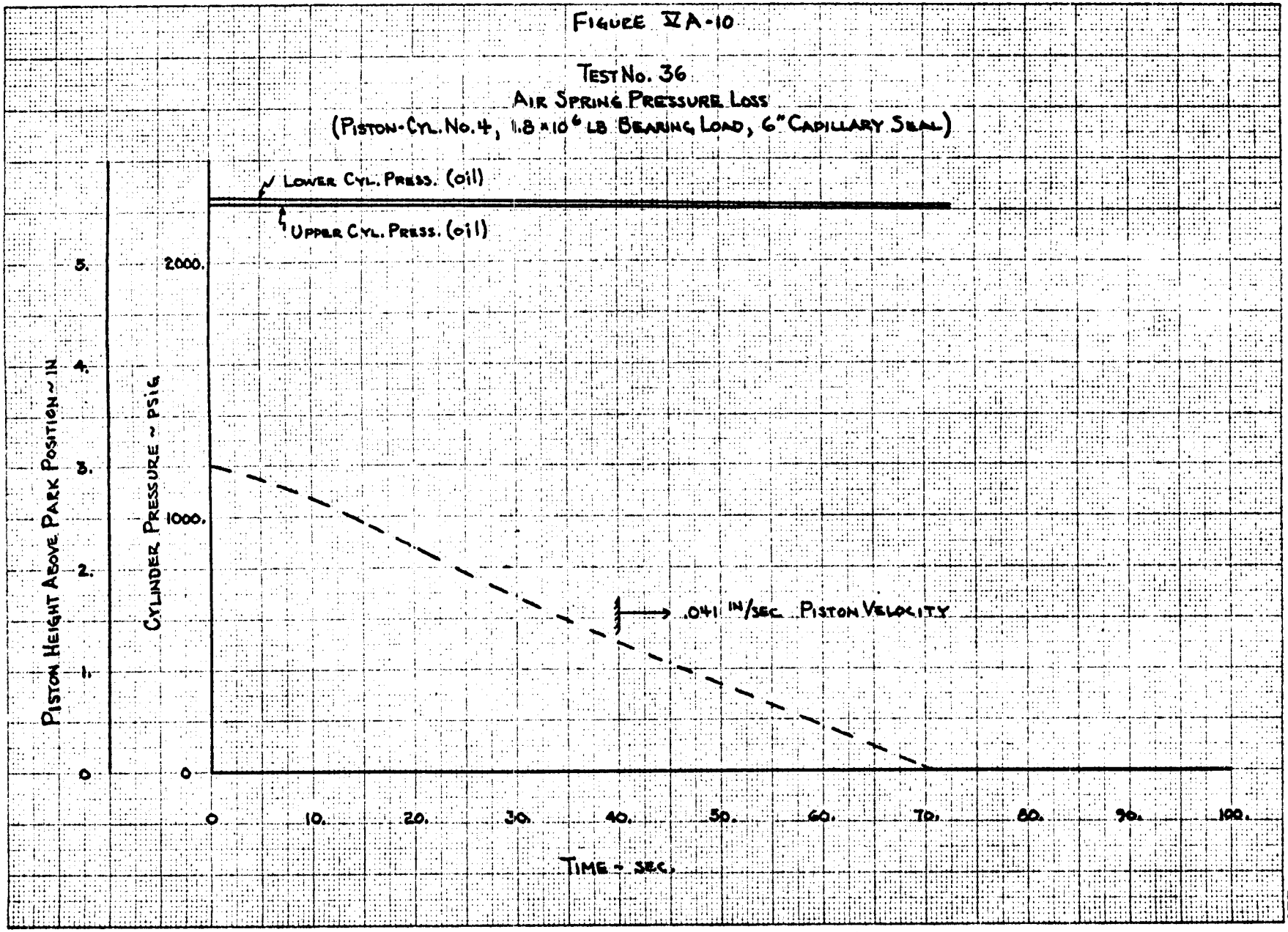

FIGURE V A-11

TEST NO. 33

HYDRODYNAMIC SUPPORT SINK RATE FROM OPERATE TO PARK POSITION

(PISTON CYL. NO. 4, 0.1 $\times 10^6$ LB BEARING LOAD, 6" CAPILLARY SEAL)

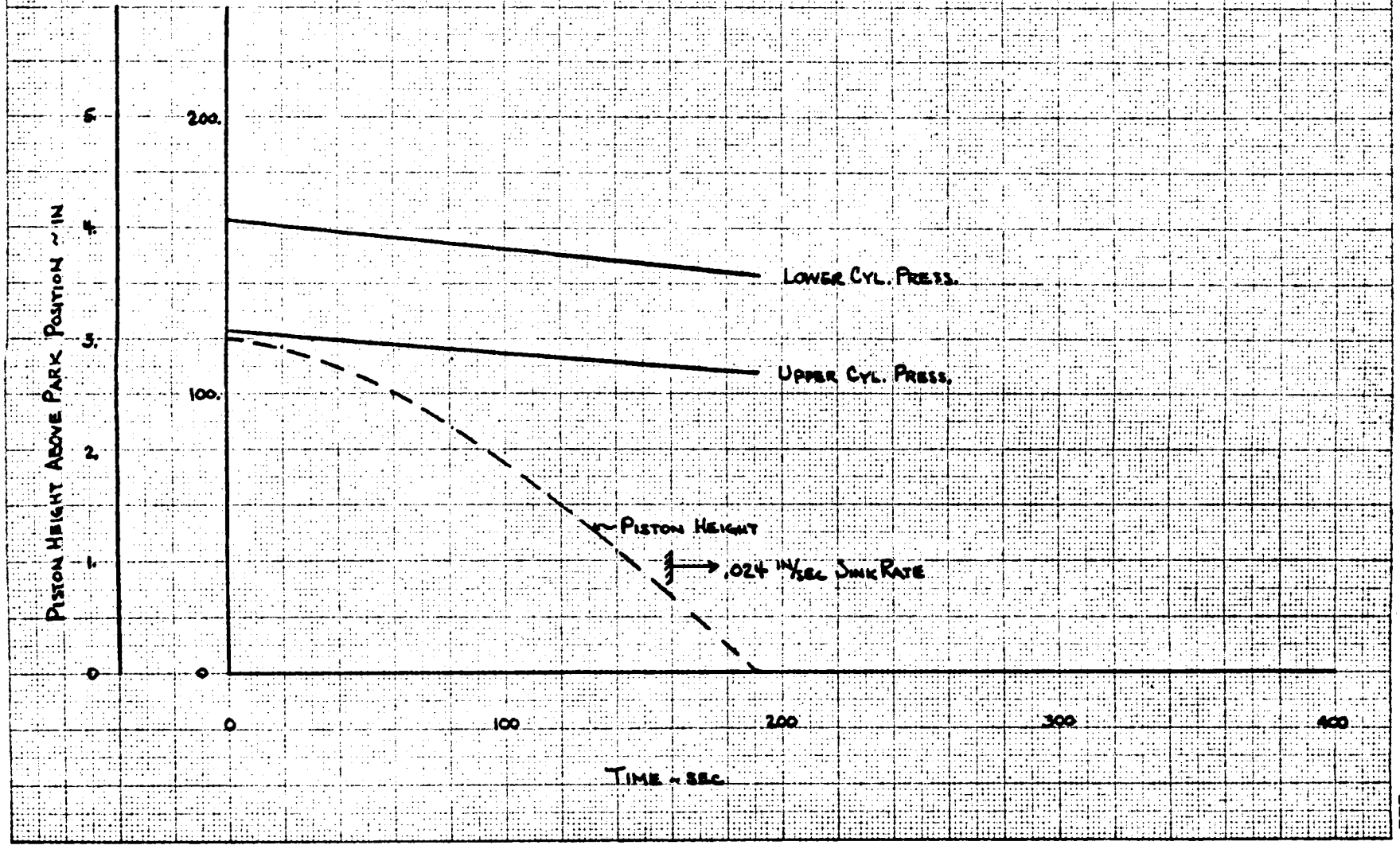

FIGURE V A-12

TEST No. 29

HYDRODYNAMIC SUPPORT SINK RATE FROM OPERATE TO PARK POSITION

(PISTON-CYL. No. 4, 1.8×10^6 LB BEARING LOAD, 6" CAPILLARY SEAL)

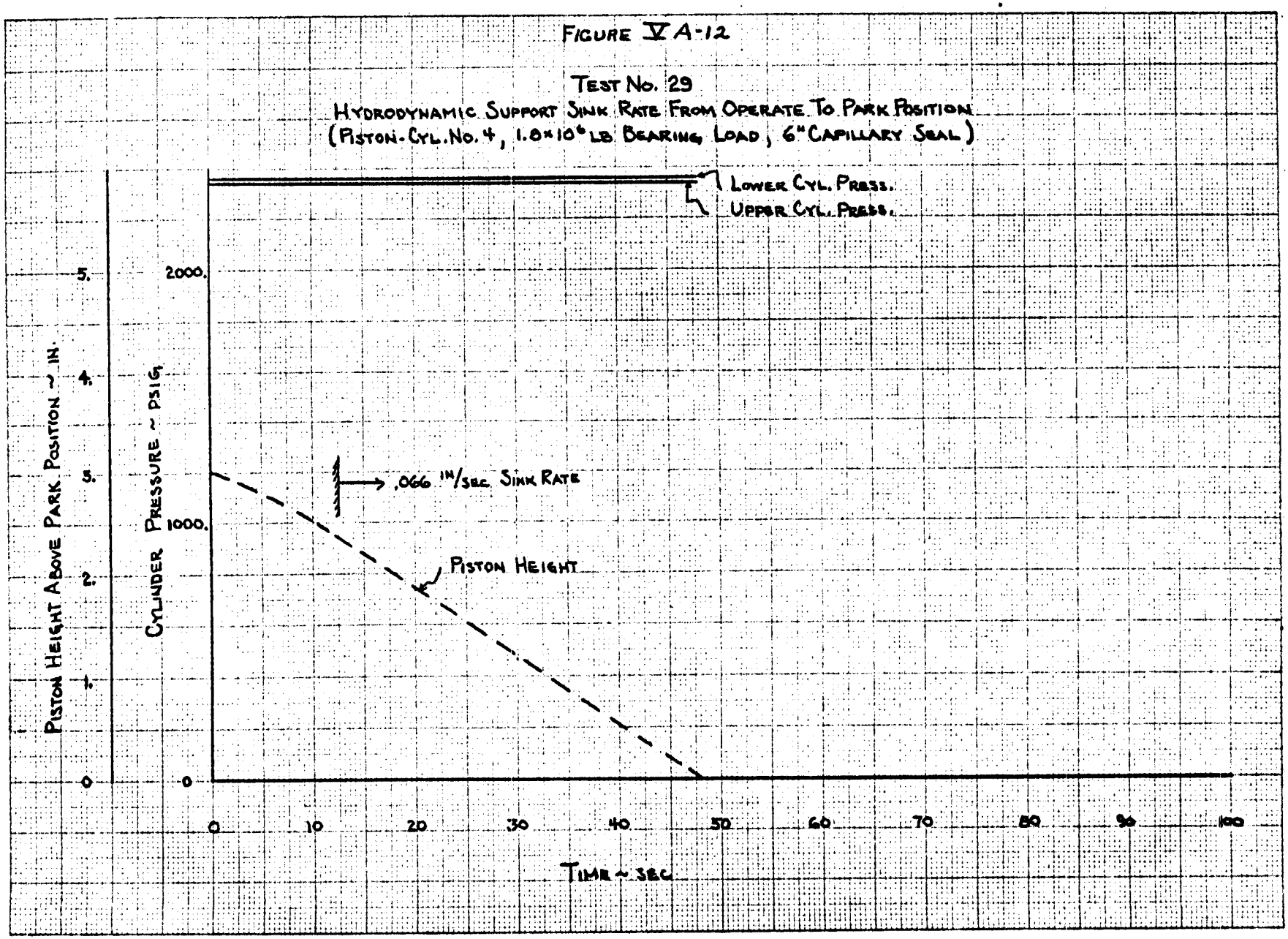

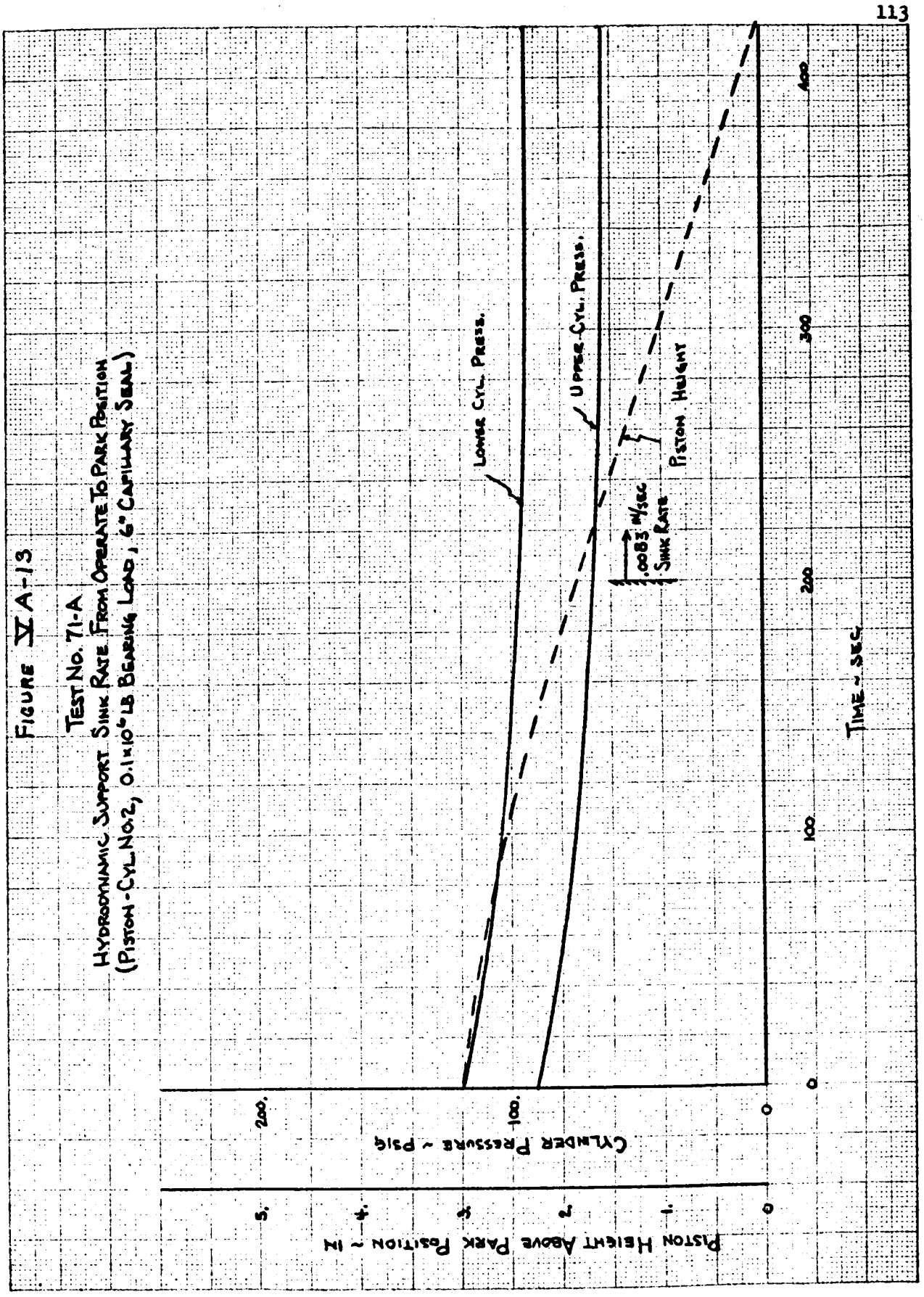

FIGURE V A-13

TEST NO. 71-A

HYDRODYNAMIC SUPPORT SINK RATE FROM OPERATE TO PARK POSITION
(PISTON-CYL NO.2, 0.1×10⁶ LB BEARING LOAD, 6° CAPILLARY SEAL)

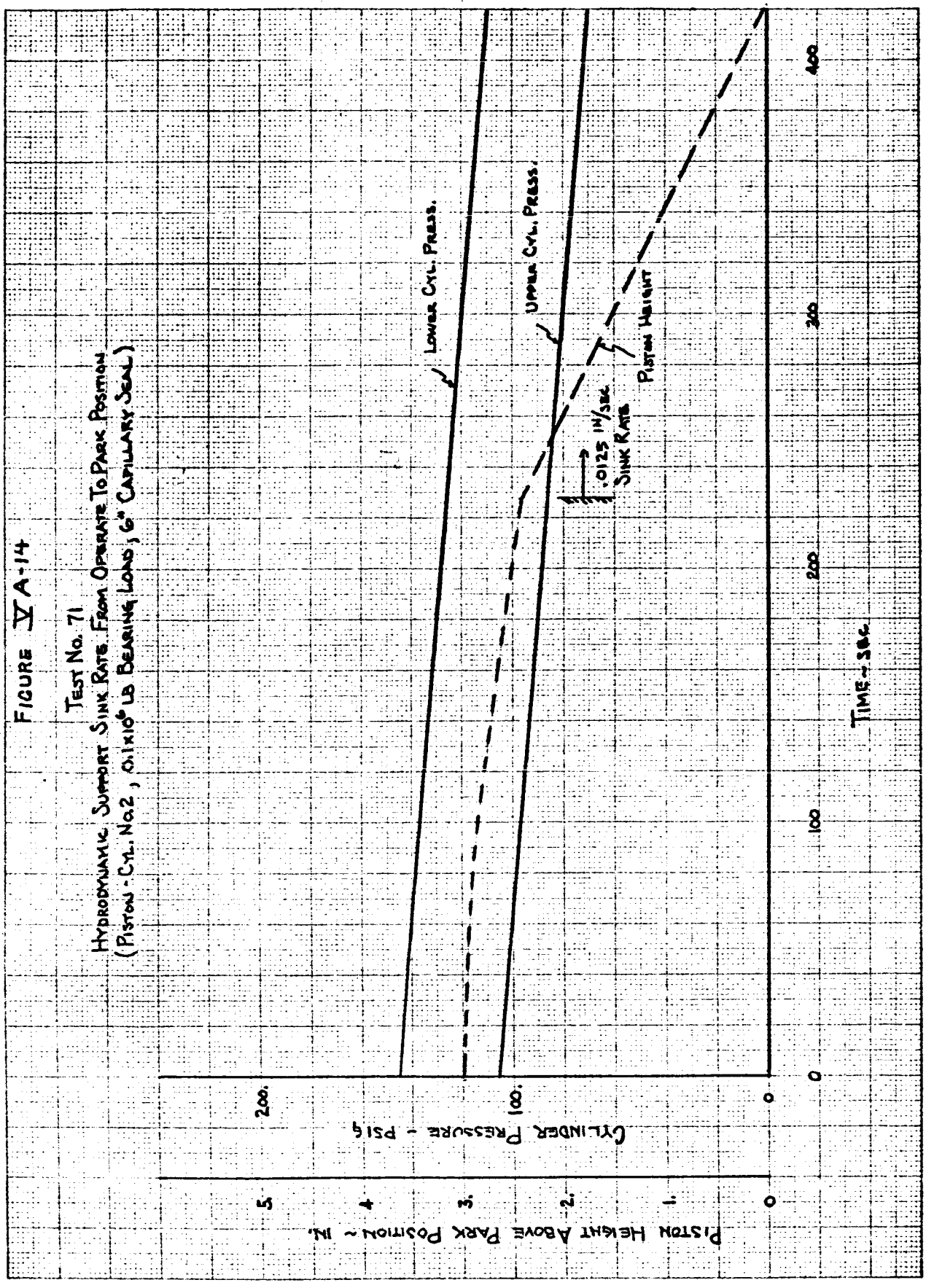

FIGURE V A-14

TEST No. 71

HYDRODYNAMIC SUPPORT SINK RATE FROM OPERATE TO PARK POSITION
(PISTON - CYL. No. 2, .01x10⁶ LB BEARING LOAD, 6" CAPILLARY SEAL)

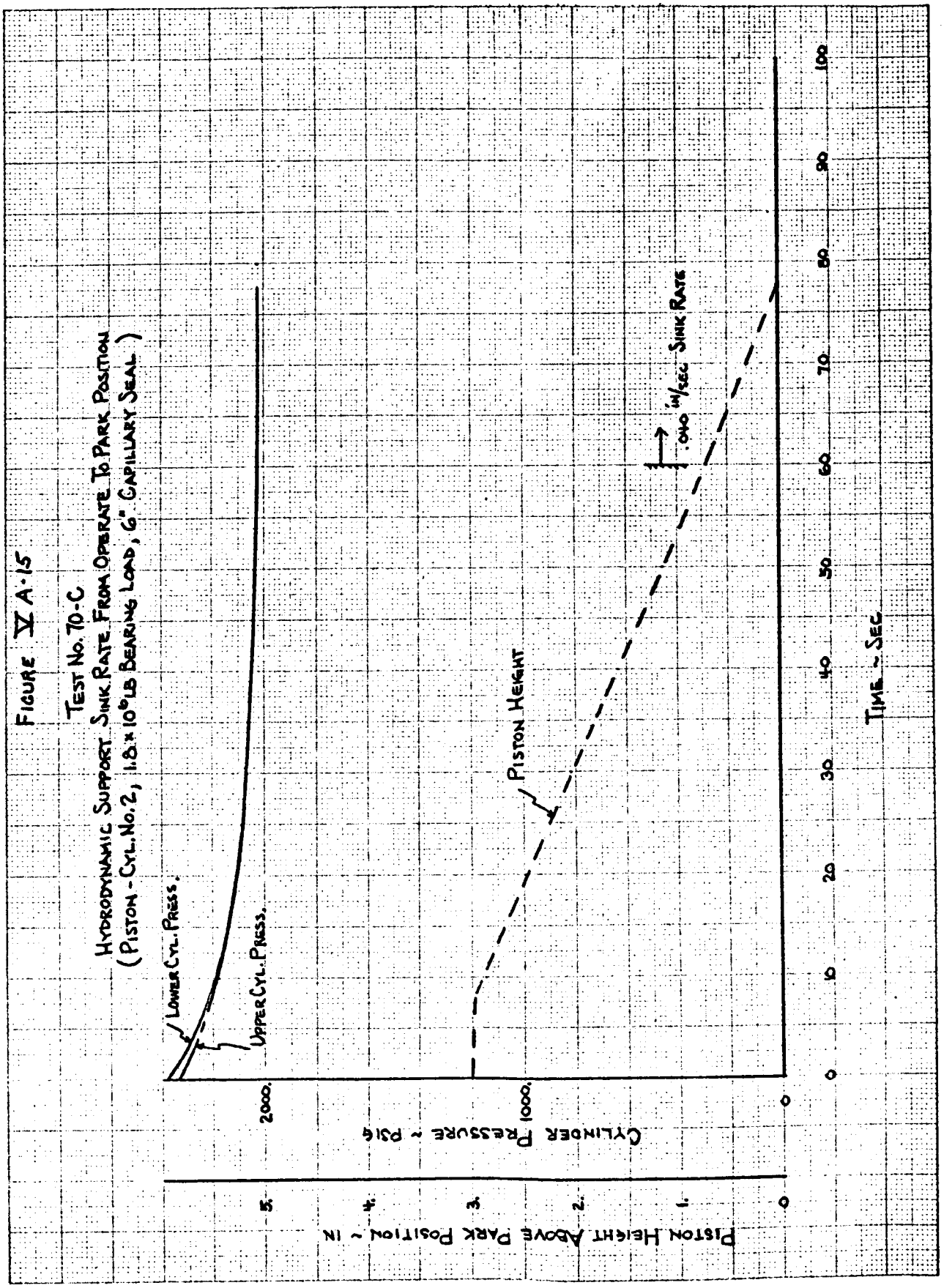

FIGURE V A-15

TEST NO. 70-C

HYDRODYNAMIC SUPPORT SINK RATE FROM OPERATE TO PARK POSITION
(PISTON - CYL. NO. 2, 1.8 × 10⁶ LB BEARING LOAD, 6" CAPILLARY SEAL)

FIGURE V A-16

TEST NO. 70-B

HYDRODYNAMIC SUPPORT SINK RATE FROM OPERATE TO PARK POSITION

(PISTON-CYL. NO. 2, 1.8×10^6 LB BEARING LOAD, 6" CAPILLARY SEAL)

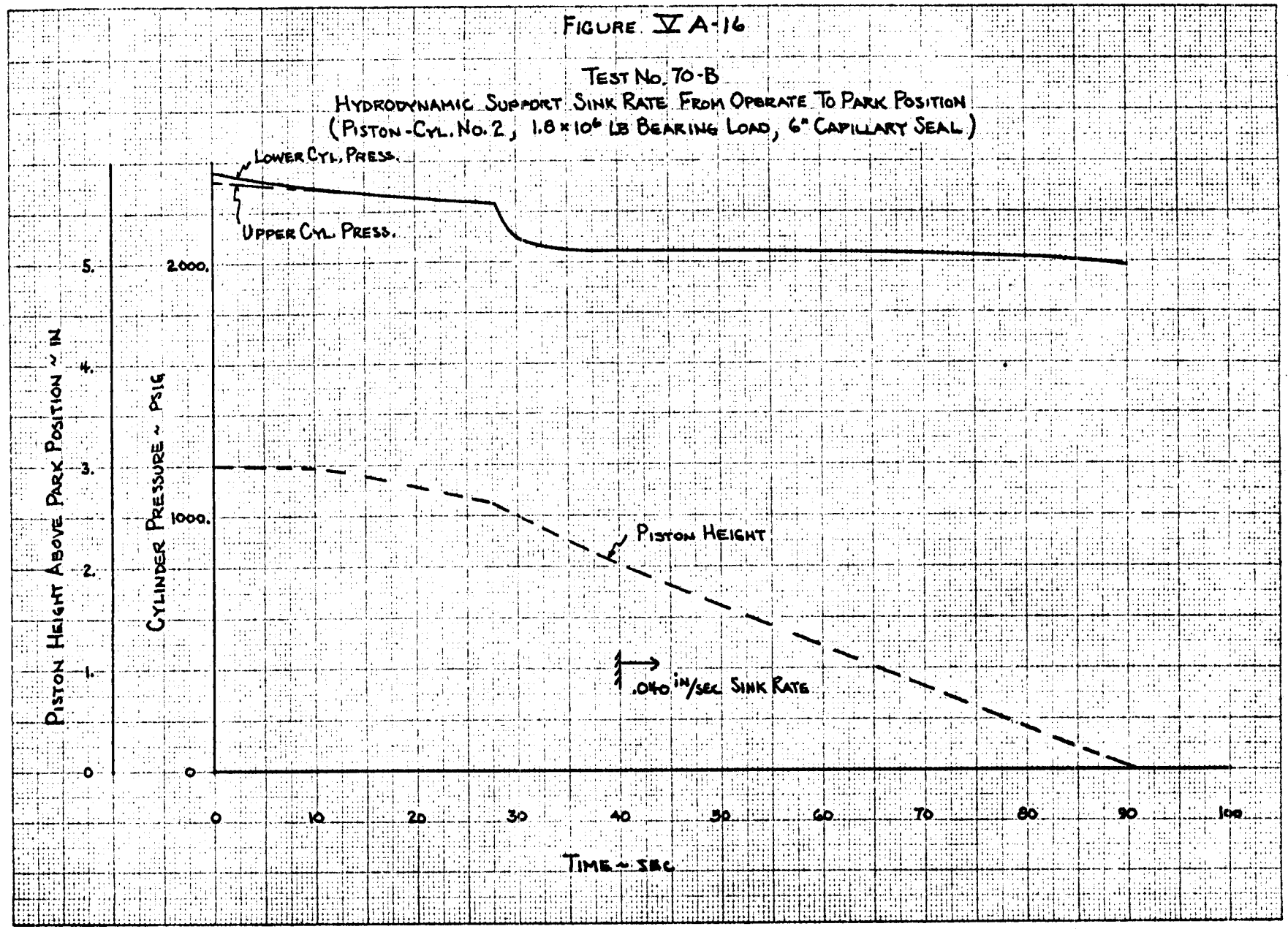

FIGURE V A-17

TEST NO. 70-A

HYDRODYNAMIC SUPPORT SINK RATE FROM OPERATE TO PARK POSITION

(PISTON-CYL. NO. 2 , 1.8×10⁴ LB BEARING LOAD , 6" CAPILLARY SEAL)

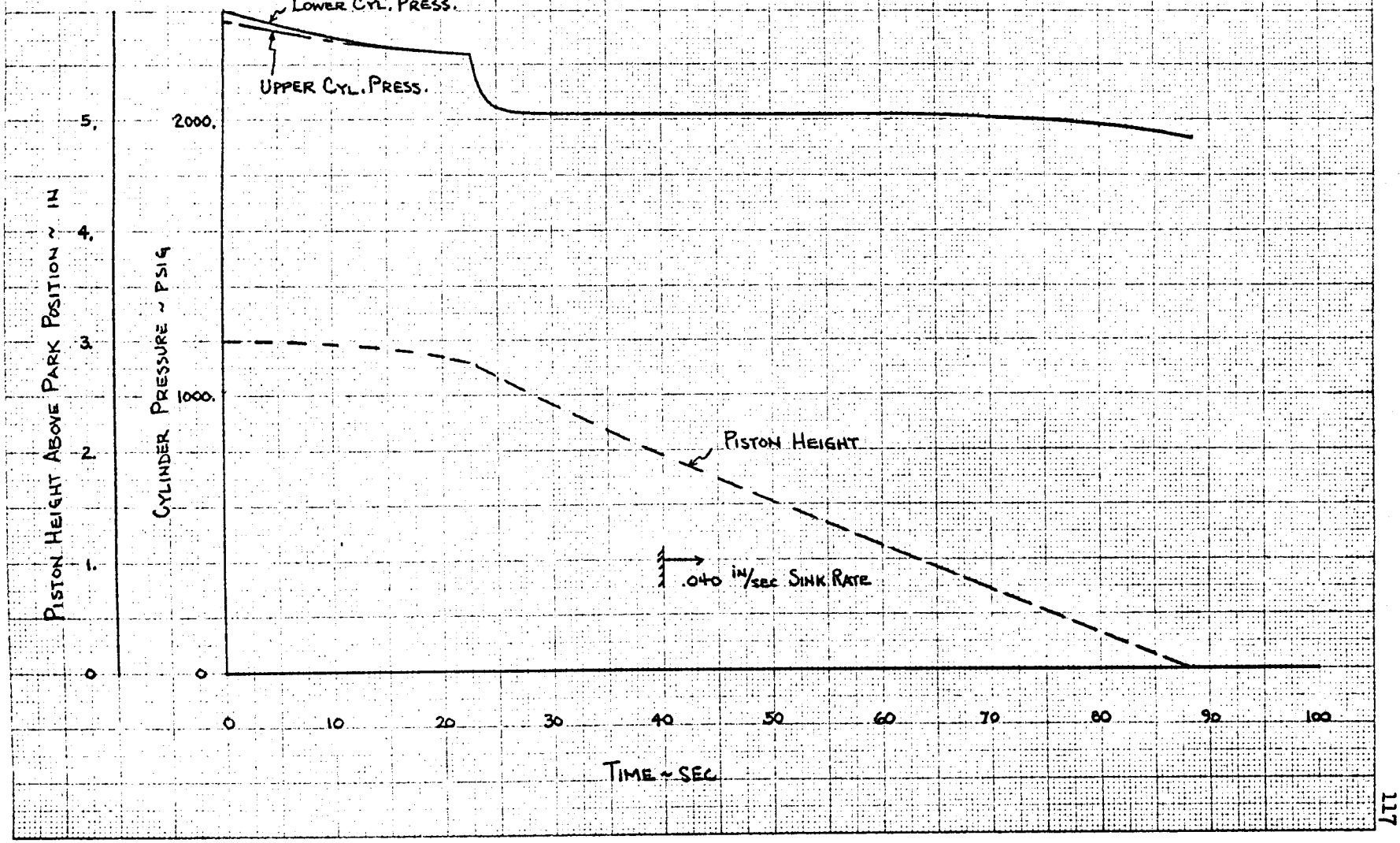

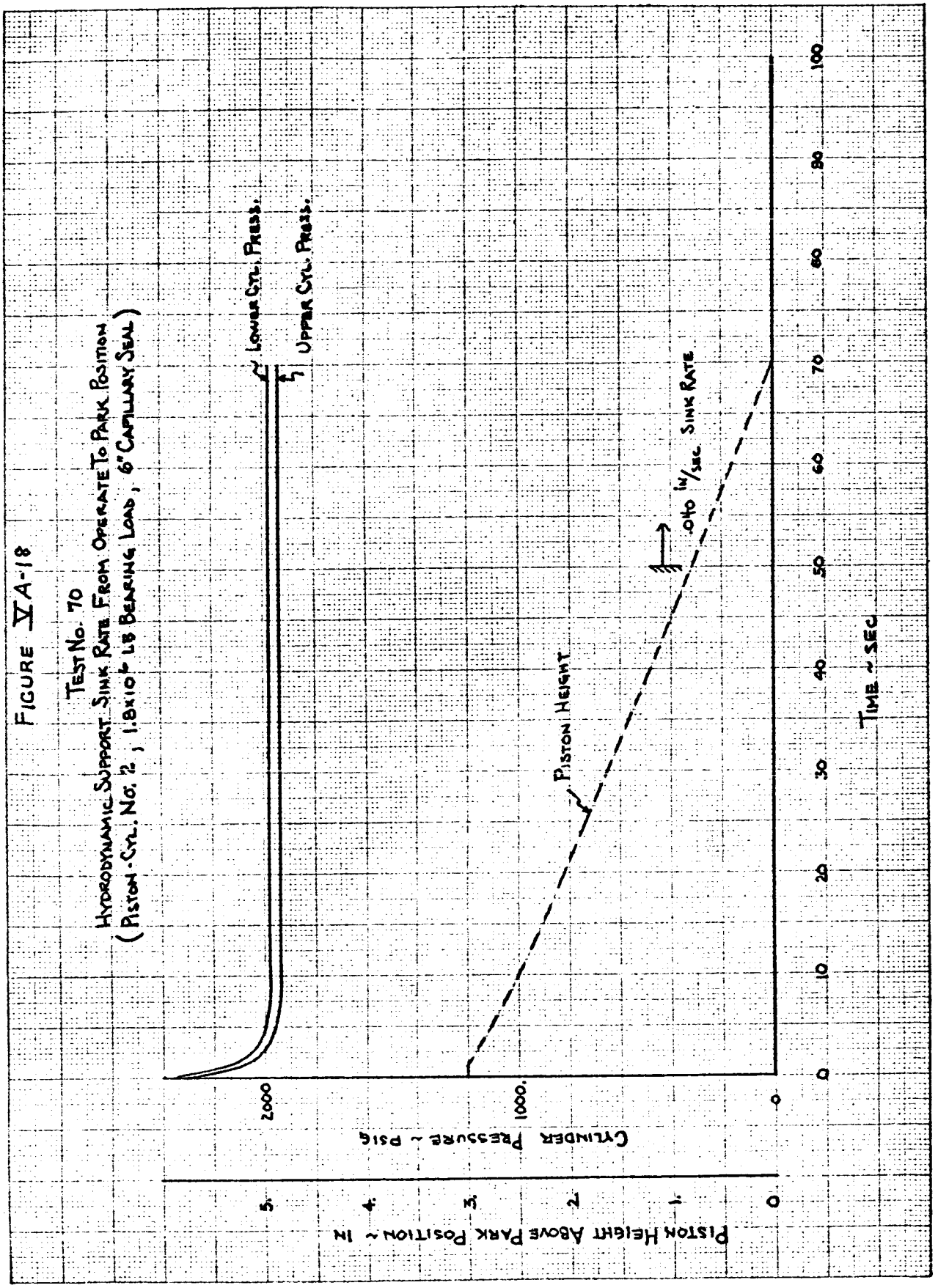

FIGURE IV A-18

TEST NO. 70

HYDRODYNAMIC SUPPORT SINK RATE FROM OPERATE TO PARK POSITION

(PISTON-CYL. NO. 2, 1.8X10⁶ LB BEARING LOAD, 6" CAPILLARY SEAL)

FIGURE V B-1

ACCELERATION AMPLITUDES FROM TEST NO. 62
(VERTICAL VIBRATION SURVEY)

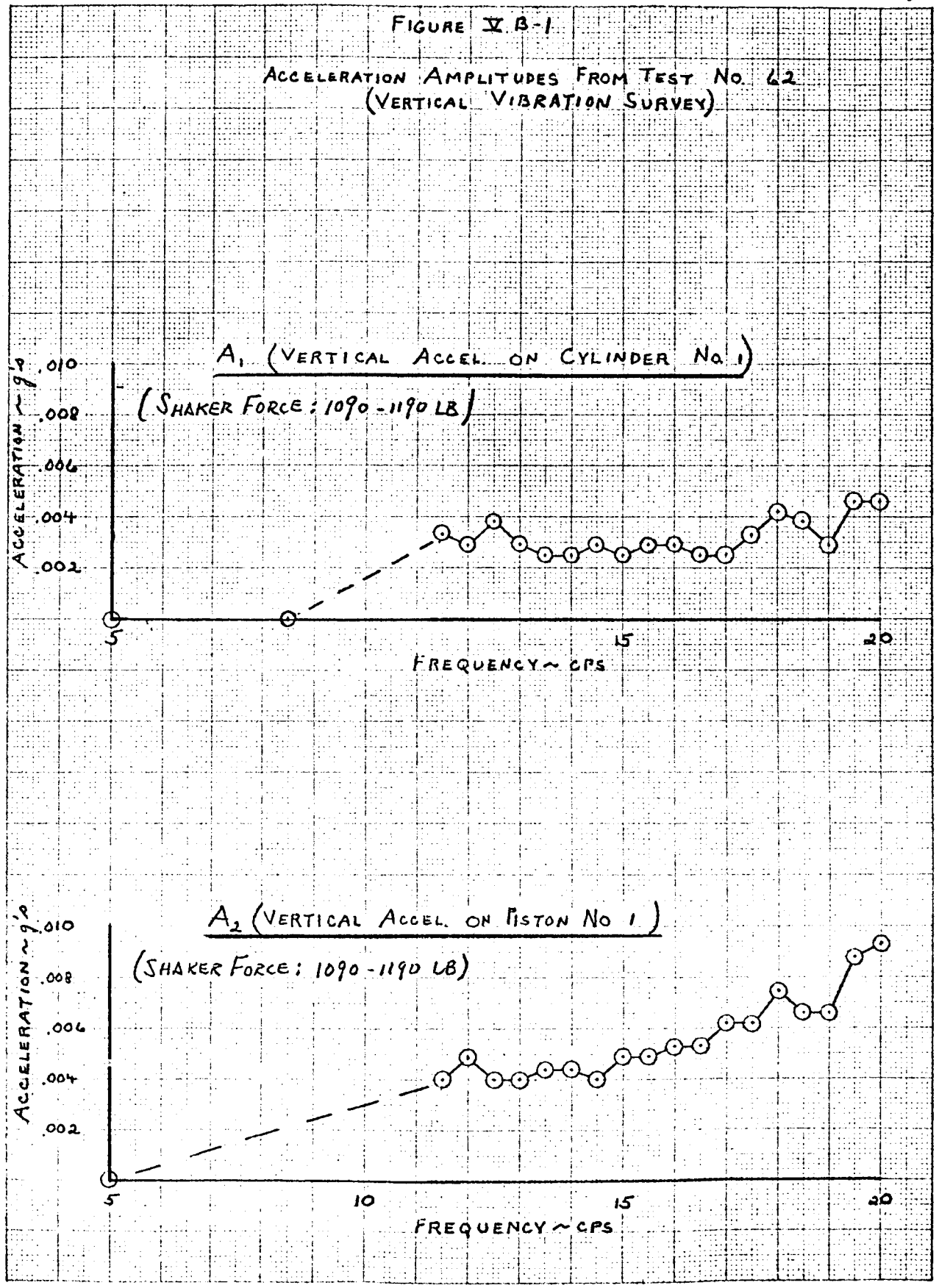

FIGURE V B-2

ACCELERATION AMPLITUDES FROM TEST NO 62
(VERTICAL VIBRATION SURVEY)

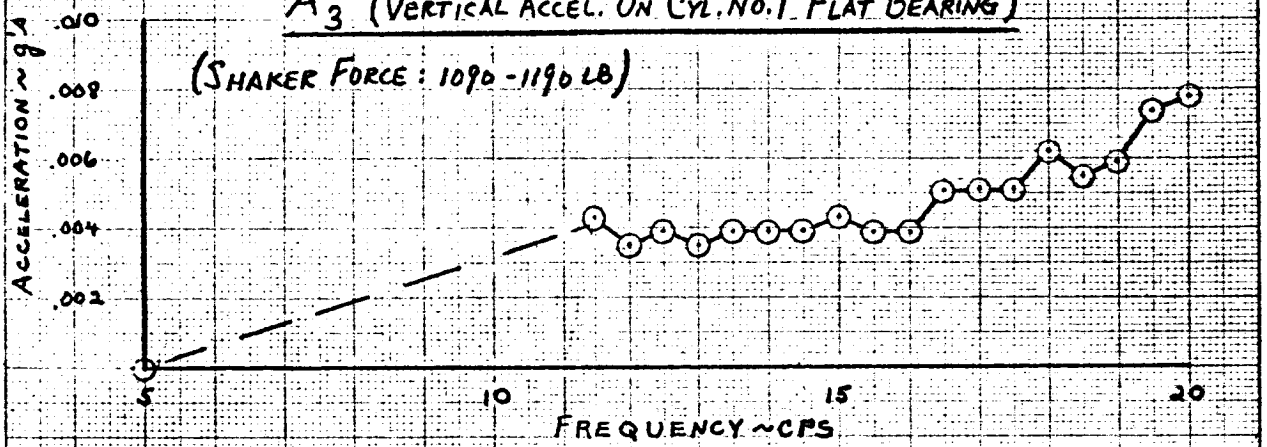

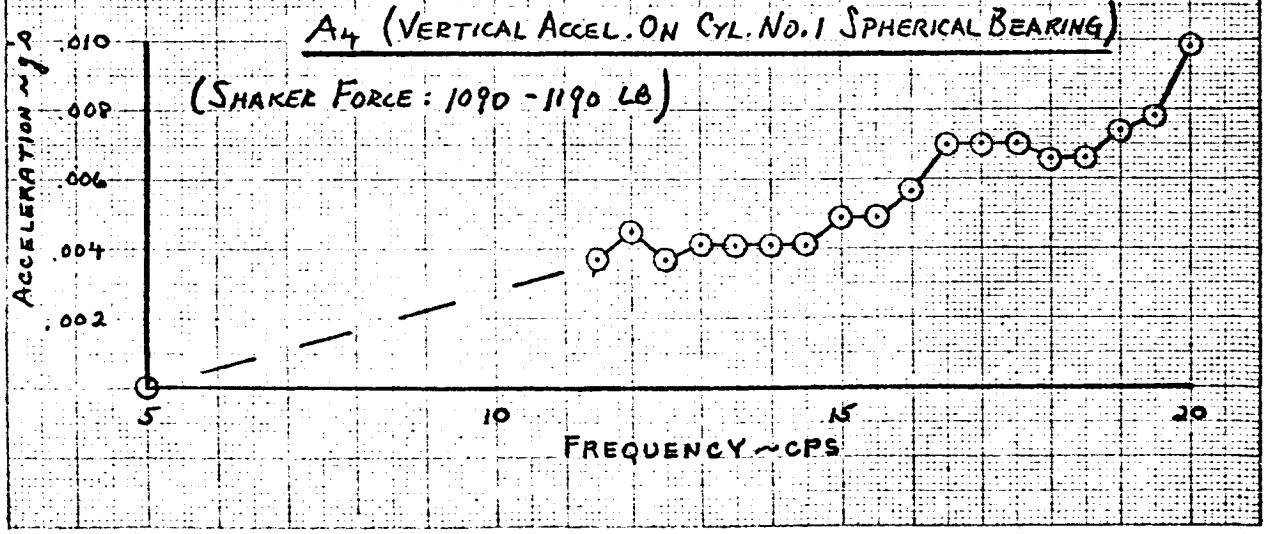

FIGURE V B-3

ACCELERATION AMPLITUDES FROM TEST NO. 62
(VERTICAL VIBRATION SURVEY)

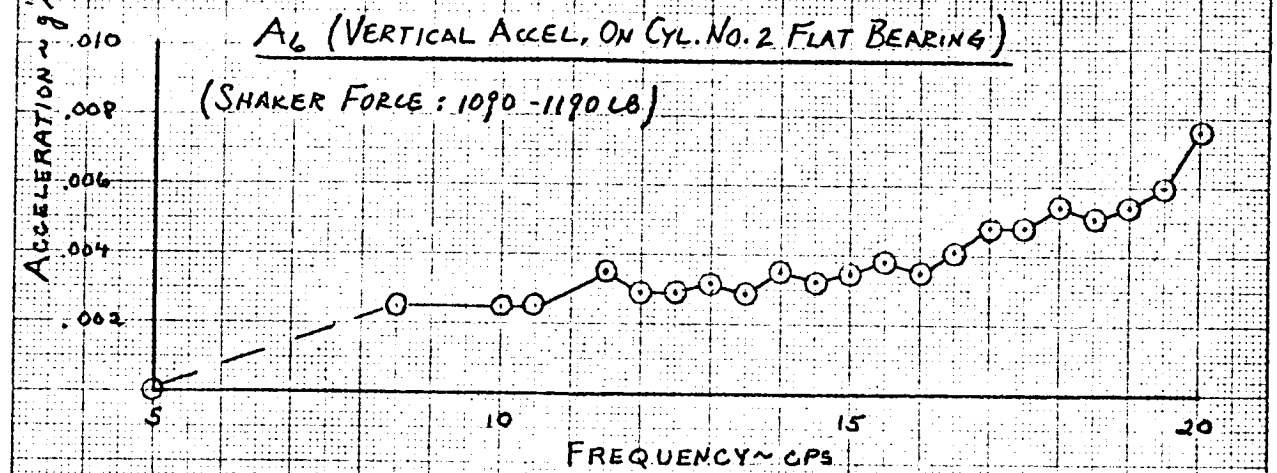

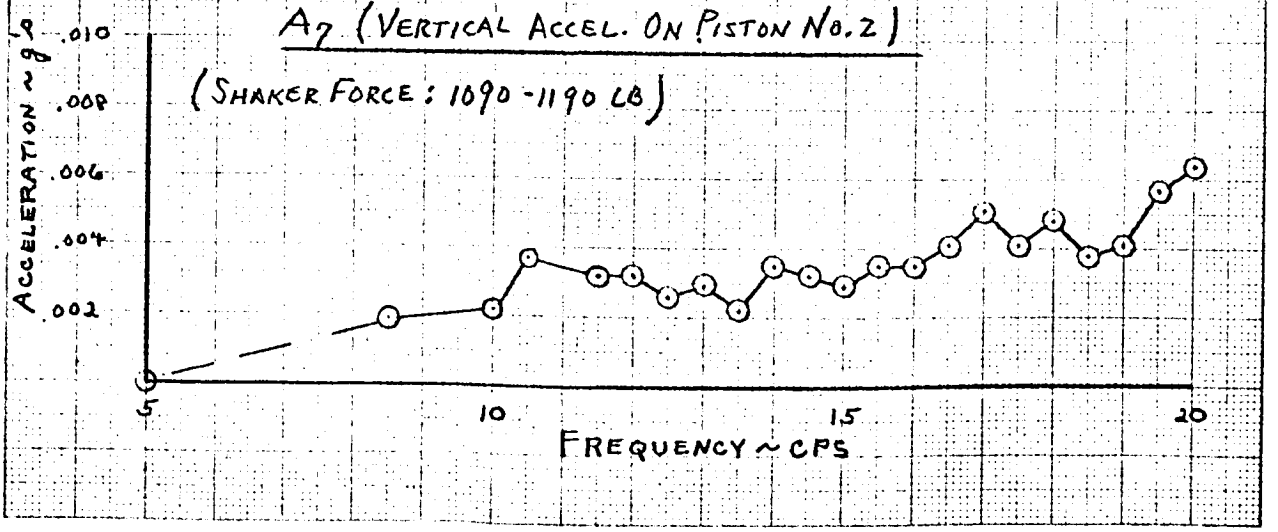

FIGURE V B-4

ACCELERATION AMPLITUDES FROM TEST No. 62
(VERTICAL VIBRATION SURVEY)

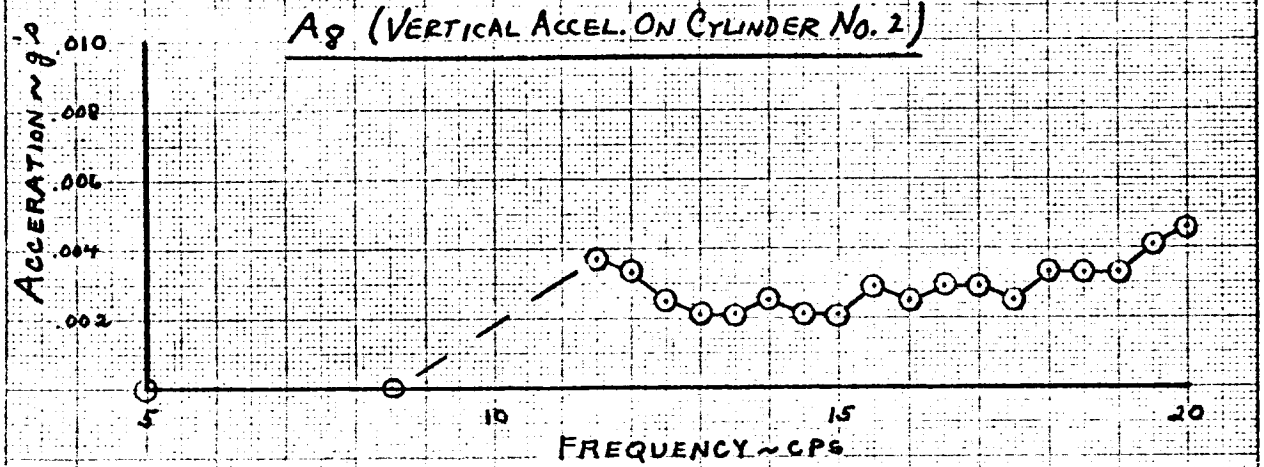

FIGURE V.B-5

ACCELERATION AMPLITUDES FROM TEST NO. 63
(LATERAL VIBRATION SURVEY)

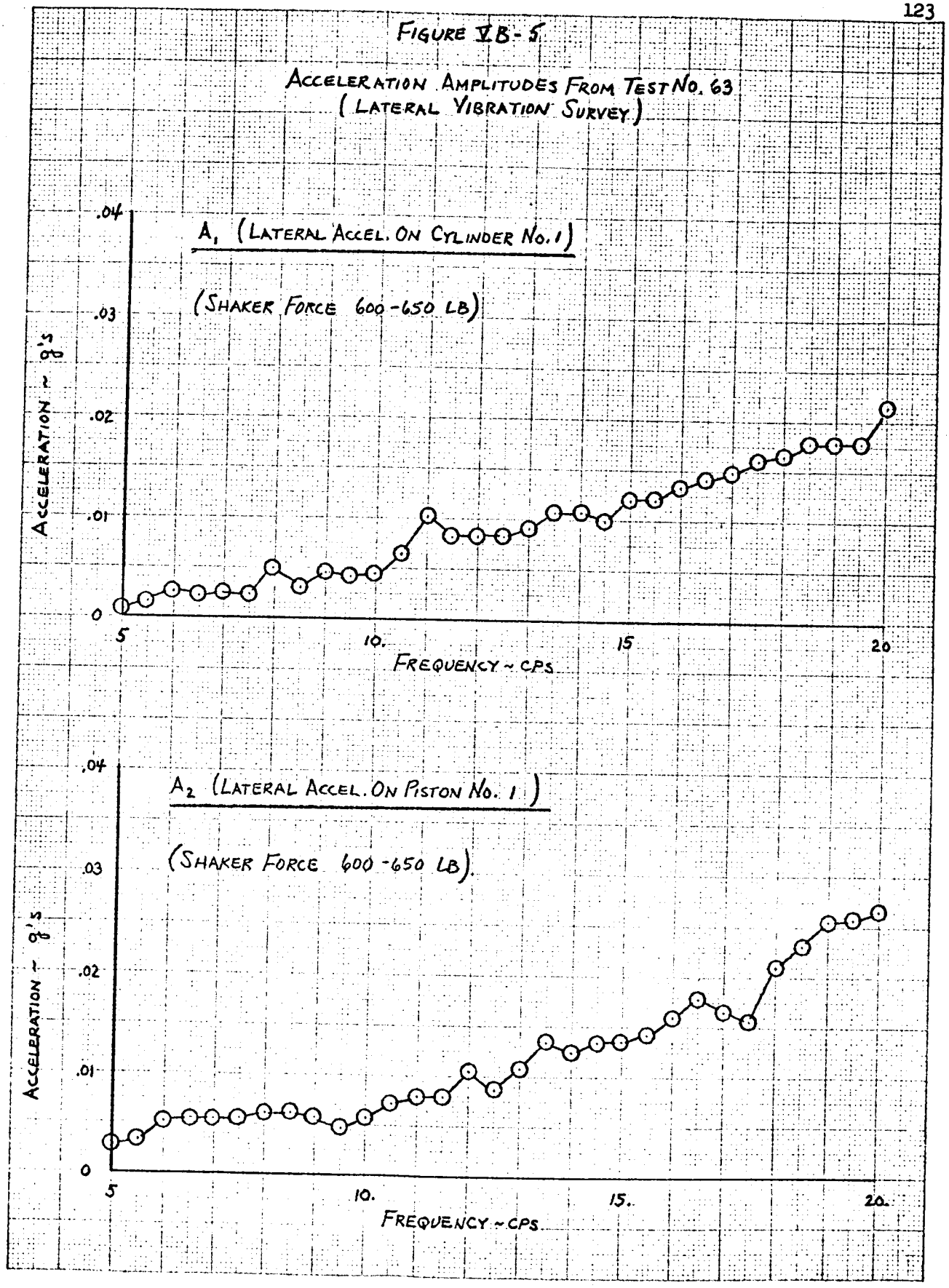

FIGURE V B-6

ACCELERATION AMPLITUDES FROM TEST NO. 63
(LATERAL VIBRATION SURVEY)

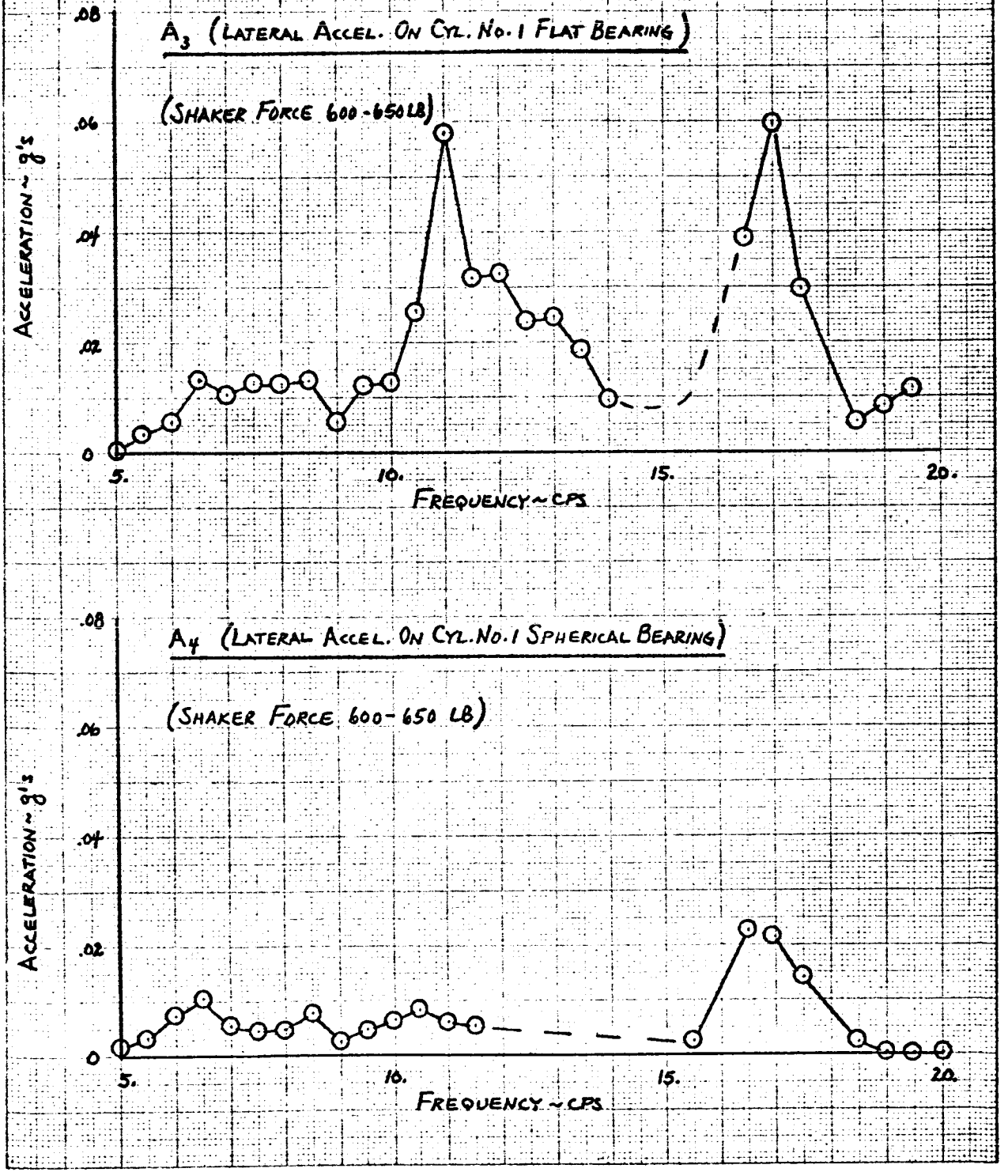

FIGURE V B-7

LATERAL ACCELERATION AMPLITUDE OF SHAKER SUPPORT STAND DURING TEST NO. 63 (LATERAL VIBRATION SURVEY)

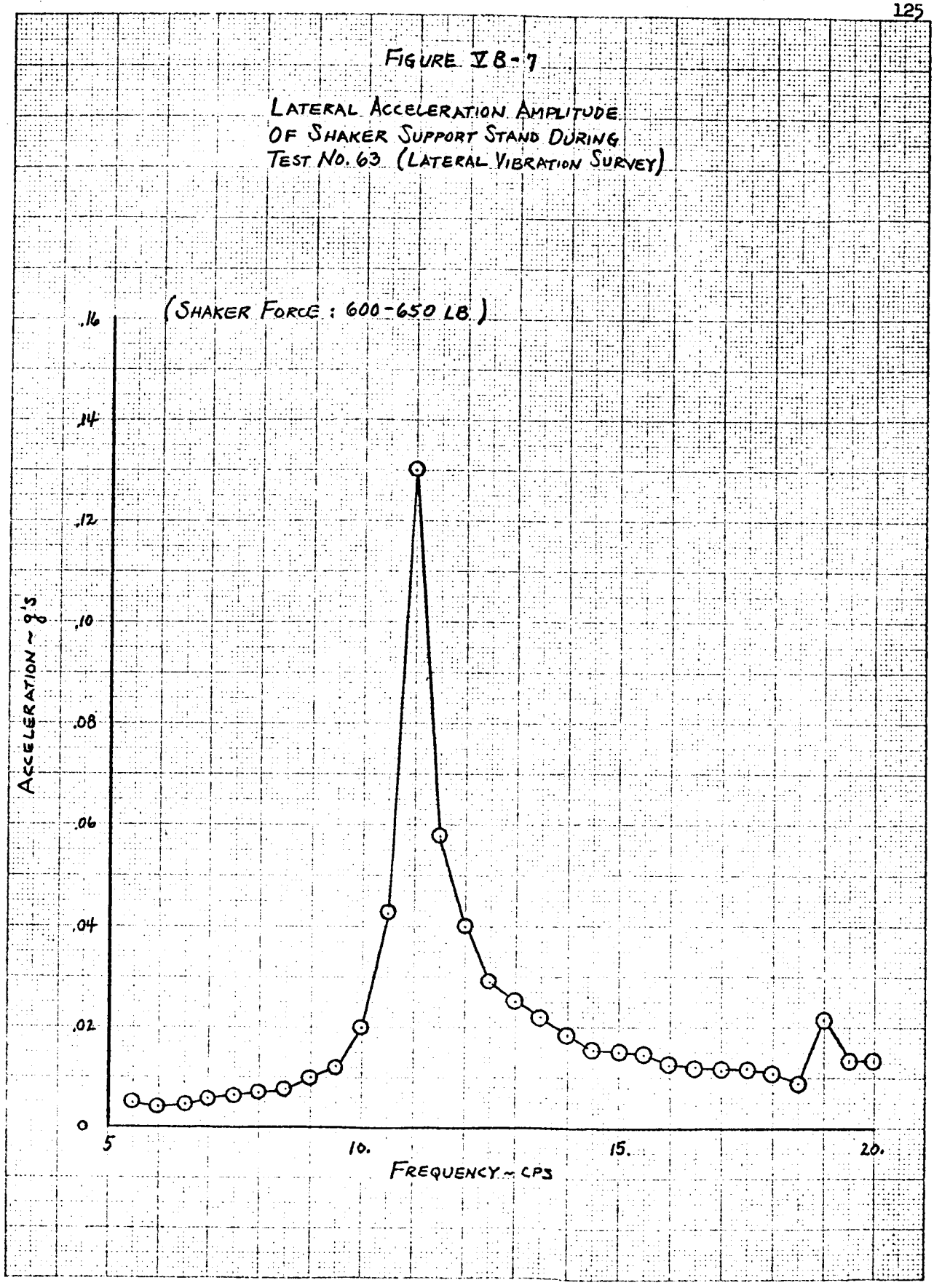

FIGURE IV C-1

CYLINDER SUPPLY SYSTEM TEST SCHEMATIC

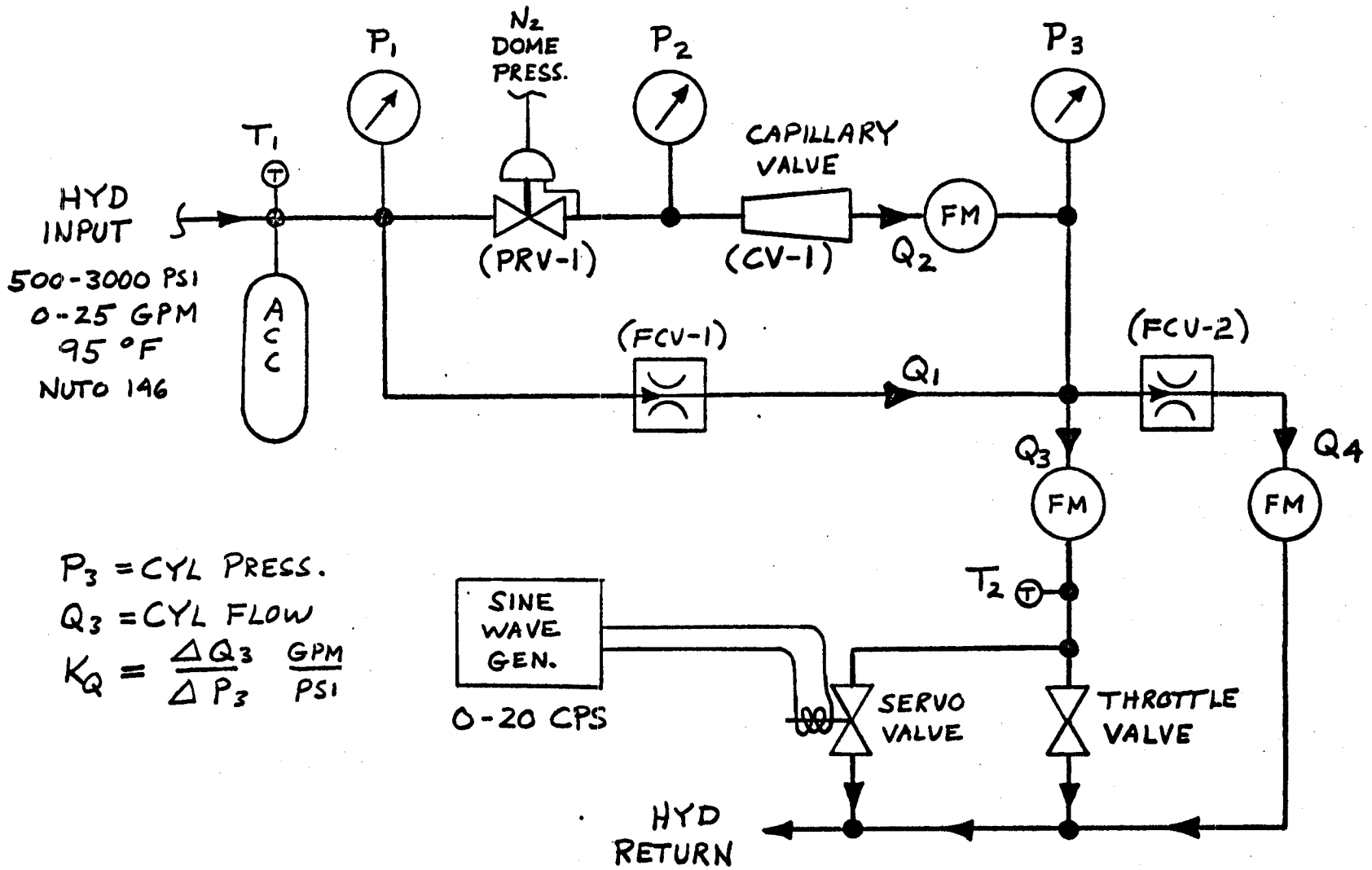

P_3 = CYL PRESS.

Q_3 = CYL FLOW

$K_Q = \frac{\Delta Q_3}{\Delta P_3} \frac{GPM}{PSI}$

FIGURE V C-2

FLOW GAIN, K_Q, VS FREQUENCY

(SIMULATING 1.8 x 10 LB. BEARING LOAD)

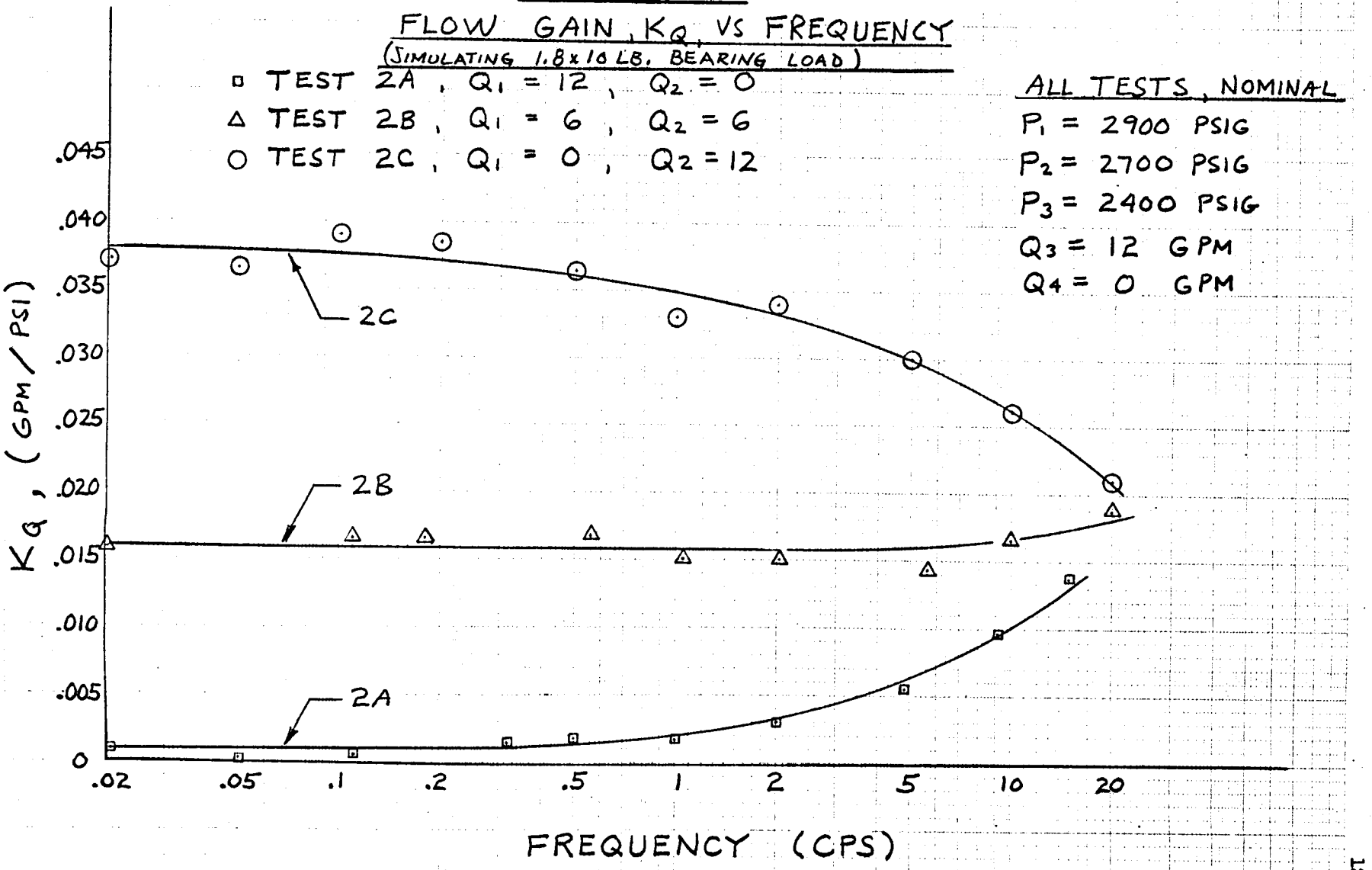

FIGURE V C-3

FLOW GAIN, K_Q, VS FREQUENCY

(SIMULATING 1.0×10^6 LB BEARING LOAD

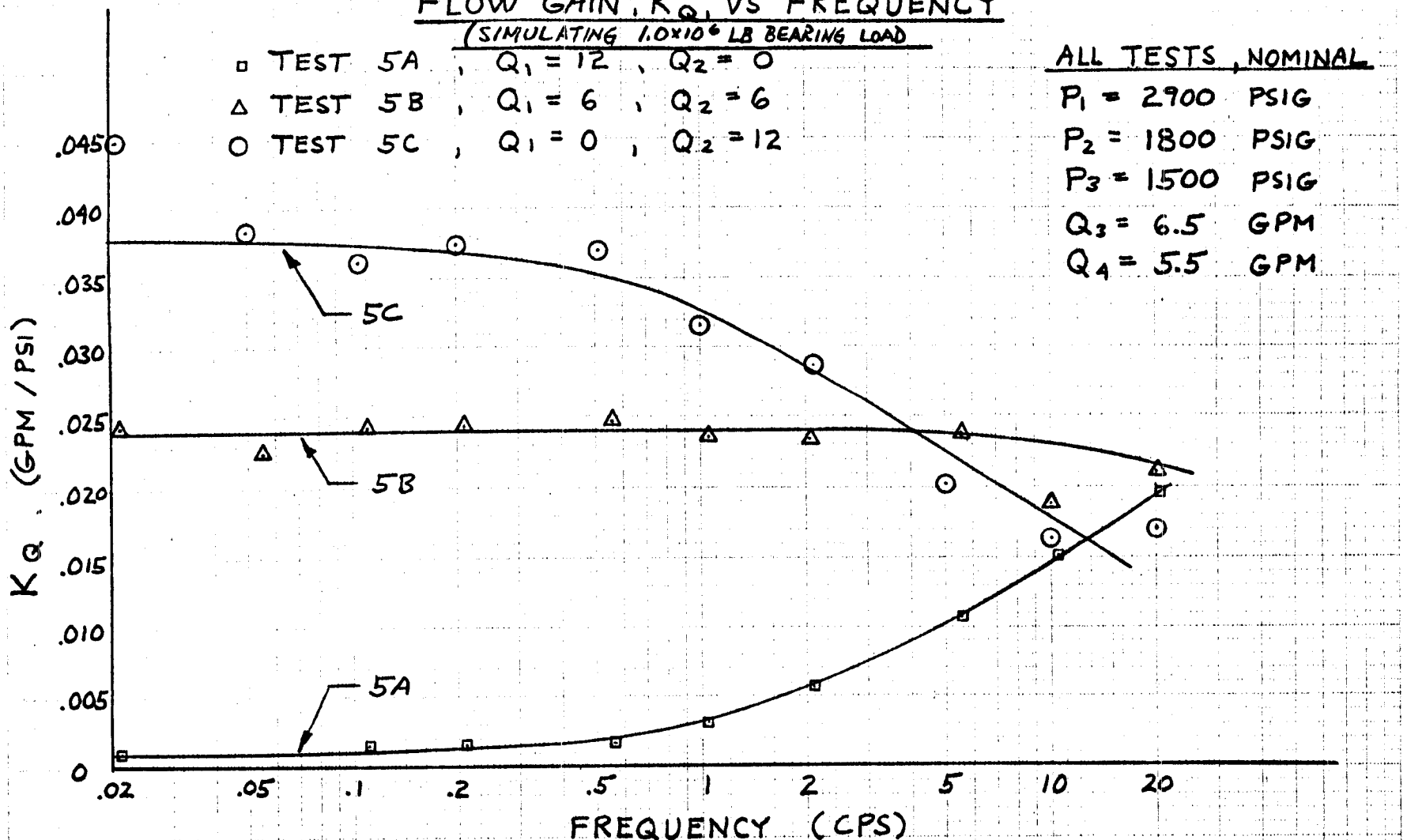

FIGURE VC-4

FLOW GAIN, K_Q VS FREQUENCY

(SIMULATING 0.44×10^6 LB BEARING LOAD)

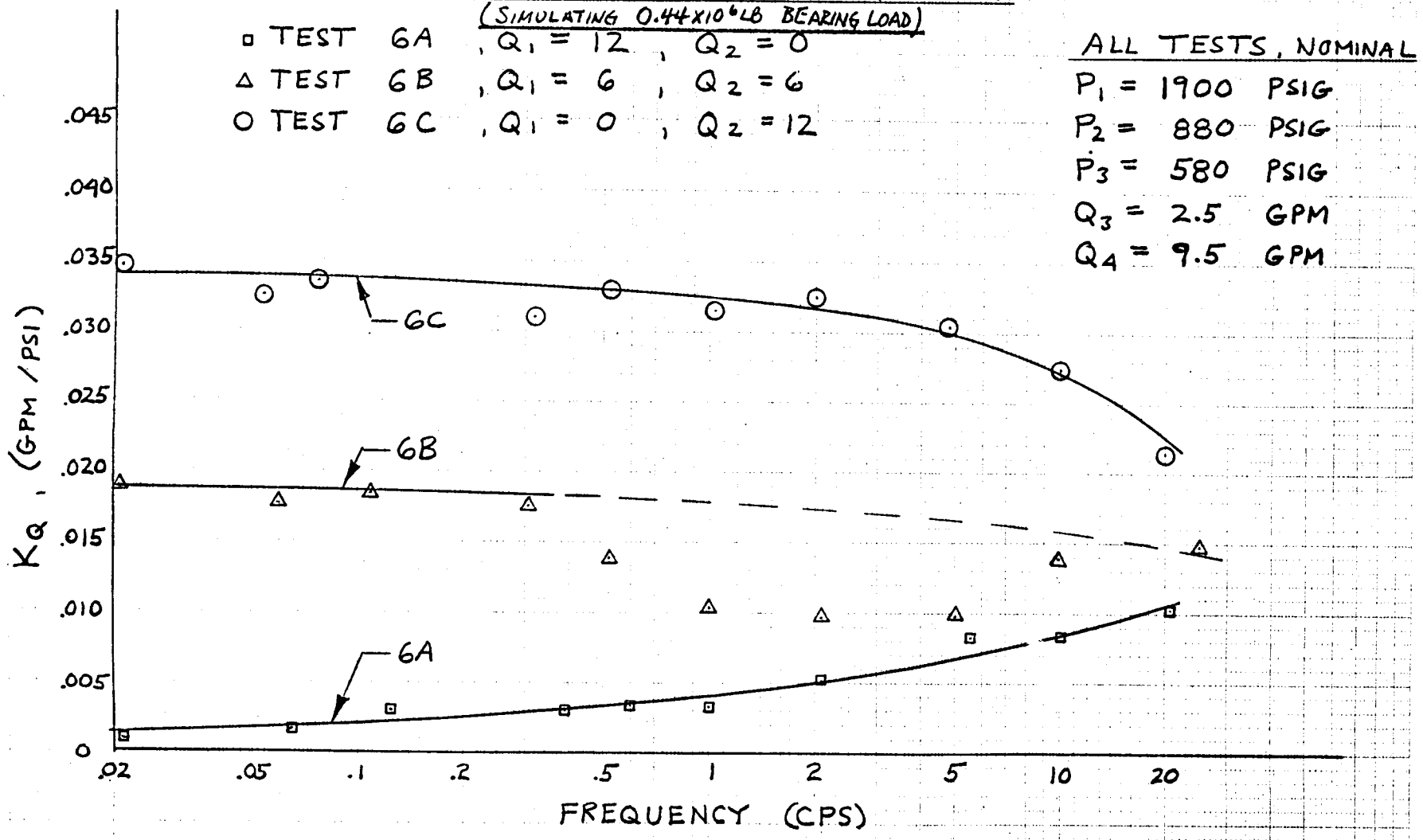

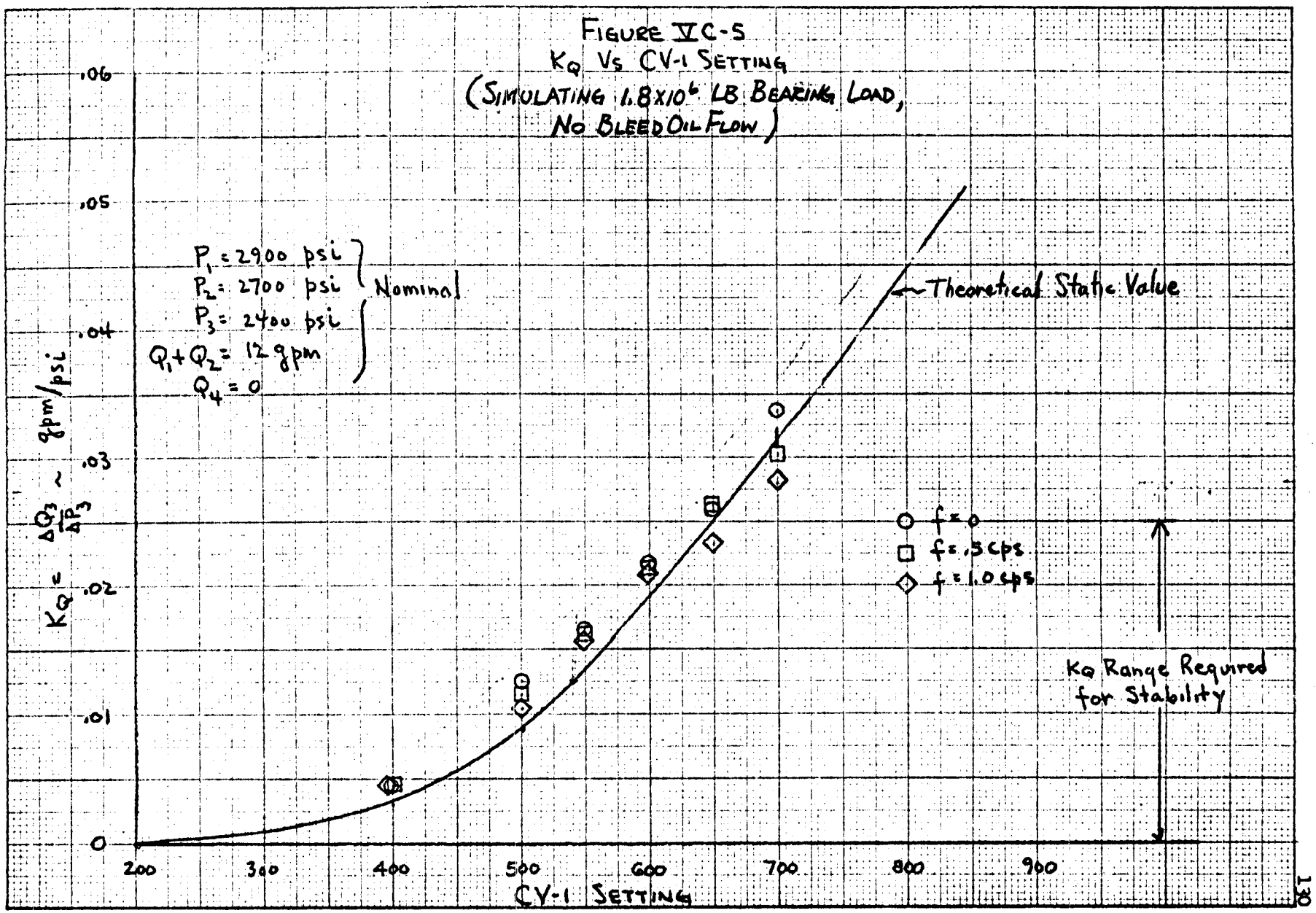
FIGURE IV C-5
K_Q VS CV-1 SETTING
(SIMULATING 1.8×10^6 LB BEARING LOAD, NO BLEED OIL FLOW)
P_1 = 2900 psi
P_2 = 2700 psi
P_3 = 2400 psi
Nominal
$Q_1 + Q_2$ = 12 gpm
Q_4 = 0
Theoretical Static Value
f = 0
f = .5 cps
f = 1.0 cps
K_Q Range Required for Stability
$K_Q = \frac{\Delta Q_3}{\Delta P_3}$ ~ gpm/psi
.06
.05
.04
.03
.02
.01
0
200
300
400
500
600
700
800
900
CV-1 SETTING

FIGURE V C-6

K_Q Vs. CV-1 SETTING

(SIMULATING 1.8×10^6 LB BEARING LOAD, 1 gpm BLEED OIL FLOW)

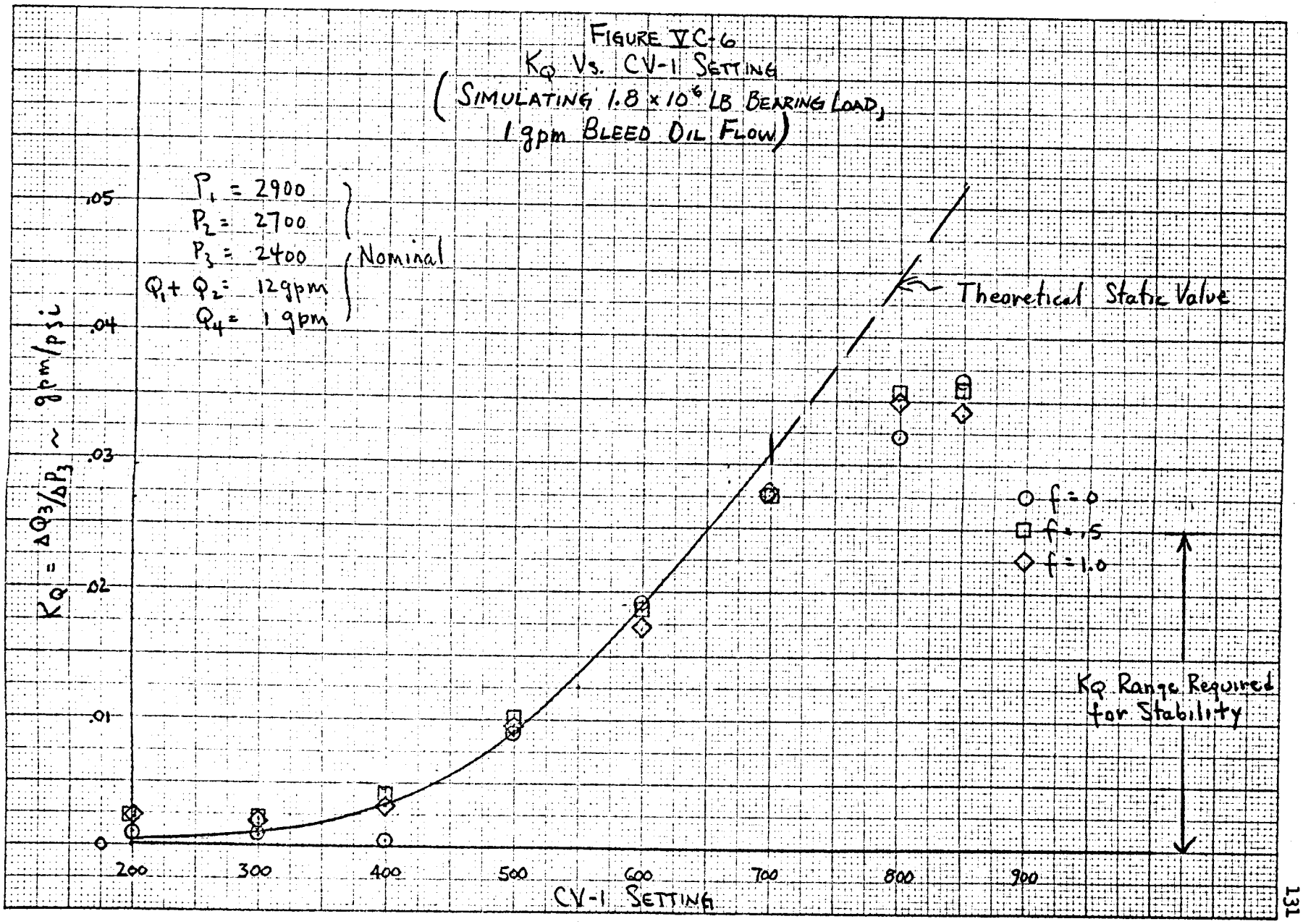

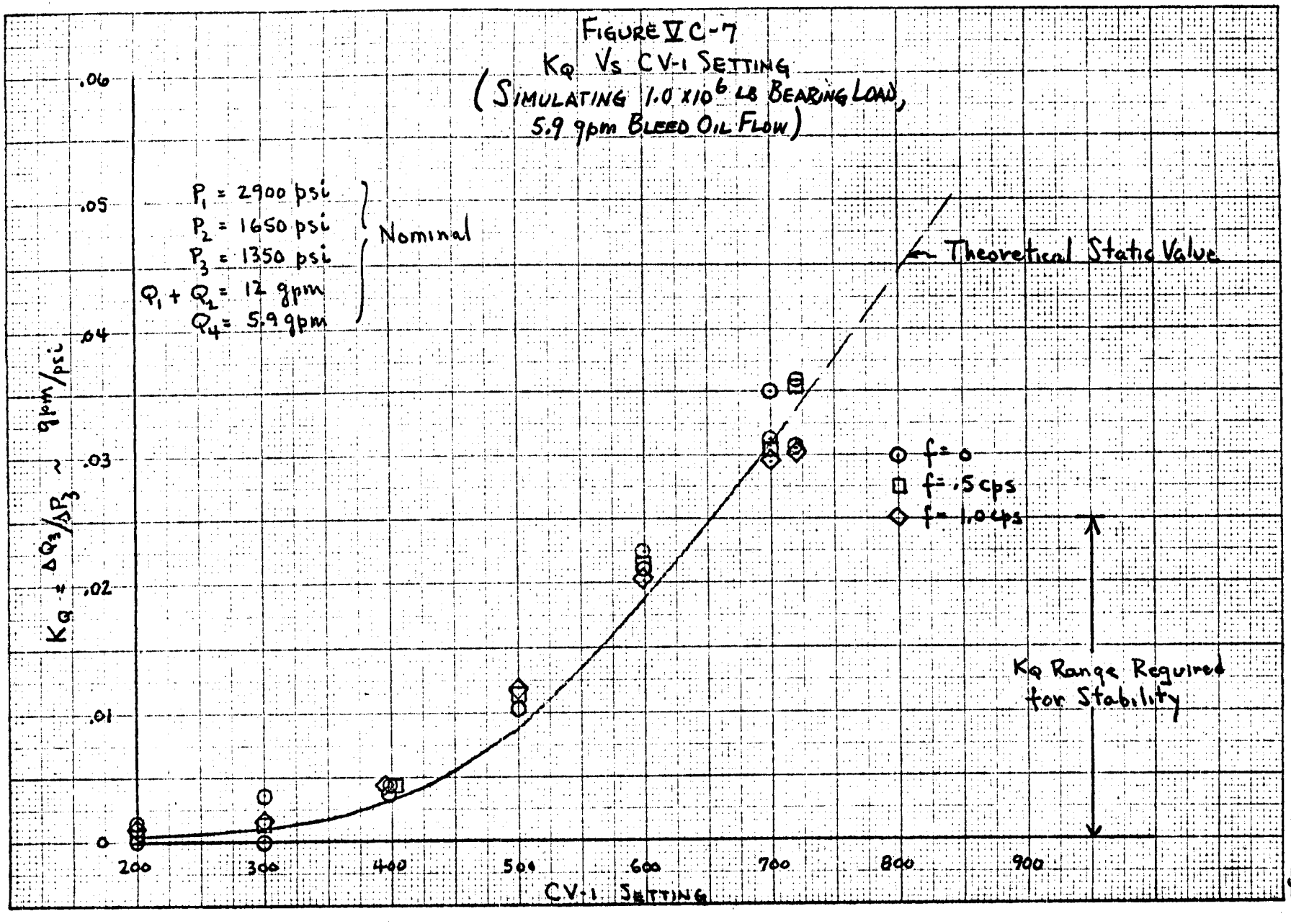
FIGURE V C-7
K_Q Vs CV-1 SETTING
(SIMULATING 1.0×10^6 LB BEARING LOAD,
5.9 gpm BLEED OIL FLOW)
P_1 = 2900 psi
P_2 = 1650 psi
P_3 = 1350 psi
$Q_1 + Q_2$ = 12 gpm
Q_4 = 5.9 gpm
Nominal
← Theoretical Static Value
f = 0
f = .5 cps
f = 1.0 cps
K_Q Range Required for Stability
$K_Q = \Delta Q_3/\Delta P_3$ ~ gpm/psi
.06
.05
.04
.03
.02
.01
0
200
300
400
500
600
700
800
900
CV-1 SETTING

FIGURE IV C-8

K_Q Vs. CV-1 SETTING

(SIMULATING 0.44×10^6 LB BEARING LOAD, 3.3 gpm BLEED OIL FLOW)

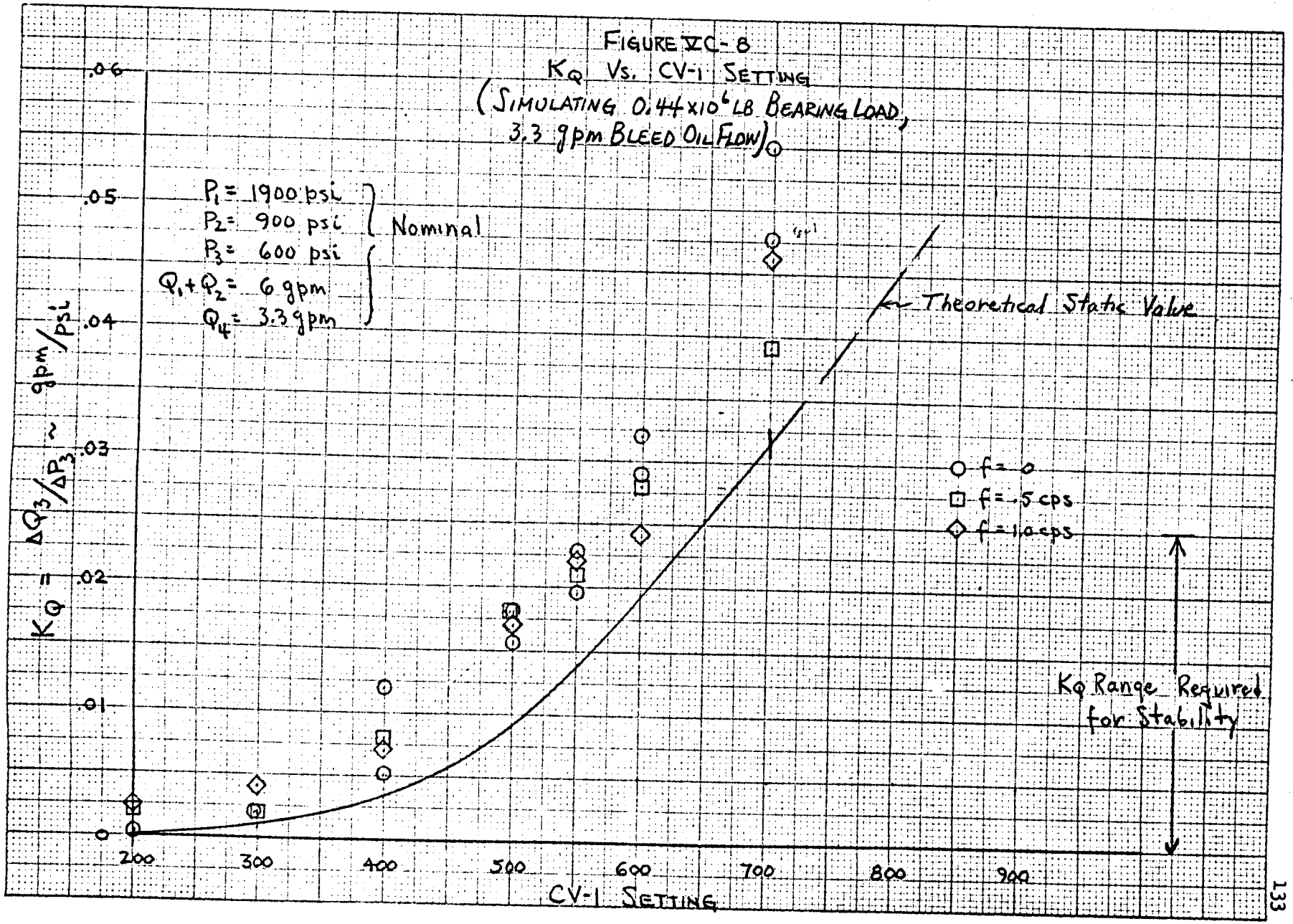

WLC 7/18/65

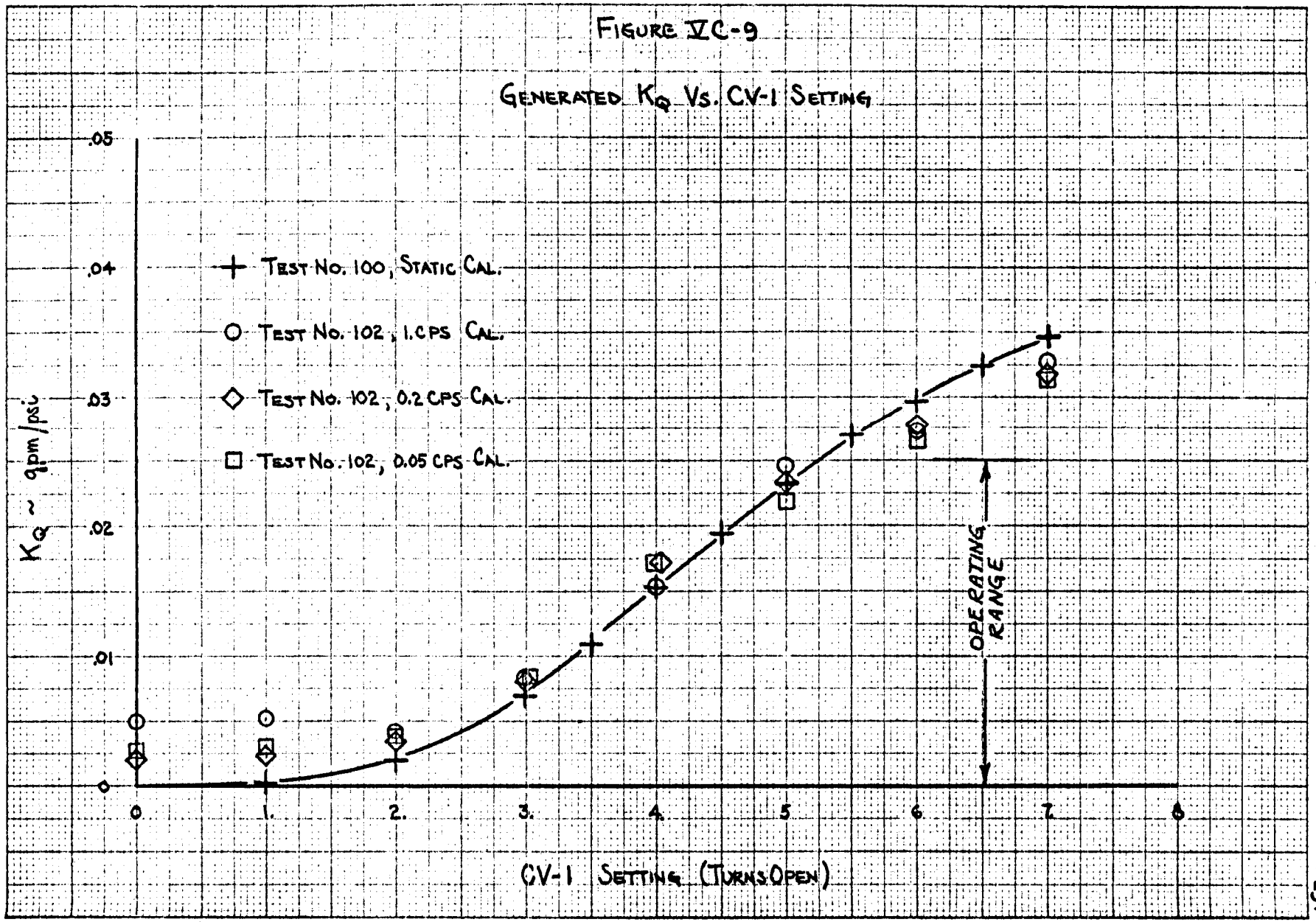
FIGURE IV C-9
GENERATED K_Q VS. CV-1 SETTING
.05
.04
.03
.02
.01
K_Q ~ gpm/psi
TEST NO. 100, STATIC CAL.
TEST NO. 102, 1.0 CPS CAL.
TEST NO. 102, 0.2 CPS CAL.
TEST NO. 102, 0.05 CPS CAL.
OPERATING RANGE
0
1.
2.
3.
4.
5
6
7
8
CV-1 SETTING (TURNS OPEN)

FIGURE V C-10

FLOW VS CAPILLARY VALVE SETTING

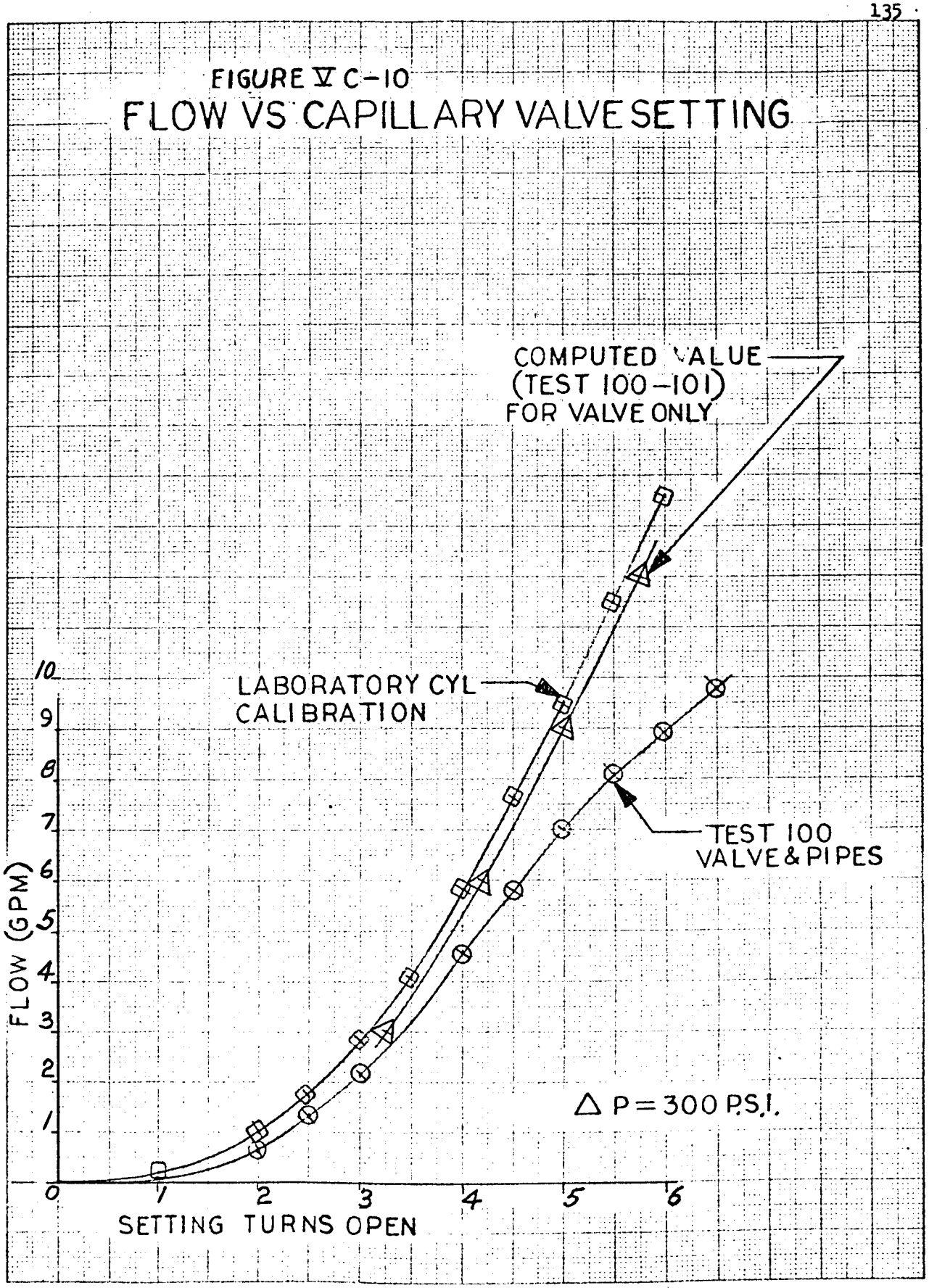

FIGURE V D-1
TEST 41.5
STATIC PISTON CHARACTERISTICS
LOWER CYLINDER FLOW VS. PRESSURE

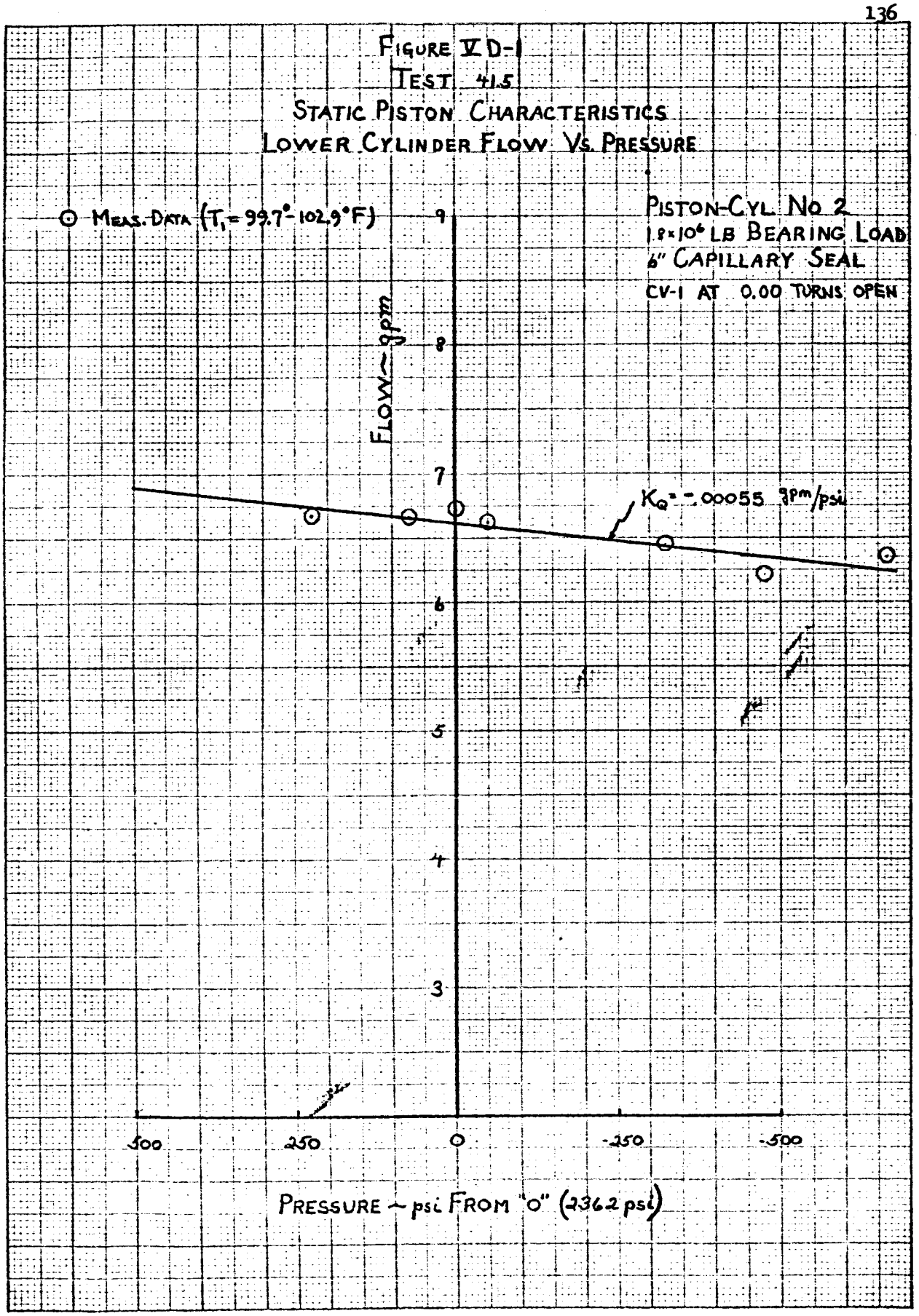

FIGURE V D-2
TEST 39-B
STATIC PISTON CHARACTERISTICS
LOWER CYLINDER FLOW VS. PRESSURE

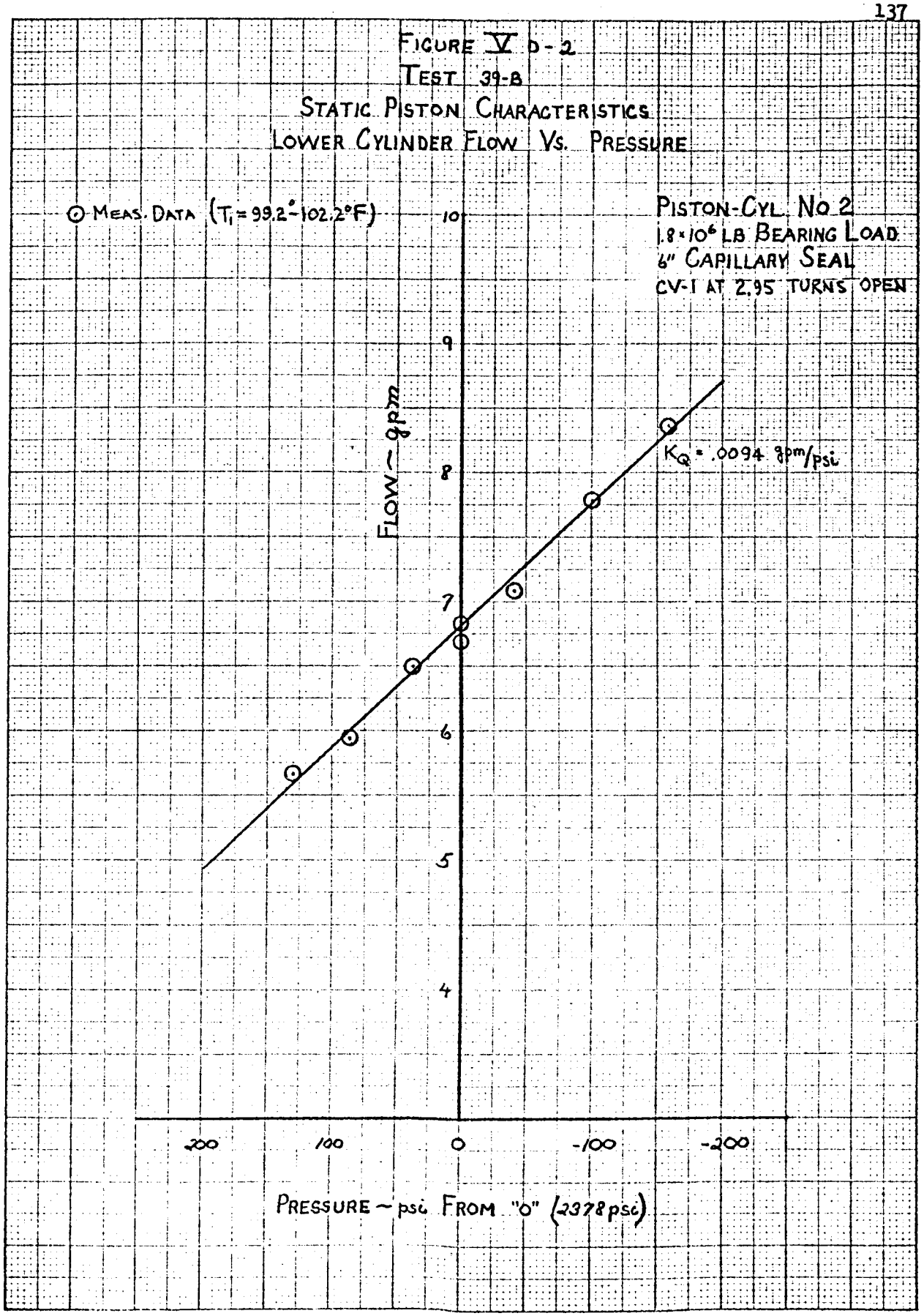

FIGURE V D-3
TEST 40-A
STATIC PISTON CHARACTERISTICS
LOWER CYLINDER FLOW VS. PRESSURE

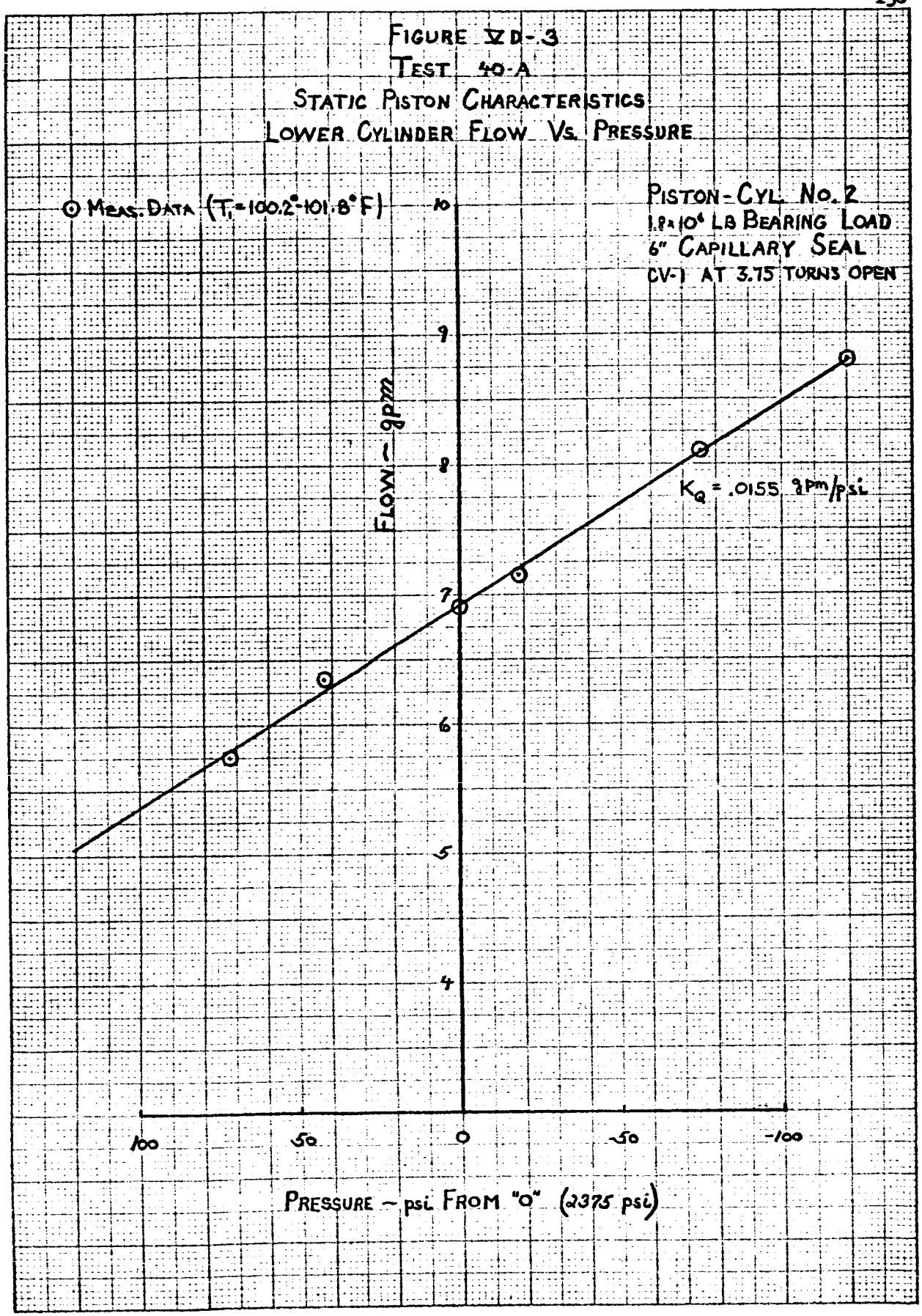

FIGURE V D-4
TEST 41
STATIC PISTON CHARACTERISTICS
LOWER CYLINDER FLOW VS. PRESSURE

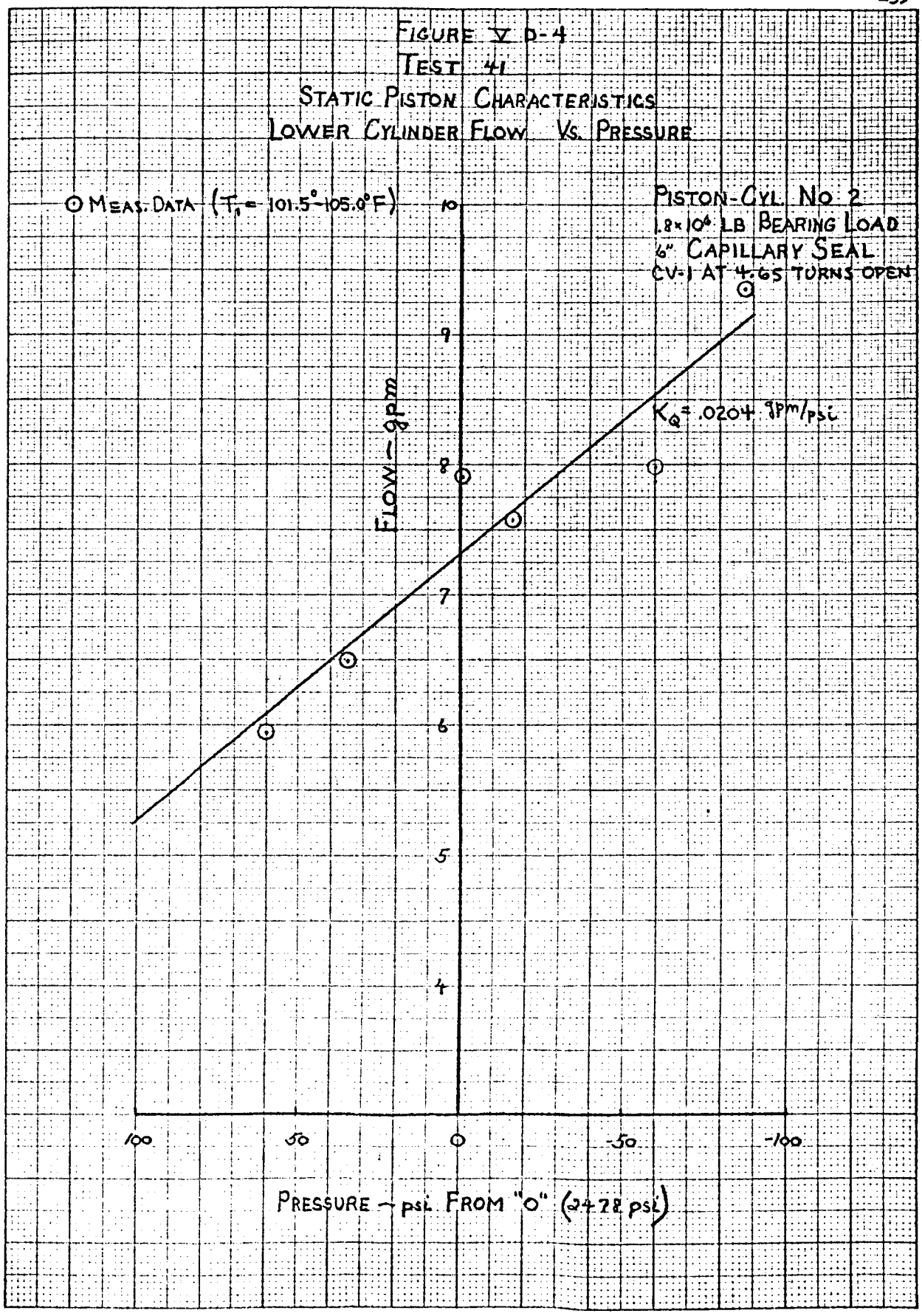

FIGURE V D-5
TEST 41-A
STATIC PISTON CHARACTERISTICS
LOWER CYLINDER FLOW VS. PRESSURE

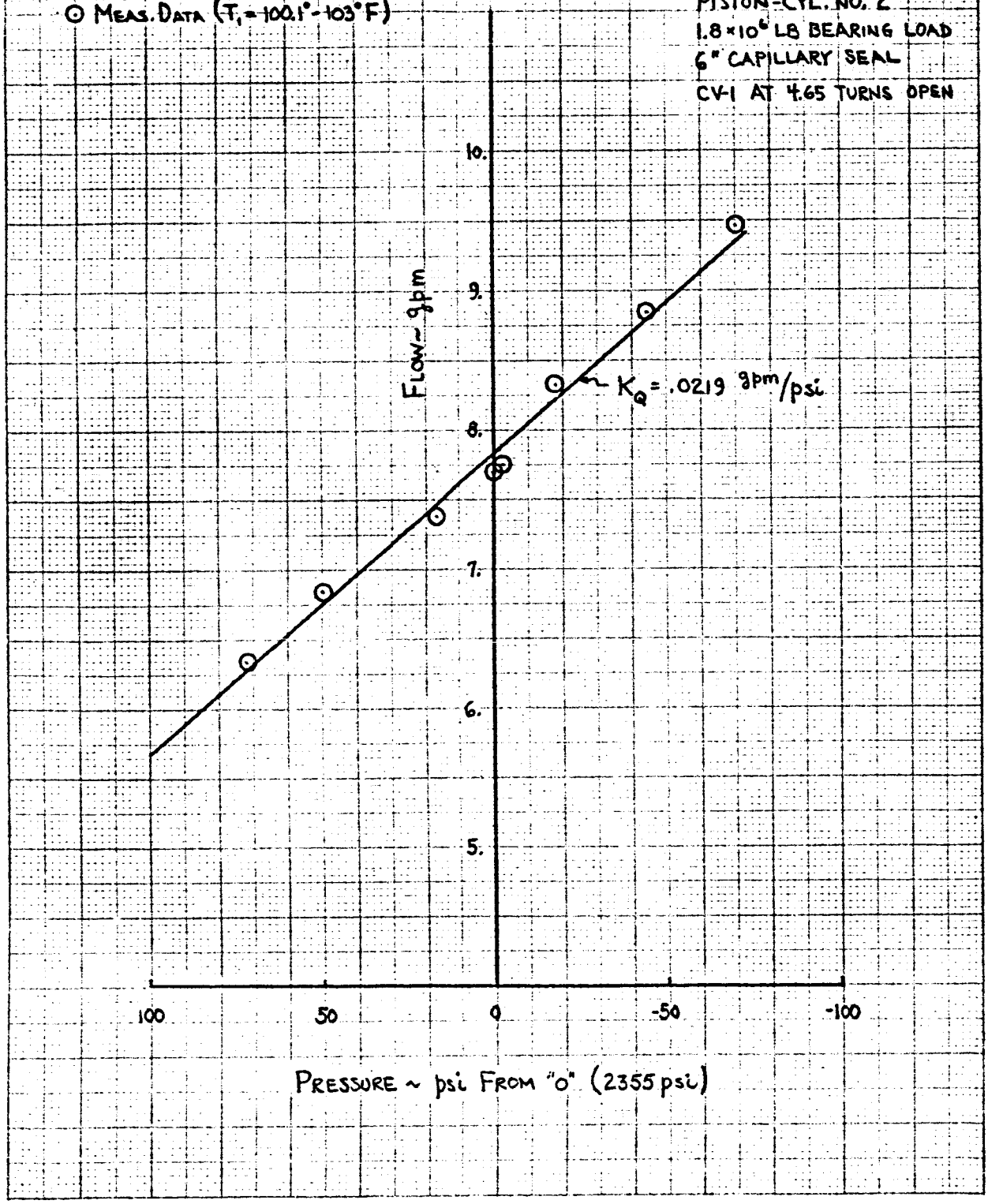

FIGURE V D-6
TEST 57-A
STATIC PISTON CHARACTERISTICS
LOWER CYLINDER FLOW VS PRESSURE

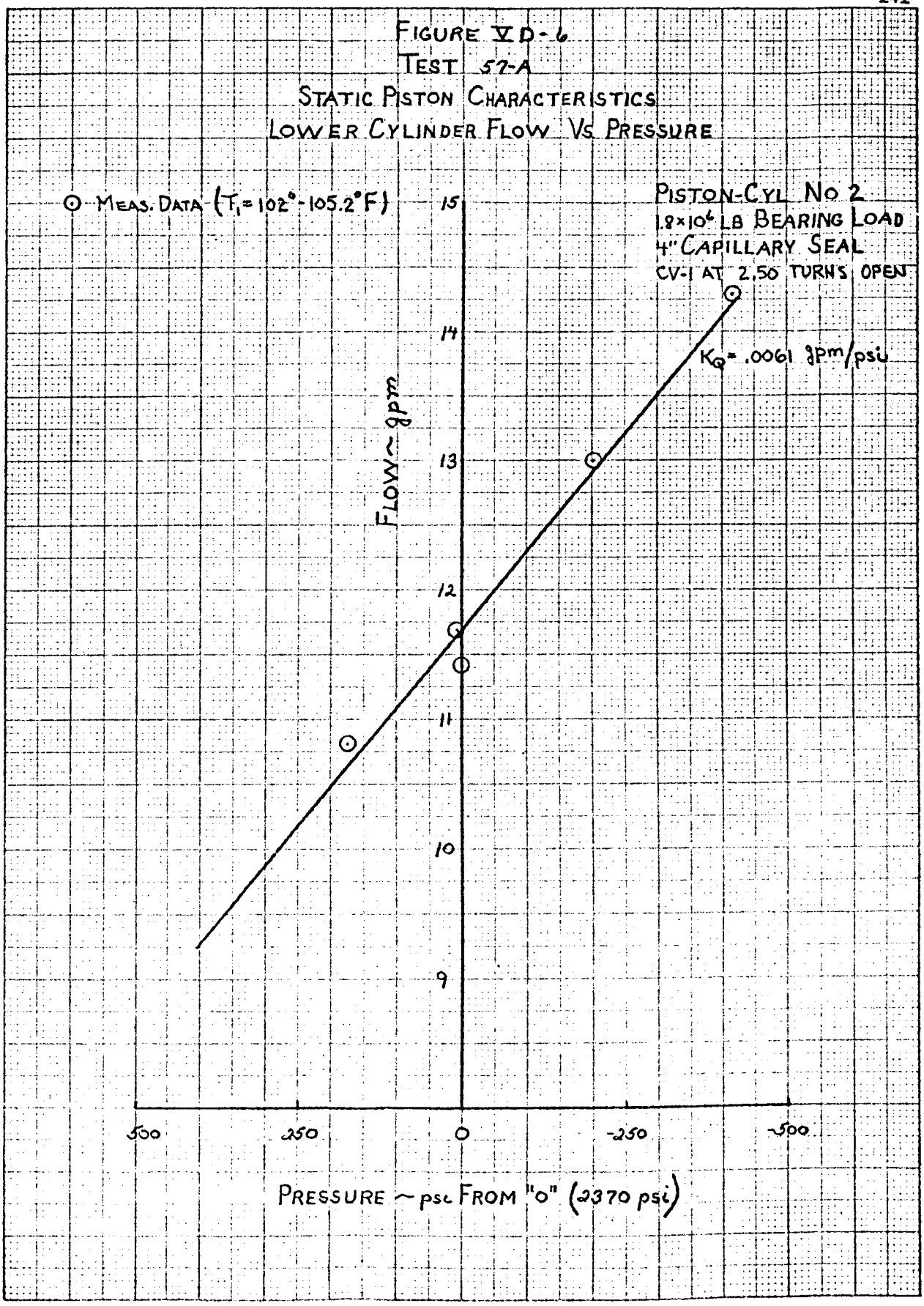

FIGURE II D-7
TEST 53
STATIC PISTON CHARACTERISTICS
LOWER CYLINDER FLOW VS. PRESSURE

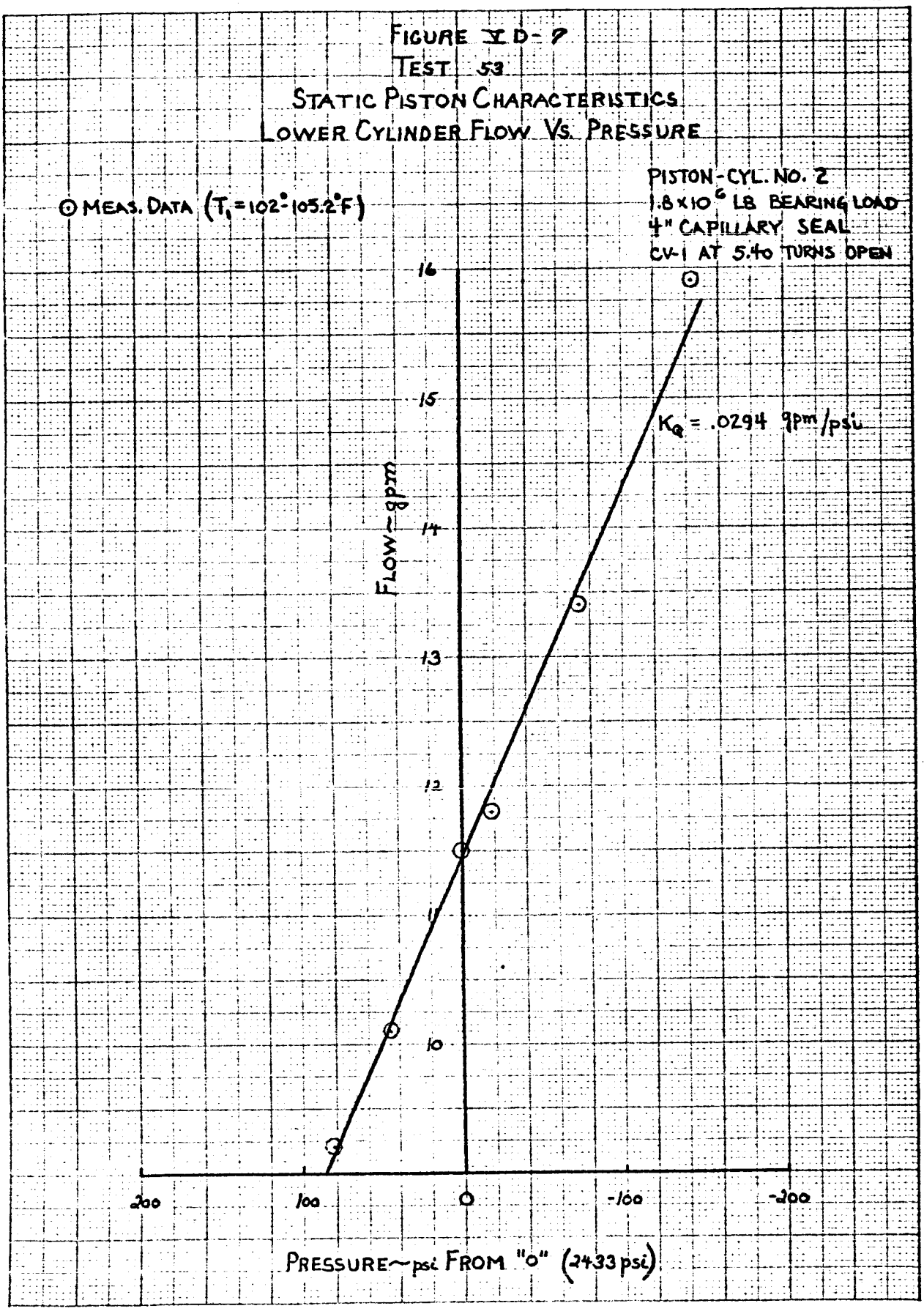

FIGURE V D-8
TEST 56-A
STATIC PISTON CHARACTERISTICS
LOWER CYLINDER FLOW VS. PRESSURE

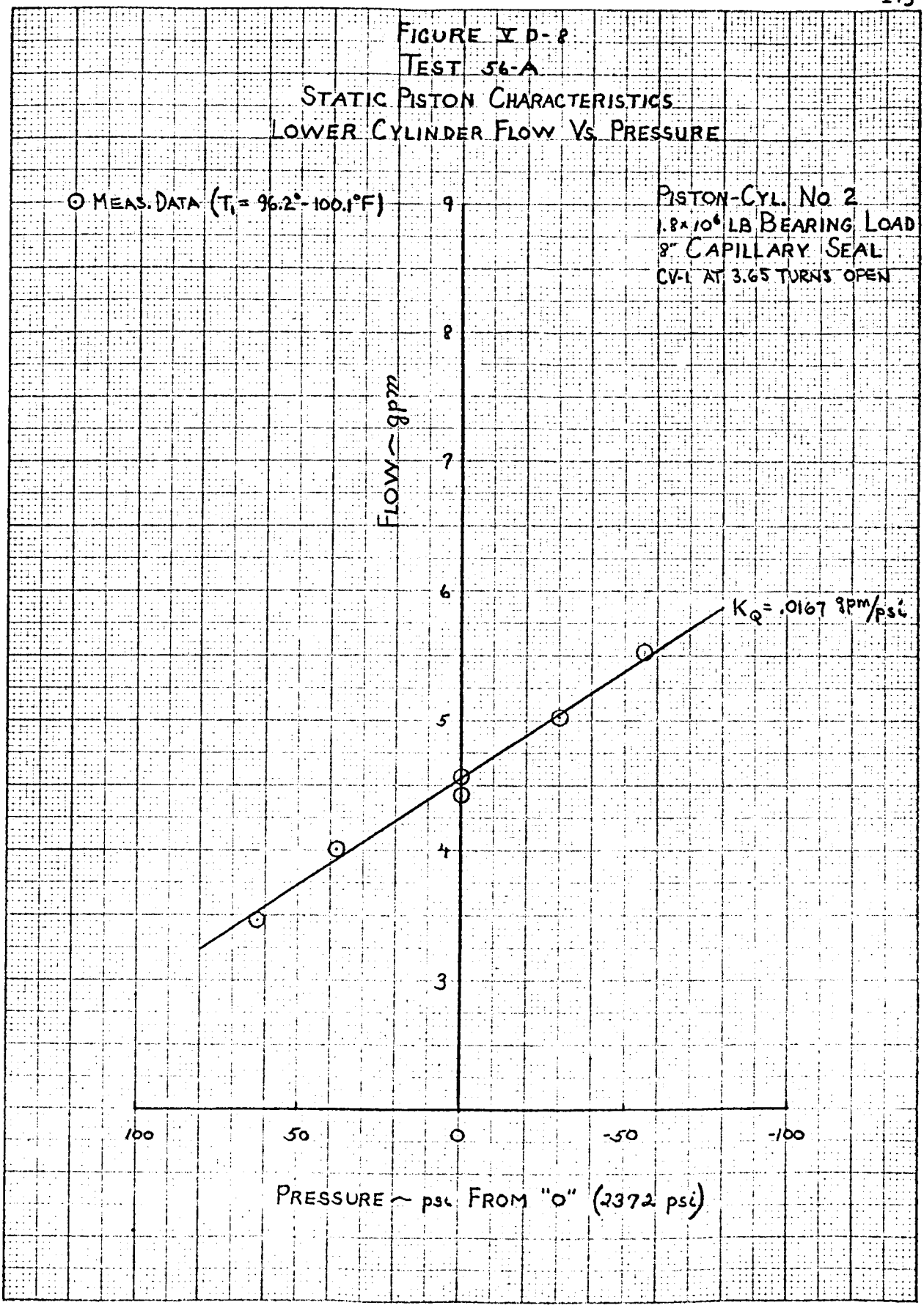

FIGURE V D-9
TEST 45
STATIC PISTON CHARACTERISTICS
LOWER CYLINDER FLOW VS. PRESSURE

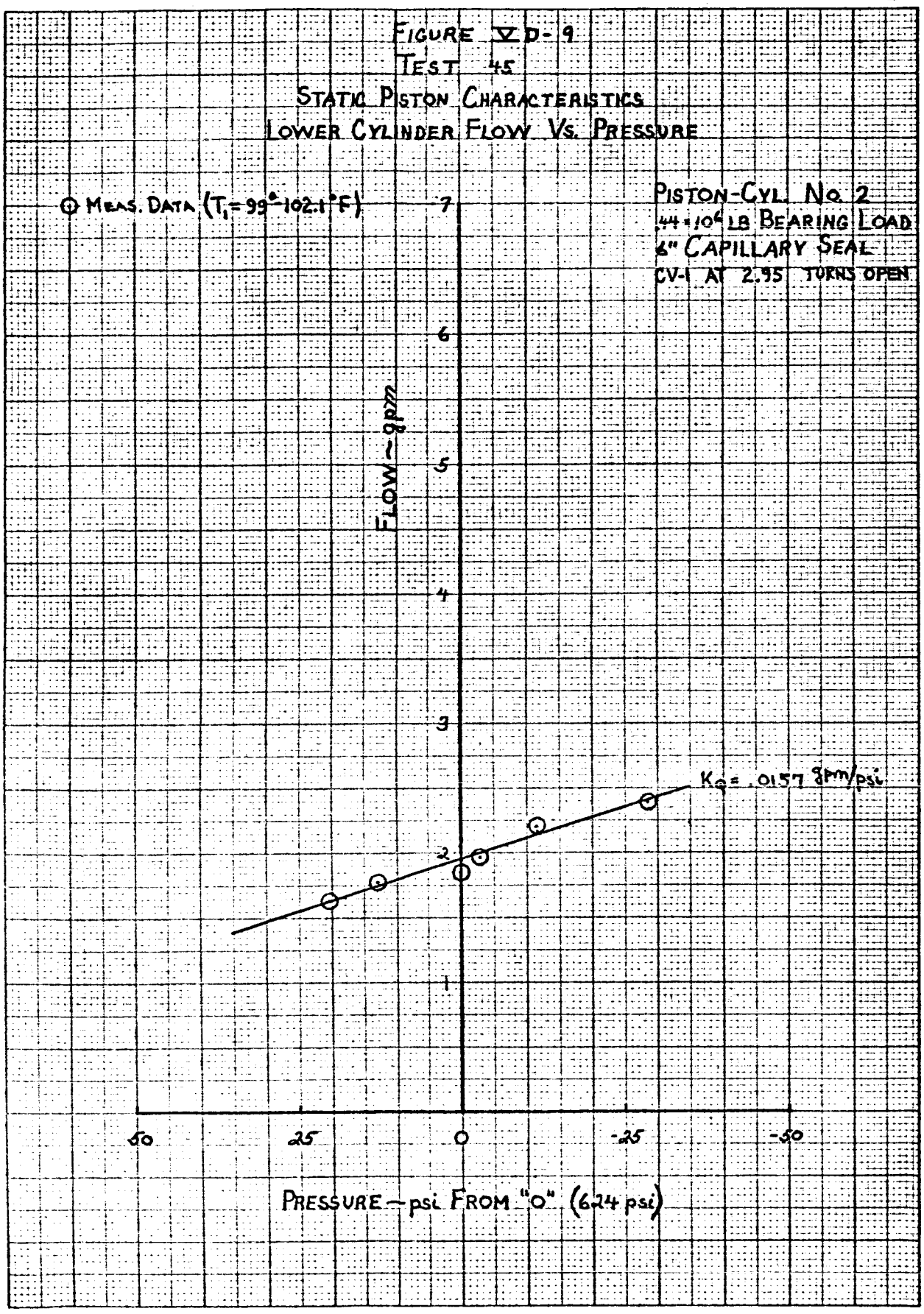

FIGURE V D-10
TEST 46
STATIC PISTON CHARACTERISTICS
LOWER CYLINDER FLOW VS. PRESSURE

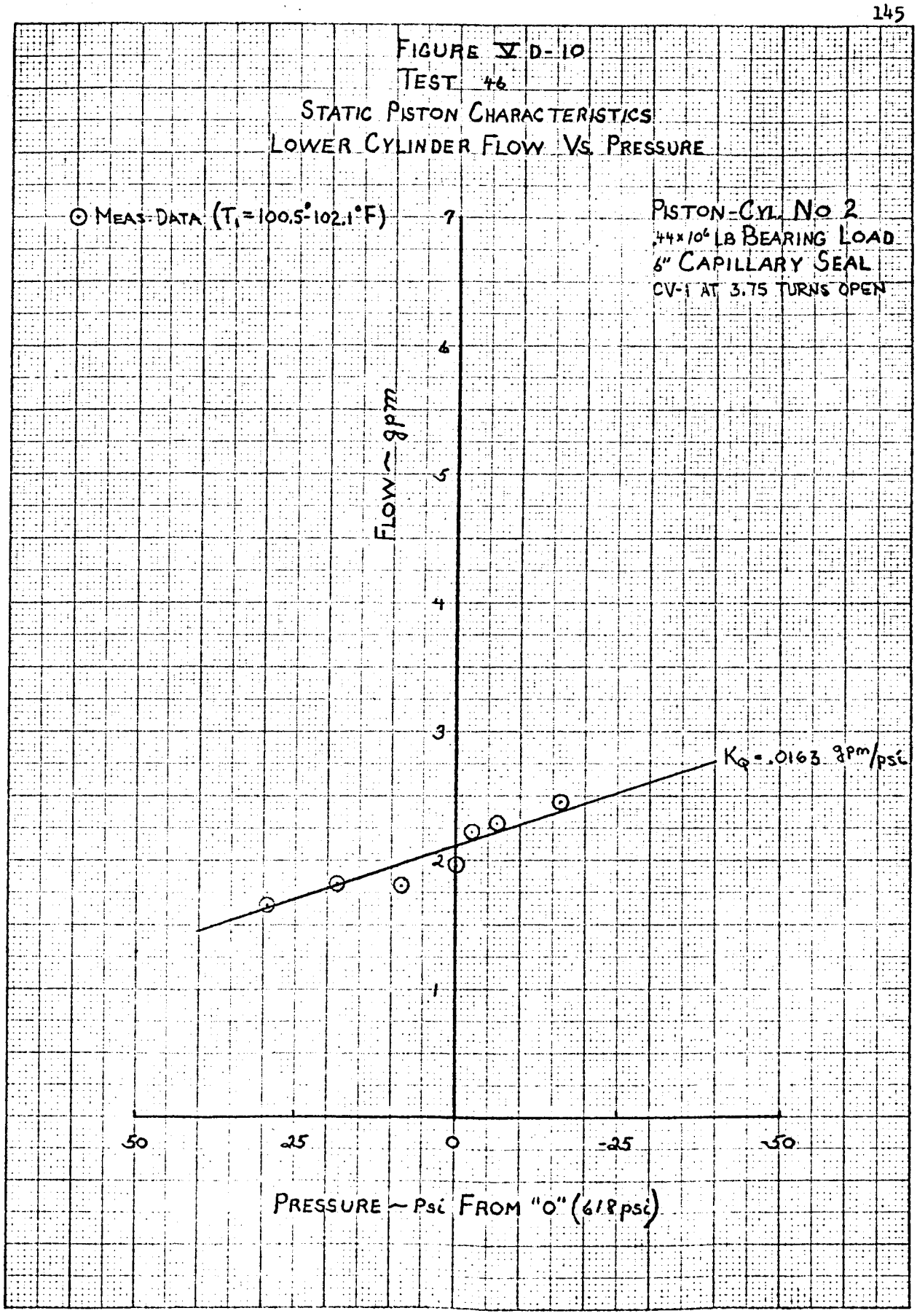

FIGURE V D-11
TEST 47
STATIC PISTON CHARACTERISTICS
LOWER CYLINDER FLOW VS PRESSURE

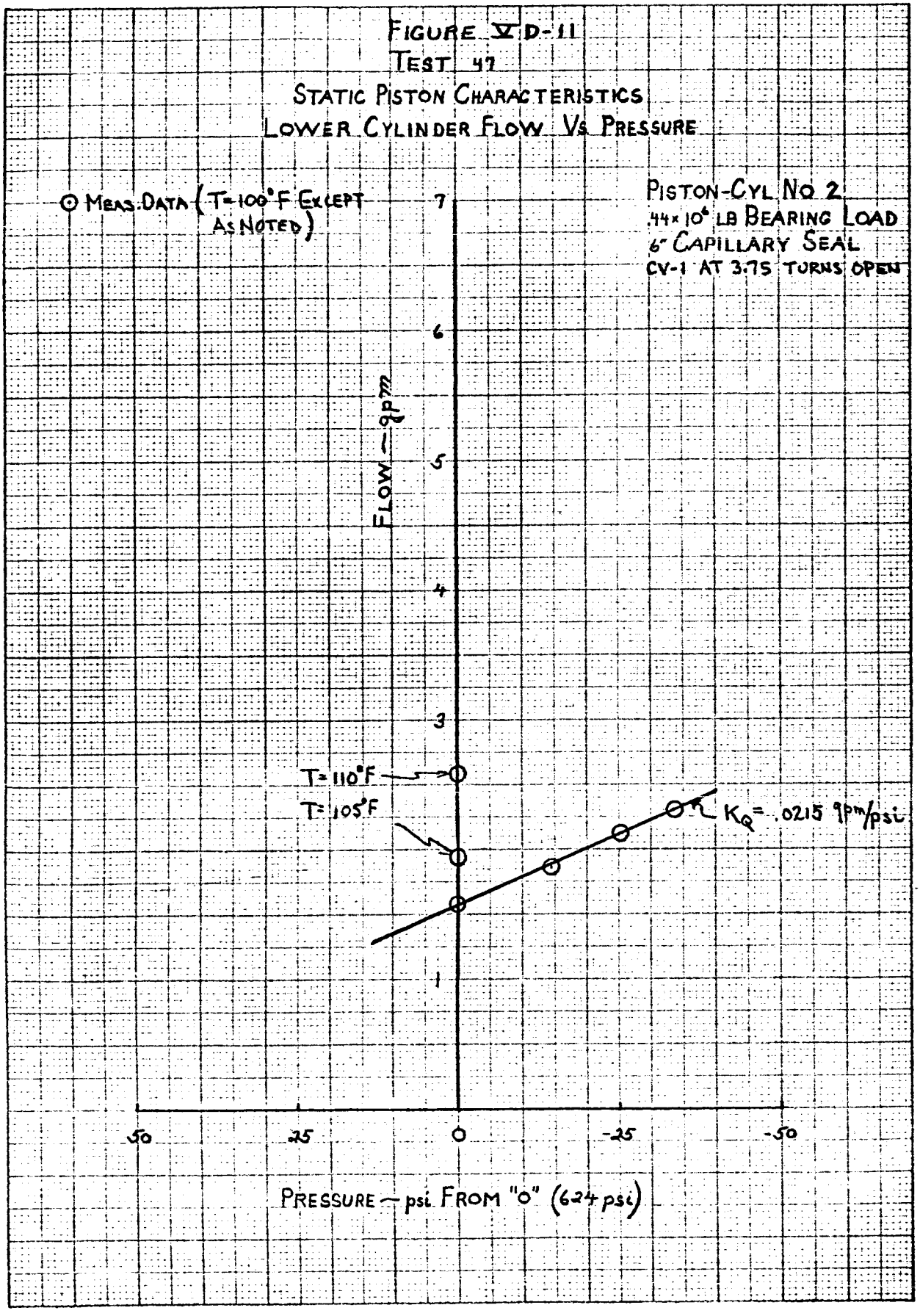

FIGURE V D-12
TEST 18-A
STATIC PISTON CHARACTERISTICS
LOWER CYLINDER FLOW VS. PRESSURE

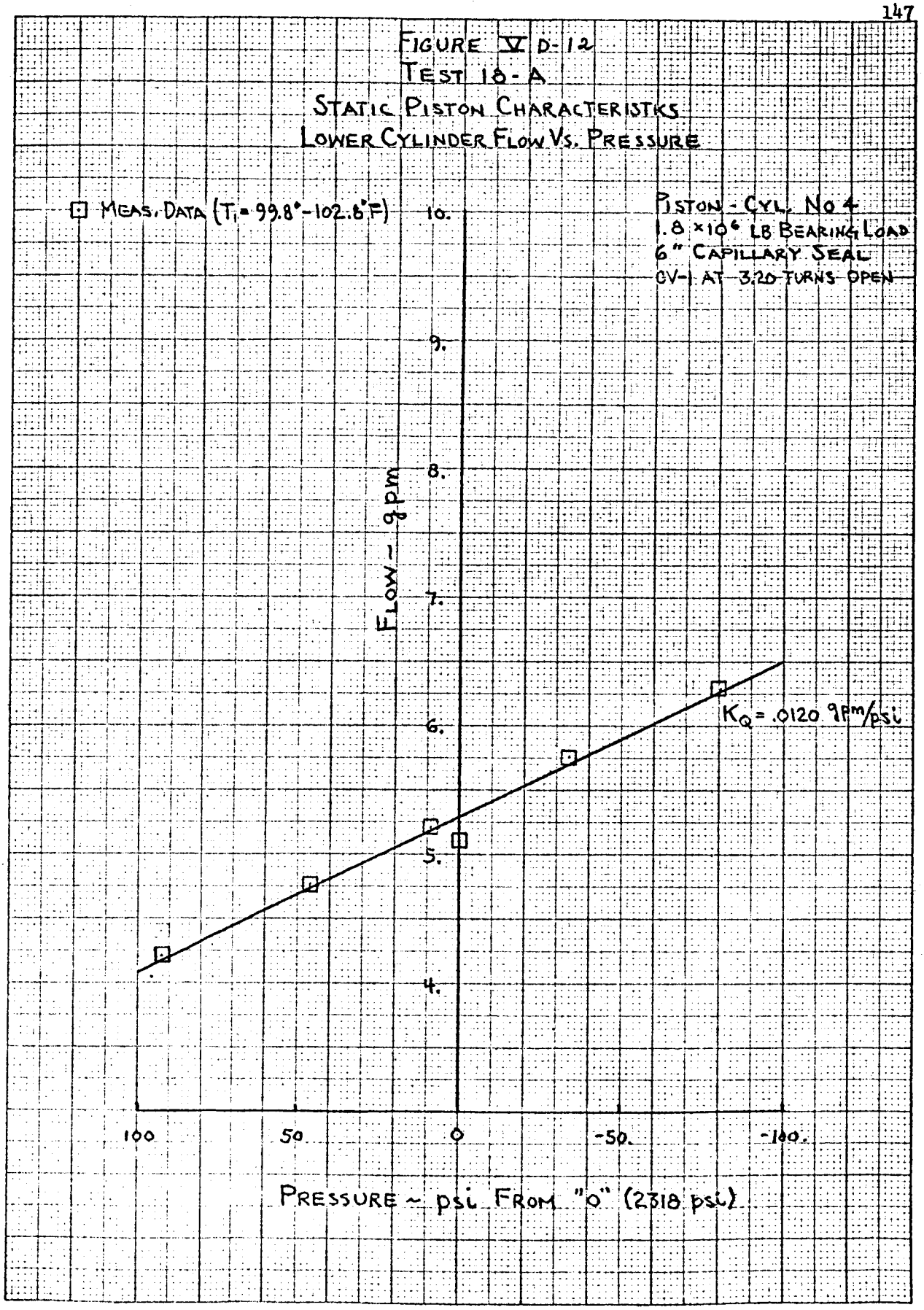

FIGURE V D-13
TEST 19
STATIC PISTON CHARACTERISTICS
LOWER CYLINDER FLOW VS. PRESSURE

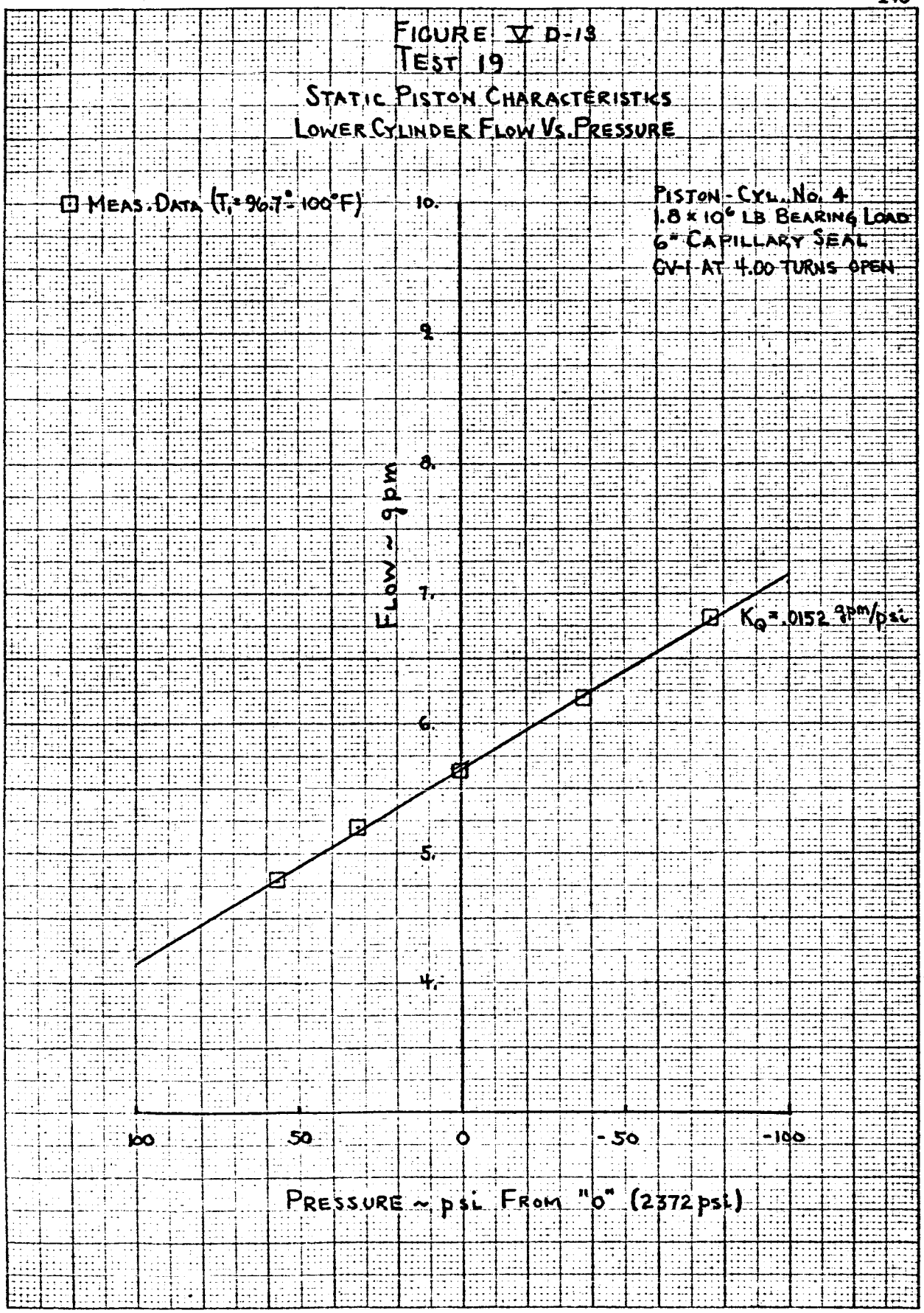

FIGURE V D-14
TEST 24
STATIC PISTON CHARACTERISTICS
LOWER CYLINDER FLOW VS PRESSURE

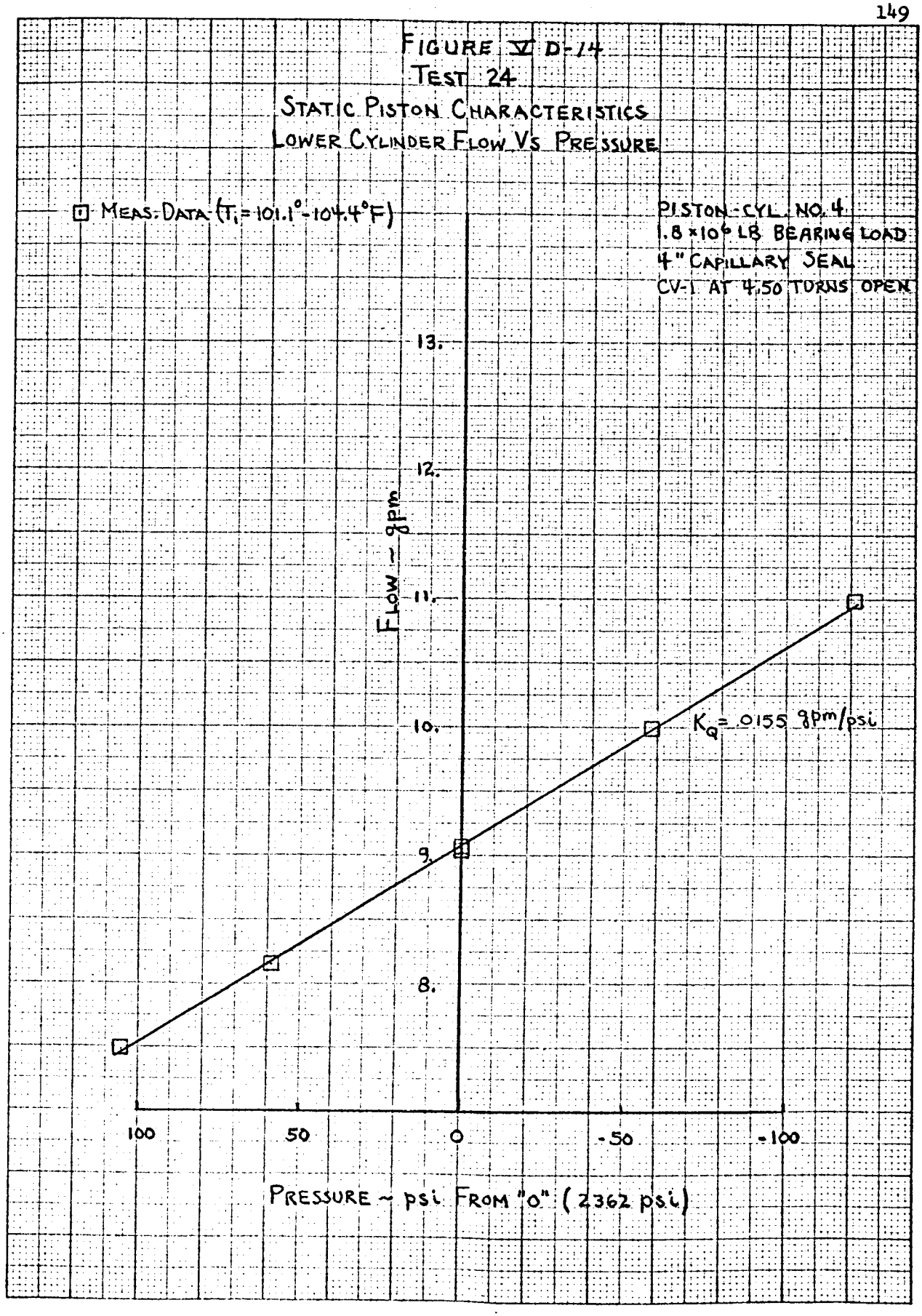

FIGURE V D-16
TEST 27
STATIC PISTON CHARACTERISTICS
LOWER CYLINDER FLOW VS PRESSURE

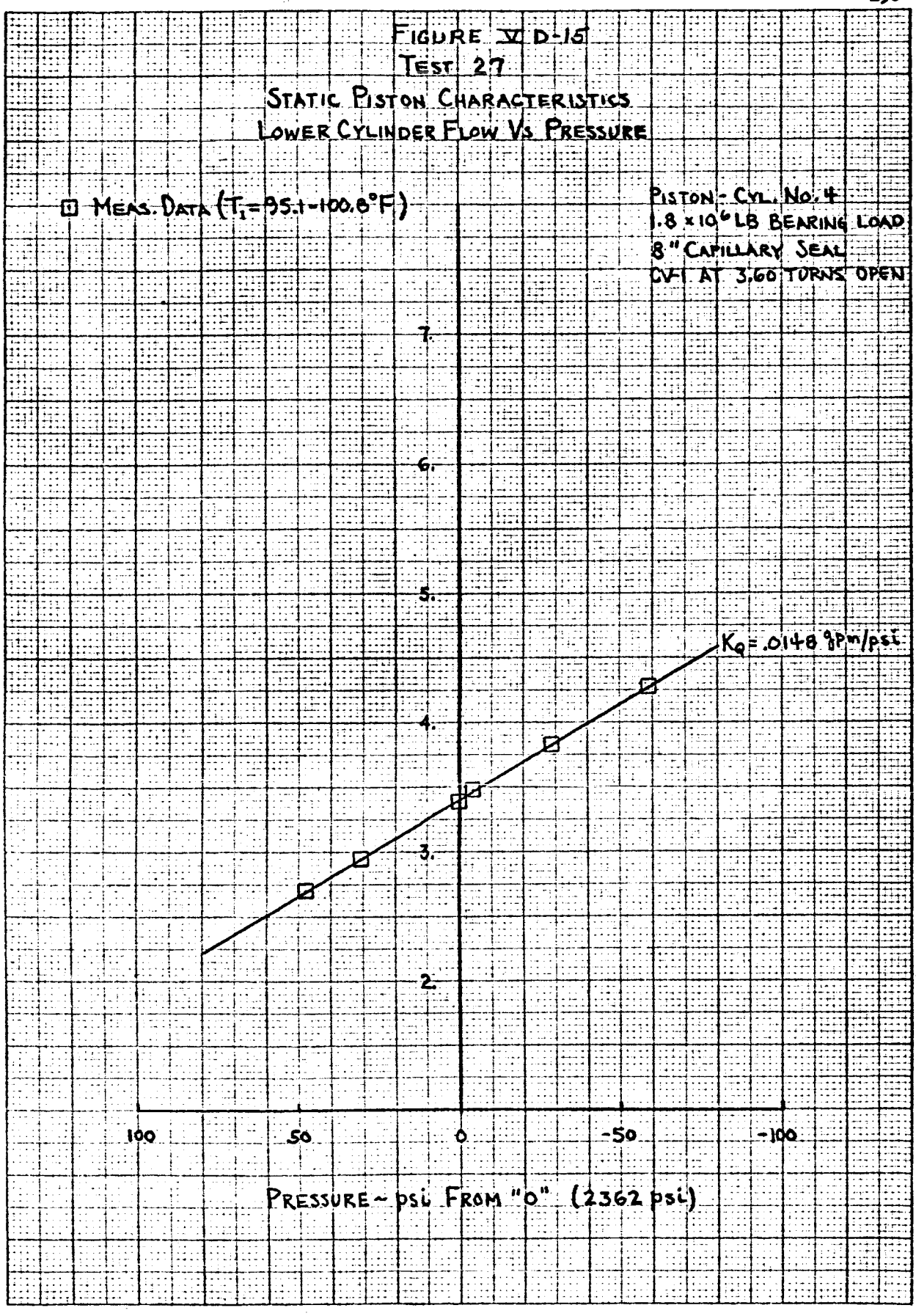

FIGURE V D-16
TEST NO 20
STATIC PISTON CHARACTERISTICS
LOWER CYLINDER FLOW VS. PRESSURE

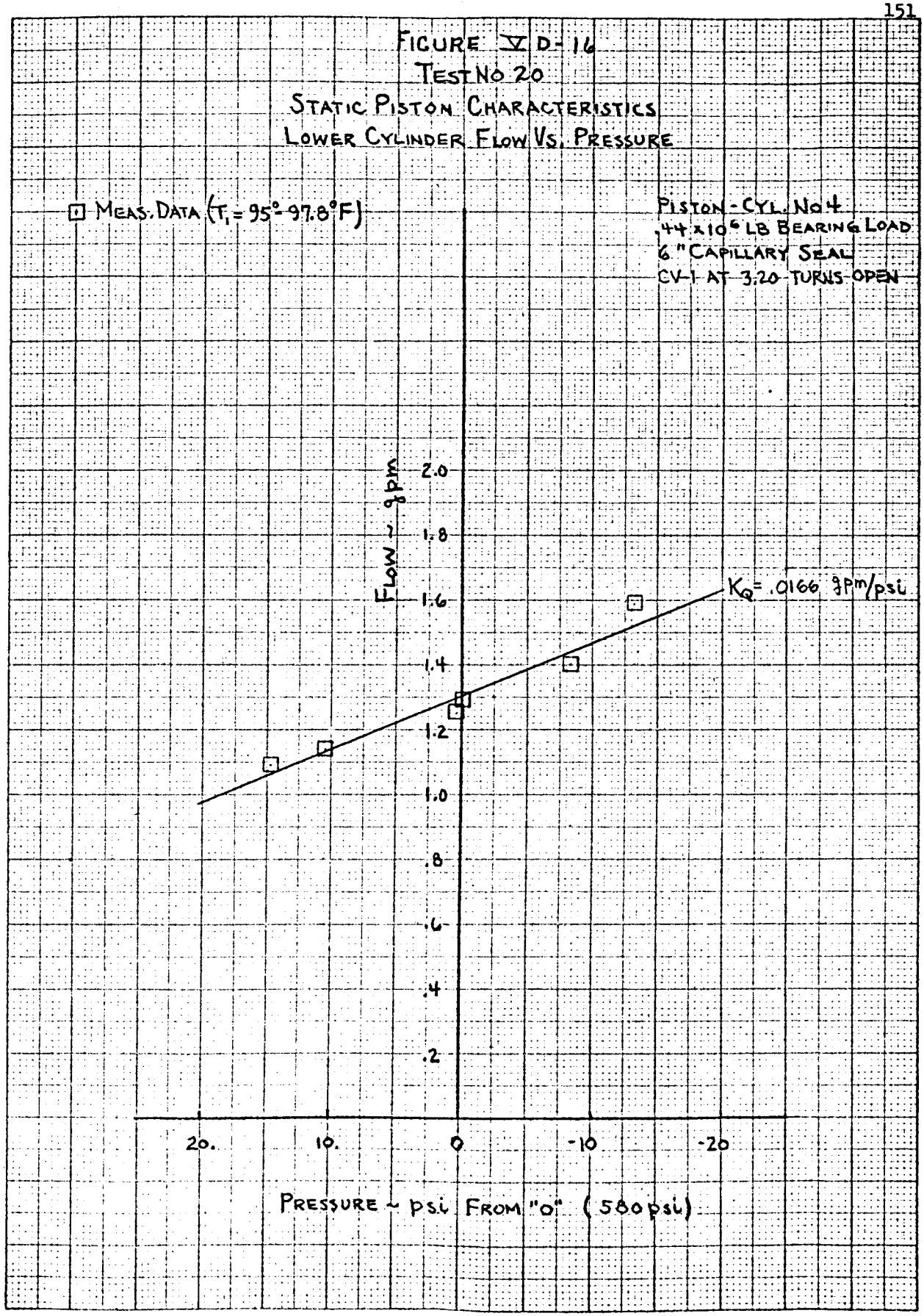

FIGURE V D-17
TEST 21
STATIC PISTON CHARACTERISTICS
LOWER CYLINDER FLOW VS. PRESSURE

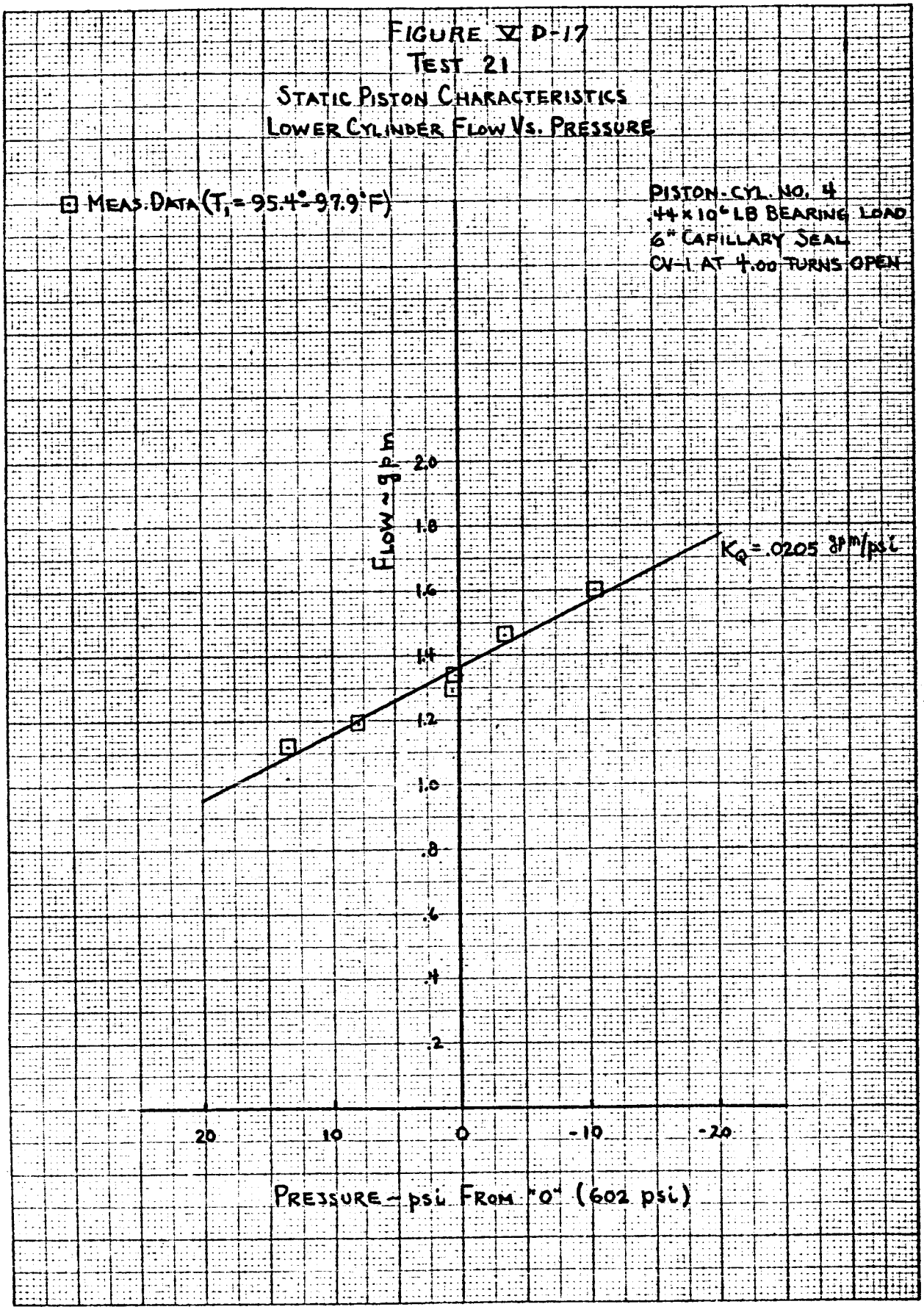

FIGURE V D-18
TEST 415
STATIC PISTON CHARACTERISTICS
LOWER CYLINDER PRESSURE VS DEFLECTION

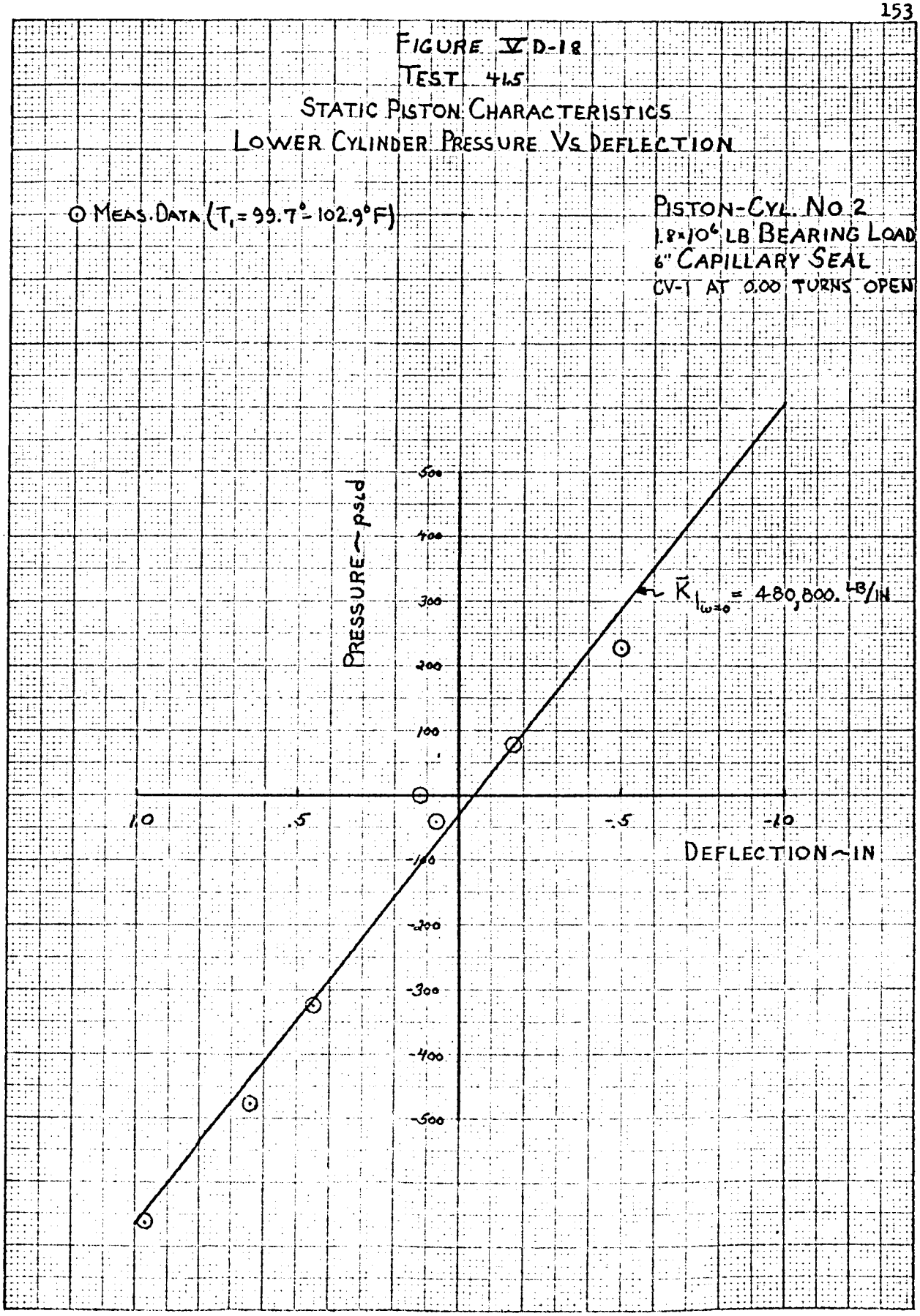

FIGURE V D-19
TEST 39-B
STATIC PISTON CHARACTERISTICS
LOWER CYLINDER PRESSURE VS. DEFLECTION

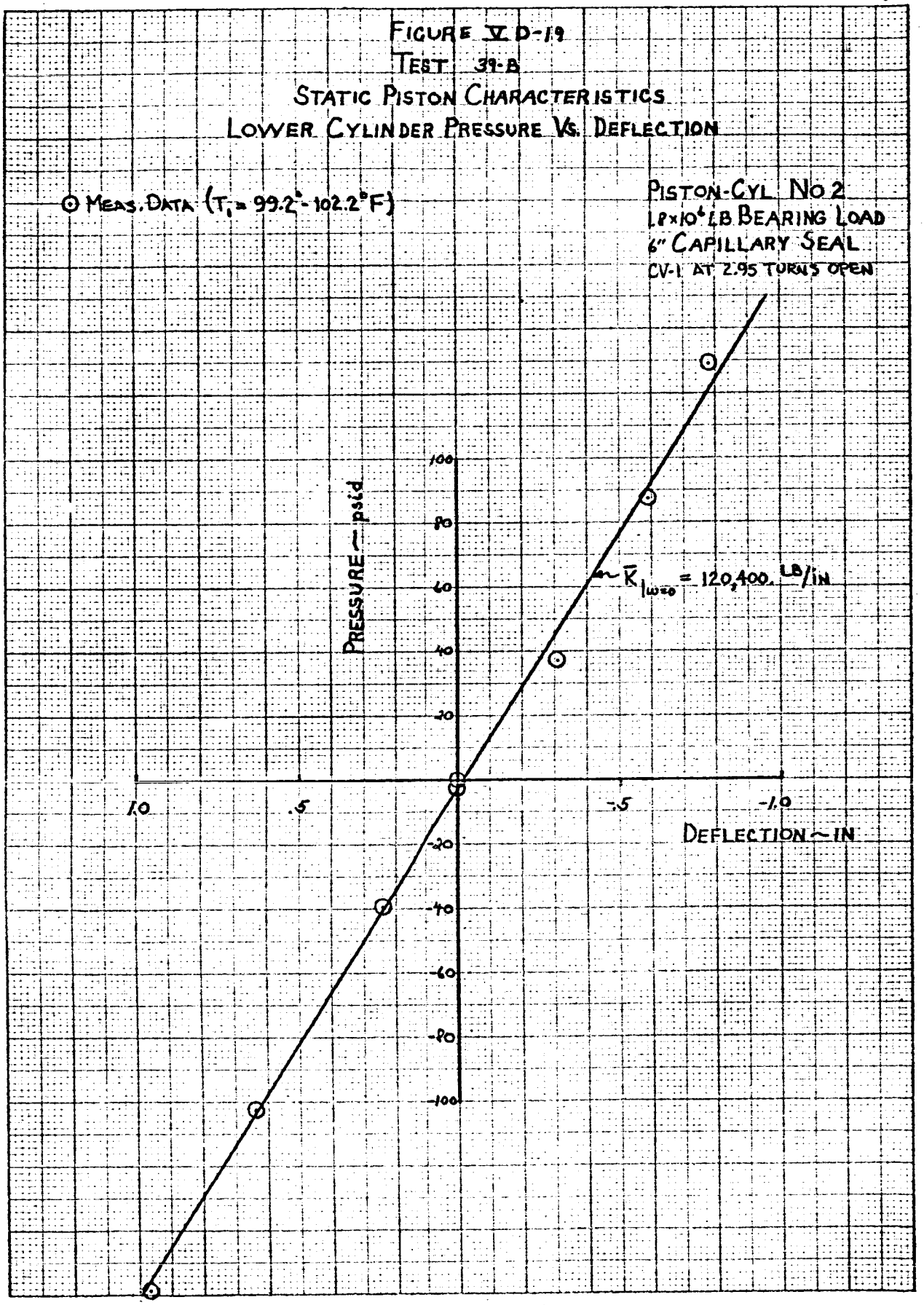

FIGURE V D-20
TEST 40-A
STATIC PISTON CHARACTERISTICS
LOWER CYLINDER PRESSURE VS. DEFLECTION

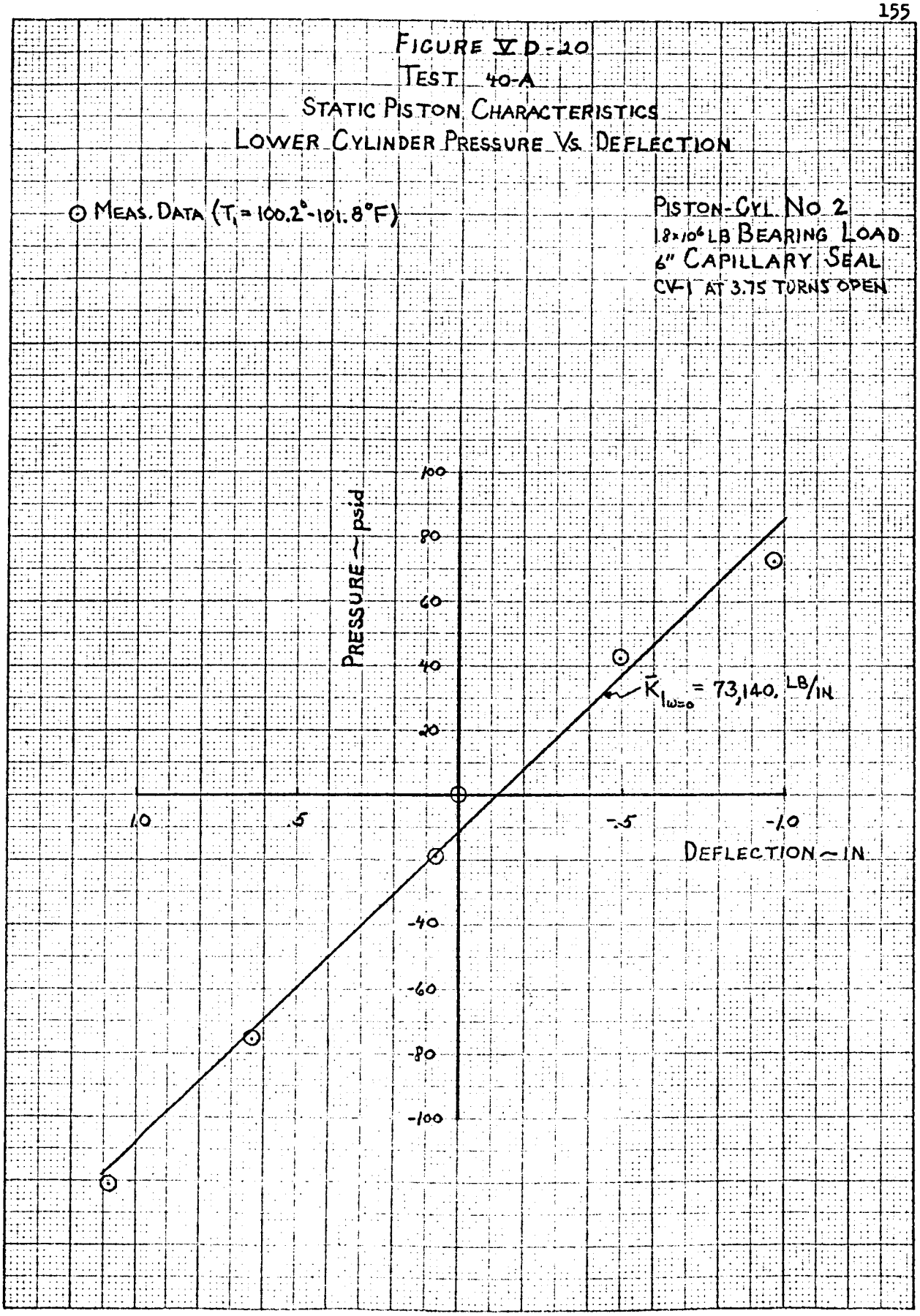

FIGURE V D-21
TEST 41
STATIC PISTON CHARACTERISTICS
LOWER CYLINDER PRESSURE VS. DEFLECTION

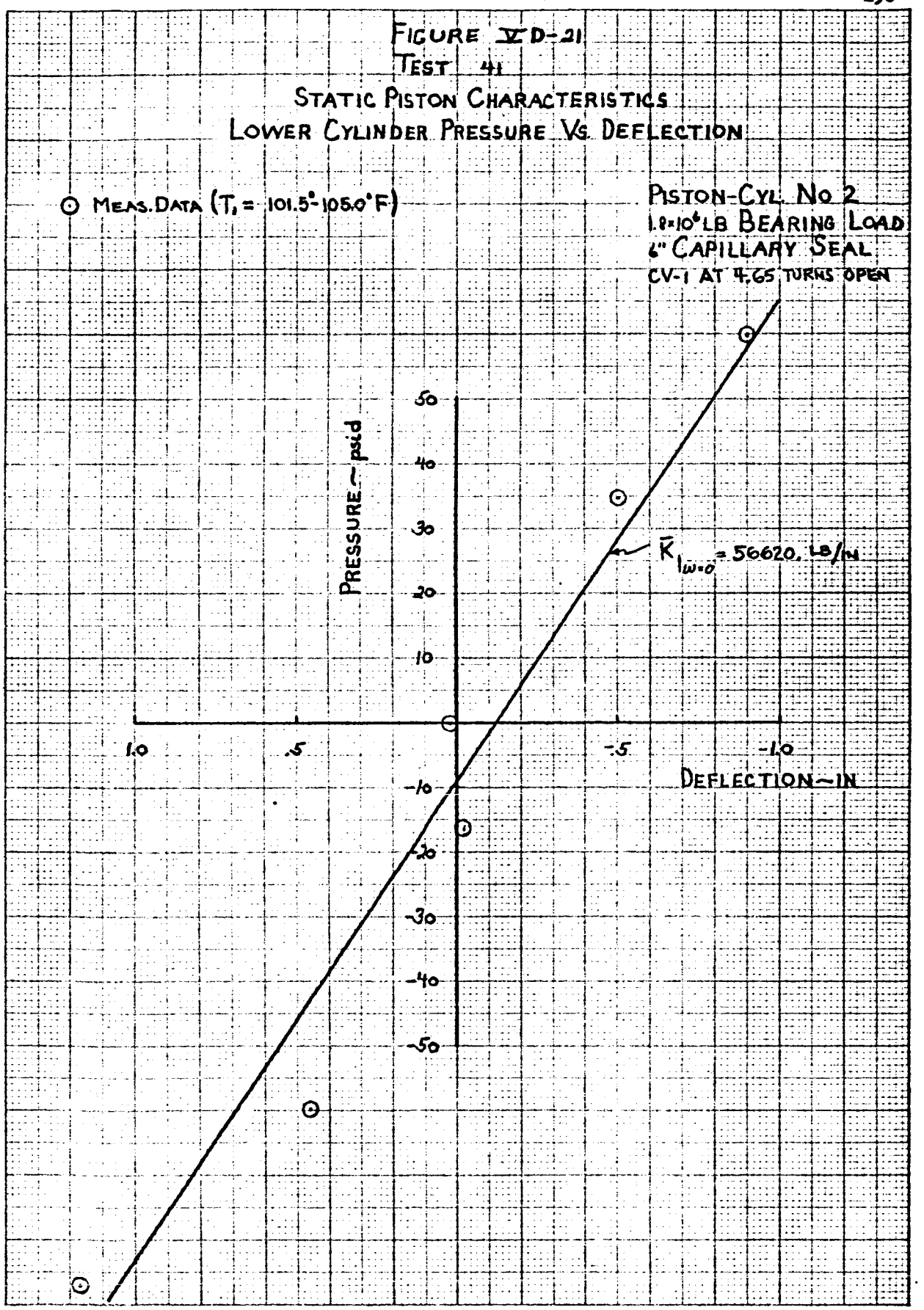

FIGURE V D-22

TEST 41-A

STATIC PISTON CHARACTERISTICS

LOWER CYLINDER PRESSURE VS. DEFLECTION

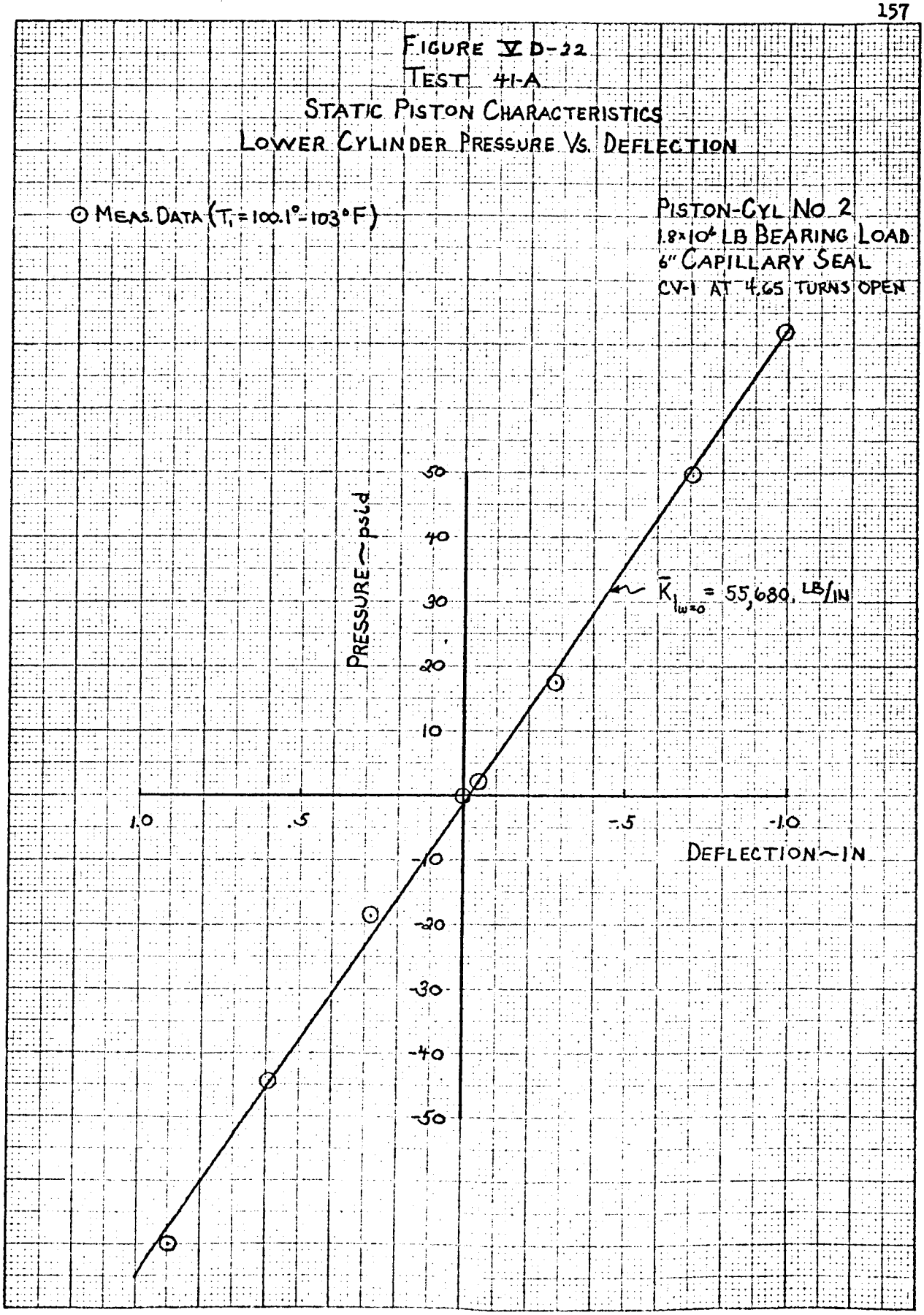

FIGURE V D-23
TEST 52-A
STATIC PISTON CHARACTERISTICS
LOWER CYLINDER PRESSURE VS. DEFLECTION

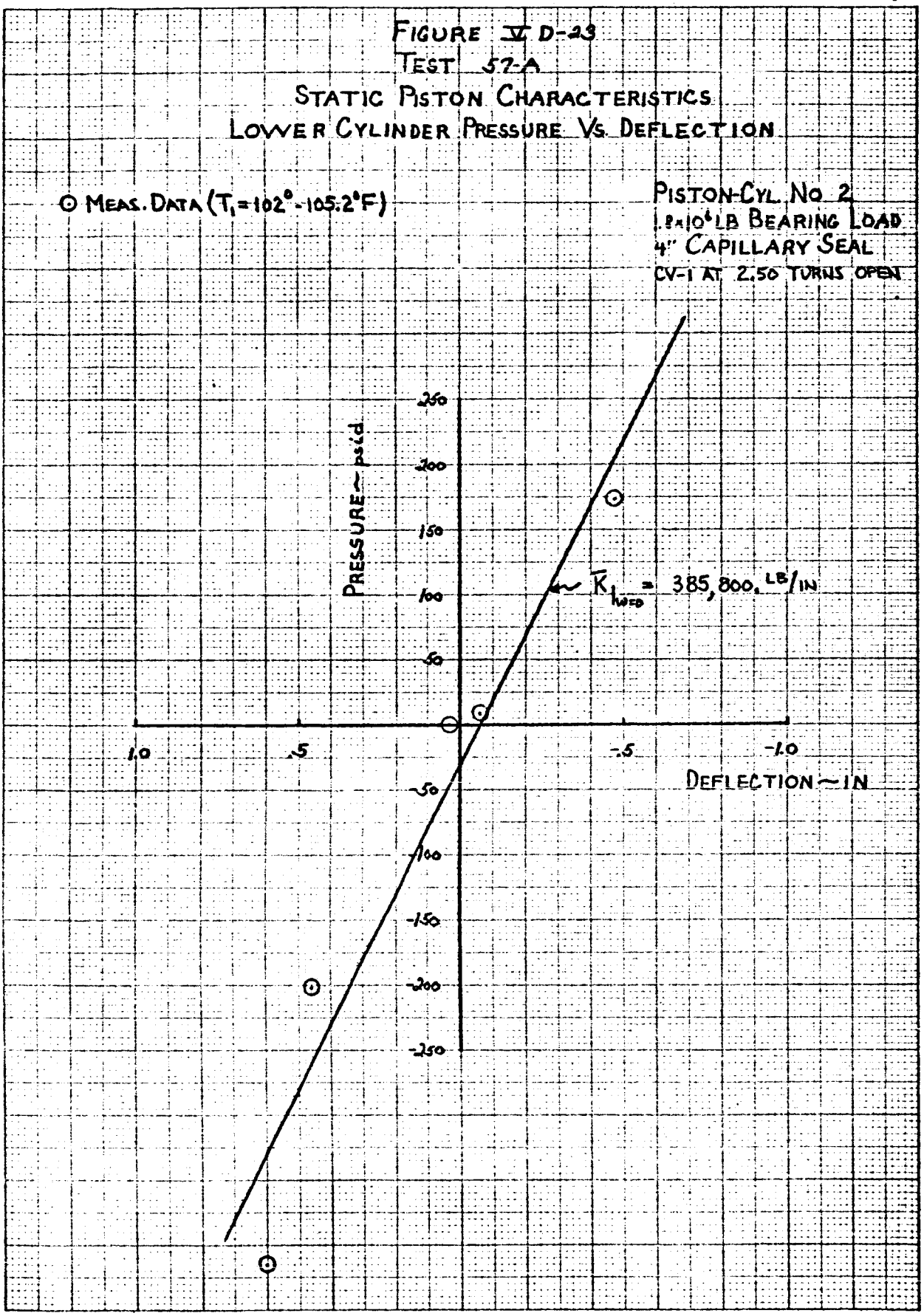

FIGURE V D-24
TEST 53
STATIC PISTON CHARACTERISTICS
LOWER CYLINDER PRESSURE VS. DEFLECTION

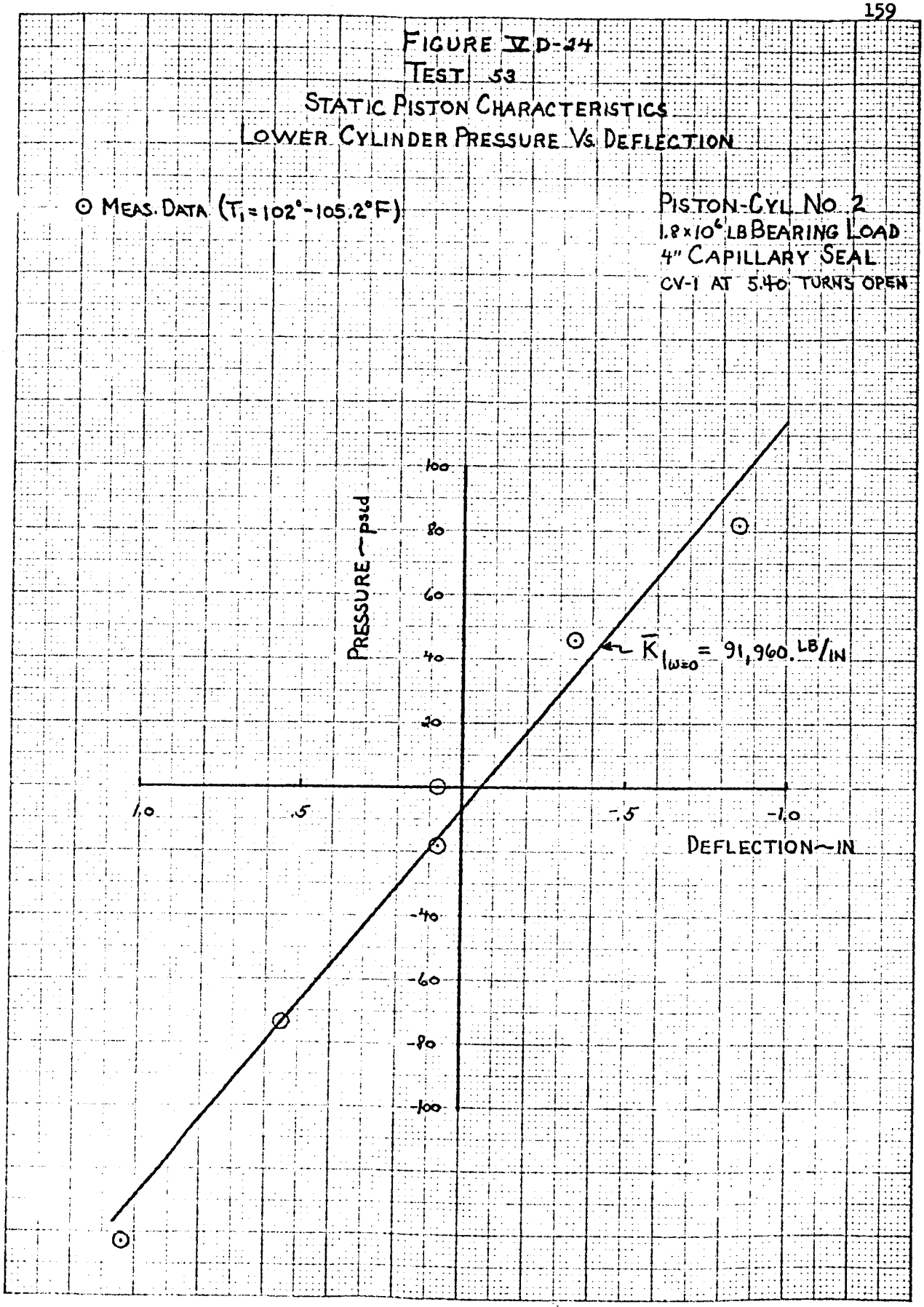

FIGURE V D-25
TEST 56-A
STATIC PISTON CHARACTERISTICS
LOWER CYLINDER PRESSURE VS. DEFLECTION

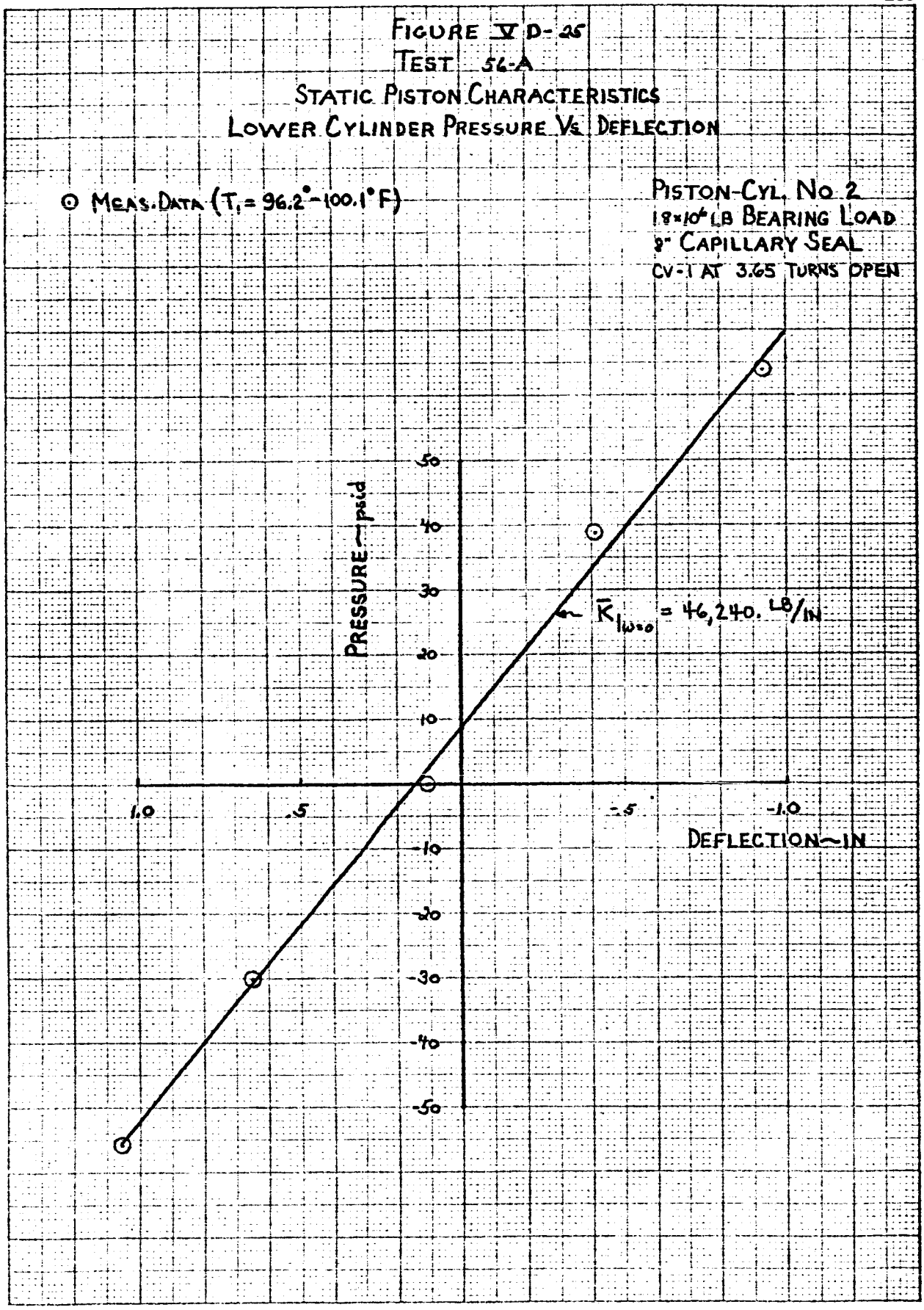

FIGURE V D-26
TEST 45
STATIC PISTON CHARACTERISTICS
LOWER CYLINDER PRESSURE VS. DEFLECTION

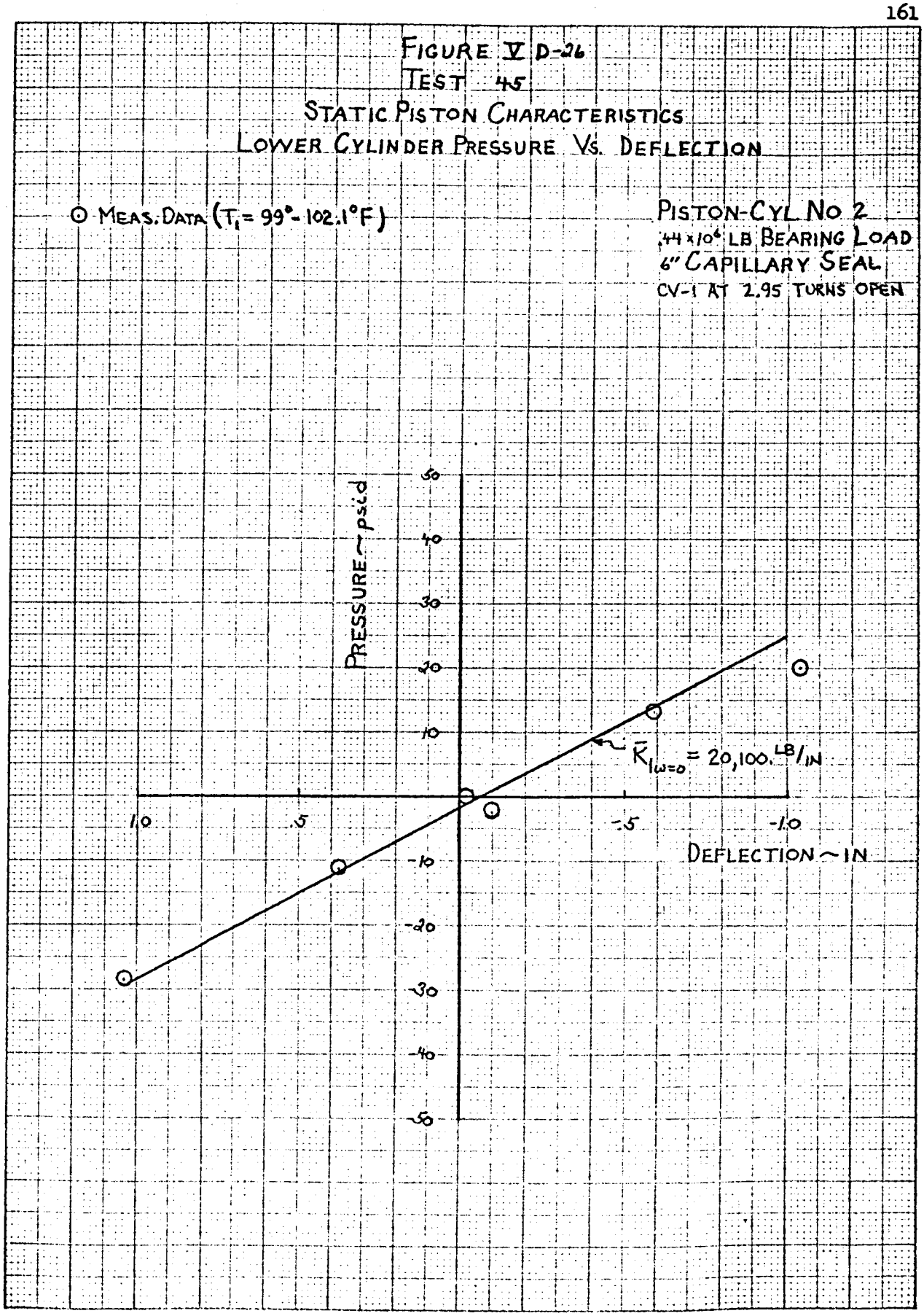

FIGURE V D-27
TEST 46
STATIC PISTON CHARACTERISTICS
LOWER CYLINDER PRESSURE VS. DEFLECTION

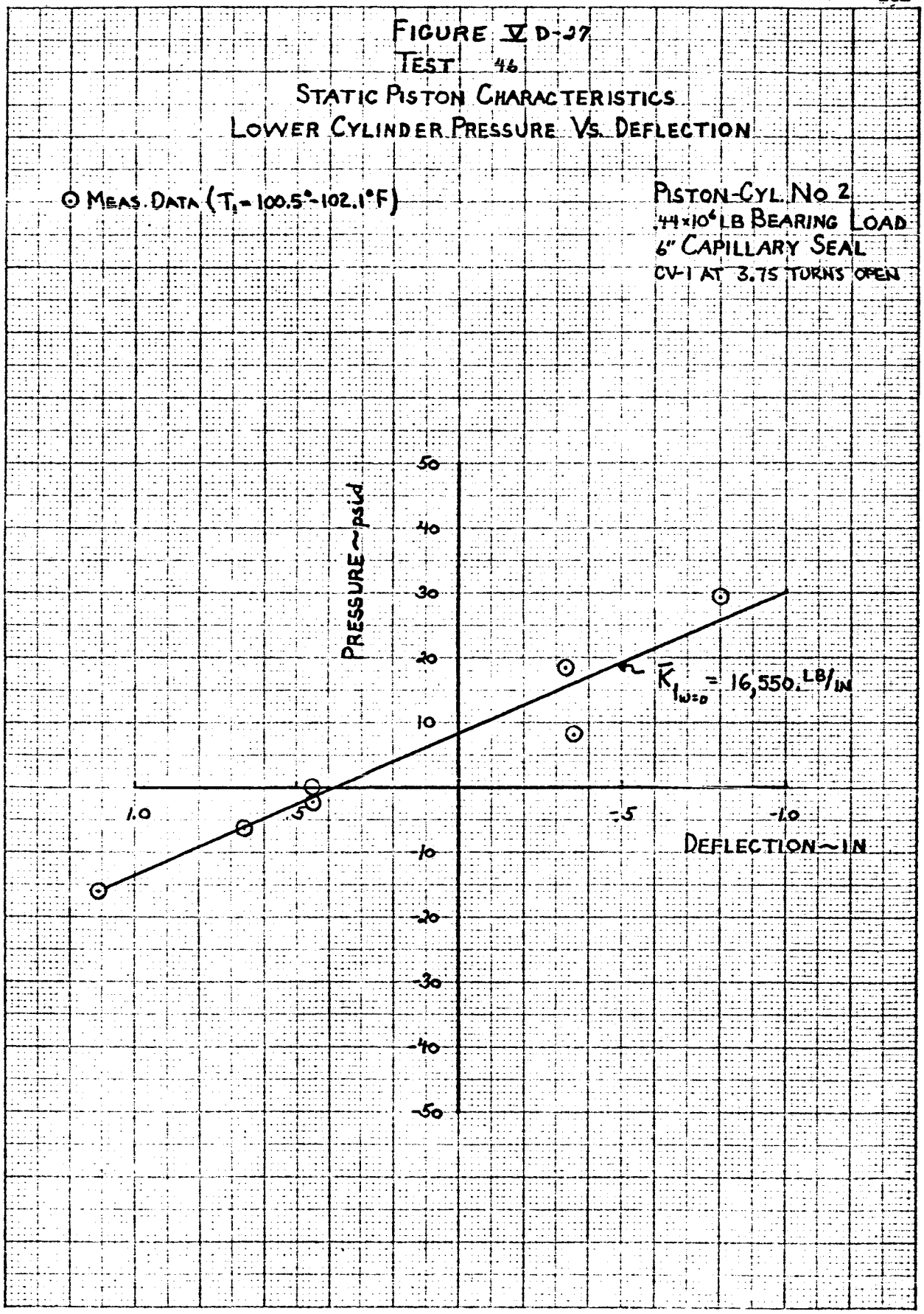

FIGURE V D-28
TEST 47
STATIC PISTON CHARACTERISTICS
LOWER CYLINDER PRESSURE VS. DEFLECTION

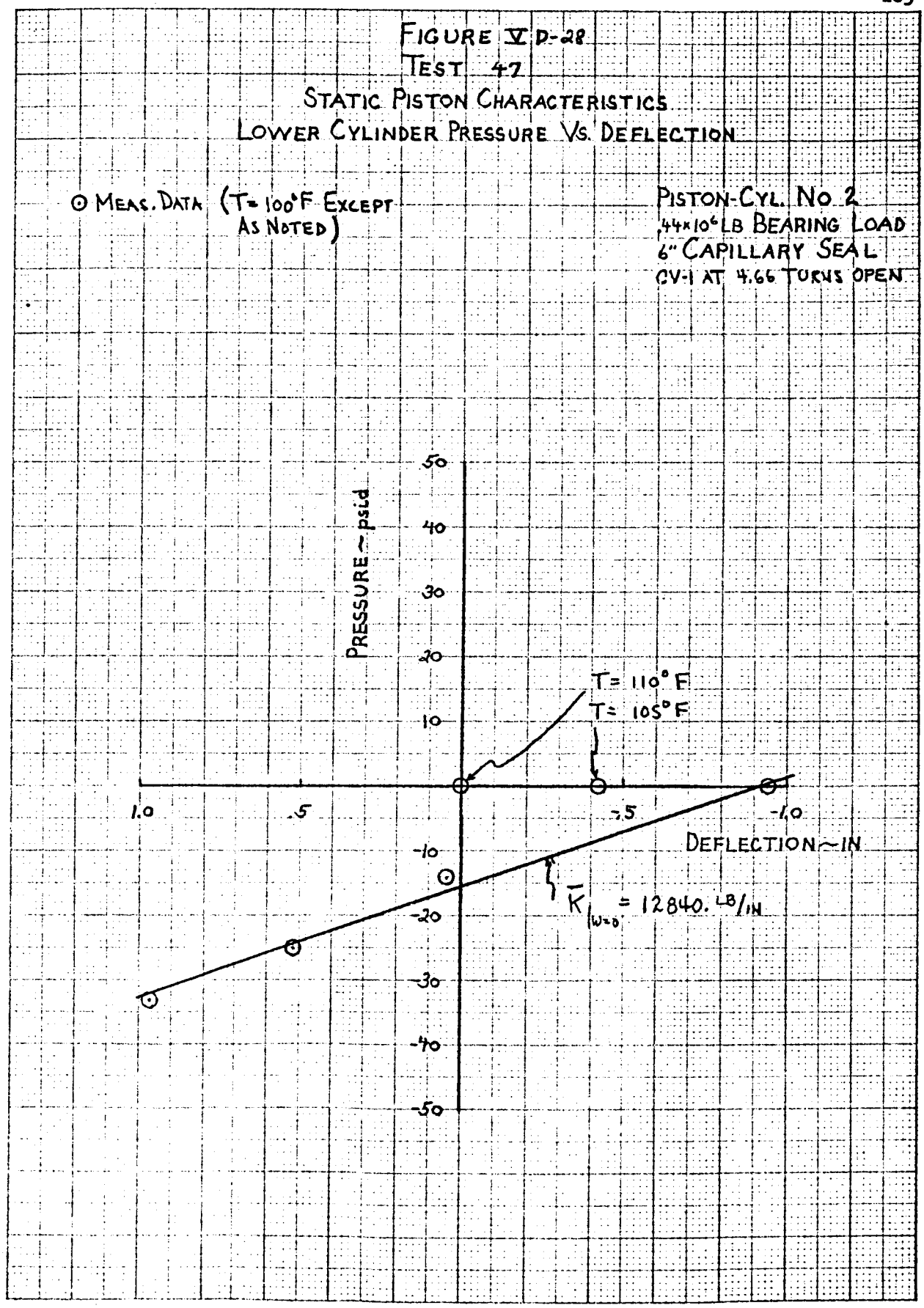

FIGURE V D-24
TEST 18A
STATIC PISTON CHARACTERISTICS
LOWER CYLINDER PRESSURE VS DEFLECTION

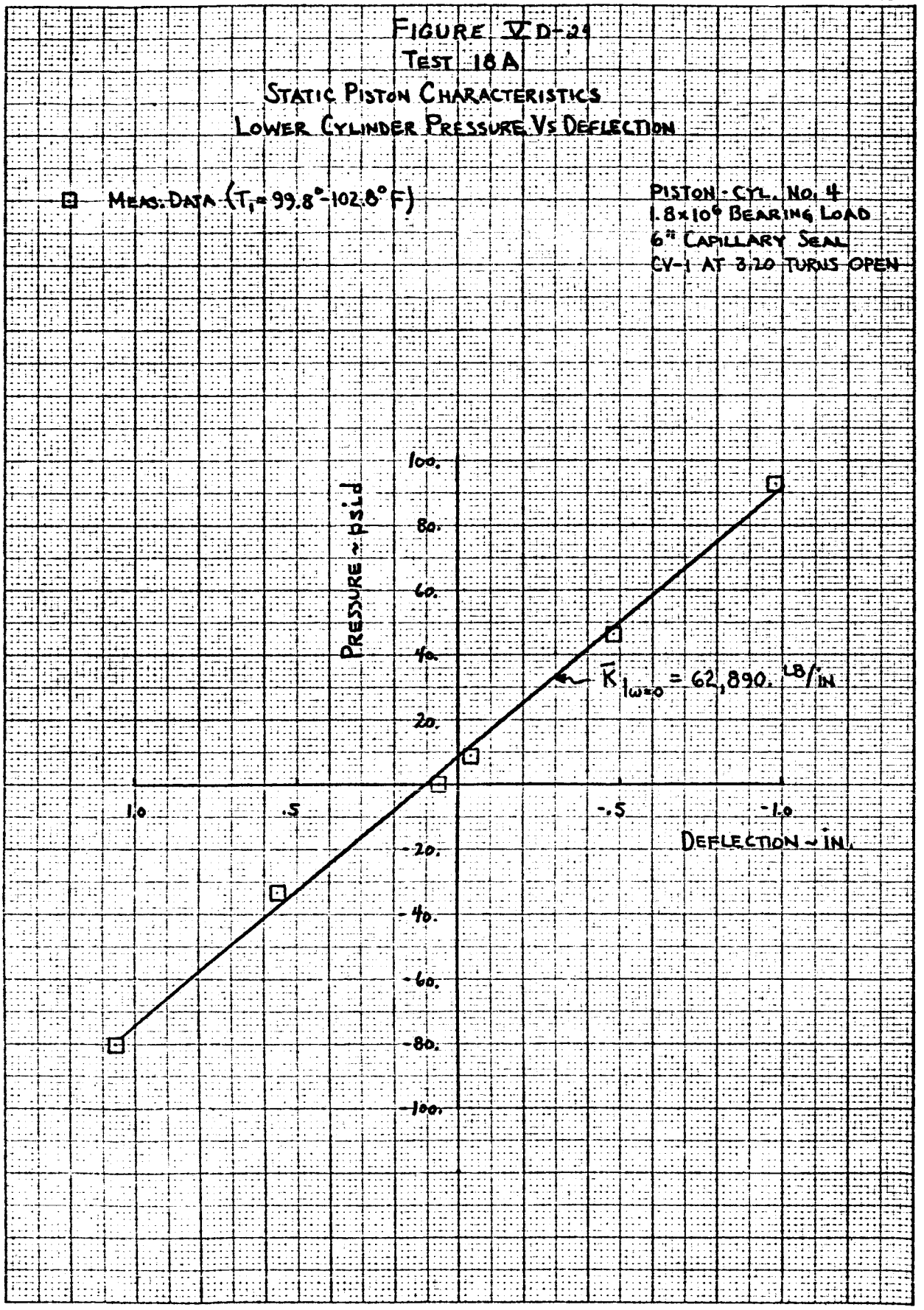

FIGURE V D-30
TEST 19
STATIC PISTON CHARACTERISTICS
LOWER CYLINDER PRESSURE VS. DEFLECTION

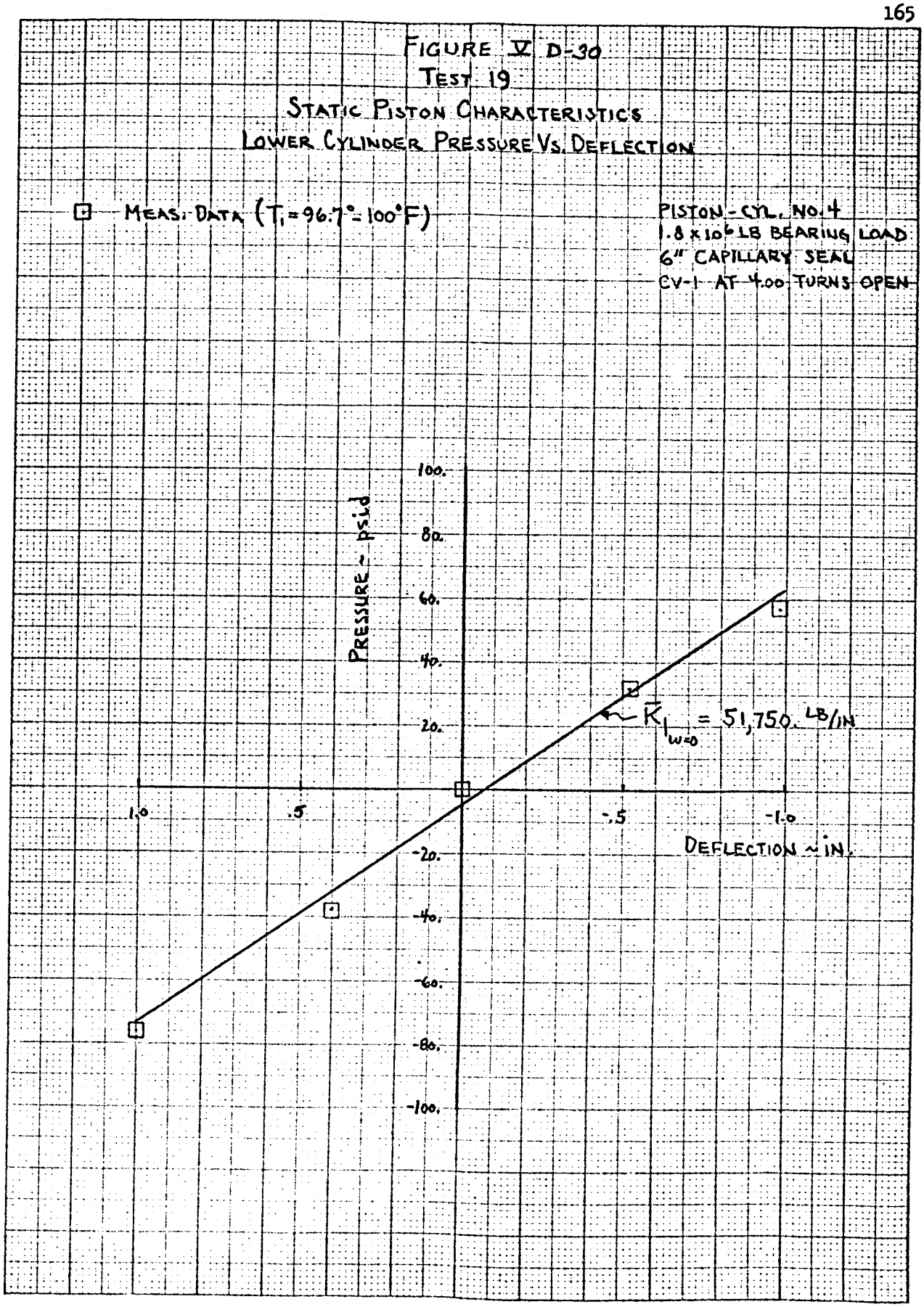

FIGURE V D-3
TEST 24
STATIC PISTON CHARACTERISTICS
LOWER CYLINDER PRESSURE VS DEFLECTION

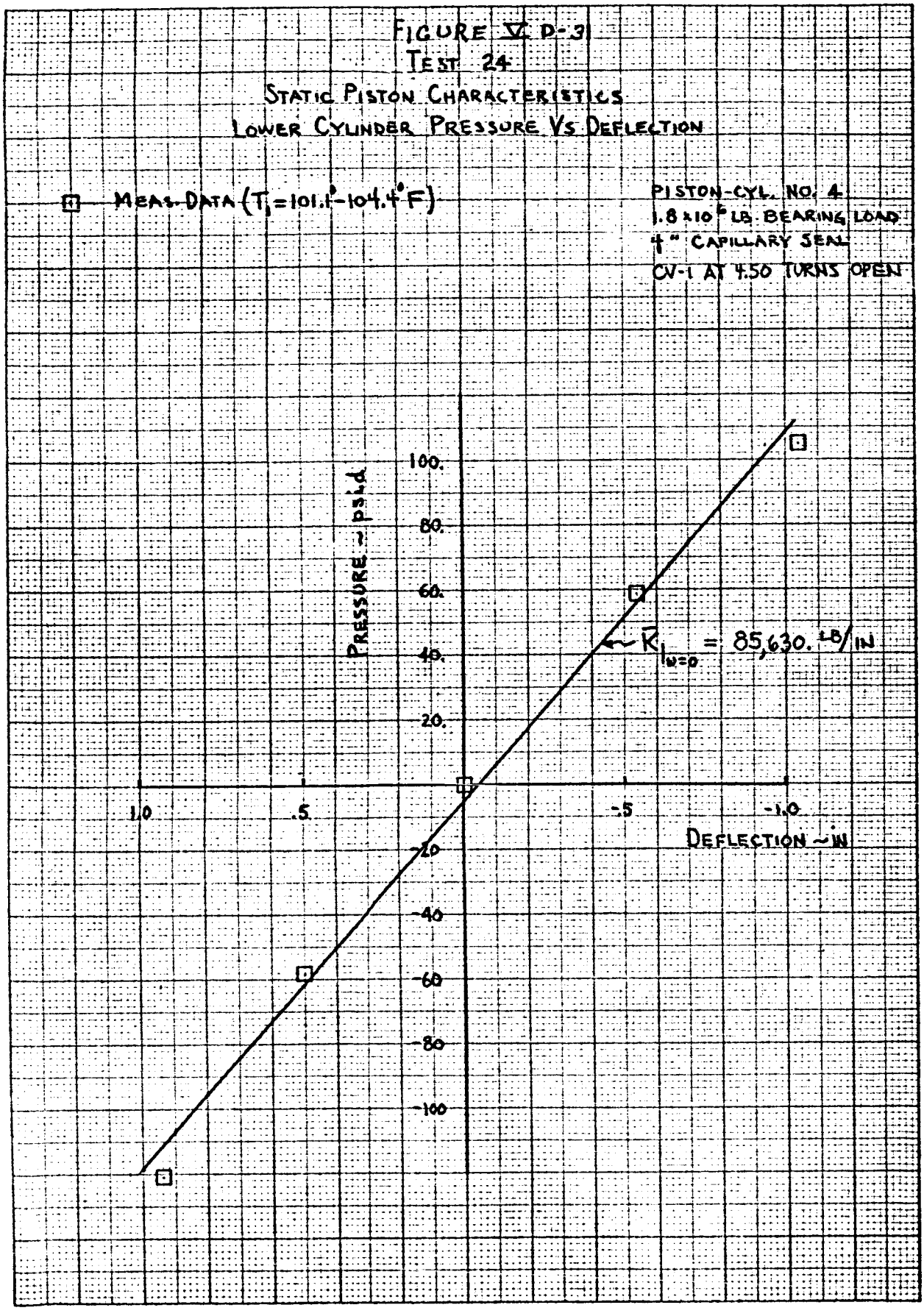

FIGURE V D-32
TEST 27
STATIC PISTON CHARACTERISTICS
LOWER CYLINDER PRESSURE VS. DEFLECTION

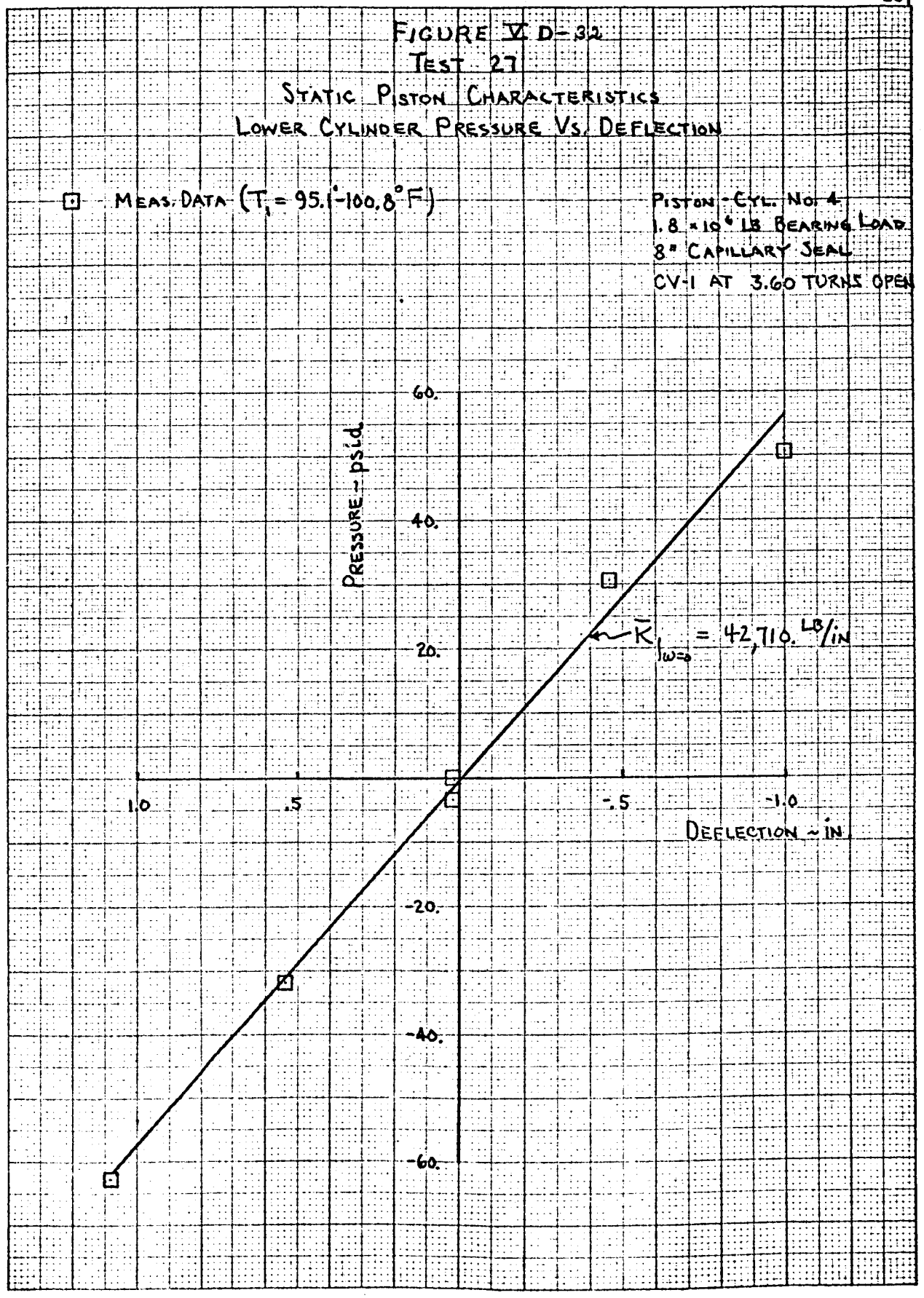

FIGURE V D-33

TEST 20

STATIC PISTON CHARACTERISTICS

LOWER CYLINDER PRESSURE VS. DEFLECTION

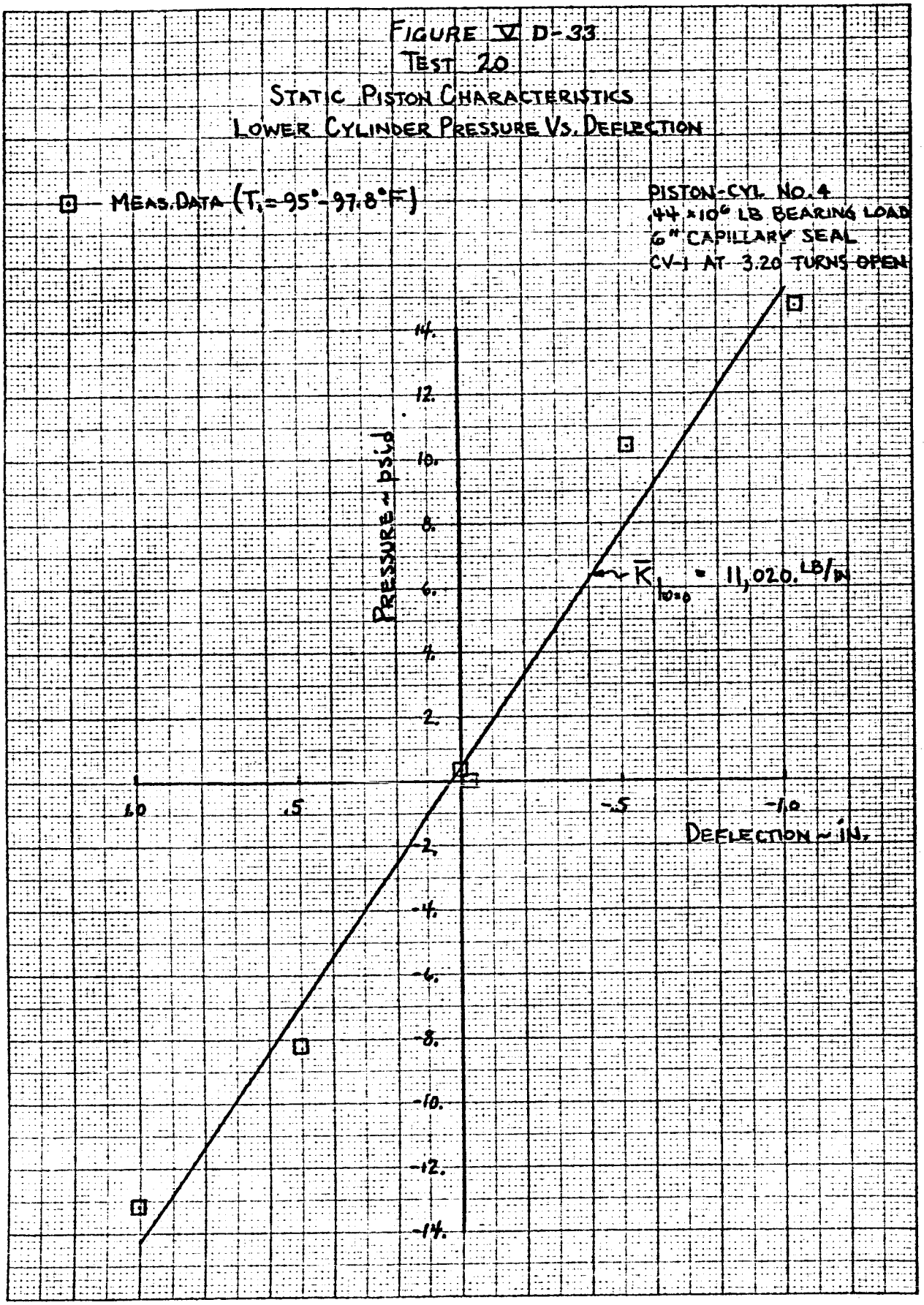

FIGURE V D-34
TEST 21
STATIC PISTON CHARACTERISTICS
LOWER CYLINDER PRESSURE VS. DEFLECTION

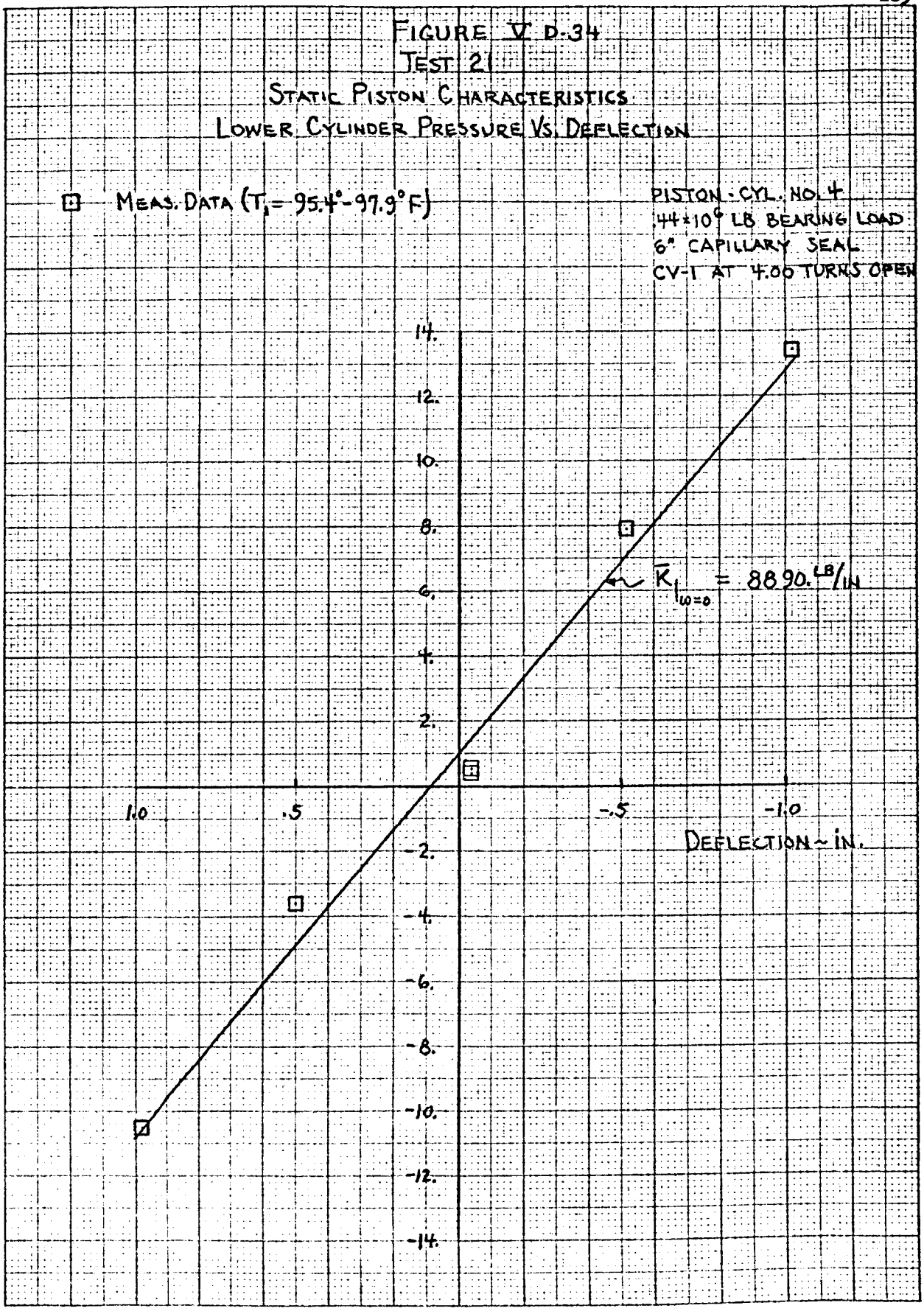

FIGURE V D-35

COMPARISON OF K_Q's OBTAINED FROM STATIC PISTON CHARACTERISTIC TESTS WITH STATIC CALIBRATION OF THE CAPILLARY RESTRICTOR VALVE (CV-1)

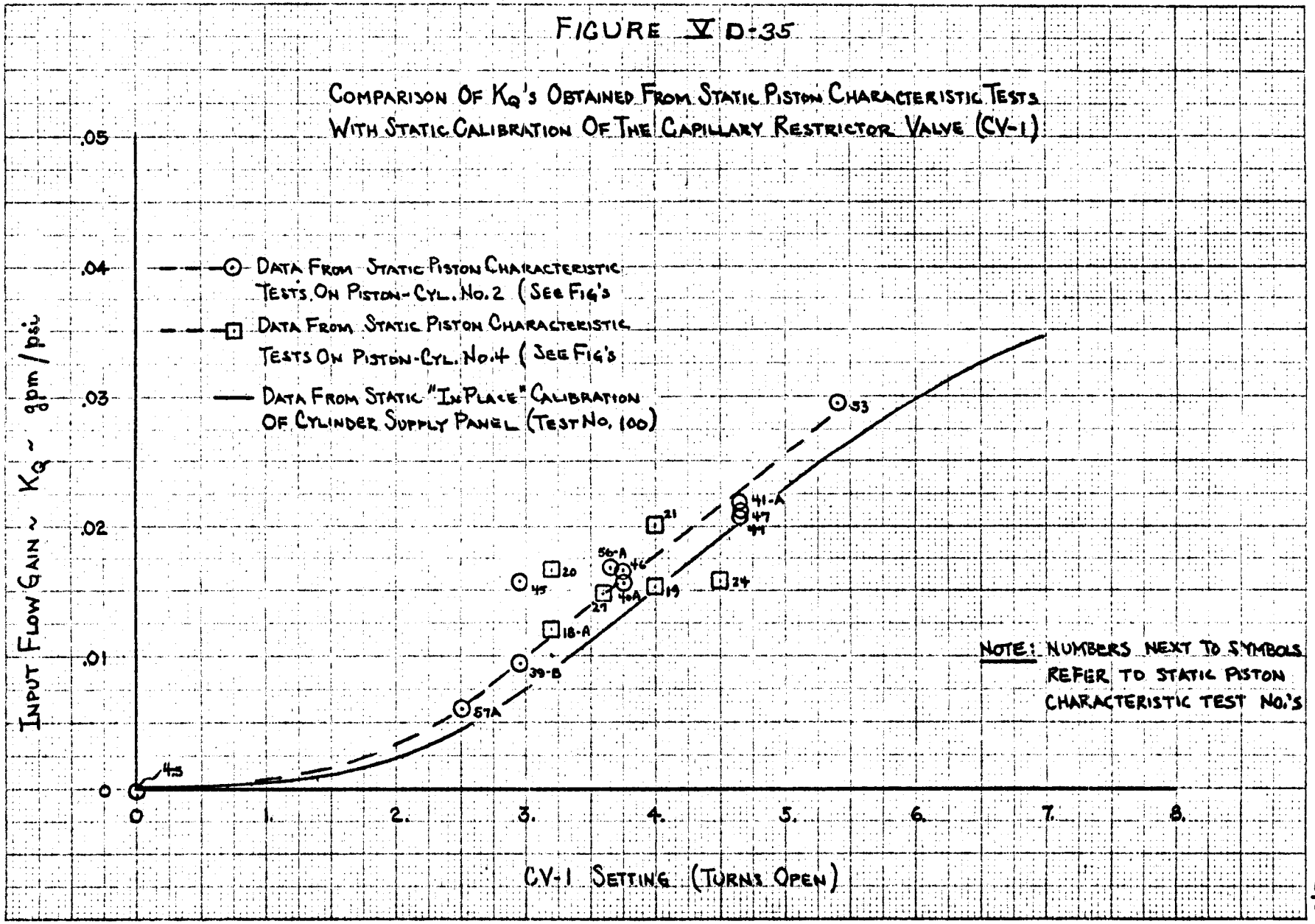

FIGURE V E-1

TEST NO. 108
(LATERAL DAMPING)

ENVELOPE OF STEM DEFLECTION IN FREE VIBRATION
(PISTON-CYL. NO'S 1 & 2, ZERO BEARING LOAD)

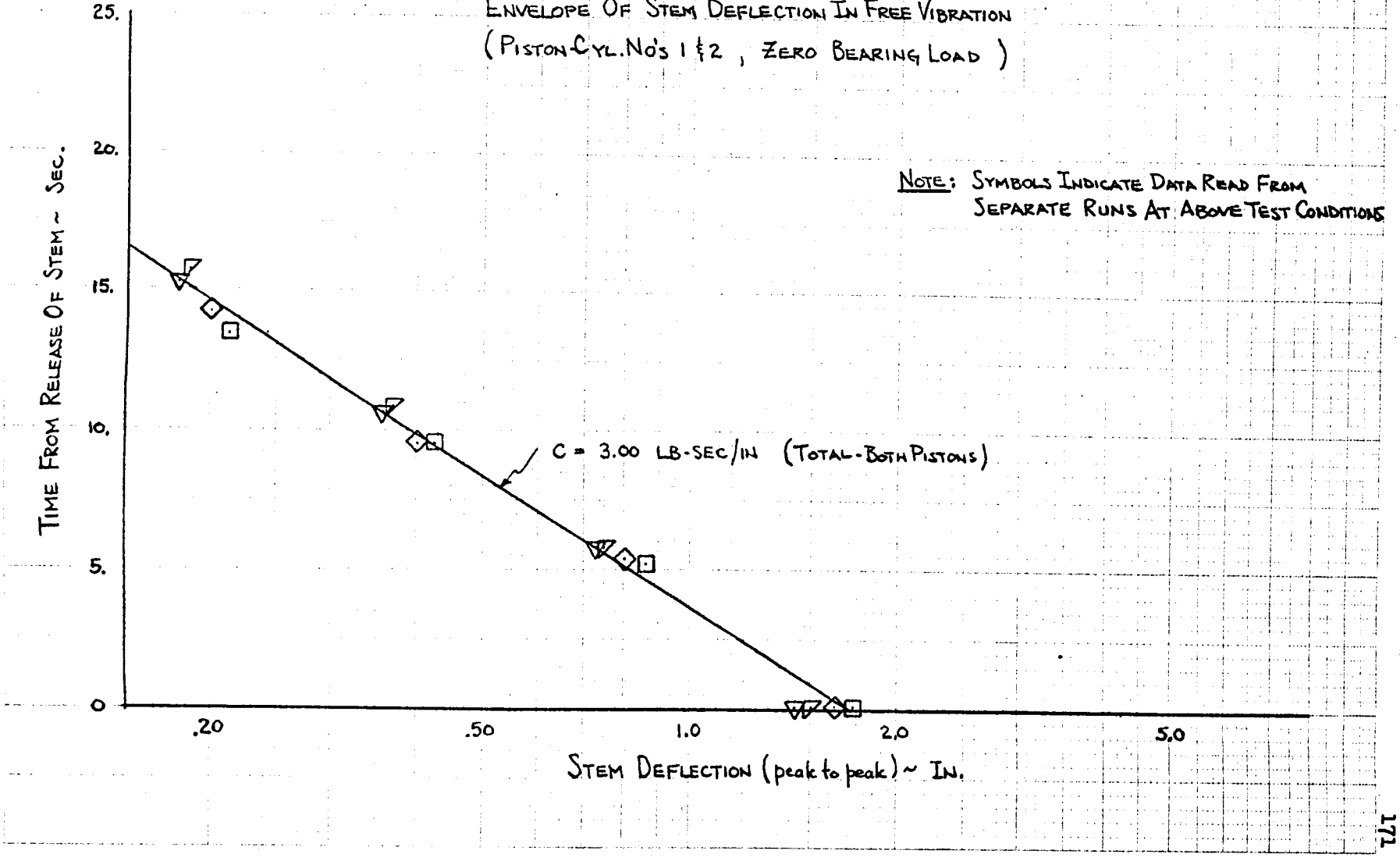

FIGURE V E-2

TEST No. 108
(LATERAL DAMPING)

ENVELOPE OF STEM DEFLECTION IN FREE VIBRATION
(PISTON-CYL. NO's 1&2, 0.1×10^6 LB. BEARING LOAD)

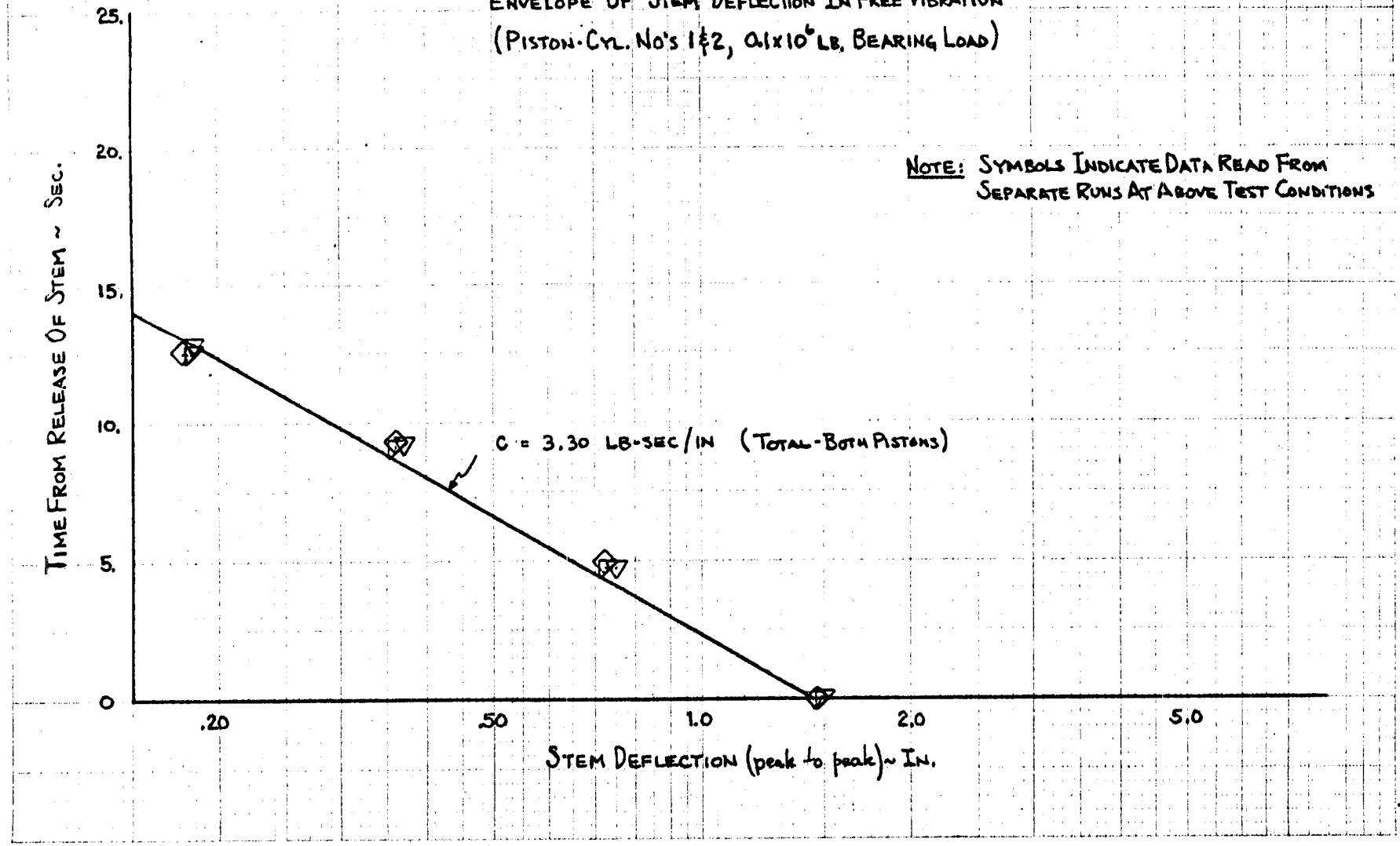

NOTE: SYMBOLS INDICATE DATA READ FROM SEPARATE RUNS AT ABOVE TEST CONDITIONS

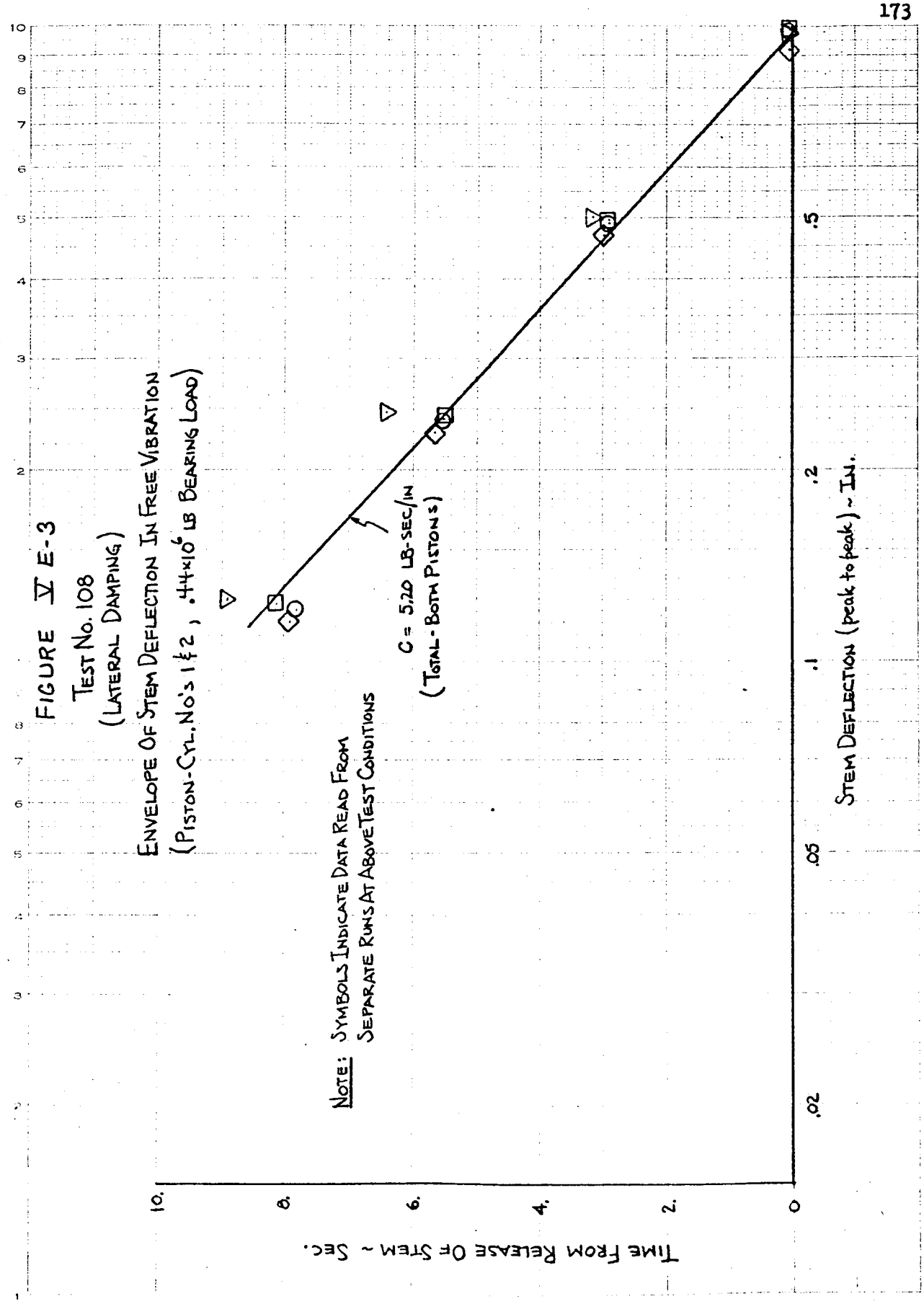
FIGURE V E-3
TEST NO. 108
(LATERAL DAMPING)
ENVELOPE OF STEM DEFLECTION IN FREE VIBRATION
(PISTON-CYL. NO'S 1 & 2, .44×10⁶ LB BEARING LOAD)
NOTE: SYMBOLS INDICATE DATA READ FROM SEPARATE RUNS AT ABOVE TEST CONDITIONS
C = 5.20 LB-SEC/IN
(TOTAL - BOTH PISTONS)
TIME FROM RELEASE OF STEM ~ SEC.
STEM DEFLECTION (peak to peak) ~ IN.
10.
8.
6.
4.
2.
0
.02
.05
.1
.2
.5

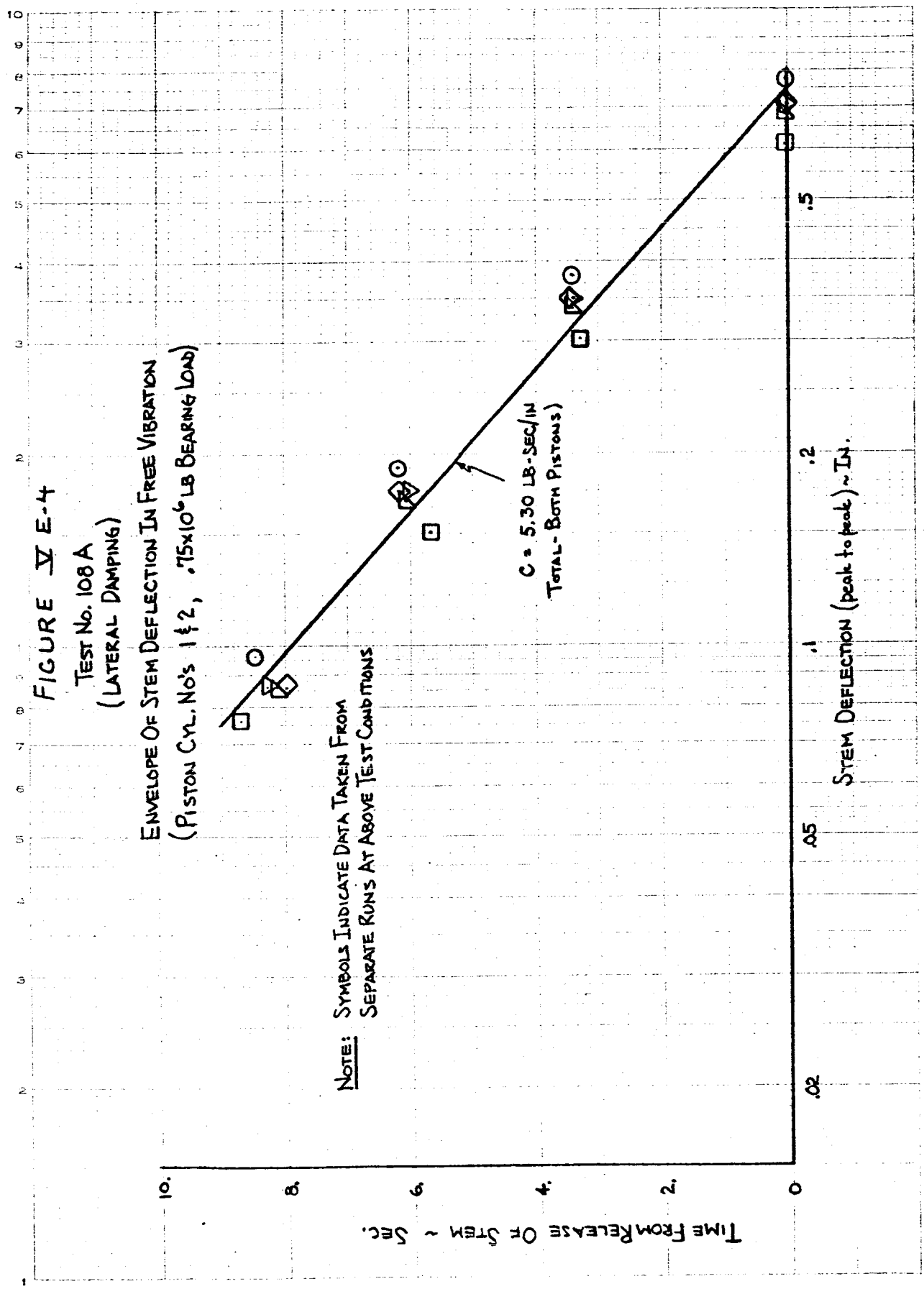
FIGURE V E-4
TEST No. 108 A
(LATERAL DAMPING)
ENVELOPE OF STEM DEFLECTION IN FREE VIBRATION
(PISTON CYL. NO's 1 & 2, .75x10⁶ LB BEARING LOAD)
C = 5.30 LB-SEC/IN
TOTAL - BOTH PISTONS
NOTE: SYMBOLS INDICATE DATA TAKEN FROM SEPARATE RUNS AT ABOVE TEST CONDITIONS
TIME FROM RELEASE OF STEM ~ SEC.
STEM DEFLECTION (peak to peak) ~ IN.
10.
8.
6.
4.
2.
0
.5
.2
.1
.05
.02

FIGURE V E-5

TEST NO. 38
(LATERAL DAMPING)

ENVELOPE OF STEM DEFLECTION IN FREE VIBRATION
(PISTON CYL. NO'S 3 & 4, .44×10⁶ LB BEARING LOAD)

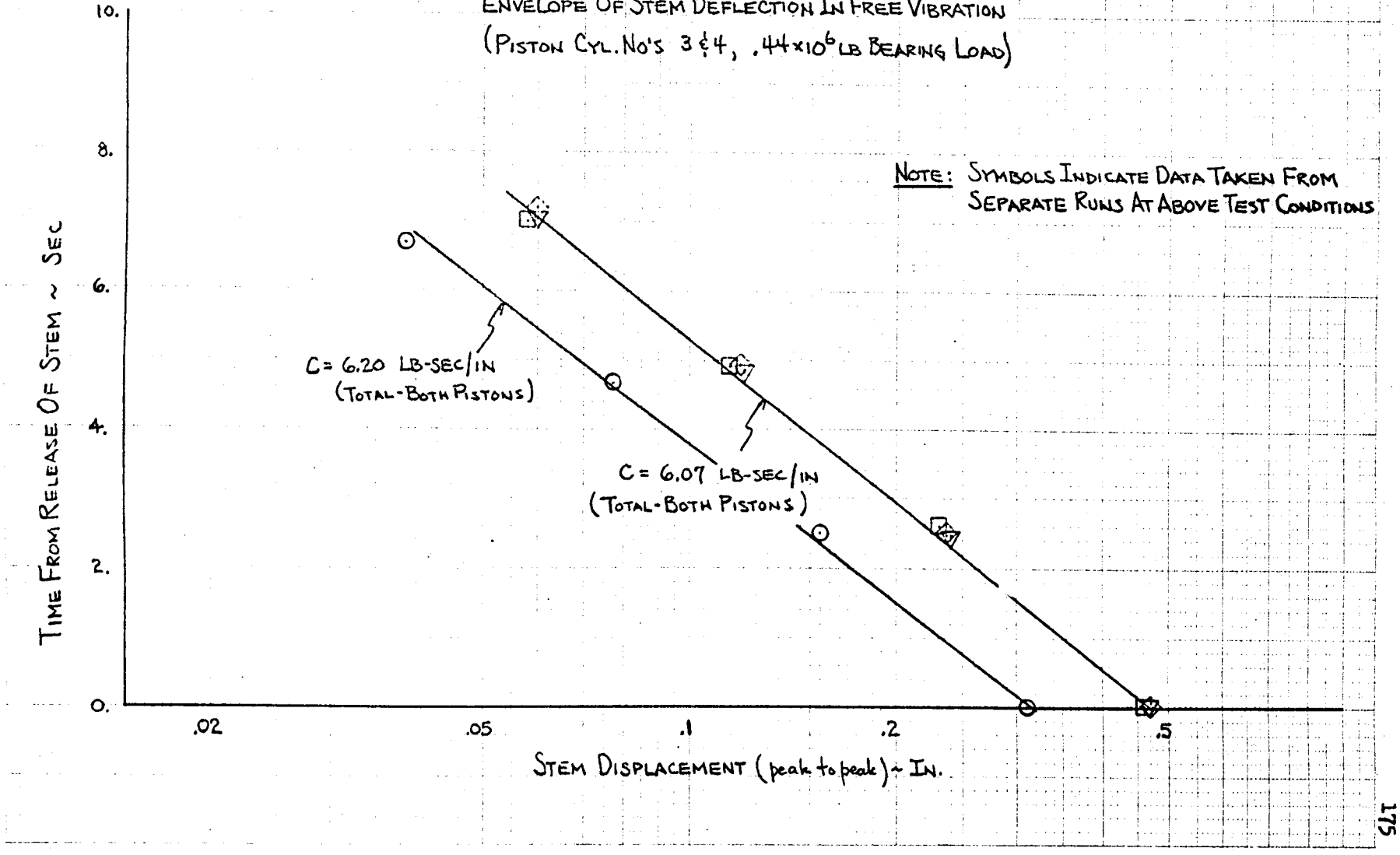

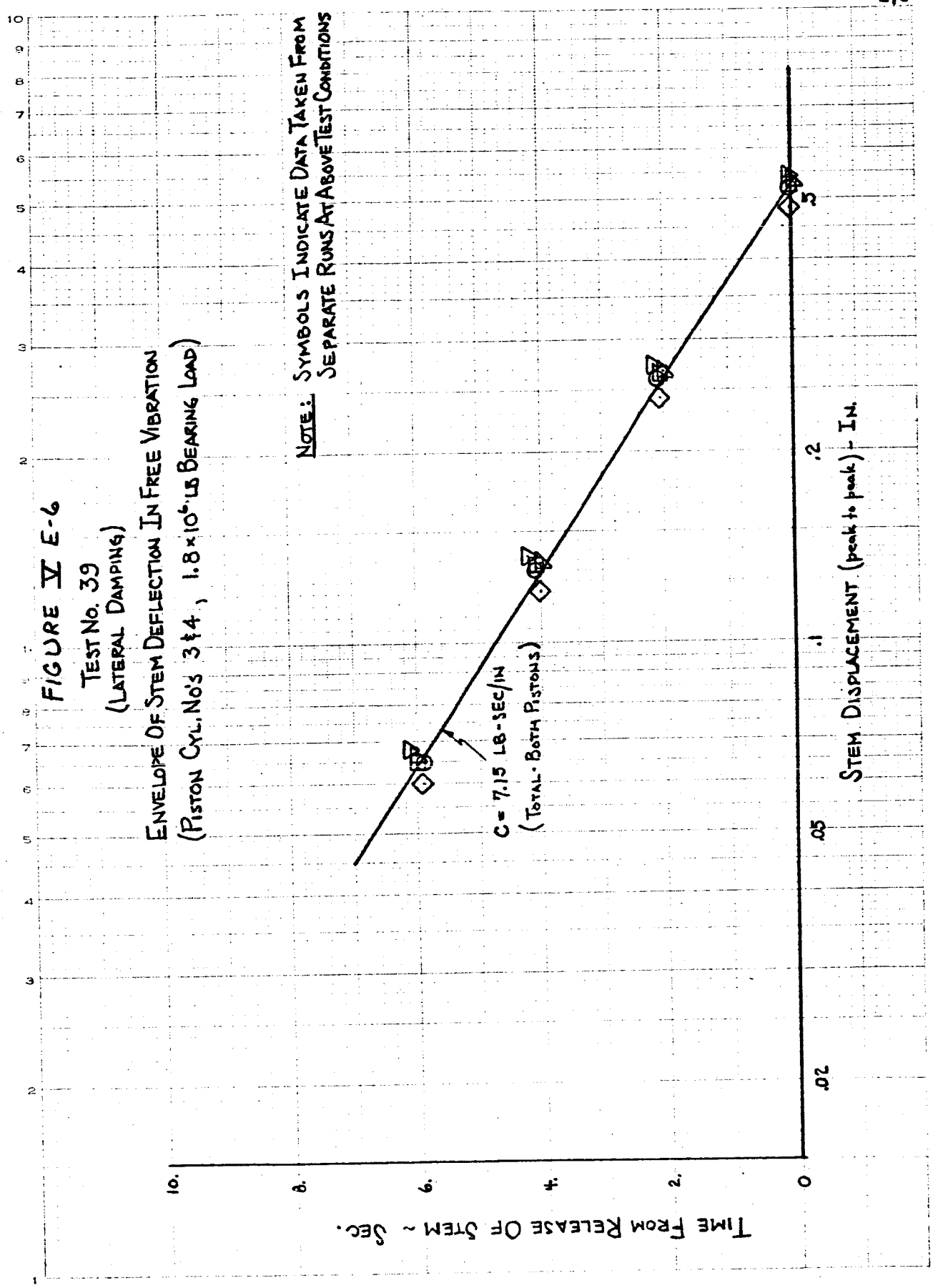
FIGURE V E-6
TEST No. 39
(LATERAL DAMPING)
ENVELOPE OF STEM DEFLECTION IN FREE VIBRATION
(PISTON CYL. NOS 3 & 4, 1.8 x 10⁶ LB BEARING LOAD)
NOTE: SYMBOLS INDICATE DATA TAKEN FROM SEPARATE RUNS AT ABOVE TEST CONDITIONS
C = 7.15 LB-SEC/IN
(TOTAL - BOTH PISTONS)
TIME FROM RELEASE OF STEM ~ SEC.
STEM DISPLACEMENT (peak to peak) ~ IN.
10.
8.
6.
4.
2.
0
.02
.05
.1
.2
.5

FIGURE V E-7

TEST No's 108, 108A, 38, 39

LATERAL DAMPING COEFFICIENT PER PISTON
AT VARIOUS BEARING LOADS FOR BOTH SETS
OF PISTON CYLINDERS

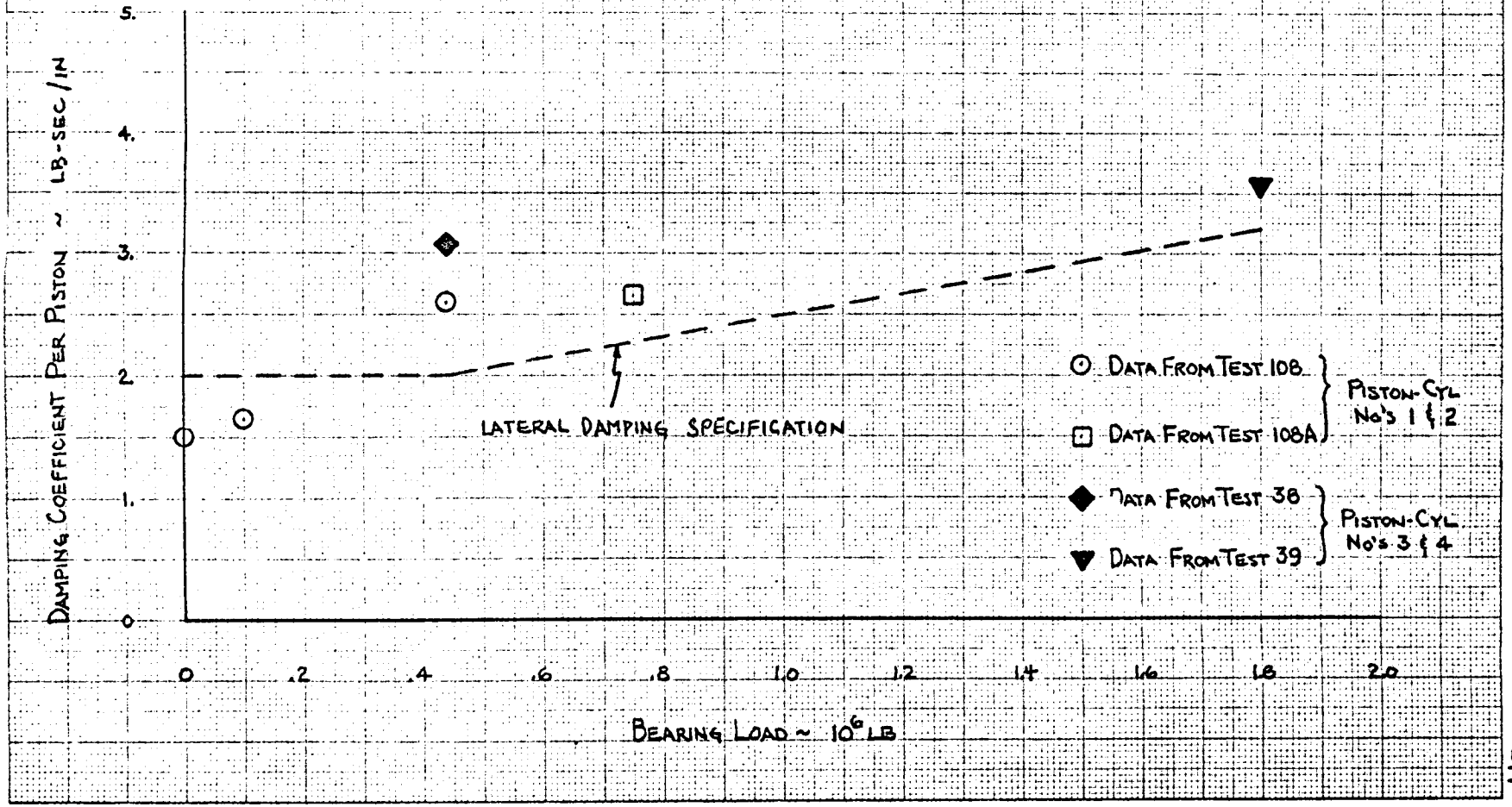

FIGURE XE-8

HYDRODYNAMIC SUPPORT TOTAL VERTICAL DAMPING
VS INPUT FLOW GAIN
(PISTON-CYL. NO. 2)

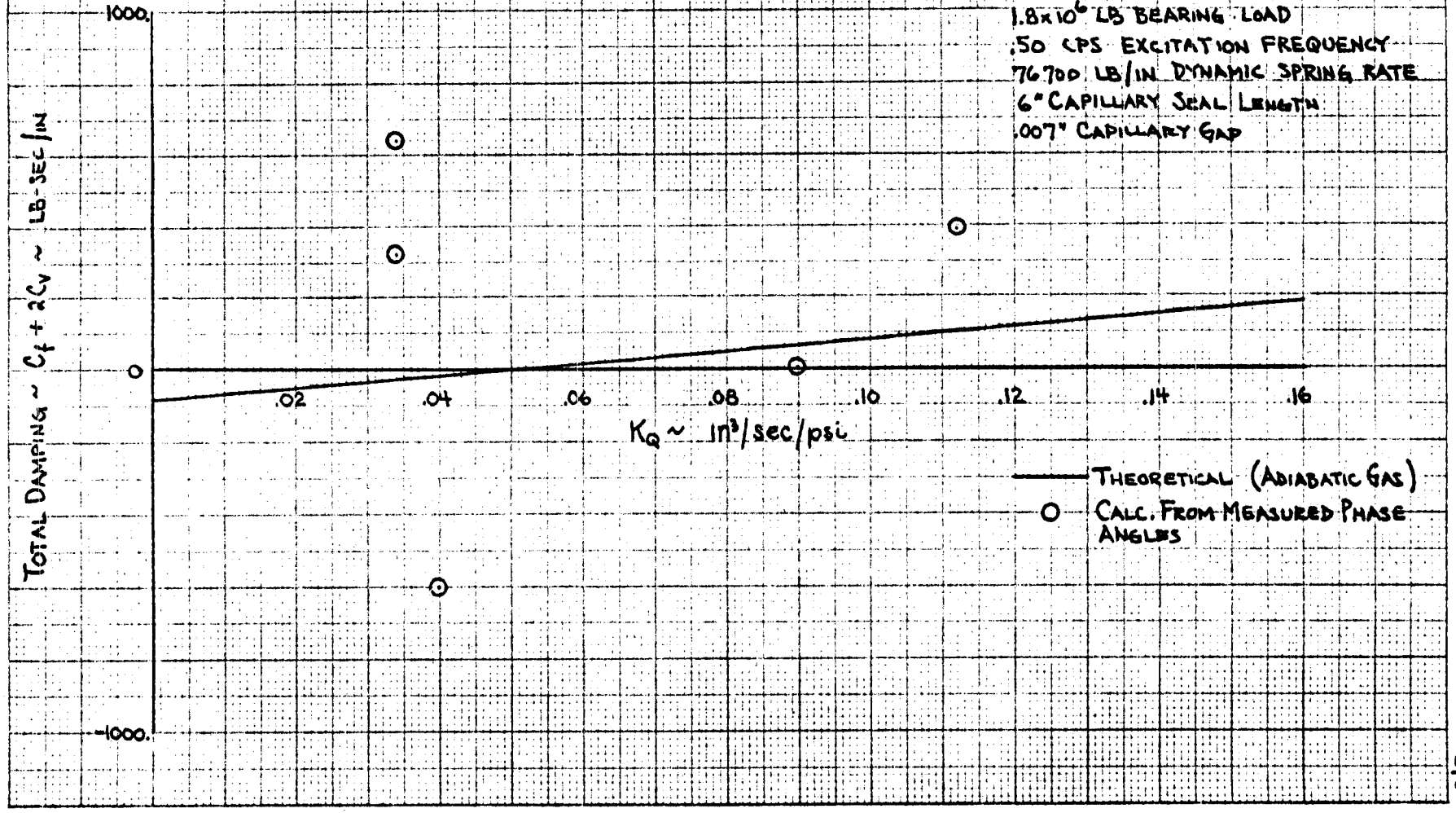

1.8×10^6 LB BEARING LOAD
0.2 CPS EXCITATION FREQ.
6" CAPILLARY SEAL LENGTH

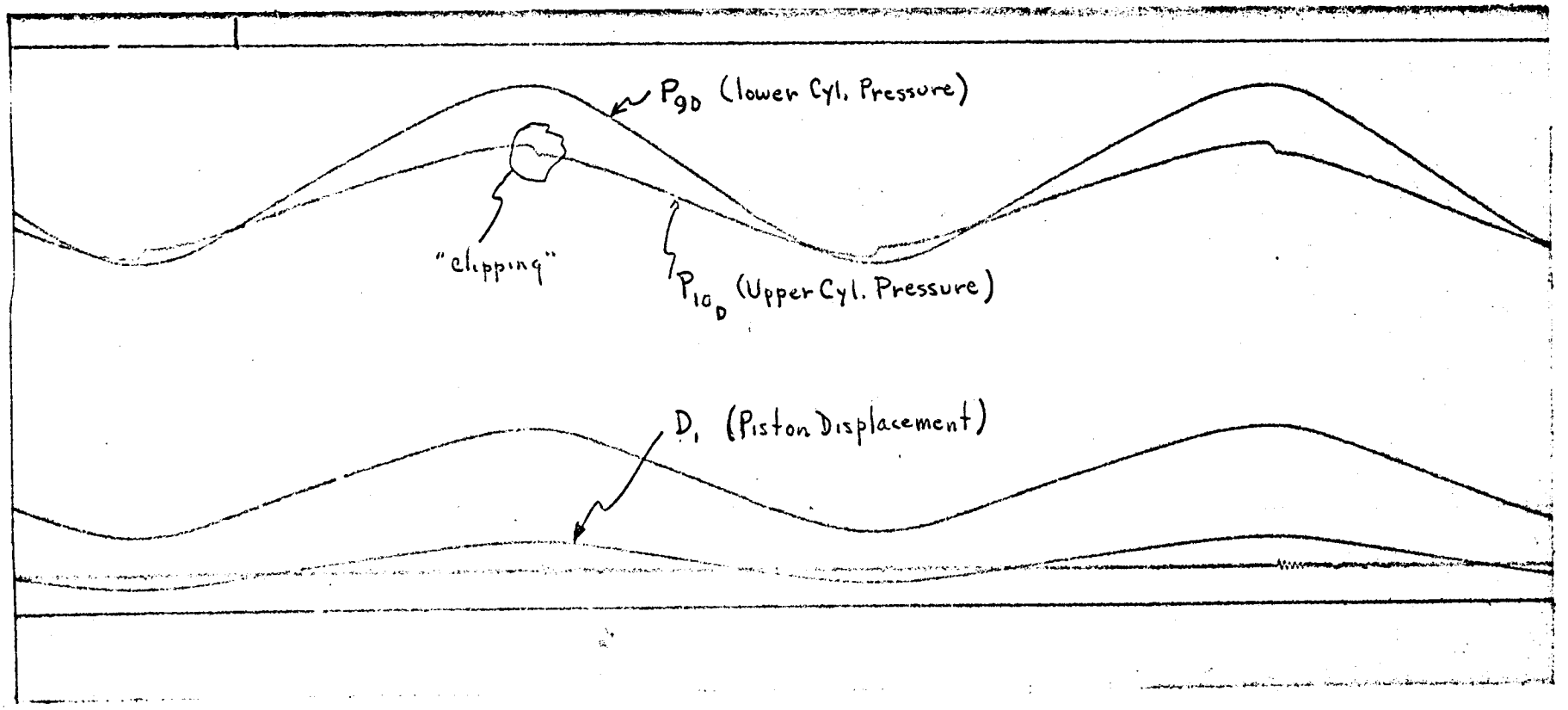

FIGURE V E-9

CYLINDER PRESSURE AND PISTON DISPLACEMENT
FROM A VERTICAL DAMPING TEST ON CYLINDER NO. 4

FIGURE IV E-10

HYDRODYNAMIC SUPPORT VERTICAL FLOW DAMPING
VS INPUT FLOW GAIN
(PISTON-CYL. NO. 4)

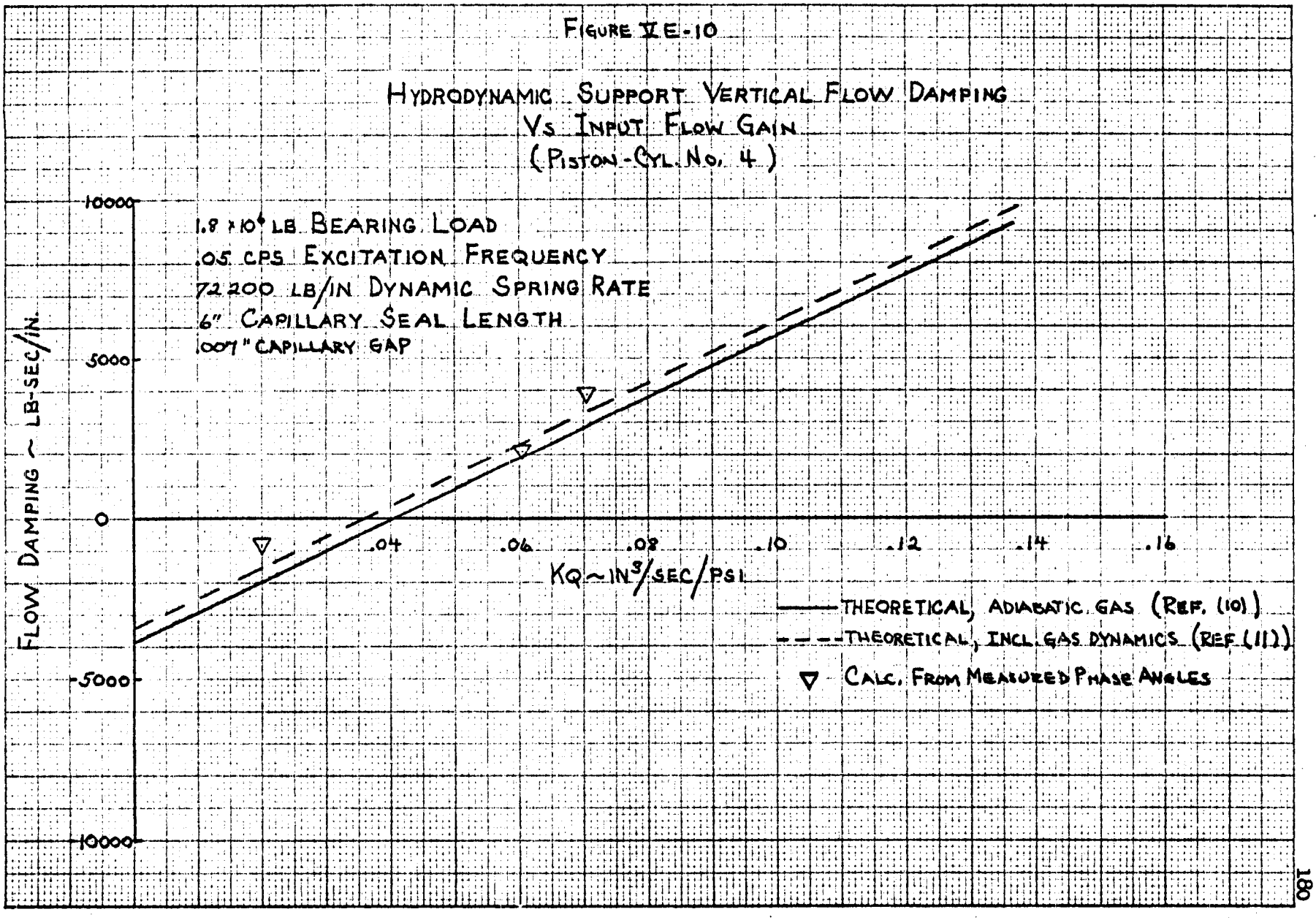

FIGURE V E-11

HYDRODYNAMIC SUPPORT VERTICAL FLOW DAMPING
VS. INPUT FLOW GAIN
(PISTON - CYL. No. 4)

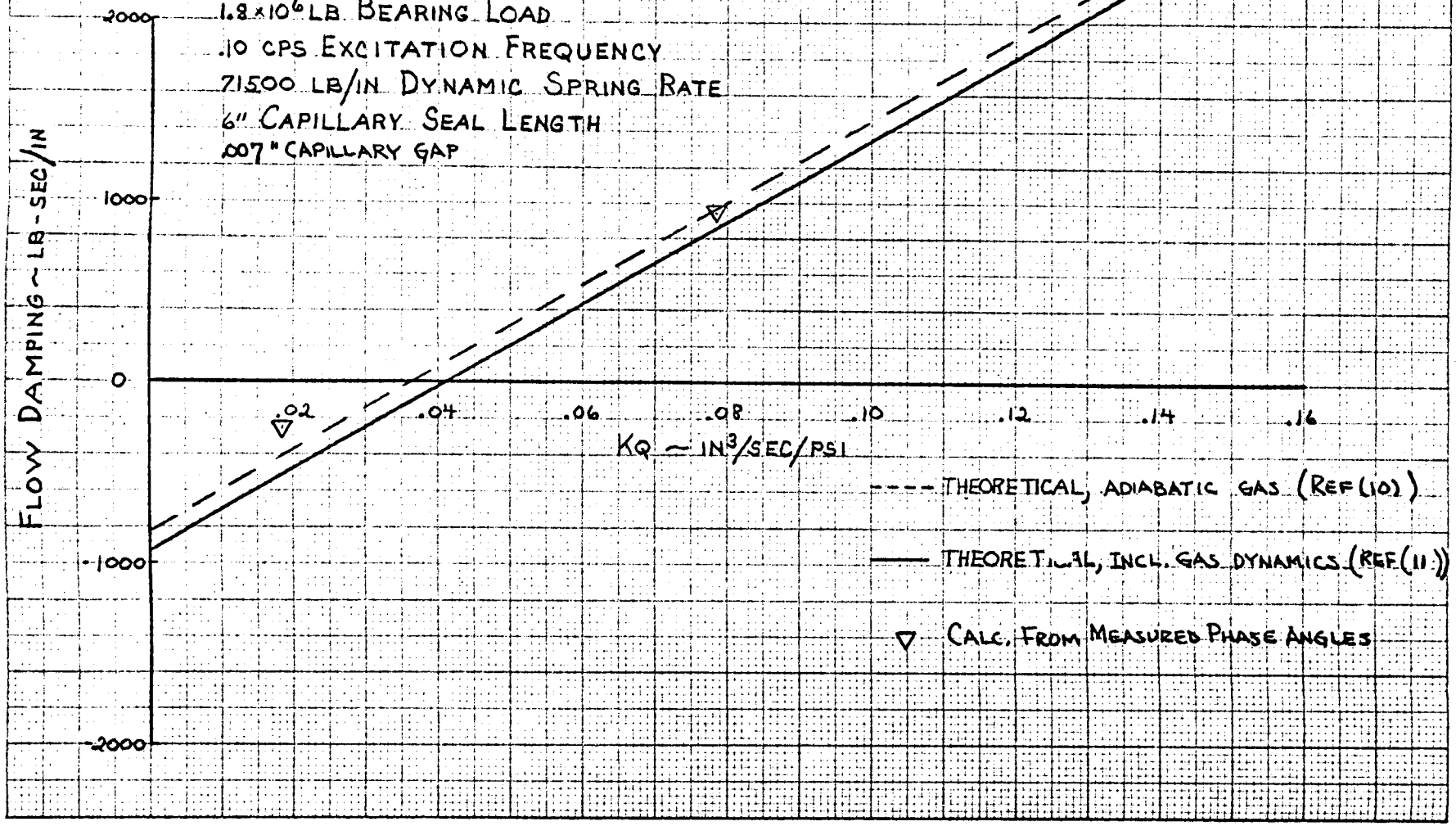

FIGURE IV E-12

HYDRODYNAMIC SUPPORT VERTICAL FLOW DAMPING
VS. INPUT FLOW GAIN
(PISTON - CYL. No. 4)

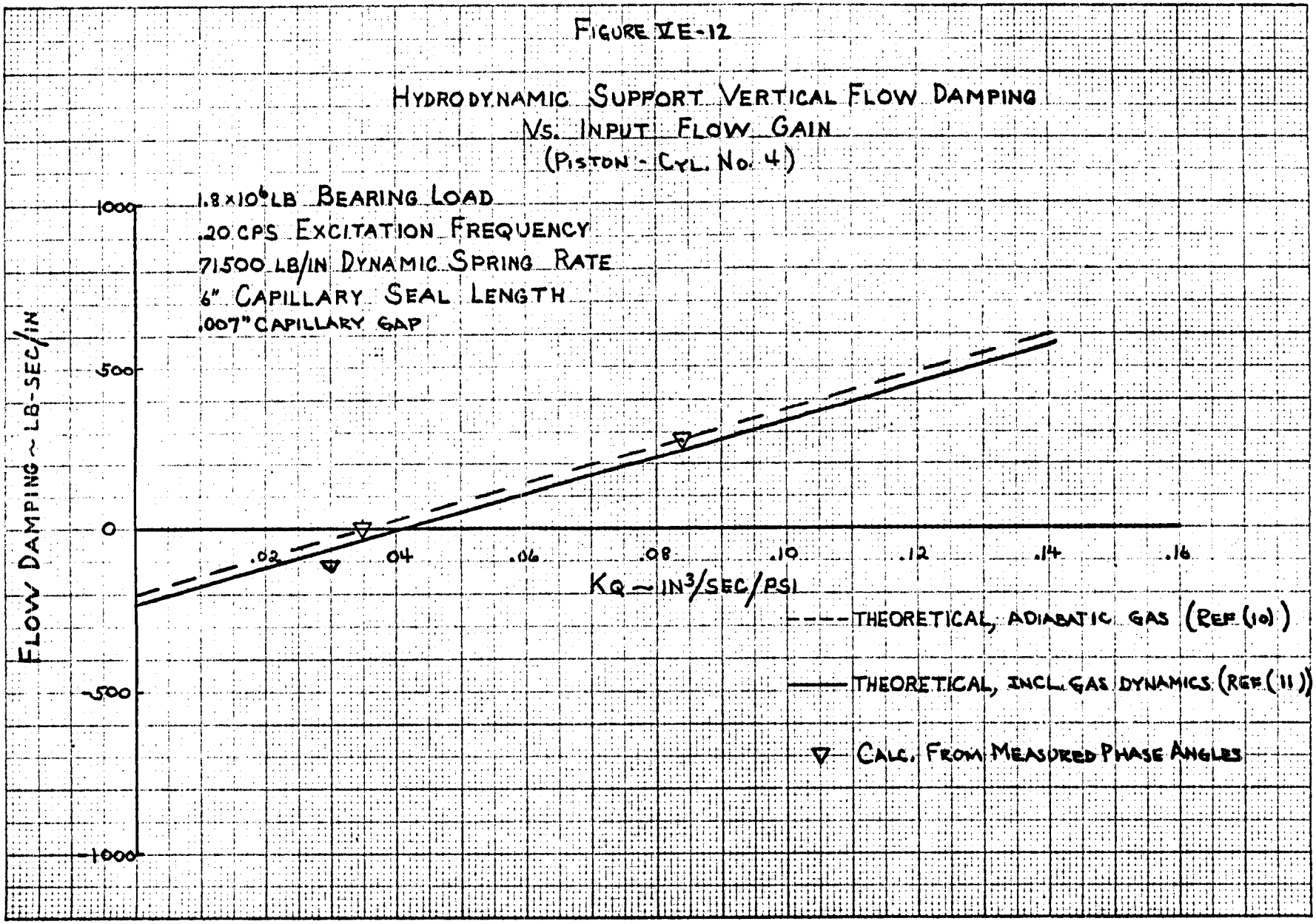

FIGURE V E-13

HYDRODYNAMIC SUPPORT VERTICAL FLOW DAMPING
VS. INPUT FLOW GAIN
(PISTON - CYL. NO. 4)

$.44 \times 10^6$ LB BEARING LOAD
.05 CPS EXCITATION FREQUENCY
15500 LB/IN DYNAMIC SPRING RATE
6" CAPILLARY SEAL LENGTH
.007" CAPILLARY GAP

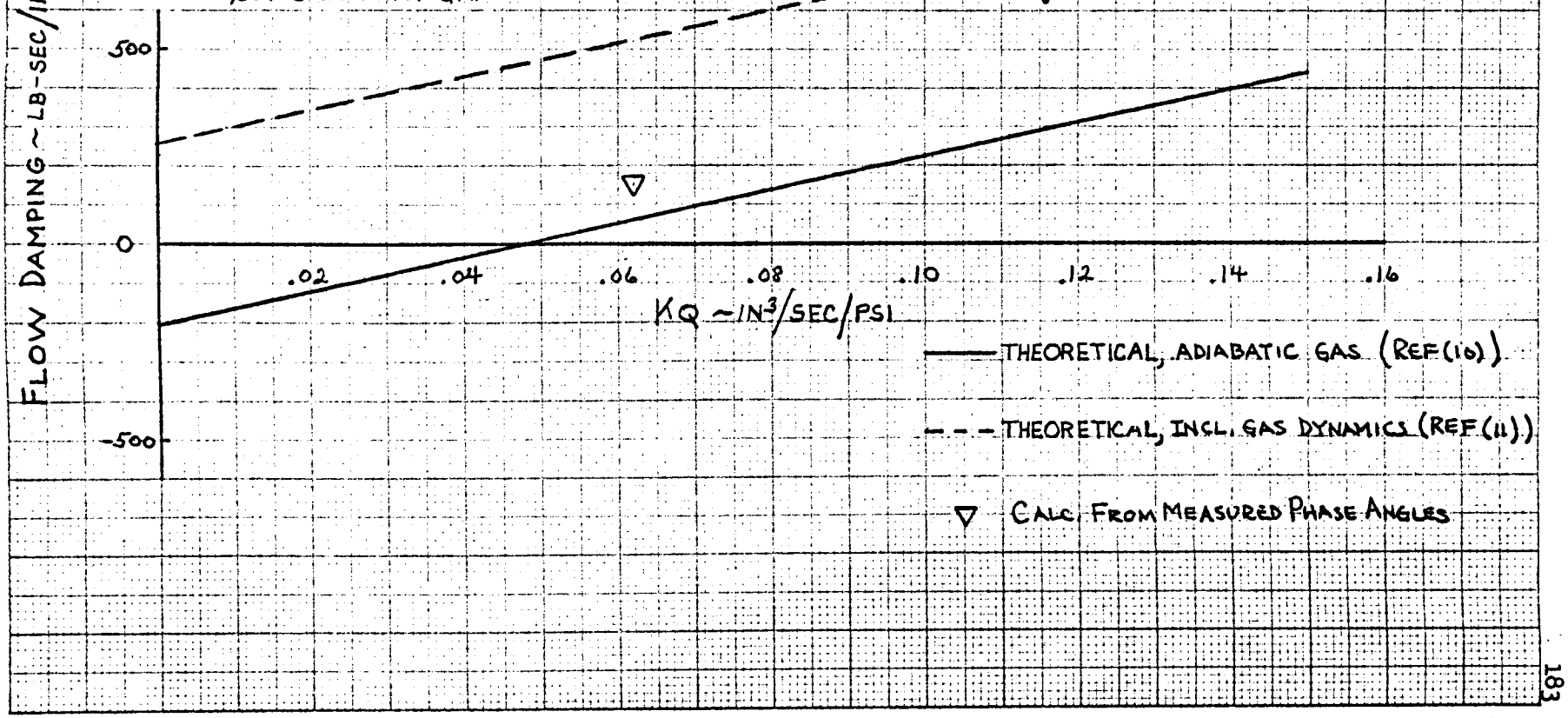

FIGURE V E-14

HYDRODYNAMIC SUPPORT VERTICAL FLOW DAMPING
VS INPUT FLOW GAIN
(PISTON-CYL. NO. 4)

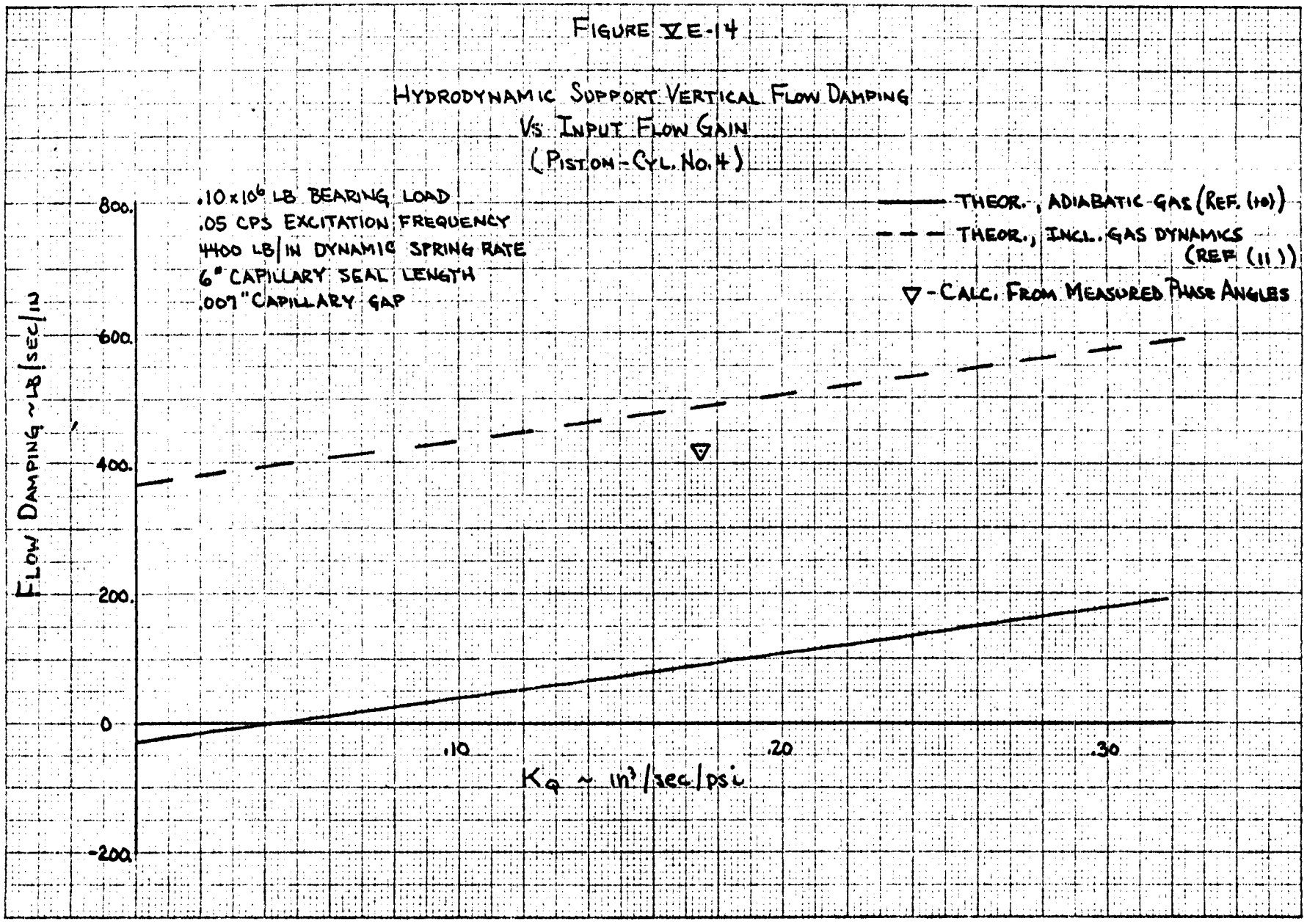

FIGURE XE-15

HYDRODYNAMIC SUPPORT VERTICAL FLOW DAMPING
VS INPUT FLOW GAIN
(PISTON - CYL. NO. 4)

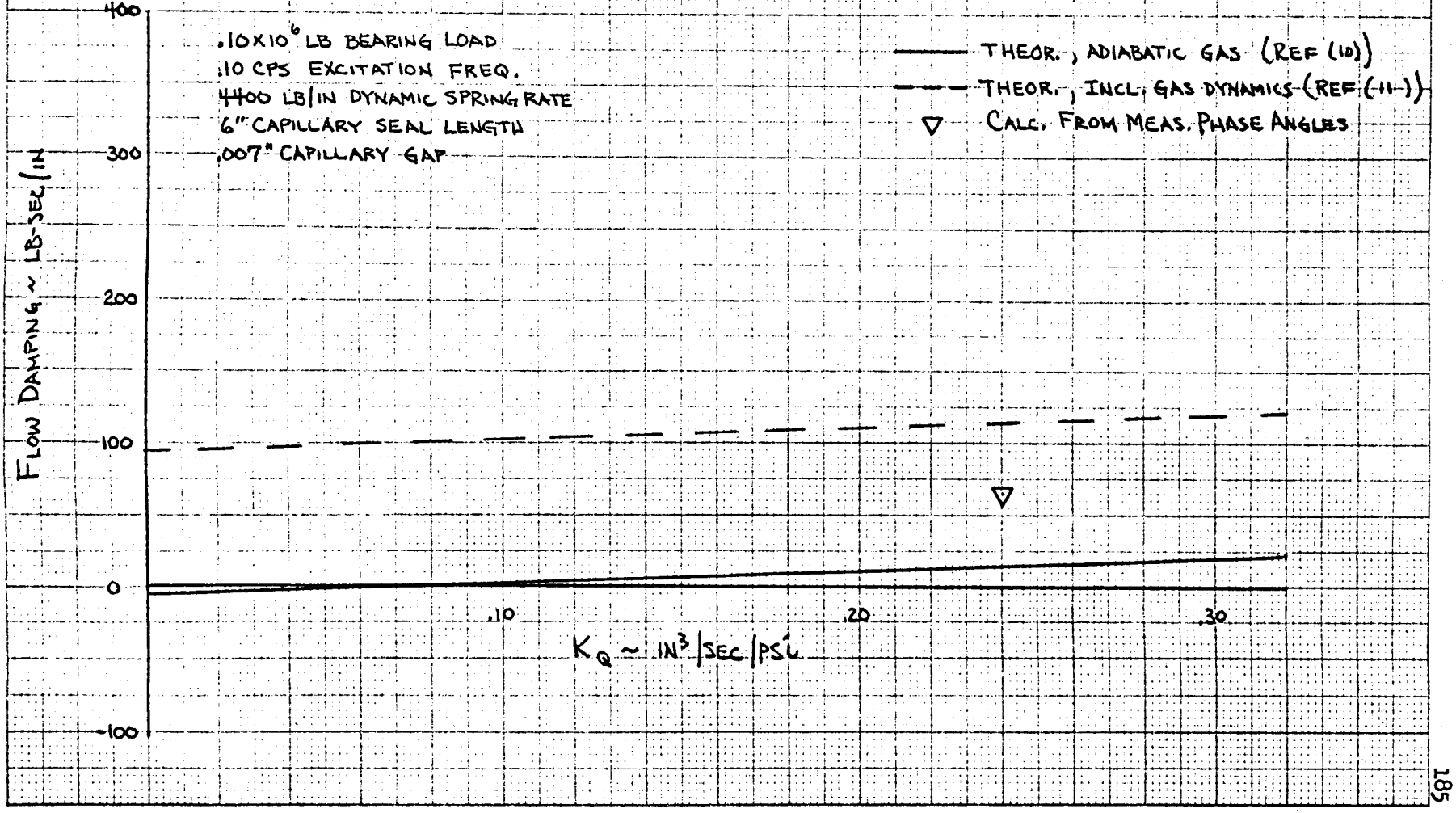

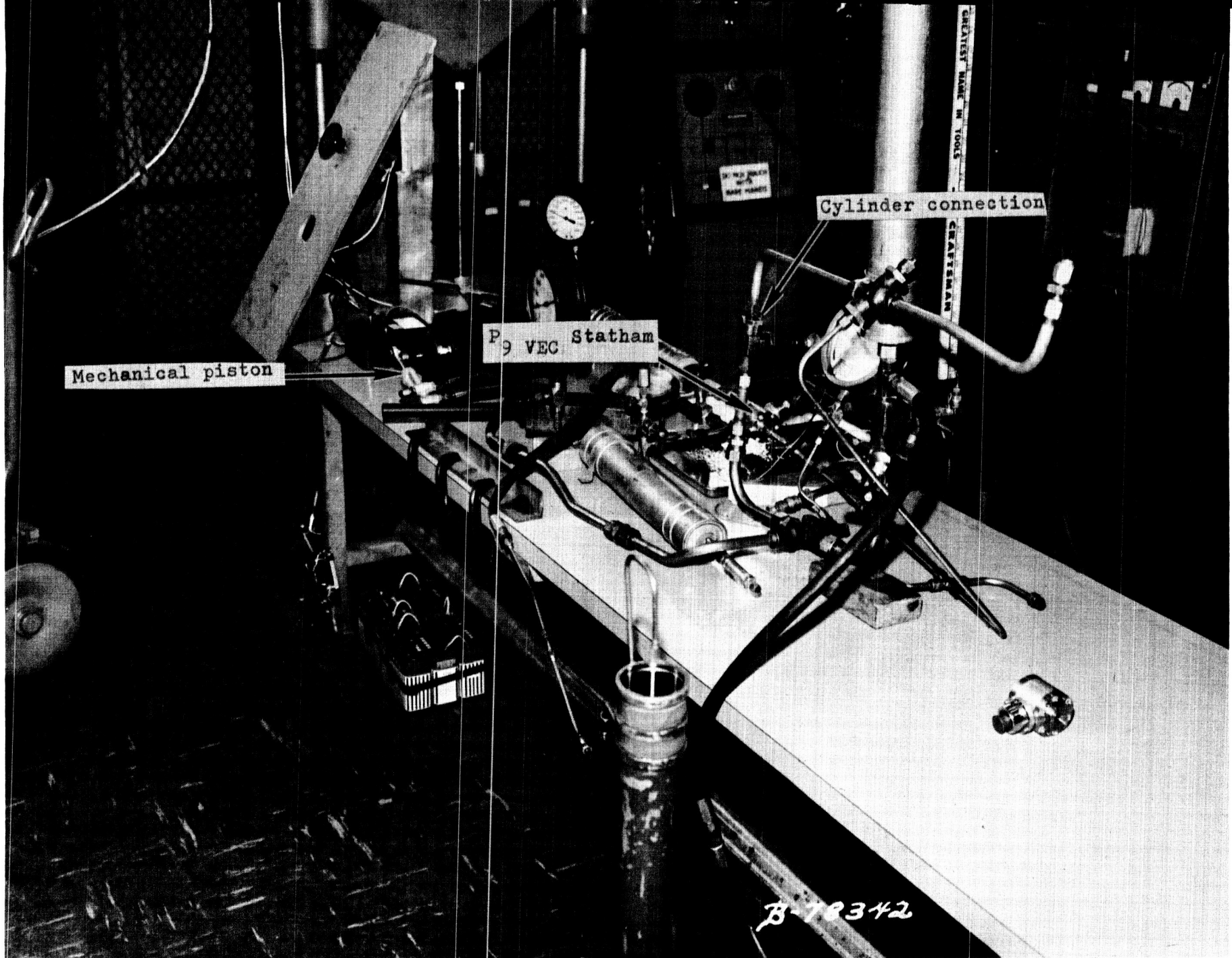

LAYOUT OF HYDRAULIC LINES USED IN PHASE MEASUREMENT
FIGURE V E-16

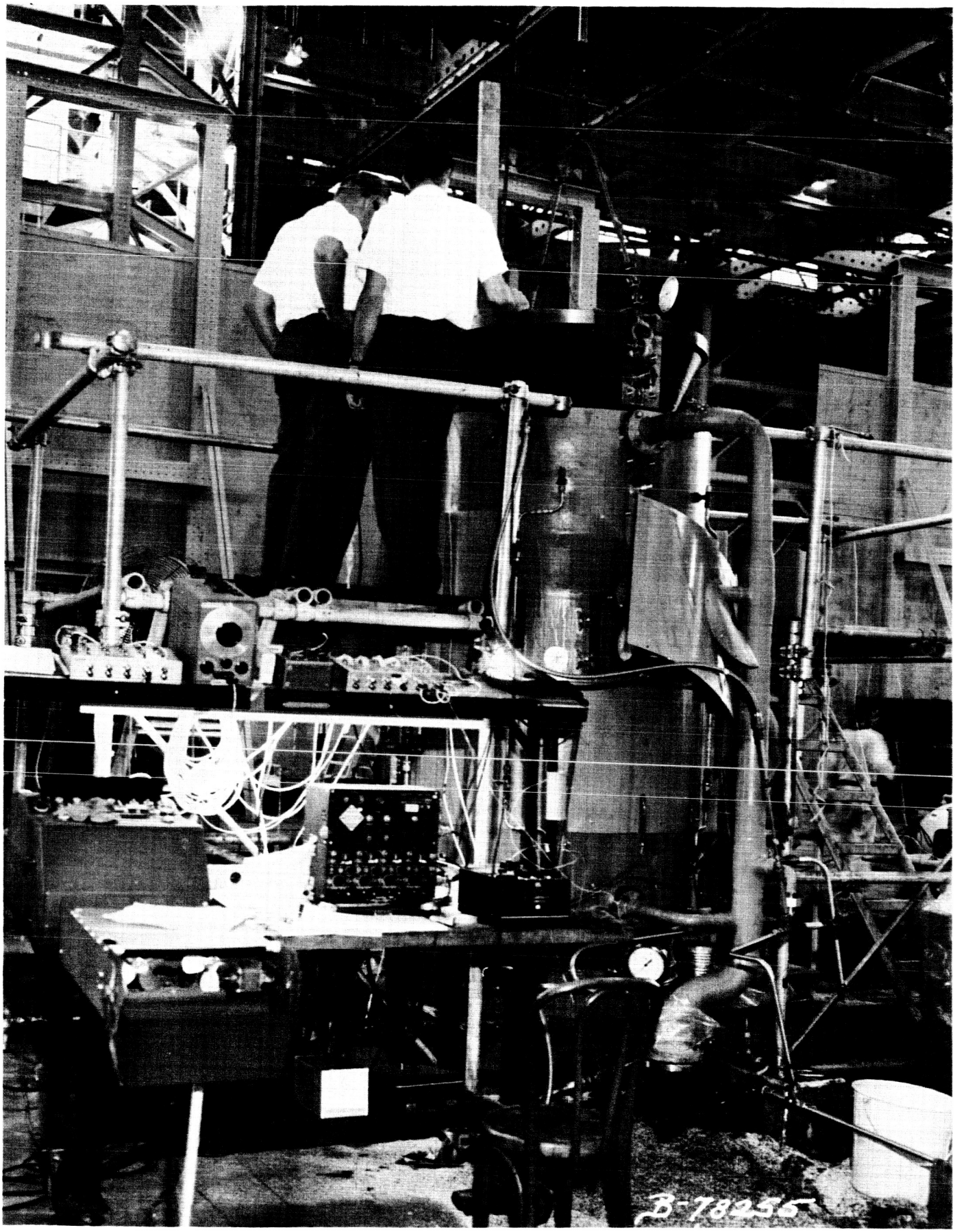

SET UP FOR VERTICAL AND ROTATIONAL
UNIT DAMPING TESTS
FIGURE V E-17

FIGURE XE-18

PISTON CYLINDER No. 4 VISCOUS DAMPING

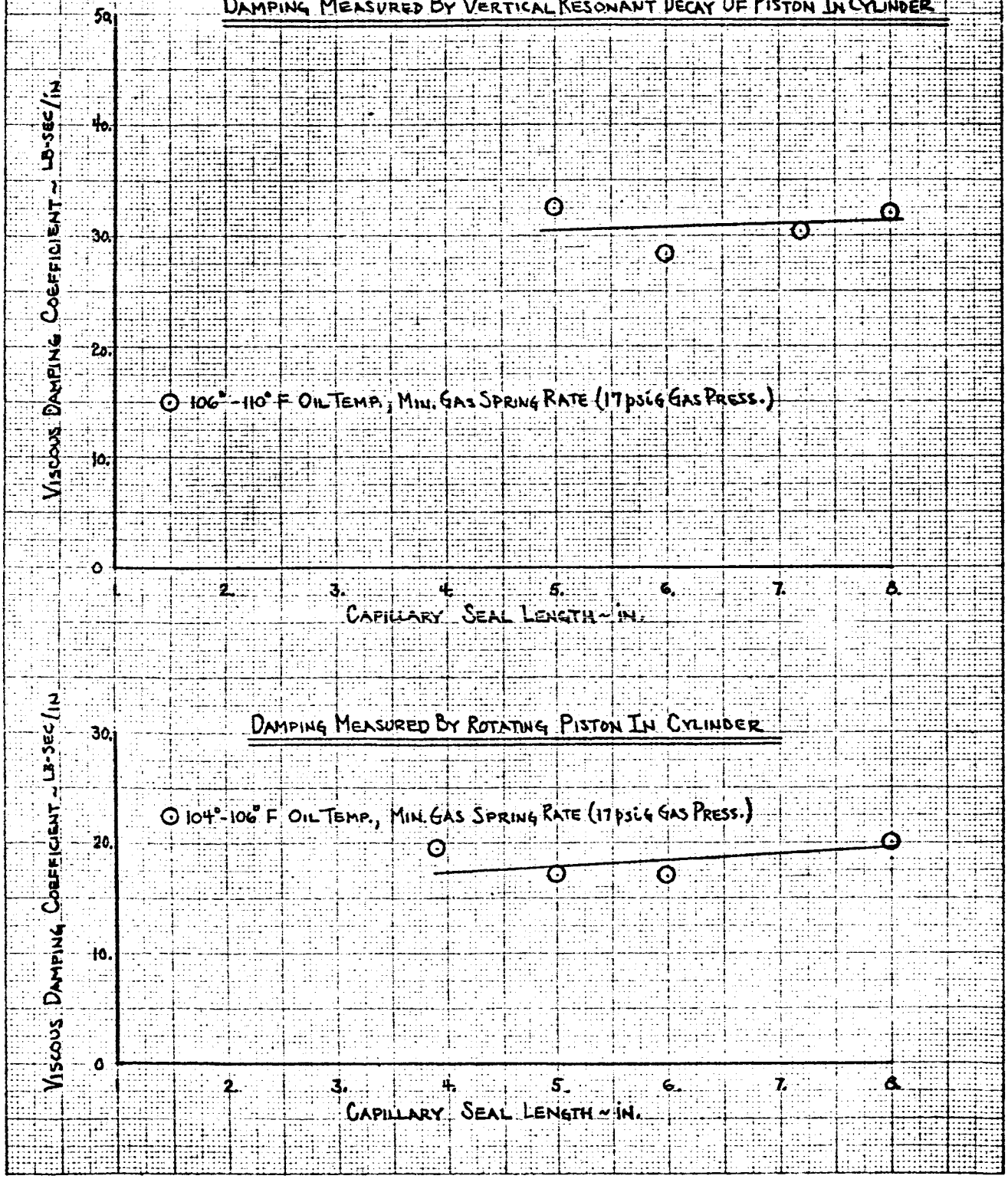

FLOAT FROM PISTON NO. 4
FIGURE V E-19

FIGURE IIE-20

PISTON-CYLINDER No. 2 VISCOUS DAMPING

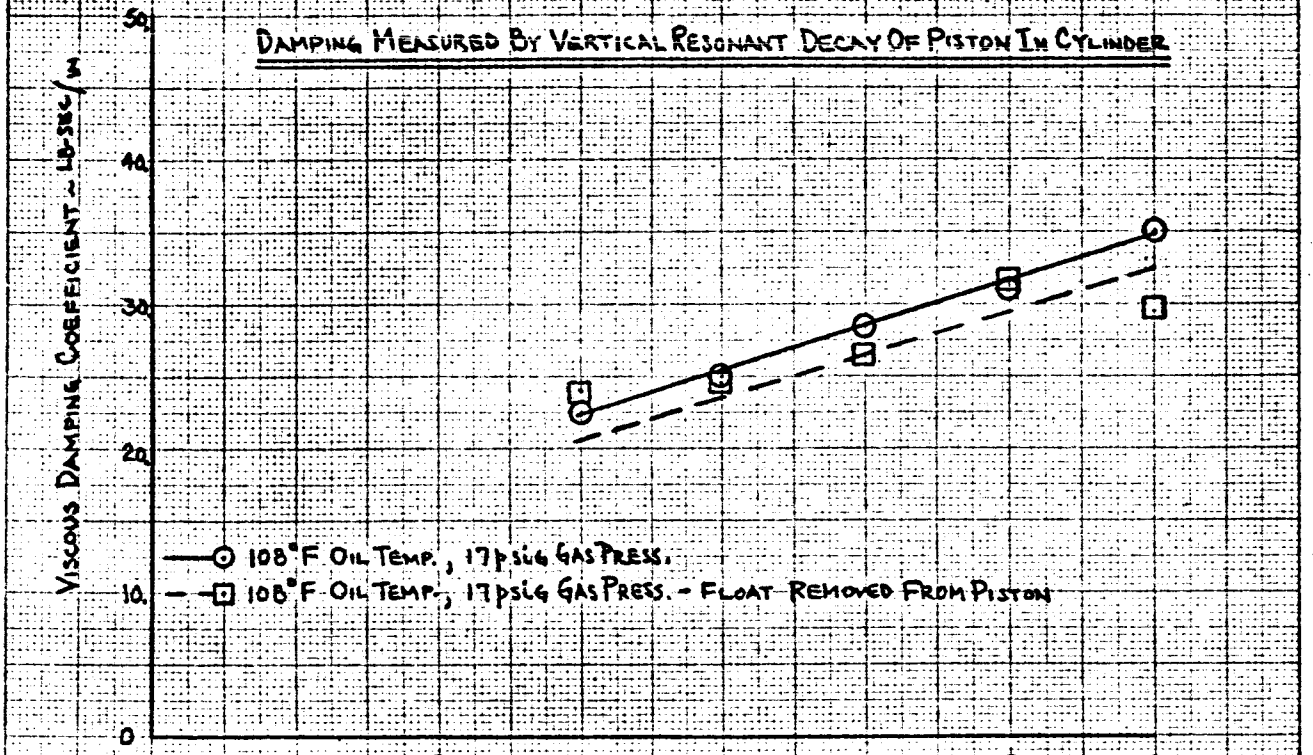

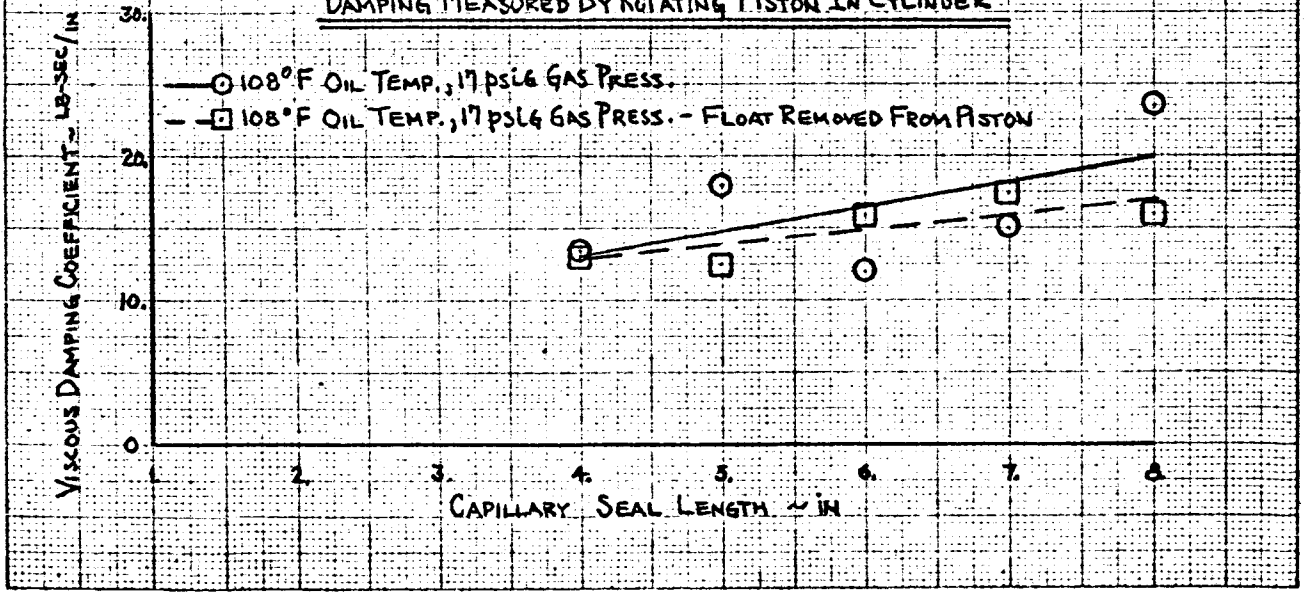

FIGURE IV E-21

PISTON-CYLINDER NO. 3 VISCOUS DAMPING

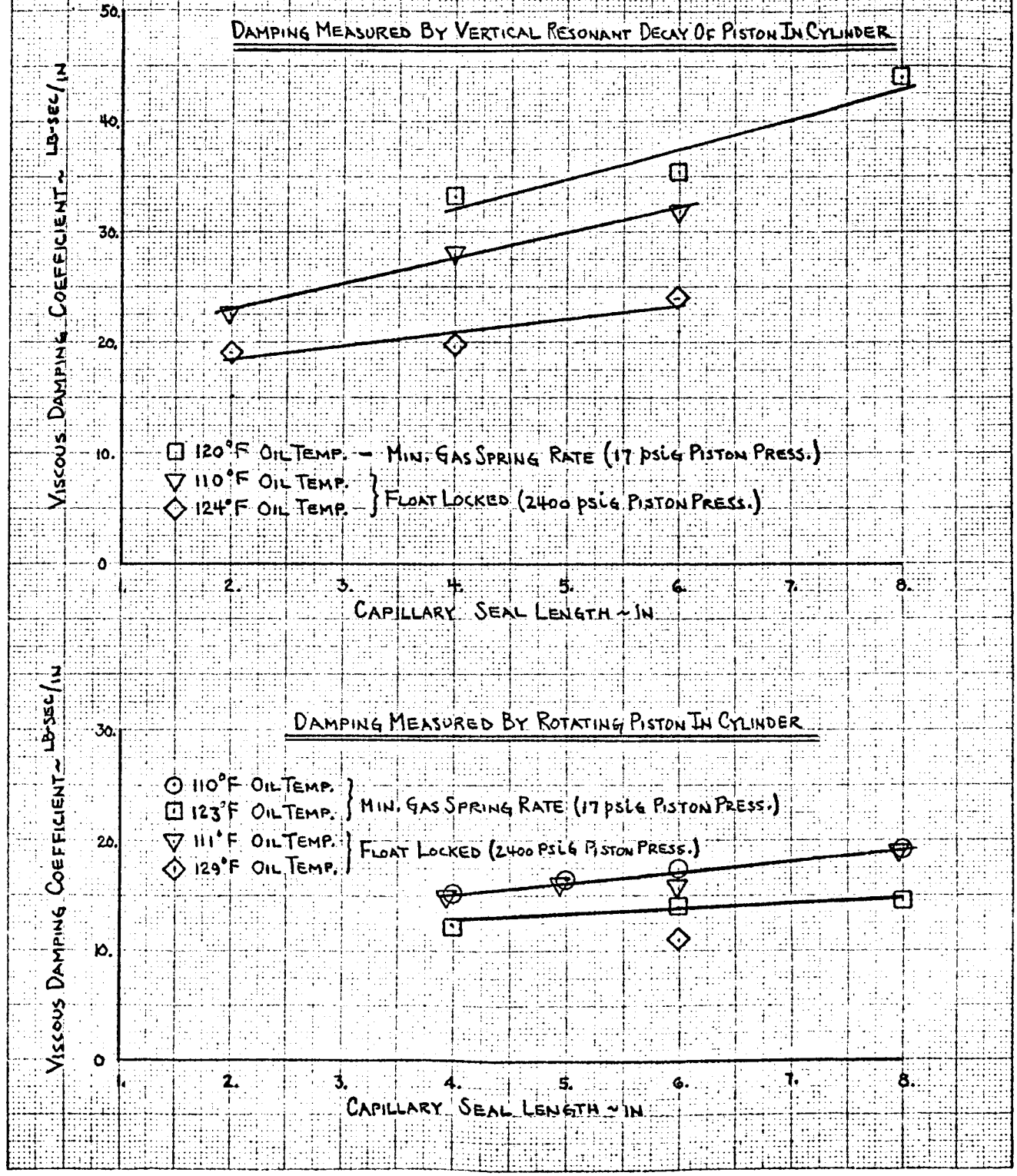

FIGURE IE-22

PISTON-CYLINDER NO. 5 VISCOUS DAMPING

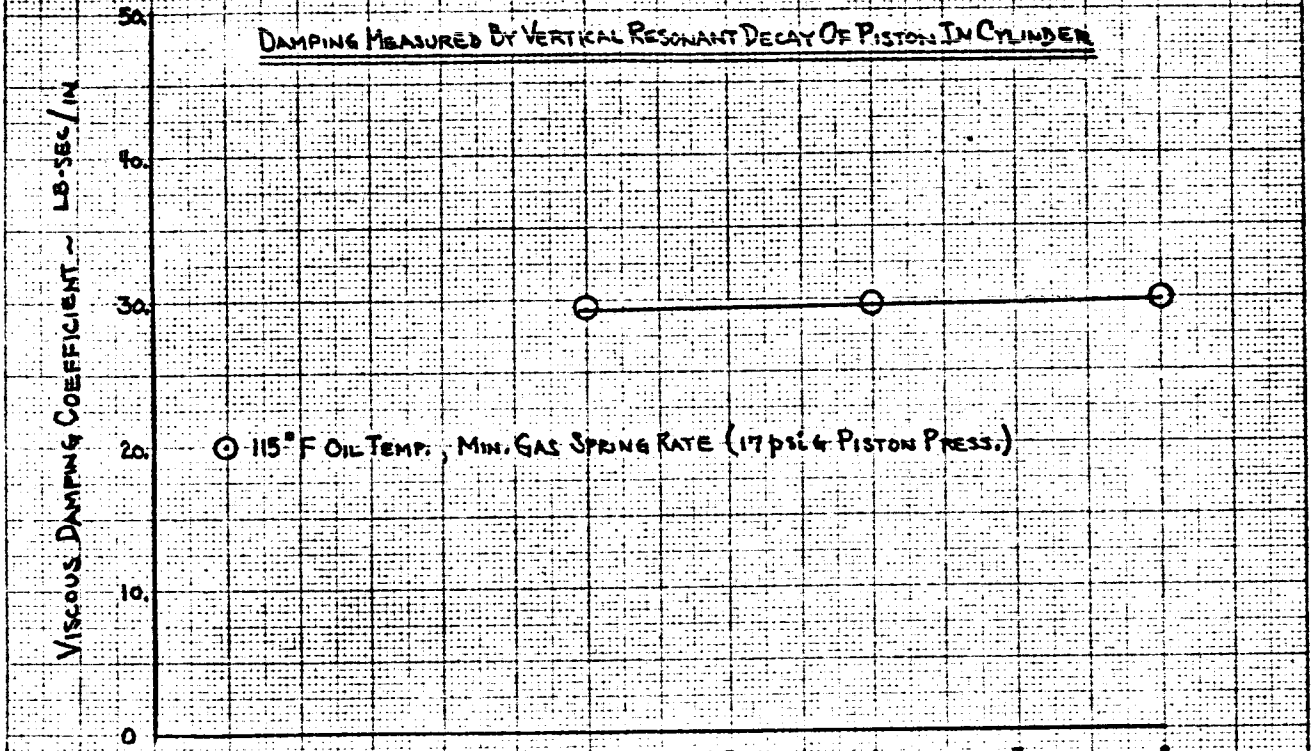

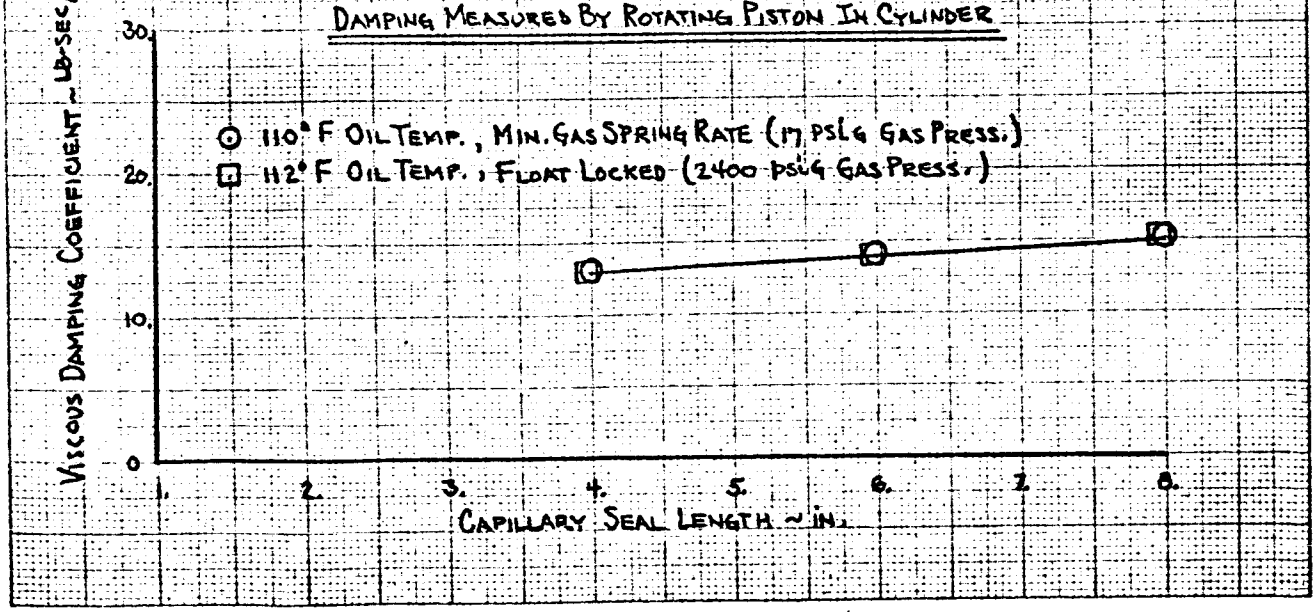

FIGURE V E-23

COMPARISON OF SEPARATE VISCOUS DAMPING TESTS ON PISTON-CYLINDER NO'S 2, 3, 4 AND 5 WITH THE THEORETICAL VISCOUS DAMPING

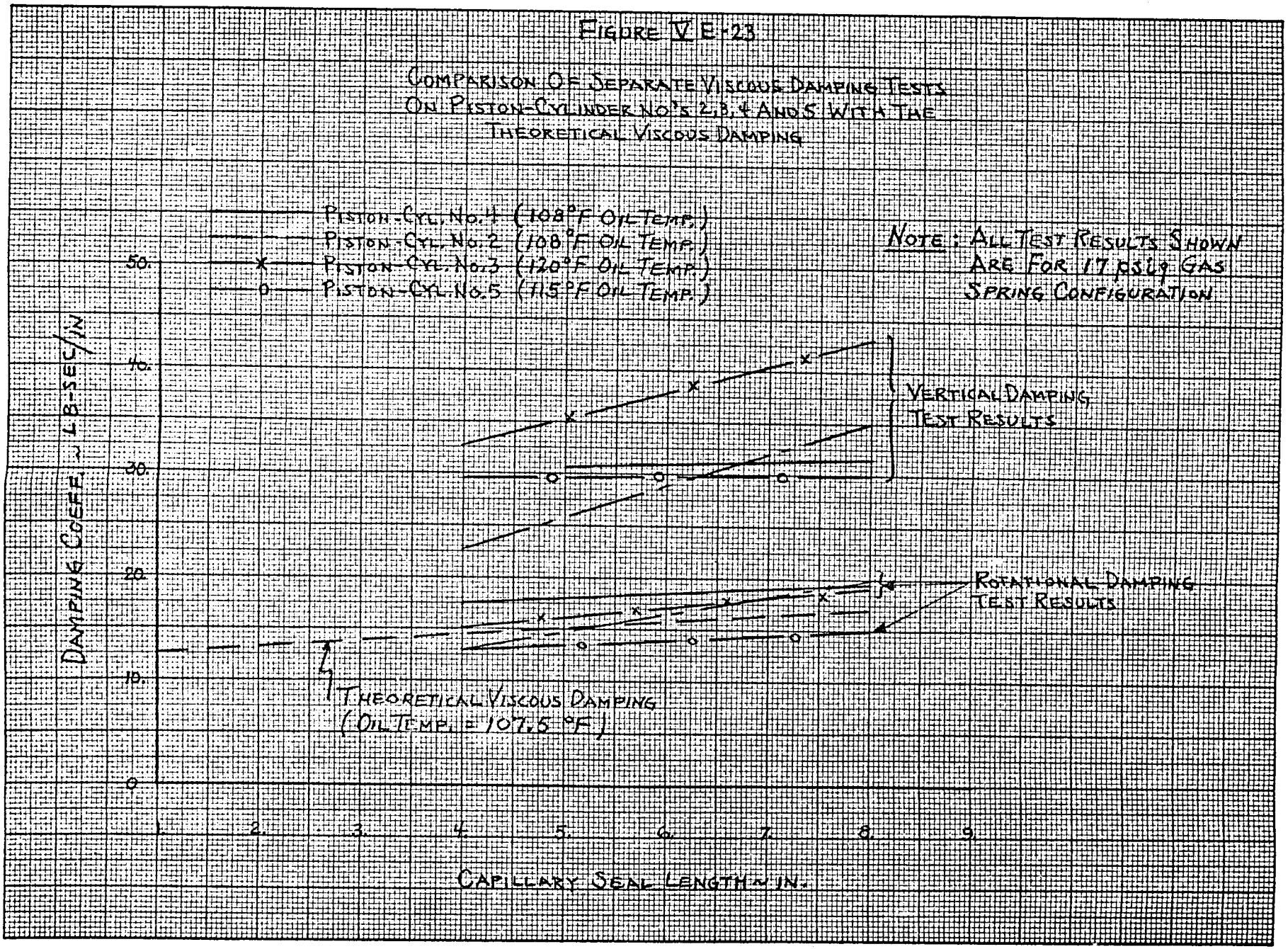

X. APPENDIX A

HEAD TO HEAD TEST SPECIFICATION

LAST CHANGE INCORPORATED A
SEE PAGE 2.0 FOR REVISIONS

88A4100403

CONTENTS

THIS DRAWING RELEASES NO PARTS - FOR REFERENCE ONLY

EFFECTIVE ON	CALC WT	DASH NUMBER	NEXT ASSY	USED ON	FINAL ASSY	TEST
			APPLICATION		QTY REQD	

DRAWN BY W. Disser DEPT. 2570 DATE 5/11/65
CHECKER R. Sonnenberger
DYNAMICS
WT ENGR
MATL- ENGR
RELIABILITY
GR ENGR G. SHOLES 5-13
PROGRAM REP.
CUST. REP.

MARTIN COMPANY
THE AEROSPACE DIVISION OF MARTIN MARIETTA CORPORATION
FRIENDSHIP INTERNATIONAL AIRPORT, MARYLAND

HEAD-TO-HEAD TEST SPECIFICATION

CODE IDENT NO.	SIZE	
38597	A	88A4100403
SCALE	SHEET	PAGE 1.0 of 15.0

E-19 (6/63)

SV3210-083

REVISIONS

SYM	PAGE	DESCRIPTION	DATE	APPROVED
A	6.0	In paragraph 3.1.1, added capillary seal lengths.	11-15-65	Jd Bone
	11.0	In paragraph 5.2.1, revised load and spring rate requirements.		

CHG.	CODE IDENT NO.	SIZE	
A	38597	A	88A4100403
	SCALE		PAGE 2.0

INDEX

PAGE	CHG.	PAGE	CHG.	PAGE	CHG.
1.0	A	7.0		13.0	
2.0	A	8.0		14.0	
3.0	A	9.0		15.0	
4.0		10.0			
5.0		11.0	A		
6.0	A	12.0			

CHG	CODE IDENT NO.	SIZE	
A	38597	A	88A4.00403
	SCALE	SHEET	PAGE 3.0

E-654 (7-61)

TABLE OF CONTENTS

TABLES

FIGURES

1.0 TEST OBJECTIVES.-

To determine the ability of the system and components to function as designed.

1.1 Determine the piston-cylinder capillary seal gap experimentally by measuring the oil flow at various pressures.

1.2 Adjust all flow control valves at operating conditions.

1.3 Demonstrate bearing redundancy. (Ref. Para. II-L)*.

1.4 Demonstrate that the bearing surfaces can be separated after bearing contact.

1.5 Demonstrate the sink rate after loss of pressure to the air spring.

1.6 Demonstrate that the piston can be raised from the park position three inches to the operate position. (Ref. Para. II-C)*.

1.7 Demonstrate the sink rate of the piston assembly when flow is interrupted to the capillary seal.

1.8 Determine the misalignment of the horizontal hydrostatic bearing surfaces due to eccentric loading. (Ref. Para. II-E)*.

1.9 Determine the total effective moving mass of the support system. (Ref. Para. II-F)*.

1.10 Determine if any components have natural frequencies below 20 cps. (Ref. Para. II-H)*.

1.11 Determine the air spring rate. (Ref. Para. II-D)*.

1.12 Measure the viscous damping characteristics of the hydrostatic bearing system. (Ref. II-G)*.

* Paragraph Number - Exhibit A, Scope of Work, Contract NAS 8-11903

2.0 SYSTEM ASSEMBLY. -

2.1 Assemble two hydrodynamic supports (88A4100410, 88A4100405-005, -011-013 and assembling bolts), into the head-to-head test stand as shown on Dwg. No. 88A4100402.

2.2 Connect the hydraulic and pneumatic system to the test stand assembly as shown on Dwg. No. 88A4100402, Sheet 7.

2.3 Connect the electrical control system to the test stand assembly as shown on Dwg. No. 88A4100903.

2.4 The supply lines feeding the bearings and the capillary seal shall be sized to approximate the longest test site line runs on the bottom piston assembly and the shortest test site line runs on the top piston assembly.

2.5 The test site pumping system will be used to supply oil to the piston assembly installed in the head-to-head test stand.

3.0 DESIGN ASSURANCE TESTS. -

Measurements to be recorded in Section 3.0 are listed in Table 3 and the measurement positions are shown in Fig. 1.

3.1 Piston - Cylinder Gap Test. -

3.1.1 To determine the piston - cylinder gap across the capillary seal the flow and pressure will be measured and compared to the flow and pressure at the calculated gap. This test will be run at bearing loads of $.10 \times 10^6$ pounds, $.44 \times 10^6$ pounds, 1.0×10^6 pounds and 1.8×10^6 pounds and an air spring rate at the maximum. The capillary seal length will be set to 4, 6 and 8 inches. (A)

3.2 Adjustment of Flow Control Valves. -

3.2.1 To adjust the ring bearing flow control valves all valves will be set to their calculated operating values and the bearing pressures and gaps will be measured and recorded. Adjustment to the valves will be made until the piston is centered in the cylinder. This test will be run at bearing loads of $.10 \times 10^6$ pounds, $.44 \times 10^6$ pounds, 1.0×10^6 pounds, and 1.8×10^6 pounds and an air spring rate set at the maximum.

3.2.2 All spherical and flat bearings will be adjusted to their calculated operating values and bearing pressures and gaps measured and recorded. Adjustments to the valves will be made if the spherical and flat bearings are not parallel. This test will be run at bearing loads of $.10 \times 10^6$ pounds, $.44 \times 10^6$ pounds, 1.0×10^6 pounds, and 1.8×10^6 pounds and an air spring rate set at the maximum.

3.3 BEARING REDUNDANCY TEST.-

3.3.1 To demonstrate bearing redundancy, one flow control valve will be closed to the spherical bearing and bearing pressures and gaps measured and recorded. Bearings shall not contact when one flow control valve is closed. This test will be repeated on the flat bearing, the upper ring bearings and the lower ring bearings. These tests will be run at a bearing load of 1.8×10^6 pounds.

3.4 Bearing Separation.-

3.4.1 To demonstrate that the bearing surfaces can be separated after bearing contact, flow will be throttled to the spherical and flat bearings until contact is established, then full flow will be re-established. Bearing pressures and gaps should return to normal when the flow does. This test will be run at a bearing load of 1.8×10^6 pounds.

3.5 Air Spring Pressure Loss Test.-

3.5.1 To demonstrate the sink rate the air spring gas pressure will be bled from the piston through a nitrogen vent valve. This test will be run at a bearing load of 1.8×10^6 pounds and the air spring rate will be set at the minimum.

3.5.2 During this test the float in the lower piston assembly will sink, then the floating procedure will be demonstrated.

3.6 OPERATING RANGE TEST.-

3.6.1 To demonstrate the operating range the piston will be moved from the park to operate position under the following conditions:

Simulated Missile Weight (lbs.) per Support	Lower Piston Air Spring Rate
$.10 \times 10^6$	Minimum
$.10 \times 10^6$	Maximum
$.44 \times 10^6$	Minimum
$.44 \times 10^6$	Maximum
1.8×10^6	Minimum
1.8×10^6	Maximum

3.7 Piston Assembly Sink Rate Test. -

3.7.1 To demonstrate the sink rate of the piston assembly the flow will be interrupted to the capillary seal and the time required for the piston to drop to the park position recorded with simulated missile weights of $.10 \times 10^6$ pounds and 1.8×10^6 pounds. The spring rate will be set at the minimum value during this test.

3.8 Eccentric Loading Tests. -

3.8.1 To determine the misalignment of the horizontal bearing surfaces the lens and flat bearing assembly will be moved from the center position in four increments until the center line of the bearing assembly is 4 inches off center. The bearing load during this test will be 1.8×10^6 pounds. Misalignment will be measured optically.

3.9 Effective Moving Mass

3.9.1 The total effective moving mass will be determined analytically.

4.0 VIBRATION SURVEY. -

4.1 To satisfy the requirement that all components have natural frequencies above 20 cps, a vibration survey of the hydrostatic bearing sets will be conducted. Two shakers (each rated at 650 lb.) will be used to excite the system at one location in the lateral direction and one location in the vertical direction. These locations are indicated in Fig. 1. The excitations will be conducted from 5 to 20 cps. If there is any indication of resonances near 20 cps the range will be extended. The bearing load for the lateral excitations will be 1.8×10^6 pounds and for the vertical excitations the bearing load will be 0.44×10^6 pounds. The minimum spring rate will be used with both bearing loads.

4.2 The dynamic response and performance of the system will be monitored at key locations during each run. The following tables list the parameters to be measured during each of the two tests. The measurement positions are indicated in Fig. 1. In addition to these measurements portable instrumentation will be available to investigate any observed resonances.

TABLE 1

Test No. 1, Vertical Direction; Frequency Excitation Range: 5-20 cps

Test Conditions:

Run No.	1
Amplitude (g's)	<0.25
Shaker Output Force	X
Bearing Load (10^6 pounds)	0.44
Minimum Spring Rate	

The following items will be recorded during each run:

Dynamic Response

1. Acceleration (vertical)

   Upper piston
   Lower piston
   Upper cylinder
   Lower cylinder
   Upper lens bearing
   Lower lens bearing
   Upper spherical bearing
   Lower spherical bearing

2. Displacement

   Upper piston (vertical)
   Lower piston (vertical)
   Upper lens bearing (lateral)
   Lower lens bearing (lateral)

System Performance

Hydraulic oil flows
Hydraulic oil temperatures
Air spring gas temperature
Hydrostatic bearing gaps (in.)

TABLE 2

Test No. 2; Lateral Direction; Frequency Excitation Range: 5-20 cps

Test Conditions:

Run No.	1
Amplitude (g's)	<0.25
Shaker output force	X
Bearing load (10^6 pounds)	1.8
Minimum spring rate	

The following items will be recorded during each run:

Dynamic Response

1. Acceleration (lateral)

   Lower piston
   Lower cylinder
   Lower lens bearing
   Lower spherical bearing

2. Displacement

   Upper lens bearing (lateral)
   Lower lens bearing (lateral)

System Performance

Hydraulic oil flows
Hydraulic oil temperature
Air spring gas temperature
Hydrostatic bearing gaps (in.)

5.0 DAMPING. -

5.1 Lateral Damping

Drawing No. 88A4100402 depicts a way to produce a vibrating system in the lateral direction. A mechanical device will be used to displace the system and then a quick release mechanism will release the system. The decay characteristics of a 1 and 5 cps free oscillating system will be used to determine the total amount of damping with the bearing loads of 1.8×10^6 and 0.44×10^6 pounds.

5.2 Vertical Damping and Stiffness. -

The moving mass in the head-to-head test (approximately 30,000 lb. weight) is much less than the moving mass in the Saturn test (approximately 0.44×10^6 or 1.8×10^6 pounds weight per support), therefore, even though the bearing loads and spring rates may be equal for the two tests, the free oscillation frequencies for the head-to-head test will be different than the free oscillation frequencies of the Saturn test.

The measured static piston characteristics and measured damping at and off resonance will be used to verify analytical predictions of system stability and to establish compliance with the maximum allowed damping specification.

The frequency effect on spring rate will be determined by comparison of the static stiffness to the dynamic stiffness at the resonant frequency in the head-to-head test.

5.2.1 Static Piston Characteristics. -

The static piston characteristics for each of the two pistons will be obtained by measuring the following:

1. Piston displacement vs. piston load.
2. Float displacement vs. piston load.

(A) The measurements will be made with bearing loads of 1.8×10^6 and 0.44×10^6 pounds at the minimum spring rate and at a capillary seal length of 6 inches for at least two input flow gains. Additional tests will be made as required to establish confidence in theoretical expectations to determine the effect of other spring rates, capillary seal lengths, and isothermic expansion of the gas spring.

5.2.2 Vertical Damping

Vertical damping at resonance will be measured with bearing loads of 1.8×10^6, 0.44×10^6, and 0.1×10^6 pounds at minimum and double the minimum spring rate.

Vertical damping off resonance will be measured with minimum spring rate at 1.0, 0.5, and 0.1 cps with bearing loads of 0.44×10^6 and 0.1×10^6 pounds, and at 0.1 cps with 1.8×10^6 pounds bearing load. Excitation will be obtained through quick release after displacement or by using two C-5 shakers (each rated at 650pounds) for all vertical damping tests with one exception. The upper piston will be used for 0.1 cps excitation with 1.8×10^6 pounds bearing load.

Damping values will be determined either by using the decay characteristics of free oscillations or by measuring the phase angle between the displacement and input force.

5.2.3 Dynamic Spring Rate. -

The dynamic spring rate can be obtained using the measured value of damping at the resonant frequency and the measured weight of the moving mass.

6.0 INSTRUMENTATION ACCURACY.-

6.1 Instrumentation required for testing shall be within the following tolerances of measurement:

Measurement	Instrument Measurement Accuracy	Overall Tolerance
Temperature	± 2.0%	± 2.0%
Pressure	± .5%	± 3.0%
Flow	± 1.0%	± 1.0%
Hydrostatic Bearing Gap	± 2.0%	± 5.0%
Change in Angle	± 5.0%	± 5.0%
Position	± 1.0%	± 3.0%
Displacement	± .2 to ± 1.0%	± 3.0%
Velocity	± 3.0%	± 5.0%
Acceleration	± 1.0%	± 3.0%
Frequency	± 1.0%	± 3.0%

7.0 PHOTOGRAPHIC DOCUMENTATION.-

7.1 A sufficient number of still photographs shall be taken to present the general assembly of the head-to-head test stand and any items of special interest.

7.2 Motion pictures shall be taken of significant aspects of the operation of the test stand.

8.0 TEST PROCEDURE AND REPORT.-

8.1 A detailed test procedure shall be written for performance of the testing and a test report shall be prepared containing pertinent test data, results and conclusions. Included in the test report shall be the photographic documentation of Paragraph 7.0.

TABLE 3

	Quantity
Oil Flow into Capillary Seal (upper and lower piston assembly)	2
Oil Flow through Adjustable Capillary (upper and lower piston assembly)	2
Spherical bearing pressure (lower piston assembly)	1
Flat bearing pressure (lower piston assembly)	1
Upper ring bearing pressure (lower piston assembly only)	2
Lower ring bearing pressure (lower piston assembly only)	6
Capillary seal pressure (upper and lower piston assembly)	2
Inlet oil temperature	1
Outlet oil temperature	1
Piston air chamber temperature (lower piston assembly only)	1
Hydrostatic bearing gap at the spherical bearing (lower piston assembly only)	2
Hydrostatic bearing gap at the flat bearing (lower piston assembly only)	2
Hydrostatic bearing gap at ring bearing (lower piston assembly only)	2
Piston position indicator	2
Float position indicator	2

INSTRUMENTATION LOCATION

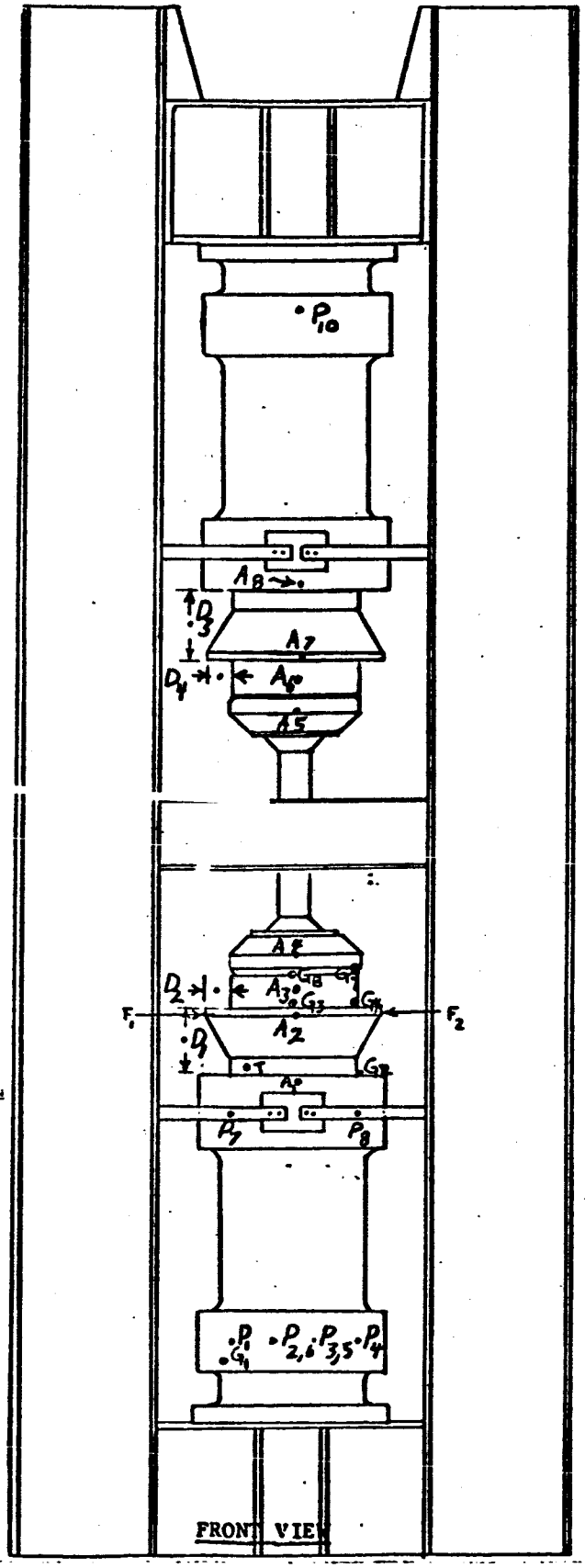

MEASUREMENTS

1. BEARING GAPS (G) 8 PLACES
2. ACCELERATIONS (A) 8 PLACES
3. PRESSURES (P) 12 PLACES
4. DISPLACEMENTS (D) 4 PLACES
5. FORCE (F) 4 PLACES
6. FLOW INDICATORS (FI) 4 PLACES

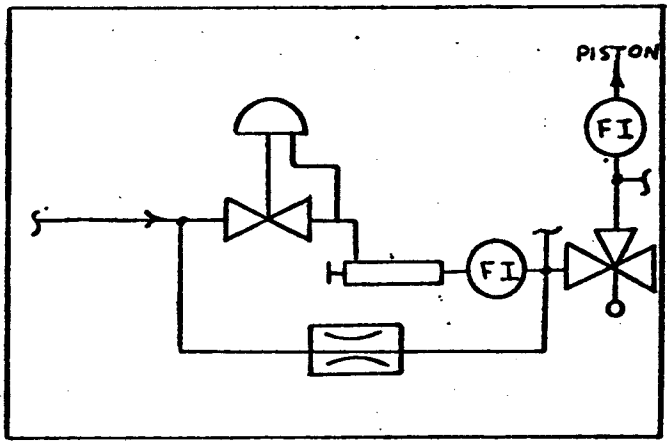

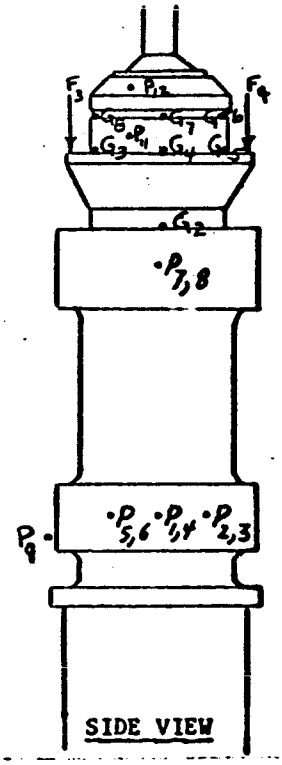

FIGURE 1